2006

ENHANCED GRAIN CROP YIELD MONITOR ACCURACY THROUGH SENSOR FUSION AND POST-PROCESSING ALGORITHMS

Matthew Wayne Veal
University of Kentucky, mveal@bae.uky.edu

ABSTRACT OF DISSERTATION

Matthew Wayne Veal

The Graduate School

University of Kentucky

2006

ENHANCED GRAIN CROP YIELD MONITOR ACCURACY THROUGH SENSOR FUSION AND POST-PROCESSING ALGORITHMS

ABSTRACT OF DISSERTATION

A dissertation submitted in partial fulfillment of the requirements
for the degree of Doctor of Philosophy in Biosystems and Agricultural Engineering
in the College of Engineering
at the University of Kentucky

By
Matthew Wayne Veal
Lexington, Kentucky

Director: Dr. Scott A. Shearer,
Professor of Biosystems and Agricultural Engineering
Lexington, Kentucky

2006

ABSTRACT OF DISSERTATION

ENHANCED GRAIN CROP YIELD MONITOR ACCURACY THROUGH SENSOR FUSION AND POST-PROCESSING ALGORITHMS

Yield monitors have become an indispensable part of precision agriculture systems because of their ability to measure the yield variability. Accurate yield monitor data availability is essential for the assessment of farm practices. The current technology of measuring grain yields is prone to errors that can be attributed to mass flow variations caused by the mechanisms within a grain combine. Because of throughput variations, there are doubts regarding the correlation between the mass flow measurement and the actual grain volume produced at a specific location. Another inaccuracy observed in yield monitor data can be attributed to inexact cut-widths values entered by the machine operator.

To effectively address these yield monitor errors, two crop mass flow sensing devices were developed and used to correct yield monitor data. The two quantities associated with crop material mass flow that were sensed were tension on the feeder housing drive chain and the hydraulic pressure on the threshing cylinder's variable speed drive. Both sensing approaches were capable of detecting zero mass flow conditions better than the traditional grain mass flow sensor. The alternative sensors also operate without being adversely affected by material transport delays. The feeder housing-based sensor was more sensitive to variations in crop material throughput than the hydraulic pressure sensor. Crop mass flow is not a surrogate for grain mass flow because of a weak relationship ($R^2 < 0.60$) between the two quantities. The crop mass flow signal does denote the location and magnitude of material throughput variations into the combine. This delineation was used to redistribute grain mass flow by aligning grain and crop mass flow transitions using sensor fusion techniques. Significant improvements ($\alpha = 0.05$)

in yield distribution profile were found after the correction was applied.

To address the cut-width entry error, a GIS-based post-processing algorithm was developed to calculate the true harvest area for each yield monitor data point. Based on the results of this method, a combine operator can introduce yield calculation errors of 15%. When these two correction methods applied to yield monitor data, the result is yield maps with dramatically improved yield estimates and enhanced spatial accuracy.

KEYWORDS: Yield Monitor, Precision Agriculture, Combine Harvester, Sensor Fusion, Geographic Information Systems (GIS)

Matthew W. Veal

4 August 2006

ENHANCED GRAIN CROP YIELD MONITOR ACCURACY THROUGH SENSOR FUSION AND POST-PROCESSING ALGORITHMS

By

Matthew Wayne Veal

Dr. Scott A. Shearer
Director of Dissertation

Dr. Dwayne R. Edwards
Director of Graduate Studies

4 August 2006

RULES FOR THE USE OF DISSERTATIONS

Unpublished dissertations submitted for the Doctor's degree and deposited in the University of Kentucky Library are as a rule open for inspection, but are to be used only with due regard to the rights of the authors. Bibliographical references may be noted, but quotations or summaries of parts may be published only with the permission of the author, and with the usual scholarly acknowledgments.

Extensive copying or publication of the dissertation in whole or in part also requires the consent of the Dean of the Graduate School of the University of Kentucky.

A library that borrows this dissertation for use by its patrons is expected to secure the signature of each user.

Name Date

_____

_____

_____

_____

_____

_____

_____

_____

_____

_____

_____

DISSERTATION

Matthew Wayne Veal

The Graduate School

University of Kentucky

2006

ENHANCED GRAIN CROP YIELD MONITOR ACCURACY THROUGH SENSOR FUSION AND POST-PROCESSING ALGORITHMS

DISSERTATION

A dissertation submitted in partial fulfillment
of the requirements for the degree of
Doctor of Philosophy in Biosystems and Agricultural Engineering
in the College of Engineering
at the University of Kentucky

By
Matthew Wayne Veal
Lexington, Kentucky

Director: Dr. Scott A. Shearer,
Professor of Biosystems and Agricultural Engineering
Lexington, Kentucky

2006

This work is dedicated to the memory of my brother Andy, who is a reminder to never take yourself too seriously and that there are more important pursuits in life than dissertations and scholarly achievement.

ACKNOWLEDGEMENTS

As my 23+ years of formal education draws to a close, I am amazed at the number of people who played a role in helping me achieve this goal. It is very reassuring to look back and see the number of people who have selflessly given of their time and resources to provide me with the means to achieve this distinction. While I am provided with limited means to offer my gratitude to those that have supported me in this pursuit, I acknowledge the efforts of everyone that has had a positive influence on my life and I offer my sincere thanks. There are a few who played a major role in this particular phase of my education who need to be recognized.

The faculty and staff within the University of Kentucky Biosystems and Agricultural Engineering Department have been a fantastic group to work with and their assistance is valued. I offer my sincere thanks to Scott Shearer whose guidance was exceedingly valuable in this final chapter of my formal education. Because of Scott's efforts, I doubt it was possible for me to have had a better Ph.D. experience to prepare me for my next career as a faculty member. I also want to thank my graduate committee, Drs. Tim Stombaugh, Mike Montross, and Keith Rouch for the advice offered and the time they put into my Ph.D. Besides Scott, I believe that Ed Hutchins played an enormous role in the completion of this degree. Ed was always there to help out when things were at their worst and the wealth of knowledge Ed possess was a great resource. The efforts of the rest of the machine shop personnel, Carl Kings, Will Adams, Lee Rechtin, and Ed Roberts are also greatly appreciated. I also want to thank Dennis Hancock, Steve Higgins, Ben Koostra, and Tim Smith for their contributions to my education.

While my time at UK has been very enjoyable, there have been tough times as well, and its only through the support family and faith in God that the strength to persevere can be found. While I have waited until the end to offer my appreciation to their efforts, they played an immeasurable role in all the success that I have enjoyed. The love, encouragement, and understanding shown by my wife, Lori, were without end and I am so grateful to her as a spouse. Without her contribution it would have been impossible to complete this work. I want to thank my parents, Jerry and Sharon for their unconditional, continual love and support. I believe that this work is a testament to the values and work ethic that they instilled in me.

TABLE OF CONTENTS

LIST OF TABLES

LIST OF FIGURES

LIST OF FILES

mveal06dissertation.pdf	9.63 Mb

Chapter One

Introduction

Preface

Precision agriculture is a methodology used by crop producers to identify and exploit variability within an agricultural field. One of the key aspects of precision agriculture is the formation of increasingly smaller, homogenous management zones that allow a farmer to customize management strategies on a much finer resolution than through traditional whole field management (Doerge, 1999). These management zones will vary in size and location depending on the type of crop input. For instance, the management zones used to develop herbicide prescription maps might vary from those used to develop nitrogen application maps. The goal of precision agriculture is to increase farmer profitability by enhancing problem diagnosis (i.e. drainage problems, pests, etc.) and improving crop input decisions (i.e. fertilizer application) (Lowenberg-DeBoer, 1997).

A popular and highly significant area of precision agriculture research focuses on the division of a field into smaller management zones. Recent production agriculture research has focused on determining what types of information and how much data a farmer should collect to define the size and location of the various management zones. Soil sampling, crop yield data, aerial imagery, electrical conductivity, and field scouting are a few of the most popular methods for collecting information regarding the variability within a field. The majority of these methods require the farmer to call on the expertise of third-party organizations to process and analyze the infield variability. Also, economic and time factors associated with these practices often limit the sampling resolution. As an alternative to methods that require third-party assistance, many crop producers have adopted yield monitoring as a means to study crop yield variability and crop response to management decisions.

Yield monitoring measures the mass flow of granular material through a grain harvester or combine. This mass flow measurement typically occurs in the clean grain elevator on a combine. As the mass flow measurements are recorded, geographic coordinates calculated by a global positioning system (GPS) receiver are also stored. Once the data is downloaded from the yield monitoring system, a crop producer can generate a yield map that will illustrate the spatial

variability of the crop yield across an agricultural field. Yield maps are extremely popular tools for the determination of management zones. Yield monitoring is popular because it allows the farmer to quickly generate a very dense data set detailing infield variability, while the operating costs are relatively low and non-recurring. The majority of the cost of utilizing a yield monitor occurs during the initial purchase and installation of the device. Because yield monitoring is integrated into the annual harvest activities, there is no considerable economic or time penalty for a crop producer to collect this data. The darker areas in the yield map generated during a soybean harvest (Figure 1.1) indicate areas of the field associated with higher levels of grain production.

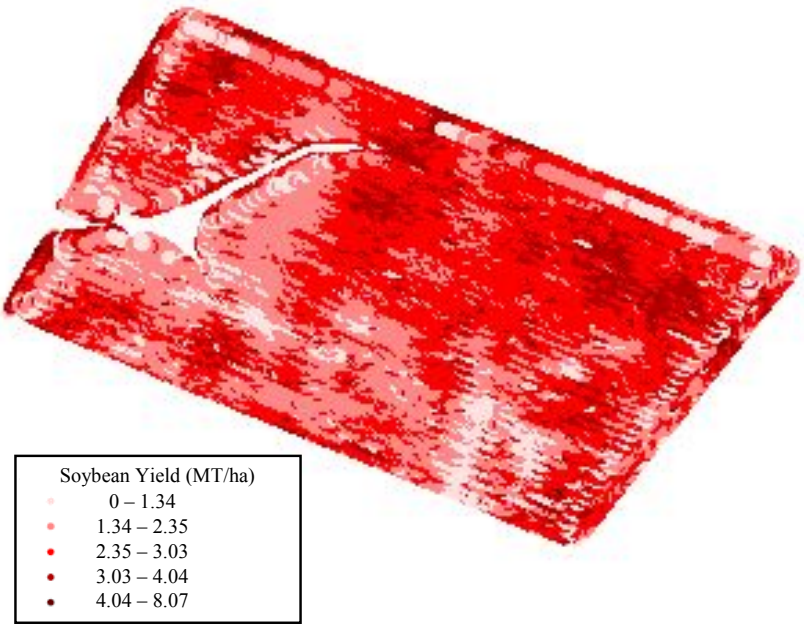

Figure 1.1. Conventional yield map for a soybean field.

To fully appreciate some of the problems associated with traditional yield monitoring systems, the basic path that plant material and grain takes as it is processed in a grain combine must be described. Figure 1.2 provides a detailed illustration of the internal components of a conventional grain combine. While conventional combine operation is described in the following paragraph, it should be noted that rotary combines are the more popular choice for new machine purchases. Rotary combines do not use straw-walkers and rely primarily on mechanical

power to separate grain from crop material. Conventional, straw-walker combines rely heavily on gravity for separation. Because a rotor is larger than the threshing cylinder in a conventional combine, crop material stays in contact with the mechanical separation device longer. Mechanical separation is faster than gravity-based separation, so rotary combines have higher capacity. Also, there is less grain damage associated with rotary machines because the rotor spins at a lower speed than the threshing cylinder in a conventional combine. One of the main drawbacks to rotary combines is the excessive amount of damage inflicted upon the plant material. This is an issue in wheat, where many crop producers bale the straw exiting the combine for animal feed.

A combine initially engages a grain crop at the grain platform (or header) where it is cut and moved to the feeder housing. The crop material and grain is conveyed through the feeder housing and then passed between the cylinder and concave where the material is threshed. At this point the grain separation process begins. As crop material passes over the straw walkers, the chaffer, and the sieve, grain is filtered out and the Material Other than Grain (MOG) exits out the rear of the combine by way of mechanical conveyance or it is blown out by the fan. Eventually the grain falls to the bottom of the cleaning shoe where it is conveyed via an auger to the clean grain elevator. Not fully detailed in this illustration is the recirculation that occurs when material passes through the chaffer but not the sieve. Material that does not fall through the sieve eventually arrives at the tailings auger and is conveyed back to the cylinder or rotor, where it is re-threshed. Mass flow is not sensed until the grain passes through the clean grain auger and is lifted to the top of the clean grain elevator.

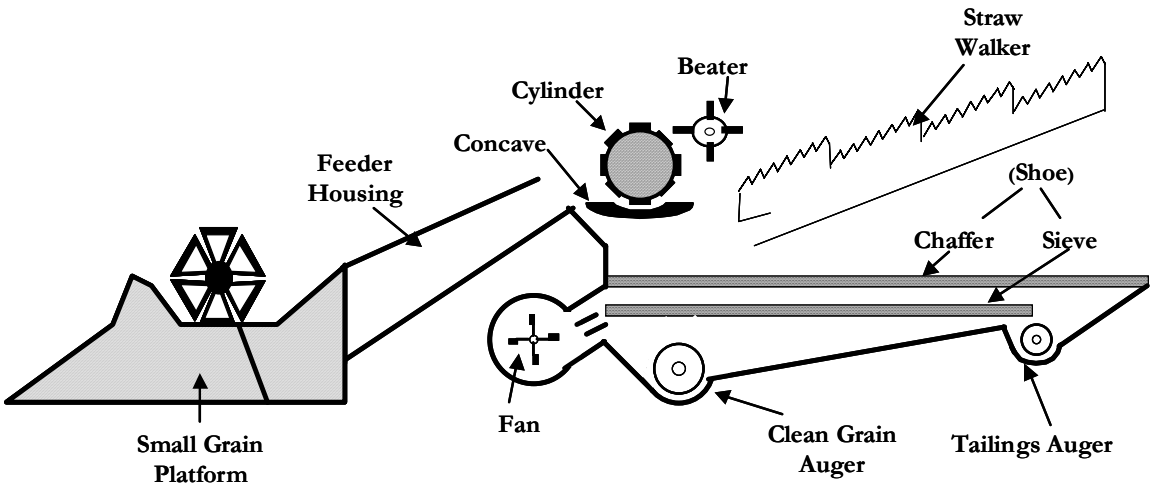

Figure 1.2. **Conventional grain combine separating and cleaning mechanisms**.

Conceptually, yield monitoring appears to be a simple means to gather crop yield data in an efficient manner. However, there are a number of issues that prevent a crop producer from using a yield map as a singular data source in the creation of field management zones. Variations in crop properties such as kernel size, grain moisture content, presence of dust or dirt on the plant, weed or pest infestations, and wind damage can affect the performance of many commercially available yield monitors (Missotten, 1996). Blackmore and Marshall (1996) identified six major sources of error associated with the operation of the grain combine that call into question the accuracy of yield maps:

- Time lag (transportation delay time) of grain through the threshing mechanism
- Unknown crop width entering the header during harvest
- The inherent "wandering" error from the GPS
- Surging grain within the combine's transport system
- Grain losses from the combine
- Sensor accuracy and calibration.

In addition to these sources of yield monitoring error, there are concerns about operational practices such as lowering and raising the header to initiate data logging and operator induced variations in combine ground speed. While there have been advancements in GPS

correction routines and improvements in mass flow sensing technologies, there are still a number of the issues identified by Blackmore and Marshall (1996) that have not been addressed. Time lag describes the time delay between the moment a plant is engaged by the combine and the moment that the mass flow measurement for the grain is recorded. A time lag value is needed to align the mass flow measurement with the geographic coordinates representing the point of cultivation for the crop. For instance, a mass flow reading will be assigned the GPS coordinates collected 13 s prior to this mass flow value being recorded. Nolan et al. (1996) observed grain transportation delays in excess of 35 seconds, which correspond to a combine traveling 49 meters at a velocity of 1.4 m/s. This is significant because most commercial systems use a constant delay time between 10 and 14 s. If a 13 s delay time is again used, the coordinates assigned to the mass flow reading in Nolan's study would be in error by 31 meters.

The time lag value is not constant and is highly variable due to combine dynamics. Combine dynamics, a term describing material transport delays, filling and emptying of the threshing and separation mechanisms, and grain recirculation, remains a major obstacle in the quest to improve yield monitor accuracy. The ground speed, incline attitude, plant material load, and whether the machine is entering or exiting a strip of grain will have significant influence on the internal dynamics of the combine and ultimately the time lag (Nolan et al, 1996). Because the time lag is subject to extreme variability and differs for each manufacturer and combine model, most yield monitors use a constant delay time value for simplicity. An incorrect delay time assumption will lead to significant over- and under-estimations of grain yield and cause random position offsets in the yield map data (Moore, 1998).

Besides throughput lag issues, another well-documented source of yield monitor error occurs when an incorrect cut- width is recorded. The cut-width is usually entered on the yield monitor's user interface and most operators use a fixed value corresponding to the maximum width the grain platform in use is capable of cutting (the effective cut-width). The effective cut-width is typically 15 cm less than the maximum cut-width. In reality, there are many instances where a partial cut-width is more accurate given the field layout or operational practices. Figure 1.3 illustrates two consecutive passes made by a grain combine and the inadequacy of using a fixed cut-width.

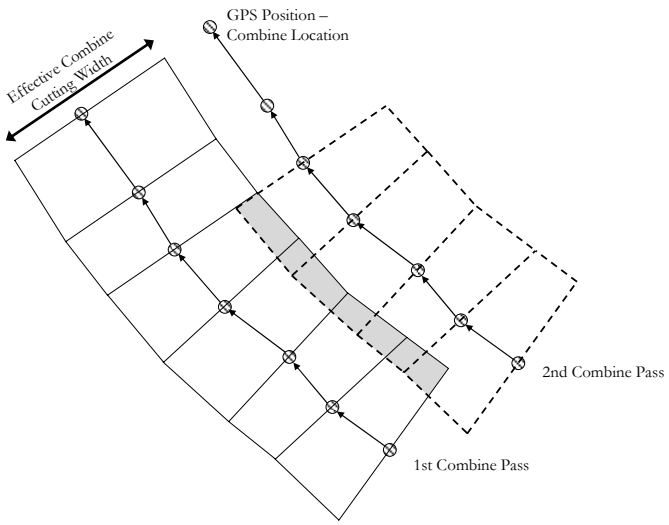

Figure 1.3. **Illustration of consecutive combine passes and the resulting error caused by the use of a fixed cutting width.**

At issue in Figure 1.3 is the gray area representing the area of overlap between the first and second combine passes. On the second pass, the yield monitor is under the impression that a full cut-width is being harvest, but there is a portion of the grain platform on the left of the combine passing over ground where the grain was harvested on the preceding pass. Therefore, to the yield monitor it appears the volume of grain entering the combine is spread out over a larger area than is the case. This will result in the yield monitor under-reporting the grain yield.

This research project was designed to resolve the two primary issues that were previously mentioned regarding the reliability of yield monitor data. Through a series of investigations, the ultimate goal was to provide crop producers with the tools to produce yield maps that reflect the actual distribution of grain within an agricultural field. The main areas of concern this project attempted to reconcile are the issues that arise from variable time delays resulting from combine dynamics and the issue of incorrect recording of combine cutting widths. To address these issues, a real-time sensor fusion mass flow correction system will be developed to alleviate time lag issues, and a post-processing algorithm will be developed within a GIS system to correct swath width errors. The rationale behind the selection of these correction schemes is covered within the literature review of this manuscript.

Justification

If a correction method can successfully improve the accuracy of yield monitor data, then crop producers will be able to assess their management decisions with greater confidence, as the yield map before them will be a more accurate spatial representation of grain produced for a given season.

Field evidence suggests the ability of yield monitors to promptly detect distinct yield differences may be questionable. In an unpublished preliminary investigation during the 2002 wheat harvest, researchers at the University of Kentucky were able to capture data that illustrates the significance of combine dynamic issues. This test was conducted in accordance with the American Society of Agricultural and Biological Engineers (ASABE) X579 Field Performance of Yield Monitors draft standard (shown in Appendix A). A test layout was established in the field by performing a series of pre-harvest operations to selectively remove grain from specific blocks in the test plot. This pre-harvest removal resulted in 6 continuous blocks that have varying grain volumes in each block. A John Deere 9500 equipped with a John Deere Greenstar yield monitoring system then harvested the test plot at constant speed. The resulting mass flow data collected by the yield monitor is shown alongside the actual grain yield present in the test plot in Figure 1.4. The key points to note are: (i) the yield monitor recorded considerable grain yields in the two blocks that had no grain present during the test and, (ii) the yield monitor was not able to reflect the full volume of grain located in the first and sixth blocks of the test.

It would appear that reallocation of the mass flow data would allow the yield monitor data to better reflect the true distribution of grain within the test plot. This could be accomplished by removing the excessive crop yield data in the blocks that had no grain present and reassigning it to the blocks where yield monitor readings underestimated the amount of grain present.

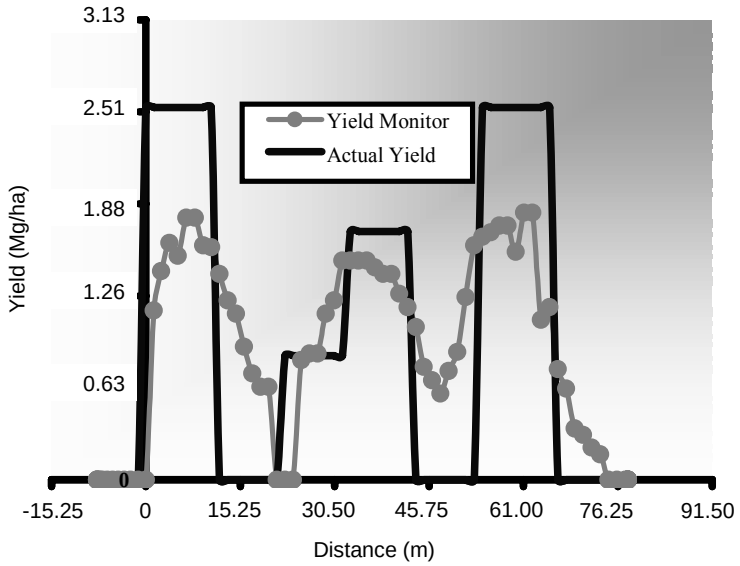

Figure 1.4. **Yield monitor response to ASABE X579 field test profile.**

By improving the delineation between areas in the field producing different volumes of grain, producers will be able to generate yield maps that capture the true variability of their fields. This could dramatically improve their management strategy as crop input prescriptions would better match the true field conditions. In addition to better management zone delineation, if the yield data reflected the true volume of grain produced in an area, a crop producer could make a more informed decision about how aggressively to attack a problematic area.

Beside spatial accuracy errors in yield maps, improper cut-width values represent a source of considerable non-random error. The main issue with improper entry of the combine's cut-width is the creation of a random source of error affecting the reported grain yield across the field. The equation to convert a mass flow reading into crop yield (the quantify of most interest to producers) is affected by errant cut-widths is found in the denominator of the first term, (Equation 1.1).

$$Y = \frac{m\left(\frac{100 - M_{HARVEST}}{100 - M_{MARKET}}\right)}{s * d * w * \rho} * \left(\frac{144 in^2}{1 ft^2}\right) * \left(\frac{43{,}560\, ft^2}{1 ac}\right) \quad \textbf{Equation 1.1}$$

where:

Y = crop yield (bu/ac)

m = mass flow (lb/s)

M = Moisture Content (%)

s = cycle time (sec)

d = cycle distance (in)

w = cutting width (in)

ρ = grain density (lb/bu)

While there have been few studies to measure how much an operator overlaps consecutive passes, it is a well-documented and cited problem when a yield monitor's accuracy is considered. The amount of overlap is unquestionably variable. As an example consider a 7.8 meter small grain platform that the operator allows to overlap by 0.8 meters. If this information was not entered into the yield monitor, then the corresponding yield map would indicate a yield value 10% below the actual crop yield. With this type of error, a crop producer could easily be lead to believe that an area is under-producing by 0.63 MT/ha or more. This misleading yield map may cause a needless waste of resources either through additional investigation into a phantom problem (i.e. additional soil sampling) or through an unnecessary change in management strategies (i.e. increased fertilizer use).

Objectives

To effectively utilize the information contained in a yield map, it is essential that a grain producer has confidence in the quality and accuracy of the data presented in the map. Current yield monitoring and mapping technologies contain flaws that can lead to the generation of suspect data. The overall goal of this research is to provide a means to correct mass flow data collected in grain combines using sensor fusion and post-processing algorithms. The specific objectives of this research are to:

1. Develop and test a prototype sensing technology that will measure biomass flow through a grain combine for the purpose of correcting yield monitor mass flow data;
2. Develop a sensor fusion technique to redistribute the grain mass flow data in accordance with the biomass flow;
3. Develop a post-processing algorithm that utilizes polygon coverages to generate correct cut-widths for single and multiple combine systems;
4. Evaluate the performance of these systems during corn, soybean, and wheat harvest under varying mass flow conditions.

Organization of Dissertation

A manuscript format has been selected for the presentation of research material in this dissertation. Individual chapters will detail the methodology employed and findings for specific aspects of this project. The initial two chapters contain material that applies to all of the work completed under this research project. Chapter One provides a general introduction to yield monitoring, the problems associated with this process, and a framework for how each problem will be addressed. The Chapter Two is a comprehensive review of all relevant literature pertaining to the quantification and correction of yield monitor problems. The subsequent chapters present methodology, data, analysis, and conclusions that are unique to each objective. Chapters Three and Four discuss the development, testing, and evaluation of specific mass flow alternative sensing devices. Chapter Three focuses on a feeder house based approach and Chapter Four looks at sensing the hydraulic pressure required to adjust the variable speed drive of the threshing cylinder or rotor on the combine. Chapter Five looks at two very distinct methods to correct yield monitor mass flow data based on the data collected by the new sensing methods. Chapter Six discusses the development and use of a GIS post-processing routine to correct errant combine cutter width entry. Chapter Seven provides a summary for these research activities as well as suggestions for future work. Supporting appendices and a list of referenced materials conclude this dissertation.

Chapter Two

Review of Literature

Yield monitoring represents one of the quickest, most economical means for grain producers to assess infield variability. By studying the yield variability across a field, it is possible for a farmer to plan future management strategies as well as determine the success of previous decisions. While the potential benefits of using yield maps to assess farm management decisions are widely known, the data constituting the yield map must be accurate for their use to be truly beneficial. The errors associated with yield monitor use are well-documented and there have been many attempts to find solutions to these sources of errors. It is the goal of this literature review to provide an assessment of yield monitoring technology, the errors associated with the technology, and methodologies that other researchers have developed to compensate for errors associated with yield monitoring.

Yield Monitoring As a Precision Agriculture Tool

Prior to the idea of precision agriculture, agriculture management was conducted on the basis of whole fields. These fields were generally defined by arbitrary boundaries such as windrows, streams, or old fences; and little consideration was given to the variation in soil series, phase, or potential productivity (Karlen et al., 1990). However, grain yields and the factors that determine yield are variable and in order for crop producers to optimize their operation it is critical that this variability is addressed. As Borgelt (1993) notes, the ability to customize crop production inputs at every location within a field creates two benefits: (i) environmental protection through the elimination of over application; and (ii) maximum profitability by optimizing yields and inputs.

Yield maps provide a producer with the basic information necessary to develop a site-specific farming strategy. These maps can be used to set up initial nutrient balances, identify areas of comparable soil fertility, and monitor the overall system efficiency (Schnug, 1993). Schnug also discusses the use of yield maps as a means to determine if the crop yield in a given area is limited by natural causes (i.e. water stress) which cannot be manipulated through

production techniques, or if the limiting factors can be manipulated through improved management strategies (i.e. increasing fertilizer applications rates). The benefit of yield maps is the fact that they are generated during typical harvesting operations, so the grain producer is not adversely affected economically beyond the initial purchase of the yield monitoring system. The result of yield monitoring is a very dense sampling of field conditions (10,000+ points/ha) that can effectively determine in-field variability, while the farmer obtains this data set without significantly increasing harvest time or costs.

The most popular means of monitoring mass flow in North America is the use of a force-impetus device mounted at the top of the clean grain elevator. This type of sensor measures the deflection as grain strikes an impact plate. As the grain completes an 180^{o} turn at the top of the clean grain elevator, the elevator paddles accelerate the granular material away from the paddles and it strikes the impact plate. The theory behind this sensing method is that impact plate deflection is proportional to the mass of grain impacting the plate. A moisture sensor is needed to correct yields at a constant moisture basis. Figure 2.1 provides a detailed illustration of the typical yield monitoring system used on a grain combine and a force-impetus type yield sensor.

Yield monitoring has been gaining interest among grain producers as a means to assess the spatial variability of conditions within the field (Stafford et. al, 1994). This is most likely attributed to the finer sampling resolution. This sampling resolution is determined by two factors, the perpendicular distance between the combine's successive passes (this is generally a function of the header width) and the relationship between sampling frequency and the forward speed of the combine. So a typical mass flow sample grid would have a mass flow reading every 2 meters along a pass and these passes would be approximately 5 to 7 meters apart. This level of resolution is sufficient to break the field into management zones that can allow for the successful implementation of site-specific farming (Lamb et. al, 1995). In addition to spatial resolution, the precision of the mass flow sensor must be considered. Howard et al. (1993) asserted that the mass sensor should record data within $\pm$5 to 10% of the actual grain weight to develop relationships between yield maps and variable rate application.

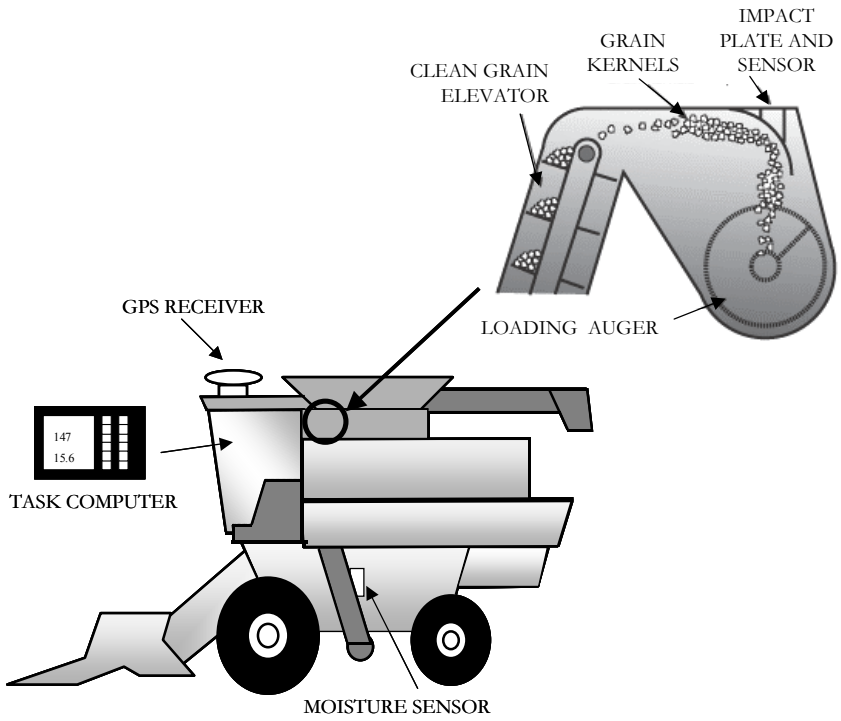

Figure 2.1. Yield monitor components and detailed illustration of force-impetus mass flow sensor (adapted from Grisso 2005).

Errors Associated with Yield Monitoring Systems

Crop producers depend on correct yield maps to perform complete, accurate economic assessments of their farm operation. Agricultural equipment manufacturers have placed a great deal of emphasis on improving the technology needed to sense grain flow in a combine for the creation of yield maps. However, there remain a number of issues that adversely affect mass flow sensing and yield monitoring systems. This dissertation is concerned with the correction of yield monitoring errors that are associated with mass flow sensing, combine dynamics and incorrect entry of combine cutting widths. However, additional error sources will be identified and discussed in detail.

A number of studies have attempted to assess the true accuracy of yield monitors. Typically, researchers compare the grain weights calculated by the yield monitor to the weight obtained from scales. Doerge (1996) performed this type of comparison and found that the yield monitor weight was within 2 to 4% of the scale weight for loads greater than 4000 kg. However,

for smaller loads the difference increased to 10%. Similar studies have been conducted in which the grain tank on the combine is equipped with scales so instantaneous as well as cumulative weight comparisons between yield monitor estimates and true grain weight can be made. Al-Mahasneh and Colvin (2000) used a combine equipped with scales to harvest grain in two cornfields and an oat field. They found the instantaneous yield monitor weights were within $\pm$1.89% of the actual weight measured by the scales for all three fields. There was an increase in this difference when the final cumulative weights were compared. The maximum cumulative difference for a single field was 6.22%; the minimal cumulative difference was 1.99%. Many of these studies were conducted under very controlled field situations utilizing plot combines; however, they do validate that it is possible to achieve the yield monitor accuracy needed to establish management zones for variable rate application. Both yield monitoring and weigh scales calculate harvest weight by integrating mass flow. Therefore, the error in weight distribution is masked by both of these methods. Total weight of grain harvested is only one aspect of yield monitor accuracy. The distribution of the grain across the harvest segment is the other part of the accuracy equation, which cannot be checked with scales.

Moore (1998) analyzed yield monitor data collected in eight fields over a period of six years. From this analysis, the most prevalent errors were identified and ranked based how badly the error altered the yield map. The following nine categories in order of distortion were found:

1) Yield map smoothing errors;
2) Regular volumetric calibration that result in yield offsets and wander over time (valid only for volumetric sensors);
3) Incorrect cut-width entry;
4) Variable time lag associated with combine filling delay, occurs at the start of each combine pass;
5) Incorrect lag time assumption;
6) GPS positioning errors that are similar to the magnitude of the cut-width;
7) Yield sensor accuracy (typically 5% or better);
8) Grain loss; and
9) Variable time lag associated with combine emptying delay, occurs at the end of each combine pass.

Among these nine items, the objectives of this research project have been drafted to correct timing and cut-width errors. Among the items that will not be addressed are yield map smoothing errors, regular volumetric calibration, and grain loss. Yield smoothing errors occur in the interpolation method use to generate a yield map from the point data and for the most part this is a user-defined issue. Volumetric yield sensors are not in widespread use in North America. Therefore, the volumetric calibration error associated with using inaccurate grain bulk mass densities is not of great concern. Grain loss is a difficult quantity to measure, as kernel loss begins the moment a combine interacts with a grain crop. For example, canola is susceptible to shatter loss because the seedpods are fragile at maturity, and when the combine engages this crop the pods split open spilling the seed to the ground.

The most common link connecting sources of yield monitor error is the degradation caused by inaccurate and variable time lag variables. Time lag is a term used to describe the amount of time required for a kernel of grain to travel from the cutting mechanism on the header to the mass flow-sensing device. This time offset must be acknowledged because it is used to assign the geographic location where the plants were cultivated to the amount of grain produced in that location. But there is inherit variability in the time lag value due to the complexity of the combine's internal structure. As the loading level within the combine separation and cleaning systems vary, there are variations in the transport delay time (Howard et al., 1993). Further complicating the ability to assess combine transport delay is evidence to suggest that adjustment of the separating and cleaning mechanisms (i.e. changing the spacing between the concave and cylinder) within the combine can lead to lag time variations of up to 2 seconds (Reitz, 1996).

There is little doubt that the grain gathered at a finite location will not pass through the combine as a single unit. Using the example of a single corn stalk and referring back to Figure 1.2 the variability of the time delay can be illustrated. Some of the kernels from this corn stalk may separate from the cob on the concave, fall straight through the cleaning shoe, and be on the fast track to the clean grain elevator. Other kernels on the same cob may be grouped in a slightly larger mass. This group of kernels would be carried across the straw walkers, fall on the chaffer, and after being sifted through the chaffer they would drop onto the sieve where they would be returned for additional threshing via the tailings elevator. This process led Lark et al. (1997) to conclude that the instantaneous mass flow measurement does not correspond to the yield at a single point, rather it represents a function of yield over a finite length along the

combine's pass. Therefore, it may more appropriate to use yield monitor data to study yield trends as the point data represents mixed grain from a 25-30 m^2 section (Arslan and Colvin, 2002a).

Arslan and Colvin (2002b) studied the response of yield monitors under a variety of field conditions that were established to create varying crop yields. There were a total of three field tests conducted in this study. In the first, scale weights were compared to yield monitor weight estimates for corn harvested in 360-meter strips. The strip was broken into 15-meter increments and consecutive increments were grouped to create segments of varying length (i.e. 15 m, 30 m, 60 m, etc.). The authors found that the discrepancy between the two weight values decreased as the strip length increased. The reason of this occurrence is combine dynamics and the filling characteristics of the threshing and cleaning mechanisms at the start of the plot. Another test looked at abrupt yield changes that were created by driving the combine through empty strips of varying width that were separated by 30 m strips of standing corn. The yield monitor did not achieve a zero mass flow reading until it passed through an empty strip of grain 18 m in length. For the 4.5 and 9 m empty strips, the yield monitor recorded significant mass flow values ranging from 2 and 6 kg/s.

Arslan and Colvin (2002b) also found that ground speed variation could lead to decreased accuracy in the yield monitor system. By raising the combine's ground speed from 8 km/h to 11 km/h the discrepancy between yield monitor and scale weight increased from 3.4% to 5.2%. This is attributed to the effects on increasing the flow rate of material into the combine and subsequent effect on combine dynamics. Missotten et al. (1996) observed a similar decrease in yield monitor accuracy but it was associated with the harvest area. When harvesting a 400 m^2 area the yield monitor had a maximum error of 5%, but this value was reduced to 3% when a 2000 m^2 area was harvested. The error was reduced to 1.7% when a 6 ha field was harvested. This decreasing error value is most likely the result of an increased sample size that reduces the effect of extremes in the data.

In addition to the transport and sensing issues, inaccurate cutting width values continue to plague modern yield monitoring systems. Currently, there is not an available means to automatically determine how much of the effective cutting width is being utilized in real-time. A yield monitor system calculates a harvest area for each mass flow reading. Therefore, for each cycle time the yield monitor records the distance traveled by the combine and the cutting swath

of the combine. Cycle distance is based on the forward speed of the combine and recorded without human intervention, but the combine's operator must manually input the combine's cutting swath. Typically, an operator inputs the maximum cutting swath and this value will be recorded as the effective cut width of the grain platform for an entire field. In practice, the effective cut width is 20 cm less than the maximum cut width.

Blackmore and Marshall (1996) describes how the incorrect entry of combine cutting width leads to a series of instantaneous errors that are associated with each data point logged by the yield monitor system. The error is not cumulative, as the yield monitor will still estimate a reasonable value for the total volume of grain produced within the field. If it were possible to harvest the same field twice utilizing the full cutting width the first time and utilizing only half of the full cutting width on the second harvest, the yield monitor would report essentially the same total grain weight. However, the harvest that used only half of the full header width to harvest the grain would produce twice the number of readings but with half the true yield value; thereby, indicating erroneous instantaneous point data.

Most yield monitor systems provide operators with the means to adjust the recorded cutting width. However, Reitz and Kutzbach (1996) point out that this feature is difficult to implement in the field. Depending on the yield monitoring system, the operator can either enter an approximate cutting width (usually rounded to the nearest foot) or the header width is divided into segments representing a percentage of the effective cutting width. Early yield monitor systems allowed the operator to specify the cutting width in 25% increments of full cutting width. Operator-based adjustments are challenging to implement because the resolution of the adjustment significantly affect the accuracy of the resulting yield map. At best, the operator has the ability to enter the cutting width in 3 cm increments. However, the percentage-based systems may have resolution in the vicinity of 2 meters. Even when manual cutting width input is available it is seldom used due to the concentration needed to operate the combine. Typically, the operator uses the same cutting width for the entire field and most often the full, effective width of the cutting platform is used.

Using the full header width is an acceptable practice as long as the full header width is engaging crop material. However, this only occurs when a combine is allowed to make a pass with standing grain on both sides of the combine. During the course of a harvest, the more likely situation would be of the combine to have a pass of harvested grain on one side and a standing

pass on the other. Usually, the operator will allow a portion of the cutting platform to overlap the previously harvested strip to insure all of the grain is harvested without making return trips to harvest any thin strips of missed crop. Based on visual inspection many operators only allow 90% of the cutting platform to engage the crop (Stafford et al, 1997). Using GPS positions collected by a yield monitor, Drummond et al. (1999) was able to study swath width inaccuracies during soybean harvest. Using vector analysis developed within a GIS engine, it was determined that on average 89% of the cutting platform was engaged with crop material and the mode was reported to be 92%. Also, there were several instances when the operator was finishing the field that the percentage of total header used dropped below 80%. Working under the assumption that the operator used the constant full header width for the recorded cutting width, the yield reflected in the typical yield map for a solid-sown crop would be under-estimated by 10%.

Besides inaccurate cutting width estimates, improper calibration is another source of yield monitor error. Improper calibration can be the result of using too few calibration data points, calibrating outside the operating parameters, or simply relying on data that is outdated (i.e. last year's calibration file). Grisso et al (2002) studied calibration error effects by changing the amount material entering the combine by varying the ground speed of the machine. When the ground speed was slowed by 20 to 30%, the flow rate of material entering the combine was reduced. For a speed increase, the material intake rate also increased. These speed variation tests were replicated on two different combines and the speed was varied such that low, normal, and high material intake rates were tested. The resulting wet weight calculated by the yield monitor was compared to the grain's true wet weight measured using a weigh wagon. Each combine had its yield monitor calibrated prior to the test operating under typical conditions (i.e. the "normal" material intake level). The test results indicated that as long as the combine was operated under the same conditions present during system calibration, the discrepancy between measured weight and actual weight was less than 4%. This discrepancy increased to over 10% when the machine was operated at speeds significantly slower or faster than the calibration speed. The yield monitors tended to over estimate the weight of harvested grain when the combine was operated at lower speeds (under capacity). For the faster combine speeds (over capacity) there was no clear distinction between over and under prediction, due to highly variable prediction errors.

Whelan and McBratney (2002) completed one of the most thorough investigations into time lag variability when they painted crops in the field and monitored how the colored material flowed through a conventional combine harvester. The colored strip of grain was located 20 m inside the plot, which assured the combine achieved steady-state operation. The clean grain elevator door was removed so that the grain was unloaded onto the surface after it passed through the clean grain auger. The results indicated that the peak flow of colored grain arrived at the end of the elevator 7 s after the colored crop was engaged. However, colored grain was found exiting the clean grain auger 25 s after the colored crop was encountered. This variable time lag for grain harvested from the same geographic location indicates the tortuous pathway that is followed by material in a grain combine. Thereby proving that a mass flow measurement is not an indication of the mass of grain harvested at a given coordinate, rather it is a mixture of grain mass for several nearby locations. It must be noted that the time lag discussed here would not be an appropriate yield monitor delay time because the transportation up the clean grain elevator is not considered.

Correction Methods for Yield Monitor Errors

Thus far, the promise of the yield monitor as a tool to develop and assess farm management strategies, and the errors preventing this technology from being used to its full potential have been discussed in great detail. At this point, the focus of the literature review will turn to methodologies that have the potential to alleviate the inaccuracies associated with yield monitoring. Data filtering, realignment of geographic coordinates, various mass flow sensing devices, cutting width correction mechanisms and yield monitoring alternatives will be discussed. Each of these items will be carefully examined so that the best course of action can be taken at the onset of this investigation and a successful yield monitor correction system will be created.

One of the most basic forms of yield monitor data correction involves the use of filters to remove data points that are perceived as containing errors. Typically, data filters locate instances within the data set that are associated with typical yield monitoring errors. Beck et al. (2001) developed a filter that removes data points with unrealistic yield values, inappropriate cycle distances, evidence of grain surging, and data collected while the combine was turning at the end of passes. It was shown that as much as 11% of the unfiltered yield map contained suspect data,

and this data was usually located along the tails of the mass flow distribution curve. Blackmore and Moore (1999) developed similar criteria for correction of yield monitor data. For instance, a maximum allowable cycle distance was calculated as a function of maximum harvest velocity and GPS positioning accuracy. Data points containing cycle distances above this maximum value were excluded from the yield map. Also, the data points at the beginning and end of each combine pass were eliminated to lessen the transport delay time variation that occurs when the separating and cleaning mechanisms initially fill and empty.

Besides filtering seemingly erroneous data points, there has been interest in developing correction programs that focus on the spatial reallocation of yield data. This correction is based on reassigning yield data to different geographic coordinates to account for variations in time lag. This could be accomplished by developing an adequate model for material transport lag in a combine. However, it would be difficult to model the material through each mechanism in a combine, so instead it is recommended that the combine should be treated as a lumped-parameter system (Searcy et al. 1989). This reduces the combine to a simple input (the header) –output (the grain flow measurement device) system that can be modeled using a first order system. Searcy also suggests the use of arithmetic averaging as a means to filter data. This is especially important if the mass flow records are not evenly spaced.

Stout et. al (1993) furthered the recommendations of Searcy and looked into the use of both first and second order models to describe transport delay in grain combines. The first order model was not appropriate as the variations in lag time were very large compared to the mean value. For the second-order model the combine was treated as a mass-spring-damper system and the results were unstable. The authors eventually settled on a fourth-order model using a 10 s moving average to smooth and filter the yield data. Birrell et al. (1996) modeled the time lag as both a simple time delay using a 4 s moving average and as a continuous first-order system. The simple time delay method calculated the instantaneous yield with little noise and additional smoothing was not required. It is essential to minimize smoothing as excessive smoothing hinders efforts to analyze short range variability. The first-order system model was much more susceptible to high frequency noise most likely caused by unsteady grain flow through the sensing device. Because of this noise component, it was difficult to determine the frequency at which changes in instantaneous yield corresponded to true yield variations. A smoothed first-order system was able to detect the step changes in mass flow that occur when a combine first

starts a pass, but this improvement came at the cost of reduced variability information. The simple time delay appears to be the better model.

One aspect of yield monitor data that has been repeated in this literature review is the idea that yield sensor data is the result of grain mixing within the combine and therefore the resulting measurement is convoluted. Whelan and McBratney (2000) discuss the use of a Fast Fourier Transform (FFT) to deconvolve the recorded mass flow signal. Using this method the variability in the yield data increased from 10% using an average transportation delay value to 17% using a deconvolution and data smoothing routine. The smoothing routine could essentially be termed a low-pass filter. This increase in variability proved to be an improvement as this value was similar to the variability determined from hand-harvested samples within the field. This procedure is extremely noise sensitive (from mechanical and procedural sources) and this characteristic becomes markedly apparent when there are abrupt changes in crop yield.

Beal and Tian (2001) developed a method known as Surface Area Ratio (SAR) to correct transport delay errors. Using a continuous 3-D surface to represent the crop yield, the SAR is defined as ratio between this area and the projection of this area onto a 2-D surface. Abrupt yield variations will lead to sharp spikes in the 3-D surface, and increase the surface area. As the time delay is shifted to a more correct value, the 3-D surface will become smoother leading to decreased surface area. The optimal time shift is determined when the minimum SAR is achieved. The authors point out that this method is very useful when multiple combines are used during a harvest. Using this method it is possible to determine the correct time delay that should be used for each combine as time delays vary based on combine manufacturer, model, and harvest settings.

The use of geostatistics as means to optimize the transport delay time value used was studied by Chung et al. (2002). In this study, two approaches were investigated and both attempted to minimize the variability between consecutive combine passes. The first method used semivariograms to identify the onset of small-scale variability within the spatial data set. The level of micro-variability is known as a nugget, which manifests itself as a point of discontinuity at the origin of the semivariogram. Semivariograms were generated for various transport delay times and the delay time that produced a nugget was considered the optimal delay time for a particular portion of the field. Chung et al's (2002) second approach was based on data segmentation using quadtree decomposition. This data segmentation method covered the

yield map with a single square and recursively partitioned the square into smaller squares until each square contained enough information to describe the yield map (this is similar to the method used to compress bitmap images). The optimal transport delay occurred when the fewest number of squares was needed to describe the yield map. While these geostatistical methods proved suitable for the correction of combine transport delay times, the authors noted that these post-processing methods are influenced by the accuracy and clarity of the field data set.

Maertens et al. (2003) brings up an important point when force impetus based sensors are used to quantify the grain mass flow in the clean elevator. Because the grain is thrown in small clusters off the elevator paddles, there is a tendency for the measured flow signal to be disturbed by the paddle rate and the resonance frequency of the mechanical sensor. For most yield monitors, two peaks will appear in the power spectrum of the mass flow data, typically one represents the first mode of the mass flow sensor and the second is due to the paddle frequency. The authors found that these disturbances could be removed using a simple second order filter at relatively low sampling rates (1 Hz). However, at higher sampling rates a double notch filter must be used. This notch filter must also have adaptive capabilities due to elevator speed variability leading to fluctuations in the paddle frequency.

Besides post-processing yield data through filters or other computational means, researchers have attempted to sense the operating parameters of a grain combine in real-time. Since the advent of the grain combine, there have been numerous technologies developed to sense the mass flow rate or feed rate of material into a combine. Typically, the emphasis has been on feed rate measurement as a means to optimize threshing capacity, increase machine efficiency, and lower grain loss. By sensing the material intake rate it is possible to vary the combine's ground speed in an attempt to maintain a constant volume of crop material within the combine. Taylor et al. (2005, 2002) discovered that the use of a feed rate sensor to dictate combine ground speed lead to a significant increase in machine capacity and ground speed when compared to the operating characteristics of experienced operators. Feeder deflection (Andersen, 1963), threshing cylinder torque (Friesen et al., 1966), and hydraulic pressure on the threshing assembly (Coers et al., 2002) are a few of the methods that have been investigated to measure crop material feed rates. Much of this work was focused on the development of intellectual property and therefore, performance data for these devices are largely unavailable.

Schueller et al. (1985) replaced the belt and pulley drive on a combine's feeder housing with a hydraulic motor to monitor the relationship between torque and material feed rate. The results indicated the torque sensor was able to quickly delineate the boundaries of step input plots where material flow rates went from 0 kg/s to 13.2 kg/s and back to 0 kg/s over a 40 m distance. The correlation between feeder housing torque and material feed rate was quite strong with an R^2 value of 0.789 (individual plots had R^2 values as high as 0.99). In addition to the torque relationship, Schueller et al. (1985) attempted to find a relationship between engine load and feed rate. The idea was that as the mechanisms of the combine fill with crop material, higher loads would be placed on the engine. The relationship between engine speed and material feed rate was not as strong as the feeder-housing torque relationship. This is most likely attributed to the fact that the engine also propels the machine, therefore terrain factors also increase engine load.

Missotten et al. (1996) described the use of a straw yield mapping system that was based on sensing crop material flow at the auger on a small grain platform. A sprocket mounted on a set of springs was placed along the tight side of the chain used to drive the header auger. As the torque needed to drive the auger varied, the drive chain tension varied, and the displacement of this sprocket was measured. Increased sprocket displacements were observed with increases in material flow rate for barley, peas, and wheat. However, the magnitude of this displacement varied for similar crops grown in different regions. Because of the presence of a series of friction clutches in the drive sprocket there were issues with slip. The platform also experienced issues with inconsistent material feed rates and instances when crop material would circulate around the auger during high intake rates. The authors found some correlation between straw yield maps and grain yield maps but this was based on visual inspection alone.

Chaplin et al. (2003) modified the clean grain elevator of a combine, so that the torque required to drive the elevator could be measured. The measurements from the torque sensor were then compared to the measurements collected by a traditional curved-plate mass flow sensor. The torque sensor was more responsive to changes in the mass flow into the clean grain elevator. However, both measurement devices failed to precisely measure flow rates below 3 kg/s, as the standard errors for both devices increased significantly at lower flow rates. At grain flow rates above 3 kg/s the standard error for the torque sensor was $\pm$5% versus $\pm$15% for the curved-plate sensor. This exercise shows that improvements in yield monitoring accuracy are

possible, however there are a drawbacks to this particular study. First, this was a static study performed in a laboratory setting and the effects of a combine's motion in the field are unknown. Secondly, an ultimately and more important to this study, this type of device is located in the clean grain elevator and the same transportation lag issues documented thus far remain problematic.

While many of these sensors have proven successful at detecting feed rate variations, there is no clear understanding of how these feed rates relate to the grain flow measurement made at the top of the clean grain elevator. Any comparisons made thus far focused on the total material feed rate that is comprised of grain and MOG (material other than grain). If a relationship between mass flow rate measurements in the clean grain elevator and mass flow measurements obtained at other locations in the combine can be determined, then it may be possible to use all of this information to produce more accurate yield data. For instance, if no material were passing through the feeder housing for a given geographic location then it is acceptable to assume there should not be a crop yield value recorded at that location. However, there has been very little research published regarding the possibility of implementing such an error-checking method.

In addition to mass flow sensing, there have been a number of investigations that have studied methodologies to either sense the current cutting width of the combine or correct the cutting width after the harvest is complete. Reitz et al. (1995) used a pair of ultrasonic sensors to measure the distance between the crop dividers on a grain platform and the edge of the standing grain crop. If the emitted ultrasonic wave struck an object within the sensor's operating range, the wave was reflected back to the sensor and the distance measurement was completed. There was a sensing range of 1.5 m. The main problem with this system was the fact that the crop edge is not clearly delineated due to stubble, stalks that jut out, fallen crops, and gaps between plants. Also, the row spacing of the crop can degrade the accuracy of the sensors. Vansichen and De Baerdemaeker (1991) and Reitz (1996) also investigated the use of ultrasonic sensors and found the mean error in the cutting width measurement was $\pm$ 0.12 m, or very similar to the row spacing for wheat. Sudduth et al. (1998) used ultrasonic sensors to measure the cutting width on larger grain platforms and found that the mean error will increase as the distance between the crop edge and the sensing element increases. Also, there appears to be concern about the use of ultrasonic distance measurement in soybeans due to canopy effects.

Another possibility for real-time cutting swath measurement would be to use some form of machine-vision. There has been success in using machine vision to detect crop edges with a camera mounted on a forage harvester (Hoffman, 1996). For this particular application the focus was to guide the machine based on the location of the standing crop. An update rate between 5 and 30 Hz was required to complete this task. It would appear that this system could be easily adapted to measure the distance to the crop edge. The major drawback to this method is there would be considerable costs in development time and operator expense to develop such a tool for swath width measurement.

As an alternative to sensing the header width in the field, researchers have investigated the possibility of using post-processing computer methods to correct swath width data. Han et al. (1997) developed a raster approach to determine the actual cutting width of a combine in the field. This method was based on the development of a high resolution bitmap indicating the field condition prior to harvest (0 = no crop, 1 = crop). As the combine travels through the field, the bitmap is updated by decrementing the cells whose centers fall within the area covered by the cutting platform. If the header area passes over a grid with a crop state value of zero, then the header width record is adjusted accordingly. Although a very small grid is desired for accurate cutting widths, in practice this is difficult to achieve. First the computing requirements for a small, lower power field computer are extreme. A single 50-ha square field using a 5-cm grid would require 25 MB. Secondly, the GPS device that the yield monitor uses to determine position must have accuracy similar to the grid size. Typically, a yield monitor will use a GPS receiver with reported accuracies of 3 to 5 meters. A number of the grid cells could have their crop status changed due to GPS drift, not due to the cutting platform actually crossing the center of the grid cell.

Drummond et al. (1999) produced a swath width correction method that was similar to Han's. While both used GIS techniques, Drummond switched to vector analysis instead of raster-based analysis. The algorithm associated with this project calculated the area covered by the header over a specified time interval. Using GPS information to ascertain the combine's heading, it is possible to generate and orient a polygon representing this coverage. If the polygon coverages are created in chronological order, then overlaps are addressed by subtracting the overlap area out of the later occurring polygon. GPS information was obtained using two real-time kinematic (RTK) GPS receivers with reported static accuracy of approximately 0.01 m.

While this vector analysis did improve yield map accuracy, the computational complexity as well as the cost of the GPS receivers made this correction routine too expensive to implement. Shearer et al. (2004) used GIS-methods similar to Drummond et al. (1999) requiring lower computational overhead with great success. The specifics of this method are discussed in detail in Chapter Six of this dissertation.

The most radical method of correcting yield monitor data would be the elimination of the data set altogether through the development of a new grain yield measurement technology. Wild et al. (2003) proposed a method to determine crop yield without relying on the measurement of material flow through a grain combine. This proposed method used radar pulses. In the test setup, a metal sheet was placed behind known amounts of chopped maize and oats. The reflected radar signal intensity was recorded after the radar pulse passed through the crop material and bounced off the metal sheet. The results of the test were promising, as the coefficient of determination relating the amount of crop material to the signal strength was between 94 and 99%. The key concern with this technology is the behavior of the radar pulse under high moisture conditions. It is hypothesized that the radar pulse could not penetrate high moisture crop material. Also, the authors note that the crop must pass through a well-defined measurement channel so the reflected radar signals can be captured. There appears to be no plan or recommendation on how this technology can be directly integrated into present agricultural practices. Another issue is that tests were only completed under static laboratory conditions.

Diker et al. (2002) proposed a less invasive method of determining the yield variation within a field through the use of remote sensing methods. Aerial imagines of a field were taken with a multi-spectral digital camera and then these images were analyzed using the red, green, and near-infrared bands. These images were compared to yield maps developed using data collected from traditional mass-flow yield sensors. The actual comparison involved the use of the Shannon-Weiner Diversity Index, which provides a means to compare the diversity or evenness of patterns associated with the yield in an agricultural field. It was hypothesized that both sensing methods would produce similar evenness patterns. Both sensing methods indicated different diversity levels within the field increased at the perimeter of the center pivot irrigation system used in the field. This increased diversity is attributed to speed variations associated with the combine harvesting headlands. If the field borders (i.e. headlands) are excluded both the remote-sensing and the yield monitor produce nearly identical diversity maps. While these

newer alternative yield data collection methods show promise, they cannot be implemented as efficiently as the mass flow sensors on a grain combine.

Based on the information compiled and analyzed in this literature review, a clear course of action has been developed to achieve the objectives of this investigation. From previous research it appears that it is possible to sense mass flow within a grain combine through means other than measuring mass flow with an impact-plate or other sensing device located in the clean grain elevator. At this point, what is not clear is the relationship between material throughput rates closer to the point of crop intake (i.e. in the feeder housing) and the grain mass flow at the top of the clean grain elevator. If such a relationship could be established then it would be possible to create a mass flow correction routine. This review also conveys the difficulty of assessing the true cutting width of the combine in real-time. The expense necessary to employ such a system and the marginal quality of the results simply warrants another alternative for correcting cutting width data. Drummond et al.'s (1999) vector-based post-processing approach is very appealing if the expense of the dual RTK-GPS and the computational requirements can be avoided. With updated GIS-engines it may be possible to improve upon this routine. The data filters and time-shift methodologies discussed will also be considered in this investigation.

Chapter Three

Development and Performance Assessment of a Feeder House-Based Mass Flow Sensing Device

Introduction

Two critical components of a yield monitoring system are the mass flow sensor and GPS receiver used to create yield maps. Spatial inaccuracies arise in a yield map when the incorrect GPS position is linked with a mass flow reading. Typically, these errors occur when the time required for the grain to travel through the combine to the mass flow sensor is different from the time delay. Typically, yield monitors use a fixed value to account for the amount of time required for grain to travel from the harvesting head to the mass flow sensor. For example, if a 12 s delay time is used as a default by a manufacturer, then the latest mass flow measurement is assigned the GPS coordinates that were logged 12 s earlier.

Unfortunately, the time required for the grain stream to travel through the combine is intrinsically unstable and highly variable. This instability is most evident when filling or emptying of the threshing mechanism occurs. To compensate for this discrepancy, it would appear that an attempt to quantify material mass flow into the grain combine ahead of the cylinder or rotor would allow for improved mass flow measurement. By recording mass flow as close to the first instance of machine-crop interaction as possible, the delay time should be more stable, the problem of varying transport delays will be avoided, and the blending of material harvested at different geographical locations is avoided.

Sub-Objectives

Yield monitoring errors could be corrected if the variability of transport delay were reduced. Quantifying material mass flow before the material arrives at the threshing cylinder or rotor may provide an opportunity to record such a measurement with reduced delay time variability. Prior to the cylinder or rotor, material flow is fairly uniform and constrained to a single path; therefore, the transport delay variability should be relatively low. This chapter

discusses the development and evaluation of one of the two alternative mass flow sensing methods developed under the umbrella of this research project. The specific objectives for this portion of this project are:

1) Develop a new feeder housing-based mass flow sensing scheme to quantify crop material mass flow prior to the threshing cylinder or rotor,
2) Develop data filters and processing techniques to enhance sensor signal values for determination of mass flow, and
3) Evaluate this device under both constant and varied mass flow conditions.

Methodology

Feeder House Mass Flow Sensor Development

Through early measurement of crop mass flow, the idea was to minimize the previously mentioned yield distortion effects caused by combine dynamics (i.e. the varying time delays associated with material movement through the separation and threshing mechanisms). A decision was made to measure material flow at the feeder housing which is located at the front of a combine. The feeder housing serves as the point of attachment for a corn head or grain platform. Crop material is cut, gathered, and fed into feeder housing via a cross auger at the back of the header. Within the feeder housing, three parallel chains with bars connected normal to the chains are used to convey crop material. As the chain loops over a drive sprocket, the bars trap the crop and drag the plant material up the feeder housing floor and into the cylinder or rotor for threshing.

There are several sensing techniques that could be used to quantify the material flow through the combine's feeder housing including, radiometric sensing, light reflectance, electrical properties of the crop, and mechanical properties of the machine. Measurement of a mechanical property on the actual grain combine proved to be the simplest and most direct means to measure biomass input to the combine. Radiometric sensing via radioactive isotope presents a variety of issues ranging from personal safety to severe regulatory constraints. Light reflectance and electrical characteristics can be compromised by the plant material properties such as nutrient composition or moisture content.

The chain tension at the feeder housing drive was measured to determine if it was correlated to grain crop input. The rationale for measuring chain tension was based on the belief that increased biomass flows through the feeder housing would result in a proportional increase in the feeder housing conveyor drive chain tension. Also, the chain driving the feeder housing is readily accessible and there is ample space to mount a sensor. An added benefit is that mass flow measurement in the feeder housing would allow for crop throughput to be sensed for all crops as opposed to sensing on the header. If sensing took place on the header there would have to be separate sets of sensors for the different heads. The sacrifice made by not sensing material flow on the header is the introduction of slight delay time variability arising from irregular cross auger feeding.

With selection of one potential sensing parameter, the focus of the project became the development and implementation of the sensing technique. (Chapter Four will present a second mass flow-sensing alternative.) Chain tension sensing could be achieved through the measurement of sprocket displacement if the drive chain was positioned with the proper orientation. The proper chain orientation would simplify the measurement by reducing the degrees of freedom within the system. To reduce the measurement of chain tension to a single degree of freedom, the path of the feeder housing drive chain was modified (Figure 3.1). This modification was accomplished through the addition of three sprockets along the tension side (top) of the feed conveyor drive chain.

The lower two sprockets help stabilize the chain and allow the chain to maintain the same path and orientation that was present prior to the alteration. Both of the lower sprockets are mounted on bearings that allow idler sprockets to rotate about two fixed shafts. The third sprocket was placed 25 cm higher than and centered between the previously added lower sprockets. This causes the chain to follow a new path that is perpendicular to the older path at the point the chain passes around the upper sprocket. The upper sprocket was mounted to a bearing attached to the feeder housing and free to rotate about a shaft fixed to cantilever beam springs. With this chain configuration, an increase in the tension on the feed conveyor drive chain would lead to a downward displacement of the upper sprocket. The displacement of the upper sprocket is proportional to the chain tension.

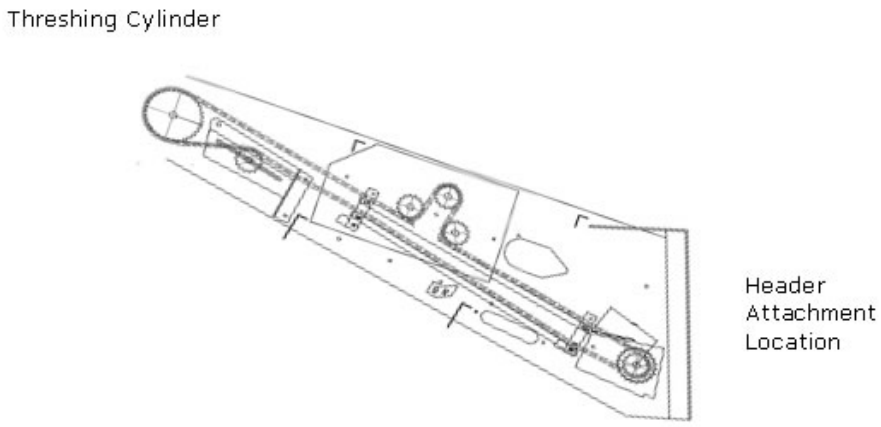

Figure 3.1. The modified feed conveyor drive chain configuration.

The final component needed to sense material flow through the feeder housing is a device to measure the deflection of the upper sprocket. Measurement of displacement was achieved with the use of a thin-film potentiometer in combination with a cantilever load cell (Figure 3.2). The cantilever mechanism was composed of two brackets interconnected by spring steel. The base support of the mechanism is rigidly attached to the feeder housing and its movement is completely constrained. The second half of the mechanism is supported by cantilever beam springs that are attached to the base support. The second support, containing the sprocket, is allowed to move vertically. As the sprocket moves with variations in the feed conveyor drive chain tension, the motion is reflected by the output of the potentiometer.

Displacement measurement is based on the relative movement of the two brackets. The spring steel used to connect the two halves serves two functions in the operation of this sensor. The first is the spring steel allows the sprocket mount to return to a neutral or zero displacement state once the tension is removed from the chain. Secondly, the steel spring facilitates sensitivity adjustment in accordance with the dimensions or type of material used to manufacture the cantilever springs. Based on estimated biomass loads, it is possible to add or subtract a layer of spring steel to change the stiffness of the cantilever beam. This stiffness adjustment would affect the range of motion and sensitivity of this system to fluctuations in material intake. Finally, a stop was added to halt displacement if the sprocket traveled beyond 2 cm. This proved to be a necessary addition in the event that the feeder housing plugged and had to be reversed to clear the obstruction. This event can create a large shock load which could cause the chain tension sensor to fail.

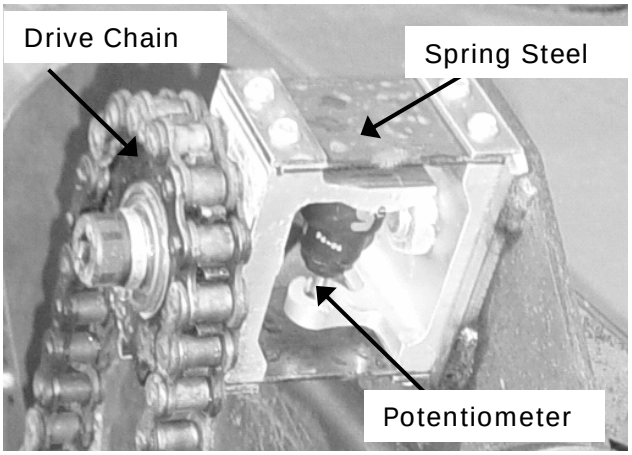

Figure 3.2. Cantilever load cell and potentiometer used to sense variations in feed conveyor drive chain tension.

The sensor selected to measure the displacement between the two brackets of the mechanism was a BEI Duncan thin-film linear potentiometer (http://www.beiduncan.com). This particular sensor was a proprietary part manufactured specifically for John Deere and previously served as the load-sensing device in older series Greenstar yield monitoring systems. This sensor was also used to sense the position of throttle and brake pedals in the operator's compartment. Potentiometers produce a variable resistance that is proportional to the wiper arm position on a resistive surface. As the plunger is depressed, the position of the wiper arm on the resistive surface changes and a voltage drop is produced by the sensor. The potentiometer must be powered from an external source (5 V for this study). At zero displacement the potentiometer output was 2.40 V, and at full displacement (20 mm) the sensor output was 5 V.

The output from the sensor was logged using a USB-based data acquisition card developed by Measurement Computing (www.measurementcomputing.com) that is capable of logging data at rates up to 1200 samples per second and is equipped with a 12 bit analog-to-digital converter. This data acquisition board was also used to provide power to the thin-film potentiometer. In addition to logging values from the sensor, differentially corrected GPS (DGPS) positioning information was also recorded. A Trimble AgGPS 132 GPS receiver was configured to output the NMEA GGA string at a rate of 10 Hz and receive a correction signal from a U.S. Coast Guard beacon located at Taylorsville Reservoir in Central Kentucky. To log the data, a Microsoft Visual Basic program (Figure 3.3) was written, compiled, and placed on a

laptop computer. The program logged two data files: a raw data file and an averaged data file. Both of the data files were stored as comma-delimited ASCII text files. The raw data file was composed of streaming data collected from the USB data logger and a time stamp from the GPS receiver. On average, approximately 400 samples per second were recorded using this method. The average data file contained data at 10 Hz. The data stored included the full GPS NMEA GGA positioning string and the averaged value for the sensor. Typically, between 30 and 40 sensor readings were averaged for each GPS position captured. A mechanical contact switch was placed on the feeder housing to detect when the header was raised, indicating the combine was not engaged in harvesting. Based on the status of this contact switch the data logging would stop when the header was raised.

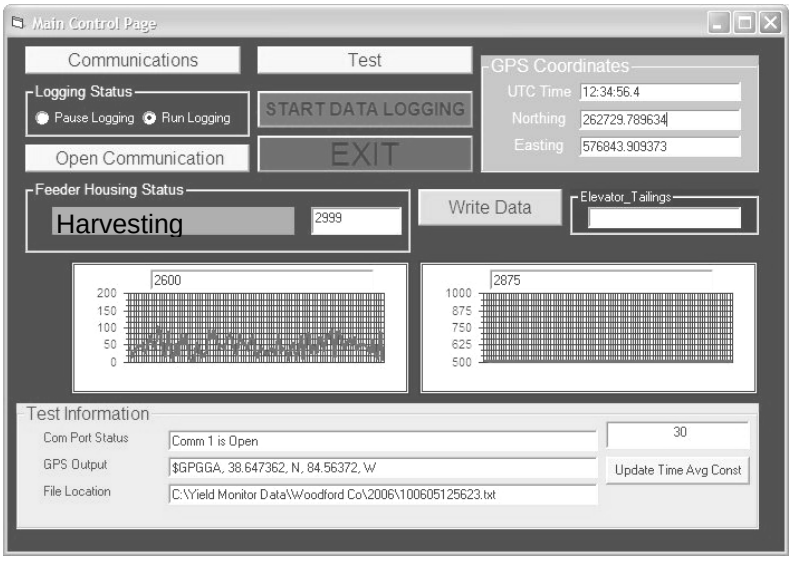

Figure 3.3. Screen shot from data acquisition program developed in Microsoft Visual Basic.

A John Deere model 9500 conventional (straw walker equipped) combine equipped with either an eight-row corn head or a 7.8 meter small grain platform was used to harvest grain crops in this study. The corn head employed in this study was equipped with hydraulically adjusted stripping plates. The combine was also equipped with a John Deere Greenstar yield monitoring system for the 2003 harvest season. For the 2004 and 2005 harvest seasons, an Ag Leader YM 2000 yield monitoring system was utilized. Each of these systems use force impetus-based sensing at the top of the clean grain elevator to sense grain mass flow. The major difference in the two systems can be found in the filtering and calibration algorithms that each employ. The

John Deere system uses a two point calibration to define a linear relationship between the mass flow sensor reading and the harvest yield. The two data points are taken at extreme low and high mass flow values. Typically, these extreme values are obtained by varying the combine's ground speed to achieve the desired effect. The Ag Leader system is a multi-point system that allows comparison for non-linear relationships between sensor output and grain yield. The two yield monitoring systems were used to establish trends that may be found in current yield monitoring technology and not as a means to conduct a performance-based comparison between the two units.

For all crop systems, the yield monitors were calibrated throughout the season to ensure accurate measurement of yield values. Also, scale weights of all loads were obtained so further correction methods could be pursued. The Greenstar yield and YM 2000 data were logged to PCMCIA cards located in the yield monitor's task computer. Data logging occurred at a rate of 1 Hz. The delay time (time from grain entering combine until the mass flow measurement is recorded at the top of the clean grain elevator) for both systems was set to 12 s. Data logging activities involving the chain tension sensor and traditional mass flow system were completed simultaneously. The data from the traditional yield monitor and the mass-flow sensing devices created for this dissertation were time registered via the GPS NMEA string. By time-stamping the two data sets it was possible to align these data sets in future analyses.

Field Evaluation

To evaluate both sensor repeatability and sensitivity, a testing program was developed to assess the value of the sensor as a means of measuring plant material throughput in a grain combine. The development and testing of this sensor occurred over a period spanning from the fall of 2003 to the fall of 2005, covering five crop harvests in central Kentucky. All three major grain crops grown in Kentucky (corn, soybeans, and wheat) were harvested during field evaluations. Testing took place at cooperator farms in Shelby County, Kentucky (38^{o} 19' 14" N; 85^{o} 14' 14" W), Hardin County, Kentucky (37^{o} 42' 27" N; 85^{o} 51' 43" W), and at the University of Kentucky's Animal Research Center in Woodford County (38^{o} 03' 07" N; 84^{o} 43' 33" W). Based on visual inspection of each field, the tests were set up in areas with relatively

uniform plant stand, size, and yield. The test blocks were located in the center portion of the field, sufficiently far away from headland rows, weedy areas, and lodged crops.

While test blocks were set up to study the effects of a variety of mass flow conditions, there was a supporting investigation performed in conjunction with the mass flow tests. This additional examination was carried out to quantify the amount of material that was being fed into the machine. Grain crop biomass exiting the rear of the machine was captured on two 6-m-wide by 31-m-long sheets of plastic that were unrolled from the rear axle of the combine as it moved across the field (Figure 3.4). The material from these sheets was weighed so that a MOG weight per unit area could be determined. Separate sheets of plastic were used to collect the material passing over the straw-walker versus material from the cleaning shoe (chaffer). A number of parameters were recorded such as the composition of the MOG exiting the combine and the MOG moisture content. The test condition where mass flow was quantified is designated MF in most figures and tables.

Figure 3.4. Obtaining Material Other than Grain (MOG) samples during the 2005 summer wheat harvest to determine the volume of material fed through the combine.

To test the performance of the sensors, a variety of evaluation plots were established within corn, soybean, and wheat fields across the state of Kentucky. Detailed sketches of the test plots will be shown in the following section. A typical field experiment was set up so a variety of different tests could be completed in the same field. Figure 3.5 illustrates how a 10 ha cornfield was divided to study sensor sensitivity to varying biomass feed rates. Some of the first tests involved the layout of six, 150-m-long straight passes (Figure 3.5). These passes were

divided into two replicates of three passes. Each pass was set up to determine the effects of allowing varying levels of biomass to pass through the feeder housing. Varying the spacing between the hydraulically actuated stripping plates on a corn head changed the amount of biomass passing through the combine. Wider settings only allow the ear to be snapped from the corn plant and much of the biomass is pulled through the stripping plates, ending up on the ground. As the stripping plate clearance is narrowed, an increased amount of material is stripped from the plant along with the ear, thereby increasing the mass flow rate through the feeder housing. The three stripper plate widths investigated were 2.5, 3.2, and 3.8 cm. The combine travel speed was fixed at 4.0 km/h for all corn tests. The straw chopper and chaff spreader were disconnected during this portion of the experiment so the amount of biomass feed through the combine could be collected and measured.

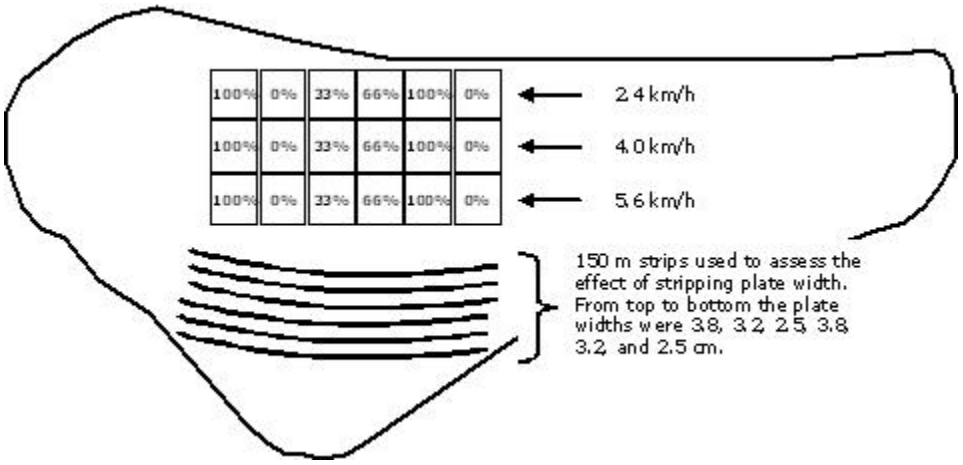

Figure 3.5. Field test schematic with 3 sets of X579 blocks and the stripping plate width test strips laid out at the bottom used in the initial field tests.

To vary the amount of biomass fed through the combine in solid sown crops, primarily wheat, the height of the cutter bar was changed. Three cutter bar heights were used to determine the sensor's ability to sense biomass feed rate variations during a wheat harvest. The highest cutter bar height was 35 cm. At this cutting height only the wheat head is cut and fed through the combine. Next, the cutting platform was lowered to 20 cm, which allows the head and some stem material to be cut and fed into the harvester. At the lowest cutting height, 5 cm, nearly the entire plant is cut and fed into the combine. The combine harvested these plots at a fixed speed

of 6.5 km/h for all wheat tests. The material was collected on the plastic sheets as it exited the combine in a method consistent with what was described in the preceding paragraphs.

The next field test was designed to study combine speed effects and evaluate the response of the sensor to changing amounts of grain and biomass input. This field evaluation was based on a draft version of ASABE Standard X579: Field Evaluation of Yield Monitors. For this test, six contiguous blocks, 27 m in length, were laid out in a single pass located in an area of uniform plant stand and size (Fig. 3.6). To simulate unique yields within each block, a portion of the plants were removed in a pre-harvest operation. Plant removal resulted in residual simulated yields of 100%, 0%, 33%, 67%, 0%, and 100% (these percentages represent the portion of the total grain volume present in the block). Because the combine was equipped with an eight-row corn head, it was impractical to remove 33% and 67% of the established corn in blocks 3 and 4. For the prescribed 33% block, 5 rows were removed with 3 rows or 37.5% of the remaining corn harvested. For the prescribed 67% block, 3 rows were removed and 5 rows or 62.5% of the corn was harvested. A cartoon of a John Deere 9500 grain combine harvesting a ASABE X579 plot is shown below (Figure 3.7). Tests conducted under the X579 draft standard are designated X579 in most figures and tables. The relevant parts of the standard are presented in Appendix A.

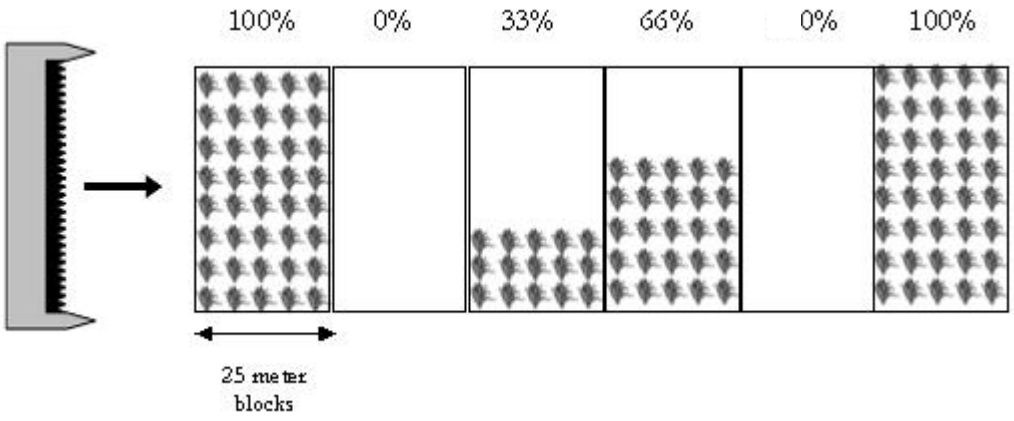

Figure 3.6. Schematic of the ASABE X579 Field Evaluation test plot.

Figure 3.7. John Deere 9500 combine harvesting the ASABE X579 Plot.

The next test plot was the interval plot, which was created by selectively cutting strips of grain crop out of the plot prior to the test. The pre-harvest strips were cut perpendicular to the combine's direction of travel during the actual harvest evaluation (Fig. 3.8). The pre-harvest strips varied in width, increasing from 1 header width to 4 header widths in increments of 1 header width. A header width was 7.62 m. Between the blocks of removed crops, a strip of crops was left with a width equal to the width of the adjoining strip of removed plant material. When the combine passed through the plot for the evaluation harvest, the machine passed through a 7.62-m-wide strip with crops, a 7.62-m-wide strip with no crops, a 15.24-m-wide strip of crops, a 15.24-m-wide strip of no crops, a 22.86-m-wide strip of crops, a 22.86-m-wide strip with no crops, etc. When the combine was passing through the strips with standing plant material present, a full header swath was cut. The sensitivity of the each mass flow sensing method could be evaluated by examining how well either sensor was able to define the border between the strips of standing crops and the strips with no crops. This is a critical test to evaluate system response to abrupt yield variations. Field evaluations conducted using the interval plots are designated IT in most figures and tables.

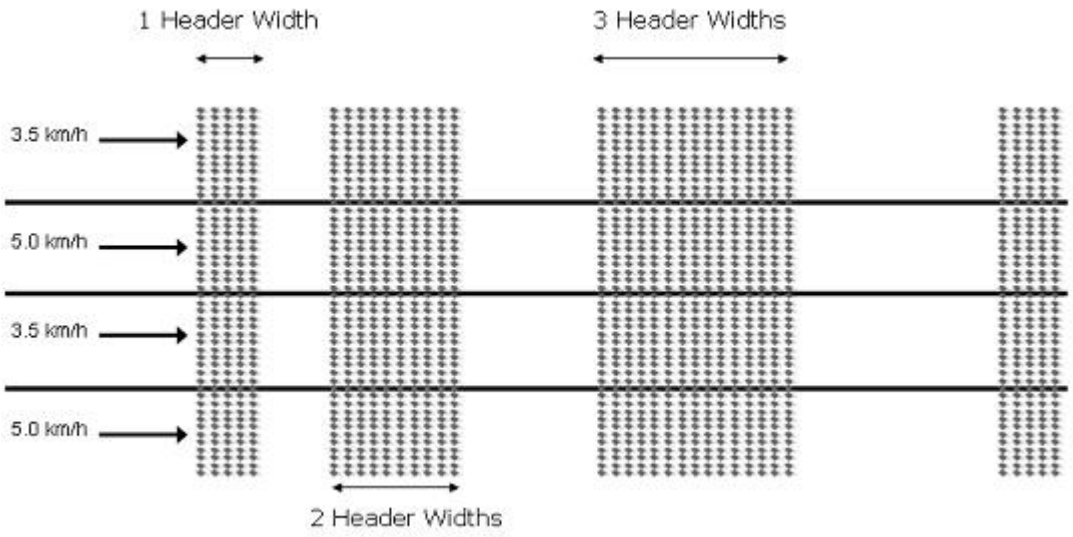

Figure 3.8. Schematic of the interval plots to test abrupt changes in crop intake.

A ramp flow test was also created (Fig 3.9). This plot was created by cutting triangles in the field during a pre-harvest operation. The triangle varied in length based on crop type, 61 m for wheat and 122 m for corn. These triangles were set up such that the combine would increase the intake of material from no grain entering the machine at the start to a full header width of material entering the machine at the mid-point of the triangular plot. As the combine traveled from the mid-point to the end of the plot the intake of material would decrease until it was again zero. This test was designed to evaluate the sensitivity of each sensor to a constant change in material flow. The ramp flow test was slightly modified for corn, as a diamond shape was laid out in the field (Figure 3.10). Every 20 m two additional rows were added to the crop intake so that the combine fed 2 rows of corn, then 4, then 6, then 8, then back to 6, then 4, etc. The final test conducted in this investigation was the full field test. For full field tests the combine conducted harvest operations in a method consistent with those used by crop producers. Data were recorded for both the force impetus mass flow device as well as for the two sensing technologies under investigation. Ramp flow and full field evaluations are designated as RF and FF in most tables and figures. Table 3.1 provides a summary of the cropping systems evaluated in this dissertation as well as the test plots utilized for each system.

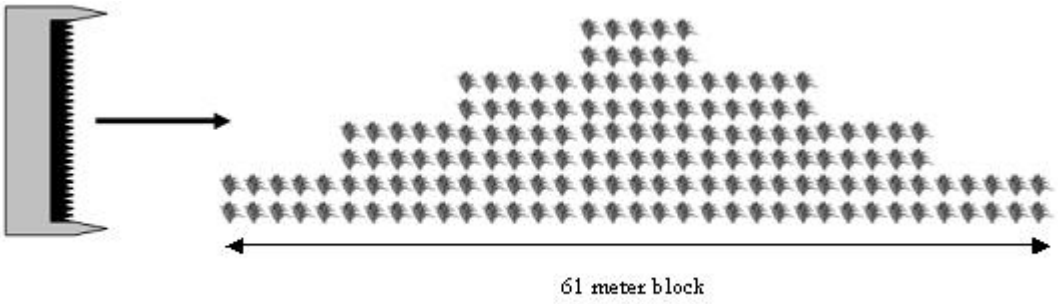

Figure 3.9. Schematic of the ramp flow plot for solid sown crops.

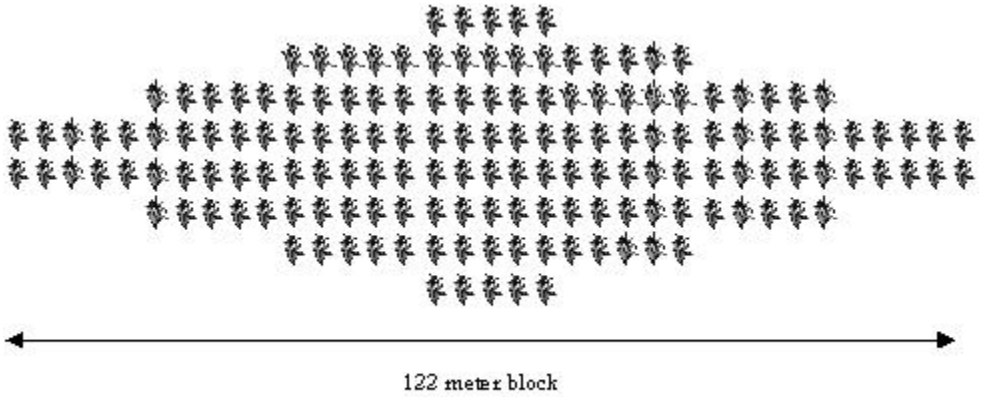

Figure 3.10. Schematic of the ramp flow plot for corn.

For each of the field plots, replicates were created within the field. The number of replicates was not uniform for every field test because the test protocol varied in accordance with yield variability and space constraints. The study involving biomass collection also affected the harvest test scheme to some degree. However, replication was used to provide a basis for statistical analysis as well as study the interaction of various machine parameters. Typically, replicates were used to study machine speed effects, stripping plate settings, and crop cutting height. The three speeds chosen for this investigation were 2.4 km/h, 4.0 km/h, and 5.6 km/h. These velocities are common harvest ground speeds. The stripping plates were set at the 3.2 cm width for all harvest activities independent of stripping plate adjustment effects. In soybeans, the small grain platform was adjusted to a float mode so the cutter-bar on the grain platform skims the soil/ground surface. Appendix B has a table listing the exact specifications for each field evaluation test.

Table 3.1. Summary of Field Tests Completed.

Harvest Period	Crop	Acreage ha (ac.)	Yield Monitor	Dissertation Sensors Used[1]	Test Completed[2]
Fall 2003	Corn	10 (25)	John Deere	FH	X579; SS; MF
Fall 2004	Corn	10 (25)	John Deere	FH & HPT	MF
	Corn	100 (247)	AgLeader	FH & HPT	X579; RF; IT; FF; MF
	Soybeans	26 (65)	AgLeader	FH & HPT	FF
Summer 2005	Wheat	47 (115)	AgLeader	FH & HPT	X579; RF; IT; FF; MF
Fall 2005	Corn	37 (90)	AgLeader	FH & HPT	FF
Summer 2006	Wheat	20 (50)	AgLeader	FH & HPT	FF

[1] FH = Feeder Housing Chain Tension Sensor; HPT = Hydraulic Pressure on Threshing Cylinder

[2] X579 = ASABE X579 Field Evaluation, RF = Ramp Flow, IT = Intervals, FF = Full Field, SS = Stripping Plate, MF = Mass Flow Calibration

Mass Flow Data Analysis

Following data collection, signal filtering was necessary to improve clarity and measurement precision for the chain tension sensor data. Filtering is commonly employed in the processing of raw data from a yield monitor, because the raw signal contains considerable noise. Matlab (The Mathworks, Natick, MA) provides a variety of toolboxes for time series analyses. For this application, Matlab was used to implement a discrete Fourier transformation (DFT) of the sensor data to determine the signal frequencies of interest. Also, the Fourier analysis can be used to identify sources of noise and then corresponding filters can be created to eliminate specific frequencies. Most likely the frequencies of interest will occur at the lower end of the frequency range. Therefore, a low pass filter was used to eliminate noise associated with the use of these sensors. Based on previous research there will be a high frequency noise component attributed to machine vibration and the motion of the paddles within the feeder house.

A solution for the proper delay time model was also studied to insure correct alignment of the sensor data with GPS coordinates. This alignment will be critical when comparisons between traditional mass flow and the new sensor data are made. Also, this delay time would

facilitate a systematic approach to mass flow correction using data from all available sensors. It appears that a simple time delay will work because of the direct path that the crop material follows from the header to the sensing location on the combine. However, first and second-order system models will also be investigated for comparative purposes. Delay time model development will be based on the sensor response as the combine begins harvest (i.e. goes from a zero mass flow state to a crop harvesting state).

Results and Discussion

Signal Conditioning

These initial signal conditioning investigations were conducted on a limited number of data files that were logged at 1000 Hz. To achieve this data logging rate, no other parameters were logged beyond the output of the Analog-to-Digital conversions completed by the USB data acquisition device. This is the only section of Chapter 3 that is concerned with the 1000 Hz data logging rate; the remainder of the chapter utilizes the 400 Hz signal which was logged with GPS and time stamp coordinates. After feeder house sensor data were collected for all three crops tested in this investigation and an unloaded combine condition, a Matlab program (Appendix C) was created to determine the frequency component of the signal. A 512-point fast Fourier transform (FFT) was utilized in the signal analysis along with the ability to clip portions of the signal that did not represent standard operating conditions. The DC component was removed from the Fourier analysis by subtracting the signal mean from each individual reading prior to analysis. Figures 3.11 through 3.14 (shown below) illustrate the common feeder house sensor output while harvesting corn, soybeans, wheat, and the zero mass flow condition. The corresponding frequency magnitude resulting from the Fourier analysis is also shown. There are occasional spikes and depressions that are indicative of feed irregularities or rocks passing through the combine.

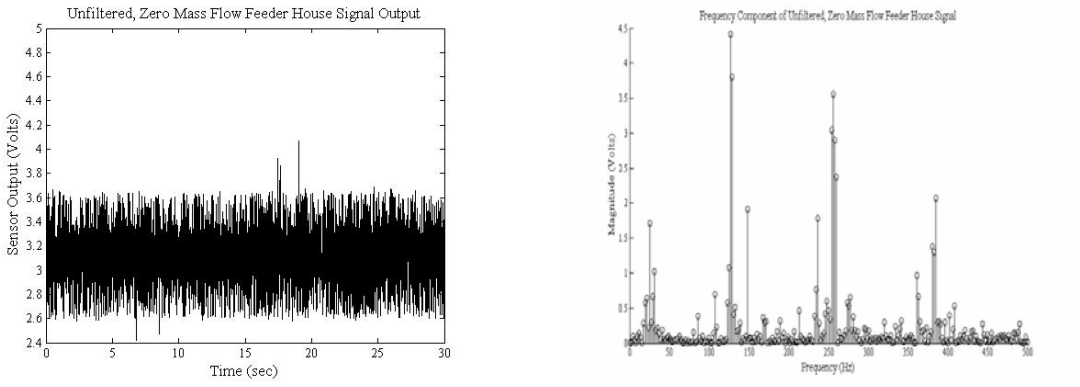

Figure 3.11. The raw feeder house sensor output and frequency content under unloaded conditions.

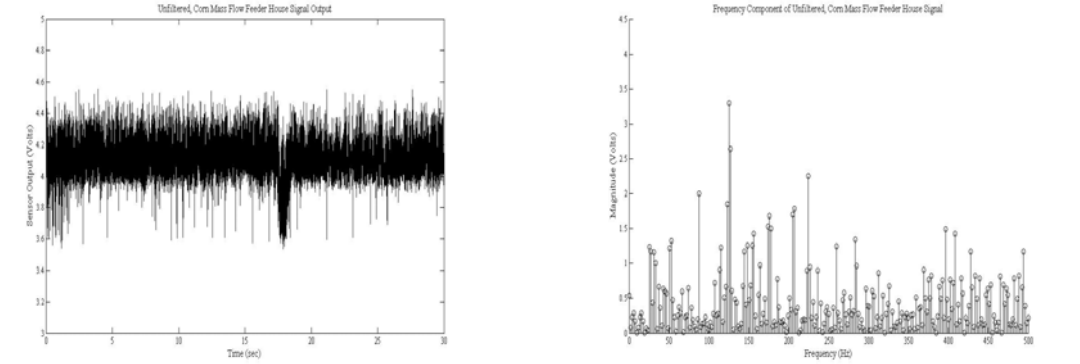

Figure 3.12. The raw feeder house sensor output and frequency content under corn harvest conditions.

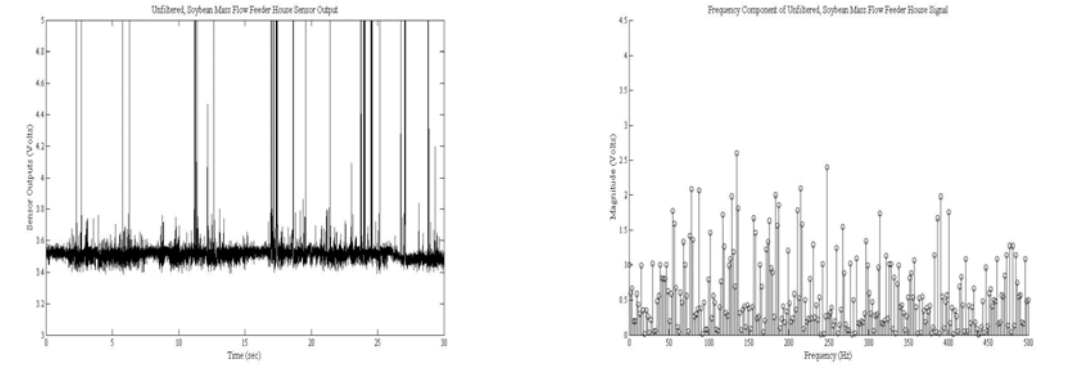

Figure 3.13. The raw feeder house sensor output and frequency content under soybean harvest conditions.

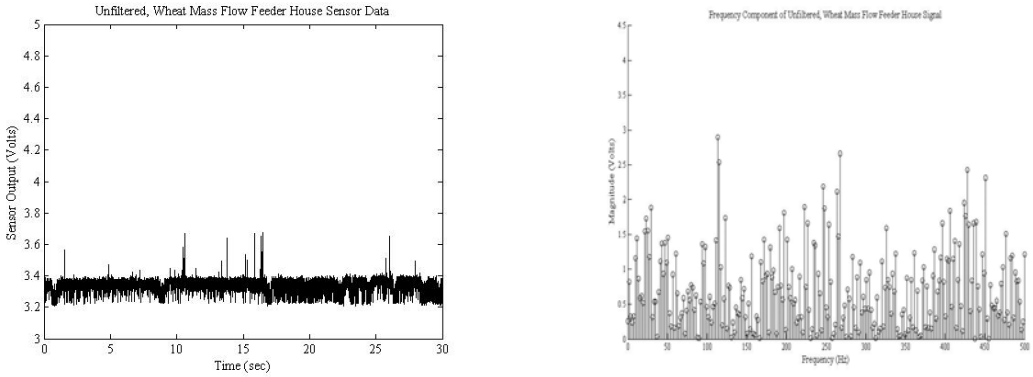

Figure 3.14. The raw feeder house sensor output and frequency content under wheat harvest conditions.

Through observation of the preceding figures, there are a number of features of this sensing method that are clear. A comparison between the mean values for the four signals plotted in the time domain above shows the promise of this sensing method. Under no load, the displacement sensor has a mean output of 3.08 V. For corn, soybeans, and wheat the mean sensor outputs were 4.11 V, 3.56 V, and 3.30 V, respectively. These voltage levels appear to correspond to the amount of biomass that would be expected to pass through the combine during harvest. Based on data collected in this investigation (discussed in upcoming sections), corn is associated with the greatest amount of biomass passing through the combine and has the highest voltage output. The soybeans and wheat would have similar biomass levels, with soybeans producing slightly more biomass.

Another observation is clipping of the soybean signal. The sensor achieves its maximum value of 5V on several occasions, indicating the maximum allowable sensor displacement has occurred. This characteristic is the result of problems encountered while using a particular crop header during the harvest of this field of beans. The small-grain platform used in this test and the logic that would allow it to function as a true floating platform is not compatible with the logic Deere & Co. uses to adjust the harvest position of their floating cutter-bars. Therefore, in the field trials this small-grain platform was subject to soil and trash build up on the harvesting head. This soil build-up led to crop clumping prior to feeding into the combine. Also, this was a double-crop bean harvest, meaning there were inherent feeding issues due to the short crop height. Essentially, the bean biomass was low enough that large slugs built up on the cutter-bar

before being fed into the feeder housing by the cross auger. Each spike is a slug of beans getting pulled into the feeder house.

Within the frequency plots, the spikes are indicative of a periodic component to the signal. This is not unexpected given the nature of the combine with a number of rotating parts and moving chains. One point of interest is the extreme magnitude of the frequency at approximately 120 Hz. This frequency correlates to the rotation of the sprocket whose displacement is being measured by the thin-film potentiometer. This 15-tooth sprocket turns at approximately 475 rpm thereby generating a vibration of 118.75 Hz. This nearly 120 Hz periodic component is evident in all four of the figures. Also, the corresponding harmonics can be seen at $2f$ (approximately 240 Hz) and $3f$ (roughly 360 Hz). The periodic components do shift slightly under crop harvest conditions (most likely attributed to damping properties of the biomass flow), so the next goal in this project was to develop an appropriate filter to remove as much of these periodic effects as possible.

To accomplish the filtering task, it was decided that a finite-duration impulse response (FIR) filter would be used. The FIR filter is a type of digital filter that is valued because of its linear-phase response. The filter will induce an additional signal. However, this delay is constant for all frequencies and the filter does not cause phase distortion. Another benefit of the FIR filter is that feedback in the filtering routine is not required, therefore mathematical anomalies (such as rounding errors) are not carried through the filtering process. FIR filters are generally more computationally efficient and have better defined transitions between the stop and pass bands with less rippling than their analog counterparts.

The FIR filter functions (IEEE Press, 1979) by multiplying the most recent N data samples by an array of constant values, known as tap coefficients. As the filter indexes to the next sample, the oldest data is thrown out.

The output of this filter in the time domain can be described using:

$$y(t) = \sum_{k=0}^{N} h[k] * x\left(t - \frac{k}{f_s}\right) \qquad \textbf{Equation 3.1}$$

where:

y(t)	=	filtered output signal
x(t)	=	raw input signal
t	=	time
f_s	=	sampling frequency
h[k]	=	tap coefficients
k	=	tap index
N	=	maximum tap value

The variable of greatest concern in Equation 3.1 is the tap coefficient, h[k], which is equivalent to the Fourier series coefficients that arise when describing the preceding equation in the frequency domain. The frequency domain equation corresponding to Equation 3.1 is:

$$Y(f) = H(f)X(f) \qquad \textbf{Equation 3.2}$$

H(*f*) in Equation 3.2 is generally referred to as the transfer function or the filter's frequency response. The desired frequency response is typically selected based on the parameters required in the filter design, such as filter type (i.e. low-pass or high-pass) and transition frequencies. Equation 3.3 shows the frequency response of a typical FIR filter.

$$H(f) = \sum_{k=0}^{N} h[k] e^{-j2\pi \frac{kf}{f_s}} \qquad \textbf{Equation 3.3}$$

Through examination of Equation 3.3, it is apparent the tap coefficients, h[k], are simply the Fourier coefficients associated with the frequency response. These coefficients can be determined by multiplying Equation 3.3 by $e^{j2\pi(kf/fs)}$ and integrating (Equation 3.4).

$$h[k] = \frac{1}{f_s} \int_0^{f_s} H(f) e^{j2\pi \frac{kf}{f_s}} df \qquad \textbf{Equation 3.4}$$

To improve the filter's performance, a window function w[k], is often used to scale down the effect of the tap coefficients at higher frequencies. This reduces ripple effects in the filter's stop

band. The window tap coefficients are calculated by multiplying the tap coefficients, h[k], by window scale coefficients, w[k] (Equation 3.5).

$$h_w[k] = h[k] * w[k] \qquad \textbf{Equation 3.5}$$

A Hamming window was used in conjunction with the filter developed for this investigation. The window scale factors for a Hamming window are given by Equation 3.6.

$$w[k] = 0.54 + 0.46\cos\left(2\pi \frac{k}{N-1}\right) \qquad \textbf{Equation 3.6}$$

As previously mentioned, a delay time is introduced when a FIR filter is used to process a particular signal. The theoretical delay time is a function of the sampling frequency (F_s) and the order of the filter (N). The corresponding equation is:

$$DelayTime = \frac{N-1}{2 * F_S} \qquad \textbf{Equation 3.7}$$

For a 1 kHz sampled signal the corresponding delay time is 0.0635 seconds; and at 400 Hz, the delay time increases to 0.15 seconds.

The FIR filter can be implemented within Matlab, and the ability to use this type of filter on a digital signal processing (DSP) microcontroller cannot be overlooked. Because the goal was to eliminate the periodic components, a low-pass filter was developed. Only the parts of the signal occurring at a frequency less than a given cutoff filter would be considered after the signal was filtered. The cutoff frequency used in this filter is 1 Hz, which corresponds to a relative frequency of 1/400 or 0.0025 (or 0.001 for the signal recorded at 1000 Hz). The Matlab code required to implement this filter is provided in Appendix C. The filtering code was added to the bottom of the same program used to establish the frequency components of the data. The frequency response and unit-step response (i.e. the tap coefficients) for the FIR filter are shown below in Figure 3.15.

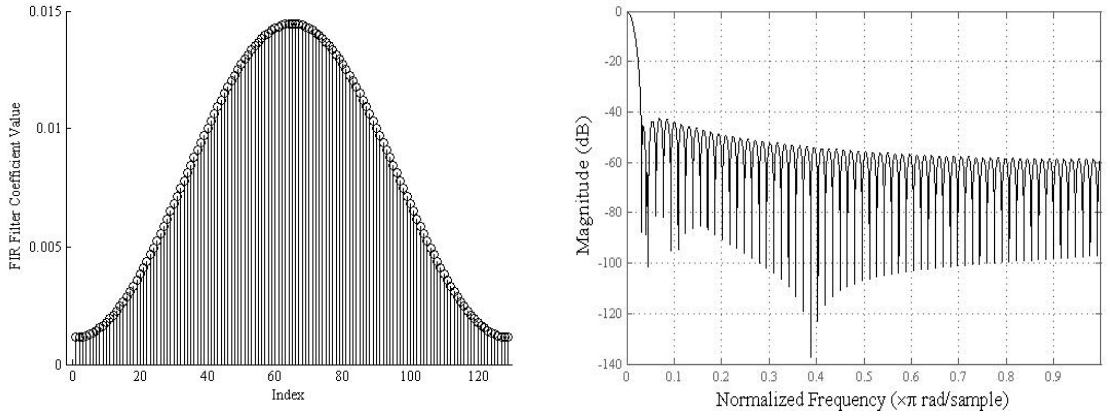

Figure 3.15. The unit-sample response of the 128-tap Hamming filter (left) and the frequency response (right). This represents a low-pass filter having a cutoff frequency of about 0.001 Hz.

To illustrate the usefulness of this filter, the original signal and the filtered signal for the four test conditions are shown next. The unloaded and soybean signals are the same ones shown in Figures 3.11 and 3.13. An ASABE X579 test plot signal for corn and wheat are shown to illustrate the utility of the FIR filter when operating under significant variations in crop material mass flow. Figures 3.16 through 3.19 all indicate that the filtering method employed on these data is acceptable, and improves both the clarity and usefulness of the data. Under a zero mass flow condition, the filtered line is near constant at 3.18 V, with a relatively low standard deviation of 0.17 Volts. In the soybean data there is an improvement as the effect of the spikes in the data are dramatically reduced. Finally, in the wheat and corn data the true mass flow trends that arises as the combine passes through grain blocks of varying biomass volumes becomes readily apparent.

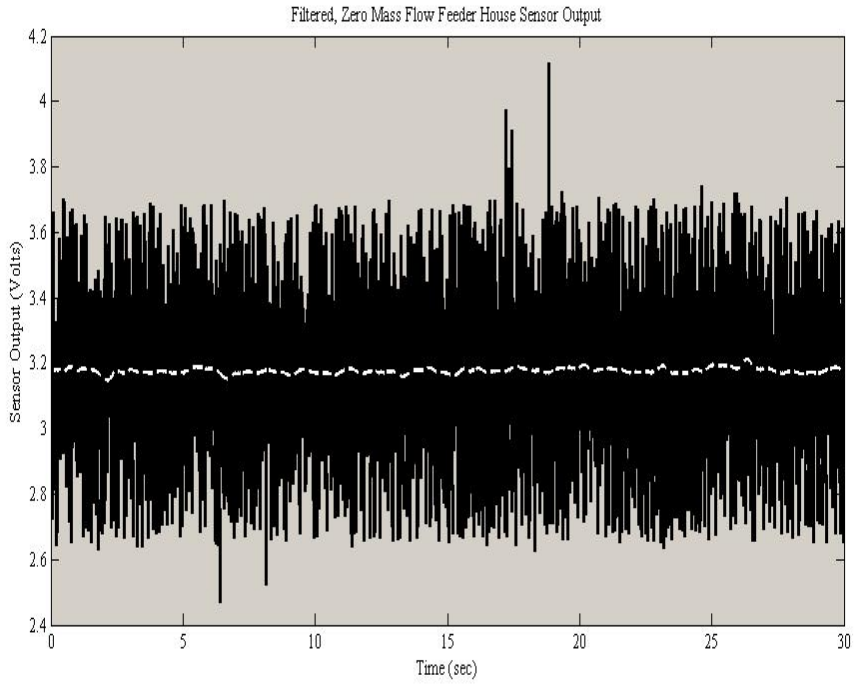

Figure 3.16. Filtered feeder house sensor output under zero mass flow conditions.

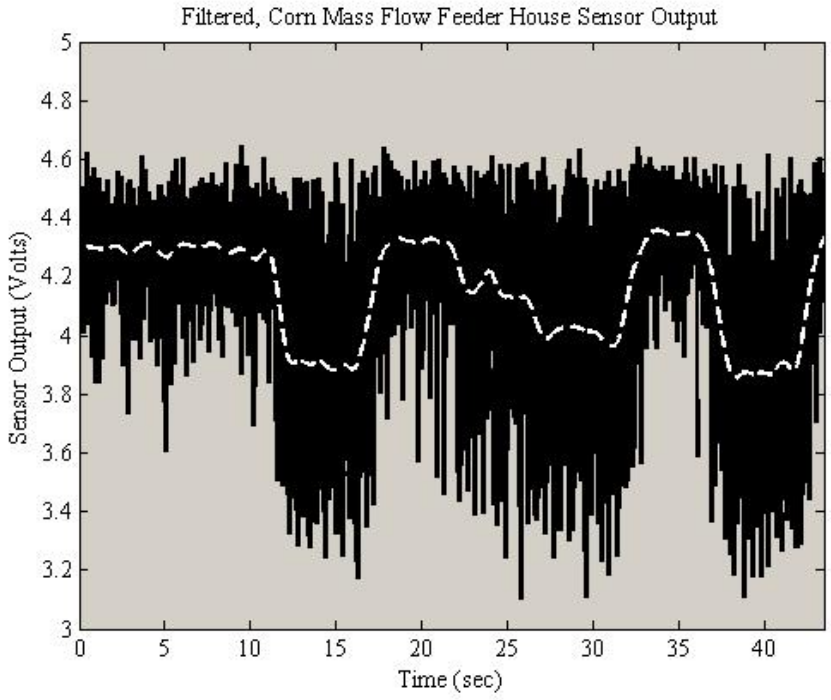

Figure 3.17. Filtered feeder house sensor output under ASABE X579 corn mass flow conditions.

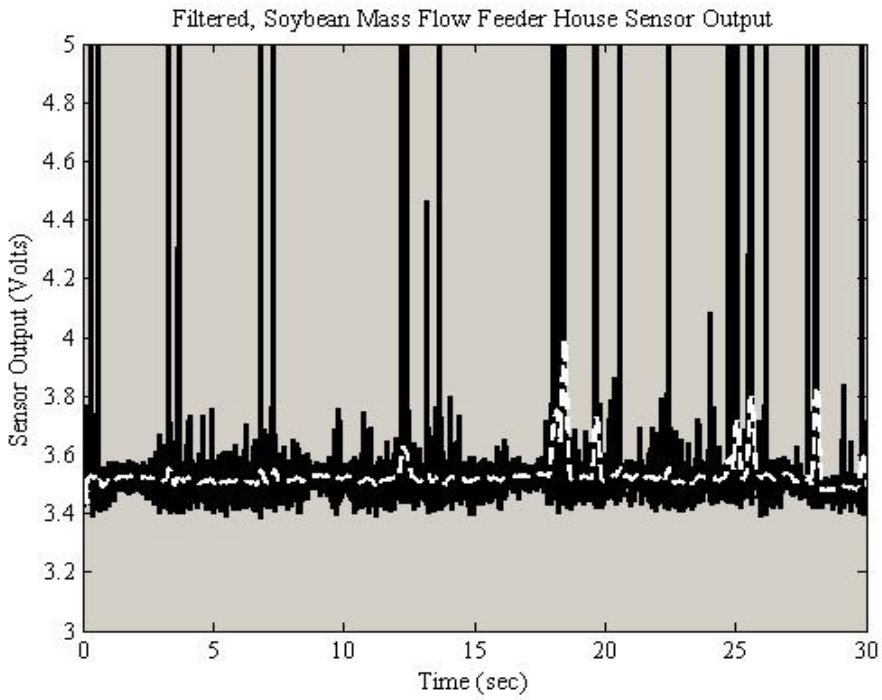

Figure 3.18. Filtered feeder house sensor output under soybean mass flow conditions.

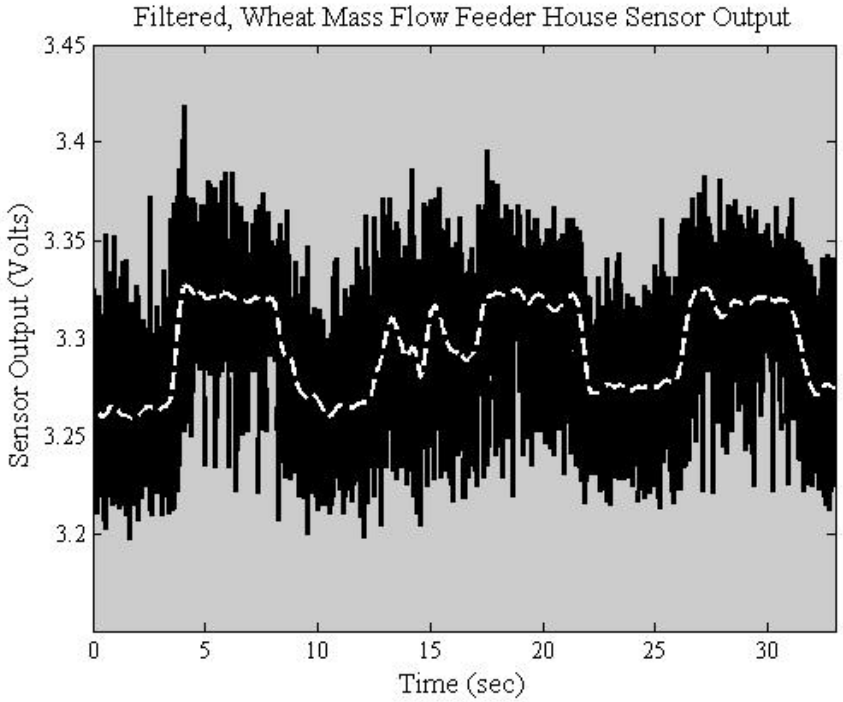

Figure 3.19. Filtered feeder house sensor output under ASABE X579 wheat mass flow conditions.

Signal Delay Time

The successful calculation of the appropriate delay time for the feeder house signal is critical. The delay time determines which set of geographic coordinates to associate with a sensor reading. Once set, it allows for the comparison of feeder house data to yield monitor data. To determine delay time, the raw sensor data were carefully studied at field locations where the feeder housing was empty and the harvesting head was beginning to interact with a grain crop. Typically, this was at the start of the pass, when the feeder housing was initially lowered to trigger data collection and engage the harvesting head with the crop. Similarly, data at the end of the passes were also studied, to determine if delay time was variable when the feeder housing was emptying (i.e. no crop material entering, only exiting). Determination of delay time variations due to combine velocity changes was also completed.

In general, the mass flow at a transitional state took the form of an "S"-shaped curve, which is best described mathematically using a sigmoidal function (Equation 3.8). Sigma Plot 9.0 (Sigma Plot, 2004) was used to determine the best fit parameters for the sigmoidal function used to describe the filling and emptying of the feeder house.

$$\hat{y} = y_O + \frac{a}{1 + e^{\left(\frac{x_o - x}{b}\right)}} \quad \textbf{Equation 3.8}$$

where: $\hat{y}$ = predicted mass flow
y_o = minimum flow rate (filling) or maximum flow rate (emptying)
a = range of mass flows
b and x_o = fit parameters based on range of *x*

The primary reason for utilizing the sigmoidal function was to provide a means to mathematically define the delay time. Using the values associated with the asymptotic tails, it was possible to determine the time required for the mass flow change to register with the sensor. Typically, the value equal to 5% of the maximum tail was used to indicate the feeder house was filling with crop material. This threshold was used just to avoid any noise associated with any residual material clearing the feeder house on initial start up. A sensor output level equivalent to 95% of the asymptotic tail indicated the achievement of steady state mass flow. Figure 3.20 provides a graphical example of this process. Typically, the four parameter (y_o, x_o, a, and b)

sigmodial function could be fitted to the data with relative success. The correlation coefficient, R^2, value resulting from these fits ranges from 0.63 to 0.92.

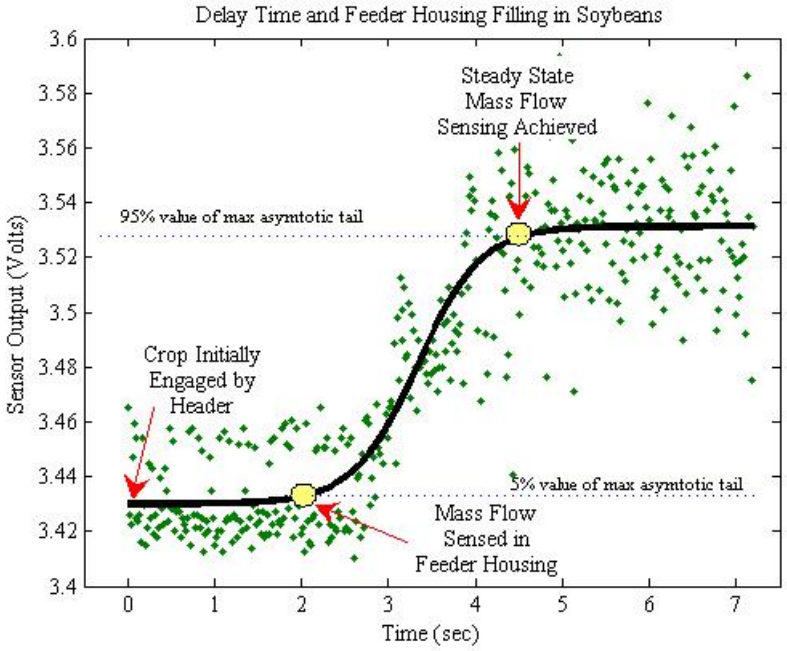

Figure 3.20. Illustrating the role of a sigmoidal function in determining delay time for the feeder house-based sensor.

From the figure, there is a two second delay that occurs from the point that the combine began harvest and the point where the mass flow was first observed by the feeder house sensor. There is an additional 2 s delay that occurs while the feeder house fills. Therefore, in this example there is a 4.5 s delay that occurs between the harvester entering the plot and the sensor output reflecting this level of biomass throughput.

Not shown in the above figure is the behavior of the filtered signal. From the earlier section discussing the filtering algorithm, it was shown that the theoretical delay time induced by the filter could be determined. At a sampling rate of 400 Hz, using a 128-tap filter, a 0.16 s delay time will result. The actual additional delay time that resulted from the filtering routine typically ranged between 0.12 and 0.28 s. The final factor to consider in the discussion of delay time is combine velocity. As the combine velocity increased the overall delay time remained relatively constant. Typically, the same 2-s lag was seen at the beginning of all of the data sets. The main difference was in the steepness of the transition from no mass flow to steady state mass flow. With every

1 km/h increase in combine velocity, 0.10 s could be removed from the transitional delay time. Given the typical harvest velocities of the combine used in this investigation, the delay time could vary by 0.50 s. Given the resolution of the positioning system (1 Hz), this variation is not a great concern.

The more interesting and variable condition is the feeder house emptying scenario. When studying corn there is a very sudden, clearly defined transition to zero flow that occurs 3.0 to 4.0 s after the flow of crop material has ceased. Within the small grains, the transition is more gradual and requires seven seconds to achieve a zero flow sensing state after harvest has ceased. The primary reason for this variation is most likely attributed to the mechanics of the harvesting head. From field observations, it appears that material lingers on a small grain platform before being fed into the feeder house. Examples of feeder house filling and emptying scenarios for all three grain crops are shown in Figure 3.21.

To simplify future modeling and sensor fusion exercises, the feeder house filling and delay will be considered as a simple step function. Given the relatively quick transition from empty to full, steady state flow, this assumption seems appropriate. When typical GPS logging rates used in yield monitoring are considered, it becomes doubtful that the true shape of this transition could be determined. So for this study, a 4.5-s shift will be applied to the feeder house sensor data. The feeder house signal logged at a specific instance in time will be assigned the geographic coordinates that were captured 4.5-s prior to the reading in question. This exercise also strengthens the assumption that using a constant value for combine delay time is erroneous. There is no mechanism within the combine to account for delay variability that occurs at the feeder house. Going into this investigation, it was assumed that the delay time at the feeder house is less variable due to the restrictive nature of the path the crop material must pass. If variability exists to a noticeable extent at this point, it can only increase as the crop material passes through the remaining threshing and separating mechanisms on a modern combine harvester.

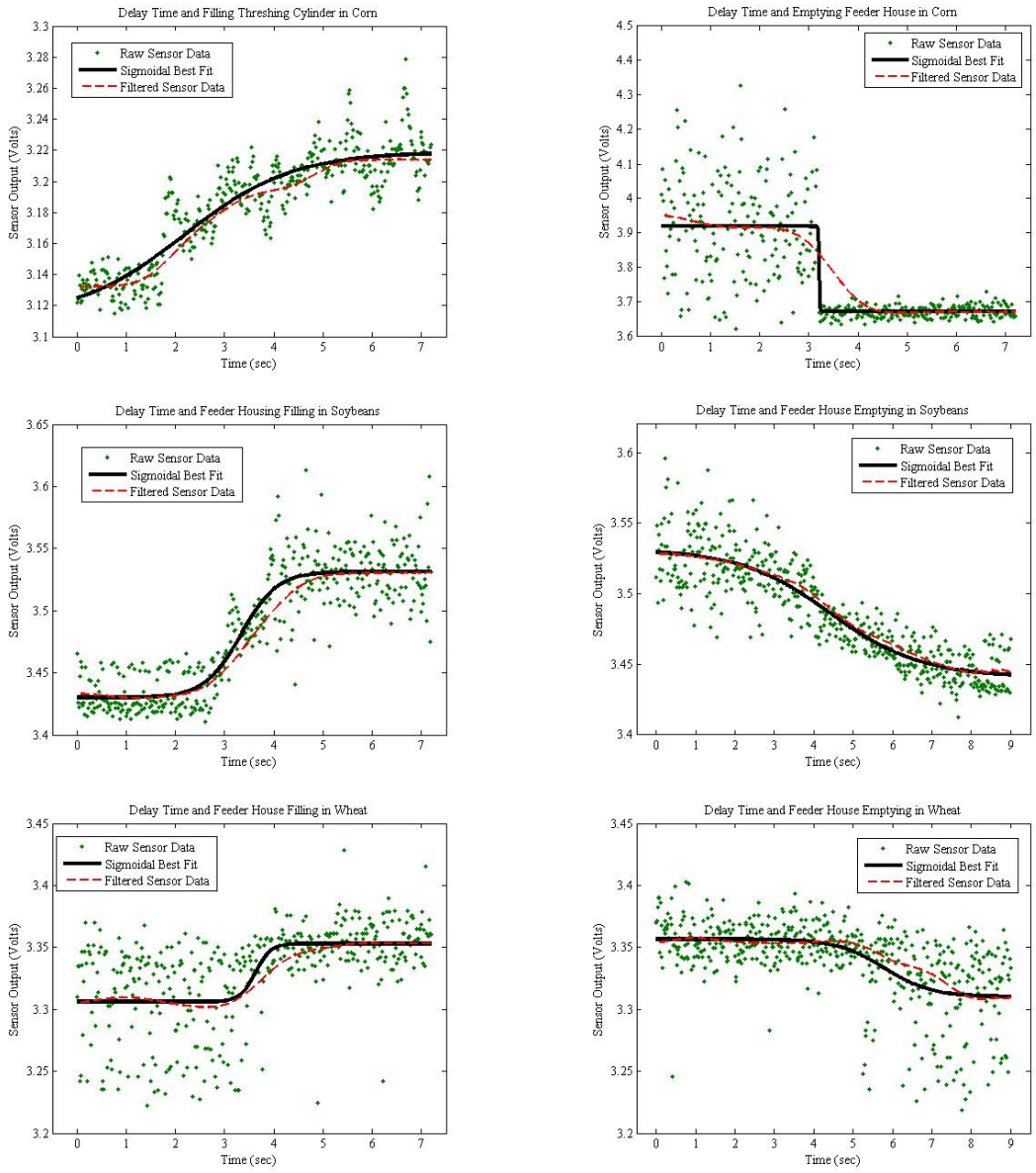

Figure 3.21 Examples of feeder house delay time and filling profiles for all three grain crops.

Sensitivity To Mass Flow Variations

Statistical analyses were carried out on both the traditional mass flow data as well as the data collected using the chain tension sensor for corn (Table 3.2) and wheat harvests (Table 3.3). Statistical analysis for the stripper plate width tests indicated that all passes had statistically similar grain yields. A similar analysis in wheat proved there were consistent grain yields regardless of the height of the cutter bar above the ground. These results are appropriate given

the fact that these tests took place in field locations with uniform grain yields. Although grain yields were statistically similar for all test conditions, the chain tension sensor indicated differences between the various stripper plate spacings in corn, and cutter bar heights in wheat. The feeder house sensor was able to detect the biomass flow variation induced by changing either stripper plate spacing in corn or cutting height in wheat.

These results were promising, since this test was set up to investigate the ability of the conveyor chain tension sensor to detect variations in the biomass flow. Typically, as stripper plate spacing is reduced, a higher rate of material is introduced to the combine. Similarly, in wheat as the cutter bar is lowered closer to the ground, the amount of wheat biomass fed into the harvester will increase. For the three corn replicates, the narrowest stripping plate setting (2.5 cm) always leads to the greatest mass flow in the feeder housing. This was confirmed by the weighing of crop material exiting the rear of the combine. The feeder-house chain tension sensor indicated there was also a significant difference in the narrowest stripping plate plots and the remaining plots. The feeder house sensor did not make a clear delineation between the 3.2 cm and 3.8 cm stripper plate settings. But there was no clear delineation in the actual mass collected from the combine for the 3.2 cm and 3.8 cm plots. This simply means given the size of the corn, when the stripper plates were opened to the 3.8 cm setting, the amount of biomass stripped from the corn plant and fed into the combine was not significantly different than for the 3.2 cm setting.

During wheat harvest there was a clear difference between all three treatments when the feeder house sensor data is considered. But this difference is evident in the biomass levels that were fed through the combine. By changing the cutter bar height, the biomass throughput increased by at least 800 kg/ha. The most likely reason that the wheat test was more successful is the fact that changing the cutter bar height physically limits the amount of crop material that can be fed into the machine. Altering the stripper plate width during corn harvest changes the potential for how much biomass will be fed into the combine. Regardless of the stipper plate spacing, the majority of the corn plant still passes through the head, and it possible for gathering chains or snapping rolls to grab onto plant material and pull it into the machine.

Table 3.2. Comparison of feeder house sensor output at varying stripping plate spacing in corn.

Feeder House Chain Tension Sensor				
Stripping Plate Width (cm)	Replication	Avg. Reading (volts)	Std. Deviation (volts)	Significantly Different From*
2.5 cm	1 2 3	3.31 3.41 3.35	0.22 0.24 0.22	3.2, 3.8
3.2 cm	1 2 3	2.92 2.71 2.90	0.31 0.27 0.30	2.5, 3.8(2,3)**
3.8 cm	1 2 3	2.65 2.37 2.45	0.30 0.29 0.29	2.5, 3.2(1,3)
Traditional Mass Flow Sensor				
Stripping Plate Width (cm)	Replication	Avg. Reading (kg/s)	Std. Deviation (kg/s)	Significantly Different From*
2.5 cm	1 2 3	5.74 5.32 5.55	0.63 0.61 0.60	None
3.2 cm	1 2 3	5.50 5.48 5.63	0.58 0.65 0.62	None
3.8 cm	1 2 3	5.37 5.68 5.48	0.58 0.61 0.54	None
Field Collected Samples				
Stripping Plate Width (cm)	Replication	Amount of Biomass (kg)	Normalized Biomass (Mt/ha)	Significantly Different From*
2.5 cm	1 2 3	53.82 53.63 54.27	3.05 3.04 3.07	3.2, 3.8
3.2 cm	1 2 3	46.14 37.66 45.62	2.61 2.13 2.58	2.5, 3.8(2,3)
3.8 cm	1 2 3	43.21 40.28 38.64	2.45 2.28 2.19	2.5, 3.2(1,3)

* Significance tested at $\alpha = 0.05$; **(2,3) refers to the second and third 3.8 cm replicate

Table 3.3. Comparison of feeder house sensor output at varying cutting heights in wheat.

Feeder House Chain Tension Sensor				
Cutting Platform Height (cm)	Replication	Avg. Reading (volts)	Std. Deviation (volts)	Significantly Different From*
5 cm	1 2 3	3.37 3.35 3.36	0.17 0.18 0.17	20 cm, 35 cm
20 cm	1 2 3	3.31 3.31 3.30	0.13 0.15 0.16	5 cm, 35 cm
35 cm	1 2 3	3.21 3.22 3.19	0.12 0.12 0.13	5 cm, 20 cm
Traditional Mass Flow Sensor				
Cutting Platform Height (cm	Replication	Avg. Reading (kg/s)	Std. Deviation (kg/s)	Significantly Different From*
5 cm	1 2 3	3.39 3.51 3.42	0.31 0.37 0.29	None
20 cm	1 2 3	3.43 3.41 3.37	0.33 0.26 0.26	None
35 cm	1 2 3	3.39 3.42 3.48	0.29 0.28 0.30	None
Field Collected Samples				
Cutting Platform Height (cm	Replication	Amount of Biomass (kg)	Normalized Biomass (Mt/ha)	Significantly Different From*
5 cm	1 2 3	48.65 62.47 36.54	2.62 2.74 2.67	20 cm, 35 cm
20 cm	1 2 3	51.78 50.87 49.20	2.15 2.27 2.24	5 cm, 35 cm
35 cm	1 2 3	34.10 33.52 34.99	1.49 1.47 1.53	5 cm, 20 cm

* Significance tested at $\alpha = 0.05$

Moisture Content Effects

Because a number of crop harvests were completed during this examination, it was possible to observe how the moisture content of the biomass affected the chain tension signal. Corn is the primary crop of concern because of its relatively long harvest period and the fact that, depending on the use of the grain, the moisture content at harvest may vary considerably. In the Fall 2004 harvest season, corn was harvested over the course of three months. The first harvest was completed in early September and the final harvest was completed in late November. During these two harvests the moisture content of the biomass dropped from 40% to 12%. Under identical operating parameters (combine speed, stripper plate setting, etc.) and similar plant material size/shape, there was a slight variation in the raw signal data. Typically, a 15 to 20% increase in the displacement of the sprocket was recorded when harvesting the wetter material. This result seems to be appropriate, given that the weight of the wetter material will be greater for the same volume of material. Also, there is a difference in the coefficient of fiction between wetter and drier crop materials that would contribute to this effect.

Spring Constant Effects

The sprocket that was being displaced as the tension on the feeder house drive chain varied was attached to the combine via two parallel cantilevers. These cantilevers were constructed using ANSI 1095 spring tempered carbon steel. The 51 mm x 89 mm x 1.5 mm cantilever had an equivalent spring stiffness of 578 N/cm. Initially, the cantilevers at the top and bottom of the sensor consisted of a single strip of steel. However, this arrangement produced an excessive amount of sprocket displacement which led to the destruction of numerous displacement transducers. Reduction in sprocket displacement was achieved by adding an additional one and one half strip of steel to the bottom cantilever, thereby producing an effective spring stiffness of 1445 N/cm for the bottom cantilever with the top remaining at 578 N/cm.

Using corn harvest as an example, the typical sensor output was 4.2 volts, which corresponds to a sensor plunger displacement of 12 mm. Using the Euler Beam equation, this displacement corresponds to a loading value of 1387 N. This reading was taken using the single strip setup. When the bottom cantilever is strengthened with the additional strips of steel, the effective cantilever stiffness is 2023 N/cm. Applying the same 1387 N load will lead to a

displacement of 6.8 mm. There is a directly proportional linear relationship in the additional spring stiffness. A general reduction in sensor output was noted when the additional strips of steel were added. However, due to the difficulty in establishing equivalent biomass throughputs, it is unknown how close the true and theoretical values are related. It should be noted that variations in the cantilever setup only occurred between field or plot activities (i.e. all comparisons are made under similar cantilever setups).

Comparison to Yield Monitor Performance

Additional analysis was performed on the data collected during the second set of tests in concurrent blocks of varying yield (ASABE X579 plots). Initially, the filtered chain tension data were plotted along with yield data collected by the traditional mass flow sensor to determine if the sensor output tracked the variations of the block pattern. The sensor data were plotted against distance. The boundaries that divided the blocks of different corn plant densities were added to the plot to establish the ability of both the chain tension sensor and yield monitor to detect changes in material throughput. Plots for the 2.5 km/hr, 5.0 km/hr, and 8.0 km/hr trials for both corn and wheat are shown in Figures 3.22 and 3.23.

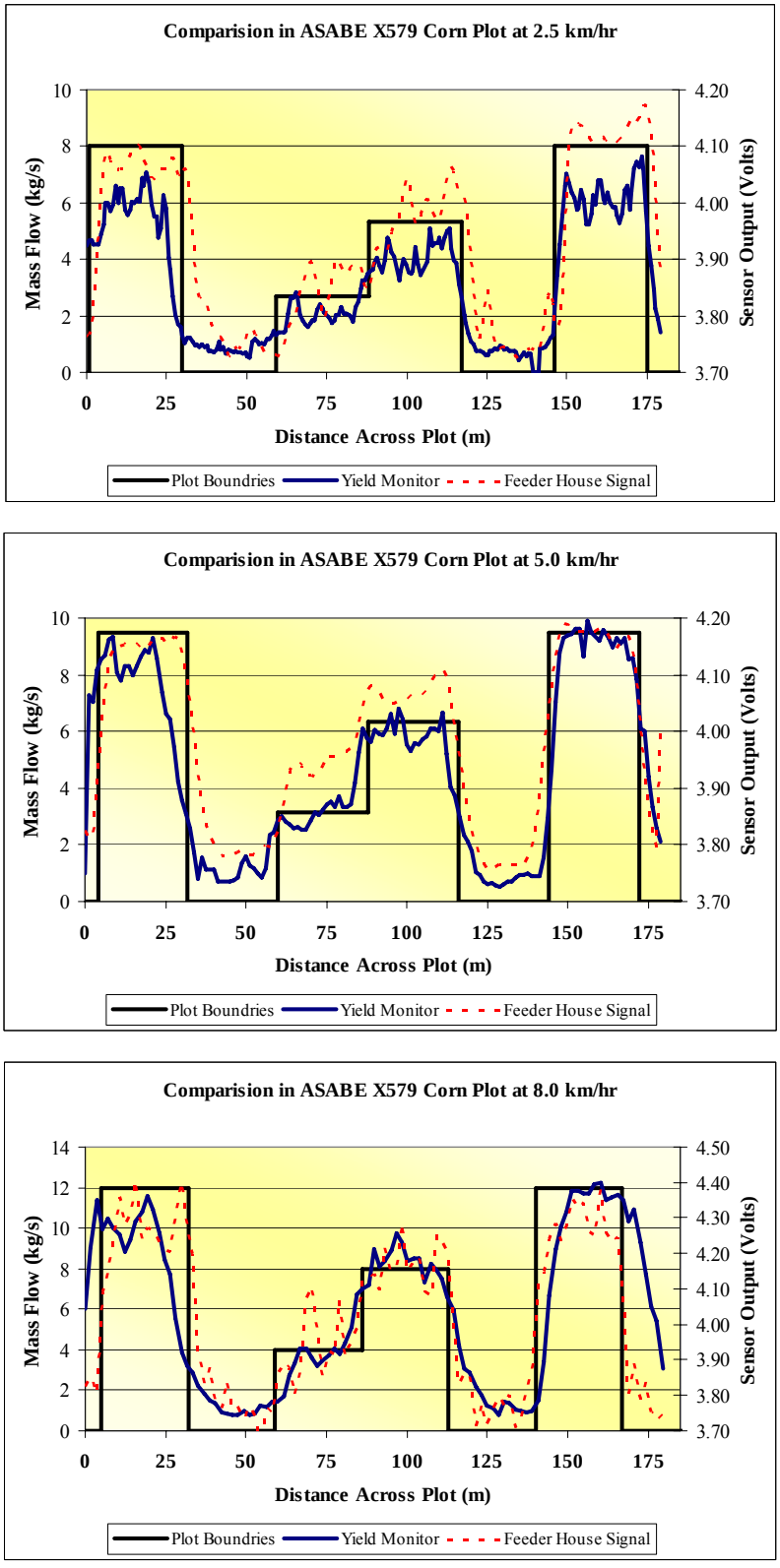

Figure 3.22. Comparison of yield monitor and feeder house sensor performance in ASABE X579 corn plots at varying ground speeds.

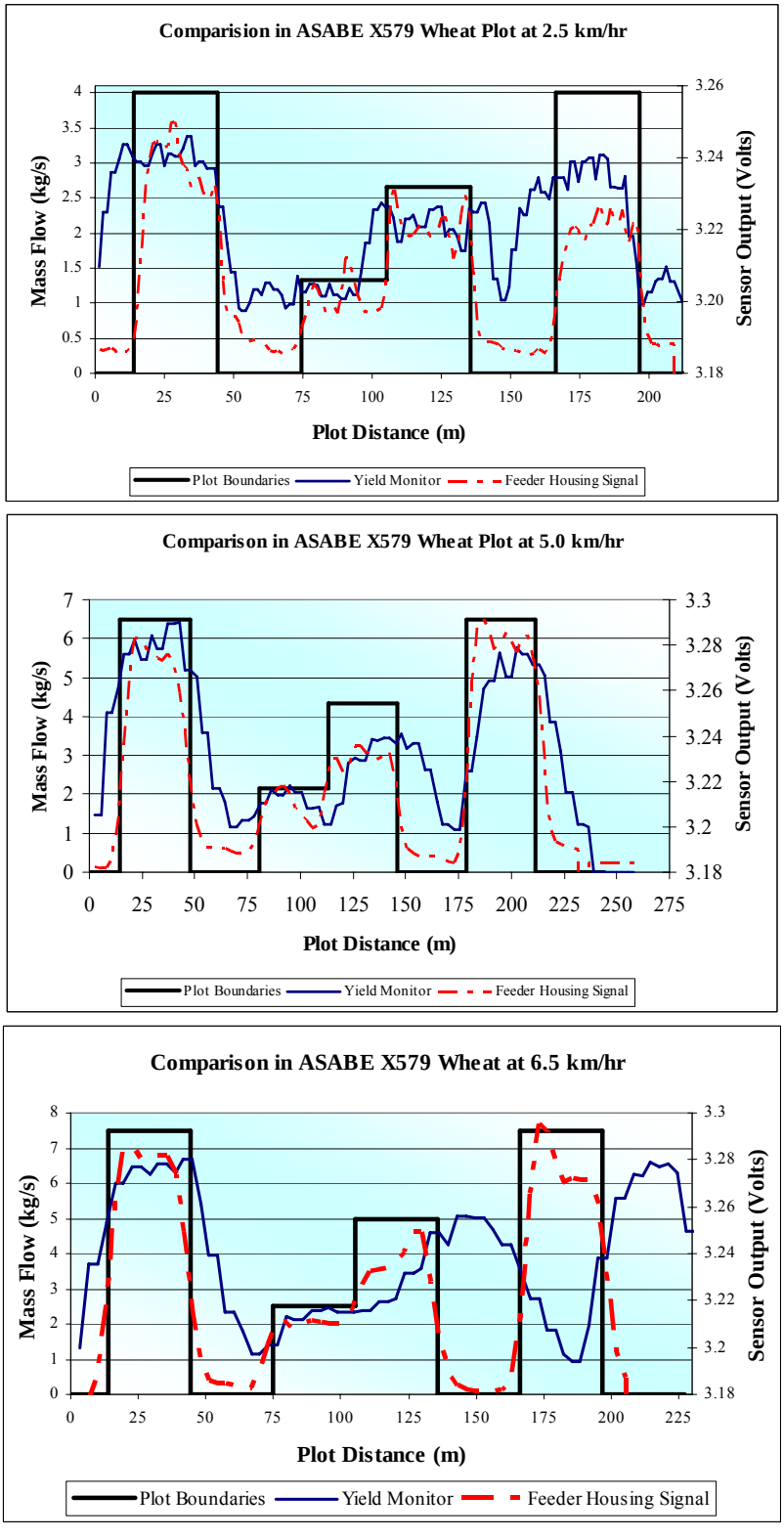

Figure 3.23. Comparison of yield monitor and feeder house sensor performance in ASABE X579 wheat plots at varying ground speeds.

A couple of trends are evident in the figures. First, both the mass flow and voltage levels increase as the combine's speed increases. As machine velocity increases, a greater area is covered in 1 s, so in that given period of time more biomass has entered the machine. The most glaring issue with the yield monitor data is the inability for the yield monitor to achieve zero mass flow in blocks with zero grain present. Meanwhile, the feeder house sensor consistently returns to similar voltage levels, 3.75 V in corn and 3.17 V in wheat, when a block with zero grain is encountered. Two other areas that the feeder house signal out performs the yield monitor is transition between plots, and ability to mimic the correct plot size. The yield monitor consistently logs data after the combine has exited the plot; even after the yield delay has been considered. The yield monitor's performance seems to improve at high flow rates such as those encountered when harvesting corn.

Box plots were developed within Matlab of the two data streams varied while harvesting plots. Box plots were setup so that the solid horizontal lines represent the lower quartile value (25^{th} percentile), the median value, and the upper quartile (75^{th} percentile) value. The whiskers that extend from the ends of the boxes indicate the extent of the data at the 2σ range. Outliers that fall beyond the 2σ are indicated using a small cross. These box plots are notched, which provides the added benefit of showing significant differences between the treatments. If the notches of two boxes do not overlap, then the median values of these boxes are significantly different at $\alpha = 0.05$. Typical box plots associated with corn and wheat harvests are provided in Figures 3.24 and 3.25.

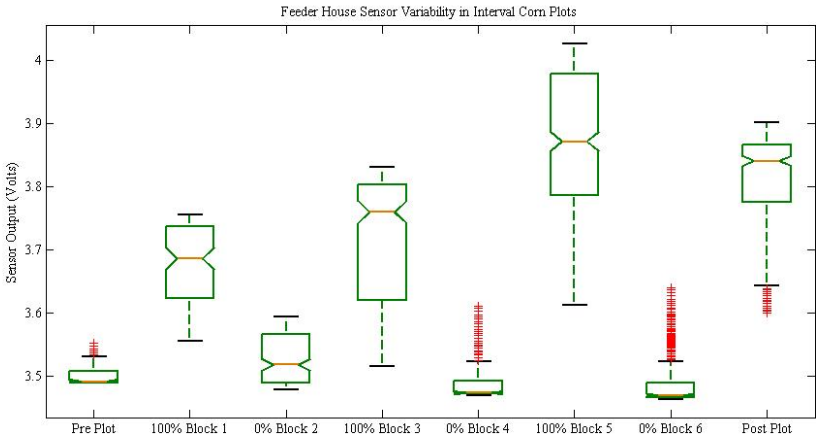

a) Feeder House Chain Tension Sensor

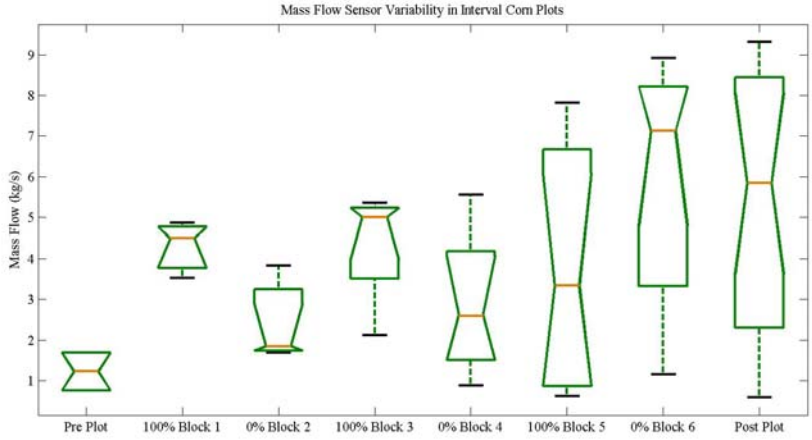

b) Grain Mass Flow Sensor

Figure 3.24. Boxplots of yield monitor and feeder house sensor performance in interval corn plots.

In the first series of box plots (Figure 3.24), the data were collected in corn interval plots. In these plots, the combine repeatedly harvested blocks that alternated between a 100% biomass level and a 0% biomass level. Examination of the box plots indicates that the yield monitor mass flow data suffers from increased variability as well as severe inconsistency. Notches for 100% blocks and 0% blocks overlap within the yield monitor data set, signifying statistical similarity between the median values of these blocks. This is a troubling trend because it is unrealistic to have blocks that have no plant material present producing grain yields equivalent to a block with

the maximum level for crop biomass present. Unlike the yield monitor box plot, the feeder house plot has a clearly discernable pattern of alternating blocks. Also, the feeder housing sensor produces a more consistent signal in the plots with no biomass present. The feeder house does suffer from irregularity in the blocks with 100% grain. The exact reason for this is unknown.

The post plot block (the material harvest outside the original test plot; last box on the right in Figure 3.24) is very interesting in this data set. In this particular plot layout, the combine passed into an area of 100% biomass after exiting block 6. The large amount of variability shown by the yield monitor is the result of a lag time delay that results in the combine experiencing a full range of flows. Basically, by the time the combine arrives at this point, the yield monitor has fallen so far behind on its transitions that the data reflect a low flow, a transition, and high flow all in the post plot block. The feeder house sensor shows the post plot block as the more accurate high condition.

In the second set of box plots (Figure 3.25), the data were collected while harvesting ASABE X579 wheat plots. On initial inspection, the increased variability within the yield monitor data set is obvious. Also, the true layout of the ASABE X579 field trial is clearly defined by the feeder house sensor. Another point to note in the ASABE X579 plots is the recurrence of two blocks as the 0% biomass level is represented in blocks 2 and 5, and the 100% biomass level is present in blocks 1 and 6. Both sensors do an adequate job of indicating the similarity between blocks 1 and 6. However, the yield monitor does not show consistency in its ability to sense a block of 0% crop biomass flow. There is a great degree of variability in the yield monitor data readings at 0% biomass flow, and the median values of the 0% blocks appear to be similar to the 33% and 67% biomass level blocks.

In the case of the ASABE X579 plots, the pre- and post-blocks were completely void of grain biomass. As with the previous set of box plots, the yield monitor data show considerable variability in the areas immediately preceding and following the actual field trial. This variability is a function of a slow transition that allows for a variety of mass flow conditions to be present in the data set at a given spatial location. Most likely this is a result of delay time variability due to the combine filling and emptying internal voids within the threshing cylinder/rotor and cleaning shoe at the start and finish of the plot. The feeder house data is not susceptible to these delay variations and is more consistent in the representation of the data.

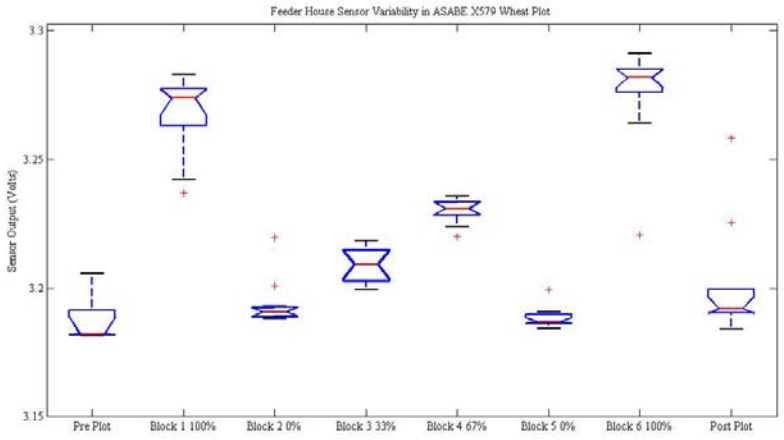

a) Feeder House Chain Tension Sensor

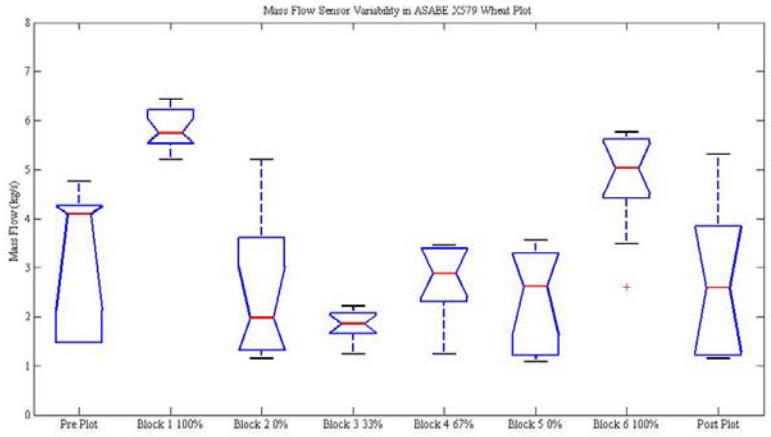

b) Grain Mass Flow Sensor

Figure 3.25. Boxplots of yield monitor and feeder house sensor performance in ASABE X579 wheat plots.

Additional statistical analysis of the data were conducted to determine if significant differences existed between the blocks of ASABE X579 plots as well as the different combine ground speeds. This analysis was conducted on both the chain tension and impact plate data sets. The results of this test are presented in Tables 3.4 (corn) and 3.5 (wheat). Included in these tables are the results of a Fisher's Least Significant Difference test (Devore, 1999) to determine how well each sensor was able to detect differences in the blocking scheme. Not shown in the table are the results from a speed comparison test. For both the chain tension sensor and the

traditional mass flow sensor, the results of the ANOVA showed combine ground speed was a significant factor influencing the output of either sensor. This result is ideal, as higher speeds increase the amount of material entering the combine at a given moment in time. However, because the combine is covering more distance on the ground, the resulting yield per unit area remains consistent and speed did not influence either sensor's ability to detect variable material input. An increase in speed essentially applies an amplification constant to the data set, but the pattern remains unchanged for a given field trial.

Table 3.4. Statistical comparison of traditional impact plate sensor and feeder house chain tension sensor performance in ASABE X579 corn plots.

Portion of Block Covered with Crop	Traditional Impact Plate Sensor			Feeder House Chain Tension Sensor		
	Mean Mass Flow (kg/s)	C.V. (%)	Different from Blocks	Mean Output (Volts)	C.V. (%)	Different from Blocks
100 %	7.49	22 %	0%, 33%	3.27	15 %	0%, 33%
0%	1.25	46 %	67 %, 100%	3.18	12 %	67 %, 100%
33 %	3.23	33 %	100 %	3.21	13 %	100 %
67 %	5.58	24 %	0 %	3.24	11 %	0 %
0 %	2.22	84 %	67 %, 100%	3.18	14 %	67 %, 100%
100 %	7.86	28 %	0%, 33%	3.28	14 %	0%, 33%
	LSD = 2.45 kg/s at $\alpha = 0.05$			LSD = 40 mV at $\alpha = 0.05$		

The statistical analysis revealed a number of interesting results with regard to chain tension sensor performance and comparison of the two different mass flow sensing devices in corn. First, both the chain tension and traditional mass flow results indicated that the output for each sensor was statistically similar for the two 100% and the two 0% biomass coverage blocks. However, both sensors failed to distinguish between the two simulated medium yield blocks, 33% and 67%. The chain sensor data showed that the 33% block was statistically similar to the completely empty (0%) blocks and the 67% block was statistically similar to the completely full (100%) blocks. The traditional mass flow sensor data indicated the 33% block was significantly different from the completely full (100%) block only. The 67% full block was significantly different from the completely empty (0%) block only. A review of the variability of the sensor output indicated a higher amount of variability with the traditional mass flow sensor readings,

particularly in the zero yield (0%) blocks. Also, the variability in the chain tension sensor output remained relatively stable regardless of the amount of biomass flowing through the combine.

A final observation for the data in Table 3.4 is the surprisingly high values for mean mass flow in the 0% blocks. It seems that delays in material transport and combine dynamics caused the mass flow sensor to record a significant amount of data after the combine had entered a block of zero yield. Figure 3.22 also indicated that mass flow never settled at zero, rather it achieved a minimal value that would allow a user to believe grain was flowing through the machine. This point supports both the need to develop additional sensors to supplement traditional mass flow data, or develop filters that can be used to post-process yield maps to improve yield estimation accuracy.

Looking through the wheat data analysis in Table 3.5, there are a couple of variations from the corn analysis. Essentially, the traditional mass flow sensor shows increased variability as significant difference was detected for blocks that had identical biomass levels. Both the 0% and 100% were different from their replicates. The feeder house chain tension sensor identified both 0% and 100% blocks to be statistically similar. The traditional mass flow sensor had a number of other instances where blocks with varying biomass levels were determined to be statistically similar. For traditional mass flow data, there is an occurrence of either similarity between blocks that were not alike or dissimilarity between blocks that were alike. Sometimes both of these conditions are present. The main concern with the chain tension sensor arose when similarity was detected between the 33% block and one of the 0% blocks and similarity was detected between the 67% block and one of the 100% blocks. However, there is still considerably less variation in the chain tension sensor versus the traditional mass flow sensor.

Table 3.5. Statistical comparison of traditional impact plate sensor and feeder house chain tension sensor performance in ASABE X579 wheat plots.

Portion of Block Covered with Crop	Traditional Impact Plate Sensor			Feeder House Chain Tension Sensor		
	Mean Mass Flow (kg/s)	C.V. (%)	Different from Blocks	Mean Output (Volts)	C.V. (%)	Different from Blocks
100 %	3.08	14 %	ALL	3.31	11 %	0%, 33%, 67%
0%	1.29	32 %	67%, 0% (2)*, 100%	3.18	4 %	67%, 100 %
33 %	1.48	35 %	67%, 0% (2), 100%	3.21	3 %	0% (2)*, 67%, 100%
67 %	2.13	19 %	0%(1), 33%, 100%	3.26	7 %	0%, 33%, 100%(1)
0 %	2.17	26 %	0%(1), 33%, 100%	3.17	9 %	33%, 67%, 100%
100 %	2.67	17 %	0%, 33%, 67%, 100%(1)	3.30	6 %	0%, 33%
	LSD = 0.45 kg/s at $\alpha = 0.05$			LSD = 47 mV at $\alpha = 0.05$		

* A value in parenthesis refers to a specific 0% or 100% block, if no parenthesis is present then the value is significantly different from both occurrences.

Yield Monitor – Feeder House Signal Correlation

Another important assessment is the relationship between crop yield and the chain tension sensor output. Figure 3.21 illustrates the relationship between chain tension sensor and the mass flow data collected during the various field activities associated with this project. The data used to generate these plots were randomly selected for the field data. This data set was then trimmed to obtain a sample that consisted of relatively steady state flow rates (i.e. zones of sharp transition were removed). The sample was then broken down into groups that represented 2.5-km/hr velocity classes. Ideally, the optimal results would be a strong correlation between the two readings regardless of machine velocity or crop type.

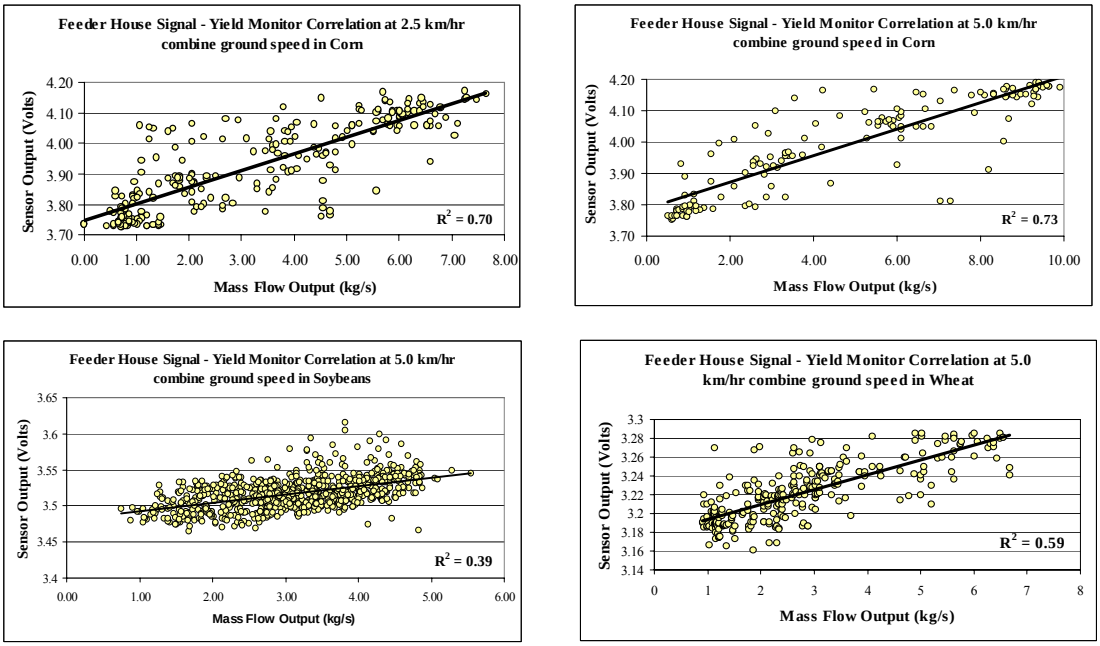

Figure 3.26. Biomass and grain mass flow relationship in three grain crops as interpreted by the feeder house chain tension sensor.

While the figure does indicate a relatively linear relationship between the two sensor outputs, there is certainly opportunity to improve upon the R^2 value of 0.39 and 0.59 seen in the soybean and wheat samples. The poor correlation in the small grains is most likely due to the poor feeding characteristics of the grain platform compared to the corn head. This correlation was completed for the sole purpose of determining if a biomass – mass flow relationship is present, but it must be noted that the devices that were used to determine this relationship are prone to errors. This data does indicate (although vaguely), that increased biomass throughput is associated with increased grain mass flow. Establishing this point is critical. Nelson (2001) determined a straw-to-grain ratio (SGR) for both corn and wheat which supports the vague relationship found in this exercise. For corn there is a 1:1 ratio, meaning for every one kg/ha of grain produced there is one kilogram of biomass grown. In winter wheat the ratio is 1.3:1. The important point is that this is only valid for similar operating conditions. As seen earlier when varying cutter bar height or stripper plate spacing, it is possible to manipulate biomass throughput while maintaining constant grain mass flow.

Summary

Modern mass flow sensing technology used to develop yield maps is subject to errors that can be attributed to incorrect swath width entry, material flow dynamics within the combine, or improper calibration. It may be possible to improve the accuracy of yield maps with the use of this supplementary sensor that measures other quantities that are related to yield. The supplementary data set can then be combined with traditional mass flow data measured in the clean grain elevator to create a superior yield map. Through modification of the path of the feed conveyor drive chain, the deflection of a cantilevered beam, measured by a thin-film potentiometer, could be used as a proxy for drive chain tension. Tests to evaluate the sensitivity of the chain tension sensor were developed and comparisons between the new sensor and the traditional mass-flow sensor were completed. Based on the testing completed during this study, the following conclusions were made:

- Variations in biomass throughput were detected by the chain tension sensor when the stripper plate adjustment on the corn head was changed to alter the amount of plant material entering the combine.
- As the combine passed through blocks with different yields, both the traditional mass flow sensor and the chain tension sensor responded in a manner coinciding with yield differences.
- The chain tension sensor operates with 10 to 20% reduced variability when compared to traditional mass flow data.
- Evidence from this study supports the notion that the chain tension sensor may have value when used to correct the mass flow sensor data in the clean grain elevator.

Chapter Four

Assessment of Threshing Cylinder Pressure as a Mass-Flow Sensing Method

Introduction

In the preceding chapter, a new mass flow-sensing device was developed and its ability to sense variations in crop material mass flow through the feeder house was documented. While this device appears to be successful at sensing mass flow variations, there is concern regarding the amount of modification required to implement this mechanism. It appeared that the feeder house chain tension sensor is susceptible to failure after repeated cycling of the reverser, which is used to clear out the feeder house when it becomes plugged. A final negative point about the feeder house signal is the signal quality and amount of filtering required to produce a useful signal. The key question being; is it possible to detect the same variations using less signal conditioning?

Therefore, it was decided to investigate other means of monitoring mass flow through a combine, in the hopes that a more easily implemented method could be used to correct yield monitor mass flow data. While feeder house chain drive configurations vary by combine manufacturer and model, the primary aim in this portion of the investigation was to find a more universal method of monitoring mass flow. This sensing method had to occur before multi-pathing of the grain stream occurred. After leaving the threshing cylinder or rotor, the grain stream can travel a variety of paths to arrive at the top of the clean grain elevator. The grain stream can pass directly through the cleaning shoe, travel through the straw-walkers or recirculate through the combine via the tailings elevator. If a mass flow sensor is placed on the straw walkers or at some point on the cleaning shoe, the flow reading is no longer representative of the crop material that was produced at a discrete location.

Therefore, measuring the load on the threshing cylinder or rotor will become the focus of this part of the investigation. All of the material passing through the feeder house is passed to the threshing cylinder/rotor; therefore, it appears that the same mass flow data logged at the feeder house would be logged again at the threshing cylinder/rotor. However, there are questions

regarding the threshing cylinder/rotor's response to crop material loading increases as well as the implications of increasing the delay time from the point of initial crop contact to the sensing location on the combine. Recirculation of crop material from the tailings elevator has the potential to compromise any sensing information obtained from the cylinder/rotor.

Sub-Objectives

The feeder house-based sensor developed in the preceding chapter was successful at detecting variations in crop material mass flow entering the combine. However, questions regarding the practicality of this sensor have led to the development of a more universal crop mass flow sensing device to correct grain mass flow data collected by the yield monitor. The specific objectives for this portion of this project were:

1) Develop a threshing cylinder/rotor-based crop mass flow sensing scheme,
2) Develop data filters and processing techniques to enhance sensor signal values for determination of mass flow, and
3) Compare the performance of this crop mass flow sensor to that of the traditional grain mass flow sensor and the feeder house-based crop mass flow sensor under both constant and varied mass flow conditions.

Methodology

Threshing Cylinder Sensor Development

The initial investigation into the development of a mass flow sensing alternative was spurred by the recent introduction of feed rate control in combines. Deere & Co. (Moline, IL) has been monitoring hydraulic pressure on the threshing cylinder/rotor's variable speed drive to control ground speed of a combine for optimizing harvest productivity. In the majority of modern combines, a hydraulically controlled variable speed drive with load-sensing capabilities drives the threshing cylinder. As a result, the hydraulic pressure on the cylinder drive will increase as the incoming material becomes harder to thresh. Under similar field conditions, it is assumed that cylinder/rotor torque increases with increasing crop mass flow. Monitoring the hydraulic pressure required to drive the threshing cylinder is less invasive than the modification

required to study feeder housing throughput. However, the sensitivity of the cylinder drive pressure to mass flow variations, as well as the usefulness of this data for the correction of yield monitor data was unknown. The cylinder drive pressure can be measured by inserting a pressure transducer into the hydraulic line controlling the piston that adjusts the variable speed drive (Figure 4.1). A 21 MPa (3000 psi) Omega PX101 pressure transducer was used to sense the hydraulic pressure required to drive the threshing cylinder. The transducer was supplied with 12 V from the combine and it gave a 0-5 V analog ouput signal. The transducer was equipped with internal voltage regulation. Typically, the cylinder required approximately 13.7 MPa (2000 psi) of pressure to operate under normal loading conditions.

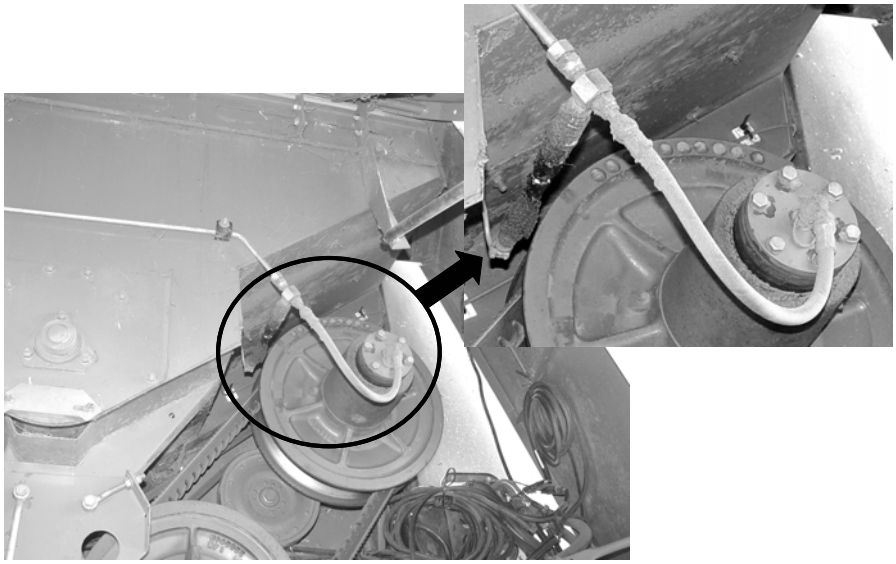

Figure 4.1. The 21 MPa (3000 psi) pressure transducer used to monitor hydraulic pressure driving the threshing cylinder.

The cylinder sensing location has the same advantages over the traditional means of sensing grain mass flow in the clean grain elevator as the feeder housing based sensor. The most obvious is the reduction in the throughput lag. A harvested crop will pass through the cylinder before many of the mechanisms (i.e. straw-walkers, transport augers, the cleaning shoe) that cause throughput lag are encountered. A second advantage is a reduction in lag time variability because the crop material is limited to a single flow path until it enters the cylinder. It is thought the delay time variability will be somewhat reduced, and a constant value lag time will again be applicable.

The analog output from the pressure transducer was logged using the USB data acquisition board with 12 bit analog-to-digital converter used in the prior feeder house investigation. For the majority of the investigations, the signal was logged at 400 Hz. A raw data text file as well as an averaged data text file was created using the same Microsoft Visual Basic program developed for the feeder house sensor investigation. The averaged data file was created by averaging the 400 Hz data every 0.1 s and listing a few additional operating parameters such as combine velocity, combine location, and header height. A few select tests were conducted at a sampling rate of 1 kHz to study the output signal parameters in greater detail. For the majority of the field tests, both feeder house sensor data and threshing cylinder data were collected and archived simultaneously.

Sensor Evaluation

With the exception of a few field tests conducted in Fall 2003, the hydraulic pressure sensor was tested alongside the feeder house based mass flow sensor. Tests were conducted on four farms in central Kentucky and tests were completed on all three major grain crops. The same series of field trials were developed, which include the ASABE X579 plot, the interval plot, the ramp flow plot, and mass flow calibration. The details on the exact nature of the field tests have been discussed in the Field Test Procedures section of Chapter Three. Similarly, the same analyses completed on the feeder house data in Chapter Three were applied to the cylinder data. The data is present in identical form, so that comparisons between the two sensing alternatives could be completed.

Results and Discussion

Signal Conditioning

Like the feeder house signal processing, threshing cylinder pressure data sampled at 1 kHz were collected for all three crops tested in this investigation. The same Matlab program (Appendix C) used to determine the frequency component of the feeder house signal, was again used. A 512-point fast Fourier transform (FFT) was utilized in the signal analysis. Figures 4.2 through 4.5 illustrate the common threshing cylinder pressure sensor output and corresponding frequency magnitude while harvesting corn, soybeans, wheat, and the zero mass flow condition.

The scaling is such that the y-axis on each figure represents a two volt range similar to the feeder house plots.

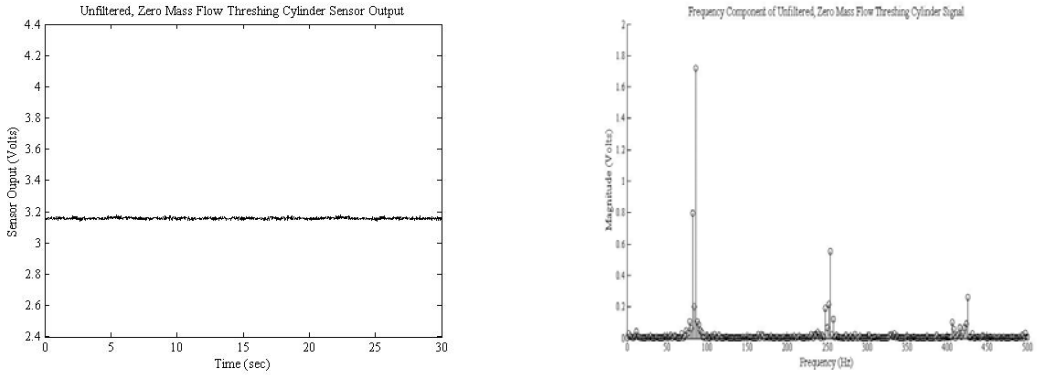

Figure 4.2. The raw cylinder drive pressure sensor output and frequency content under unloaded conditions.

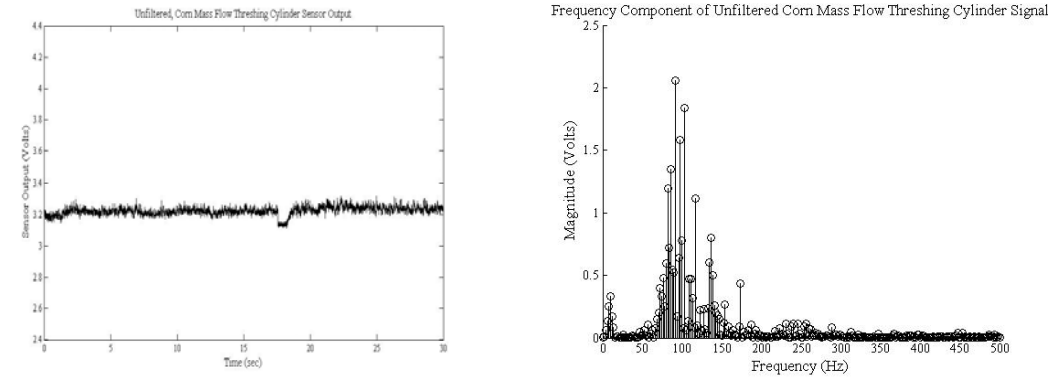

Figure 4.3. The raw cylinder drive pressure sensor output and frequency content under corn mass flow conditions.

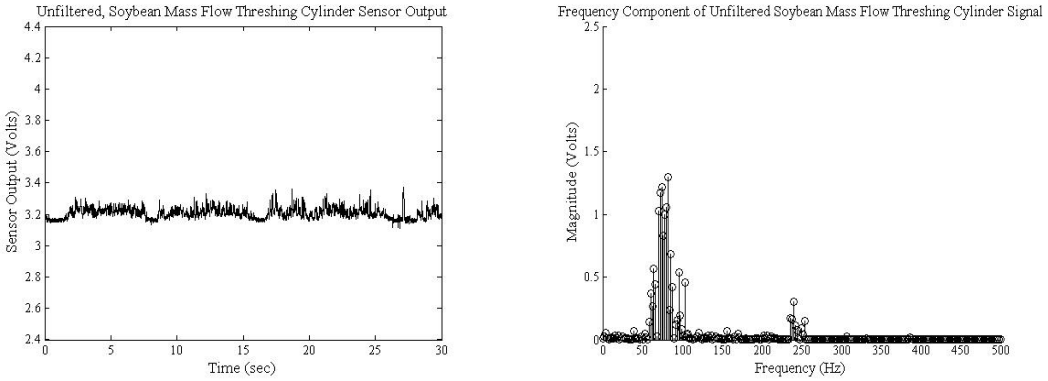

Figure 4.4. The raw cylinder drive pressure sensor output and frequency content under soybean mass flow conditions.

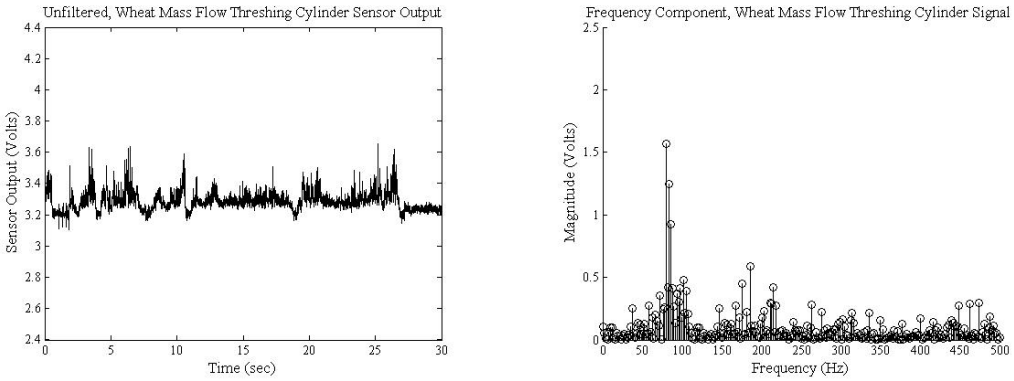

Figure 4.5. The raw cylinder drive pressure sensor output and frequency content under wheat mass flow conditions.

One obvious feature of this signal is the relative low variability within the signal. Unlike the feeder house signal, which had peak-to-peak amplitudes approaching 2V, the threshing cylinder signal rarely varied by more than 0.4 V across a plot. From a frequency perspective, there are obvious frequency spikes in the vicinity of 100 and 250 Hz. At this time there is not a clear answer as to the nature of this frequency disturbance. There would be a pulse close to 220 Hz due to the rotation of the 10 rasp bar cylinder turning at approximately 1300 rpm. As before, a low-pass FIR filter was used to remove these higher frequency periodic components. Figures 4.6 through 4.9 provide examples of the filtered data sets. The filtering appears to be appropriate as mass flow trends become readily apparent after the filtering is applied. Note that the unloaded threshing cylinder has an average voltage reading of 3.16 volts, which corresponds to 13.1 kPa (1900 psi).

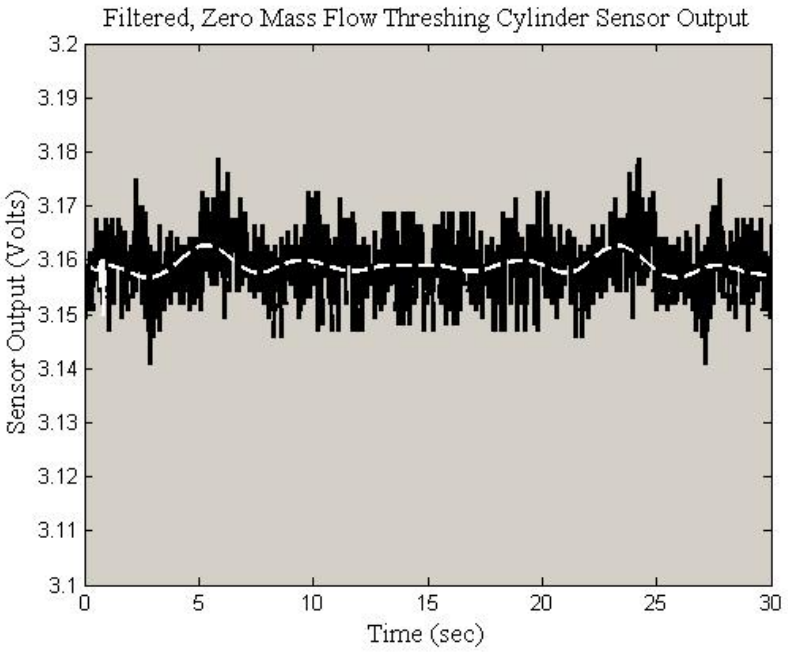

Figure 4.6. Filtered threshing cylinder sensor output under zero mass flow conditions.

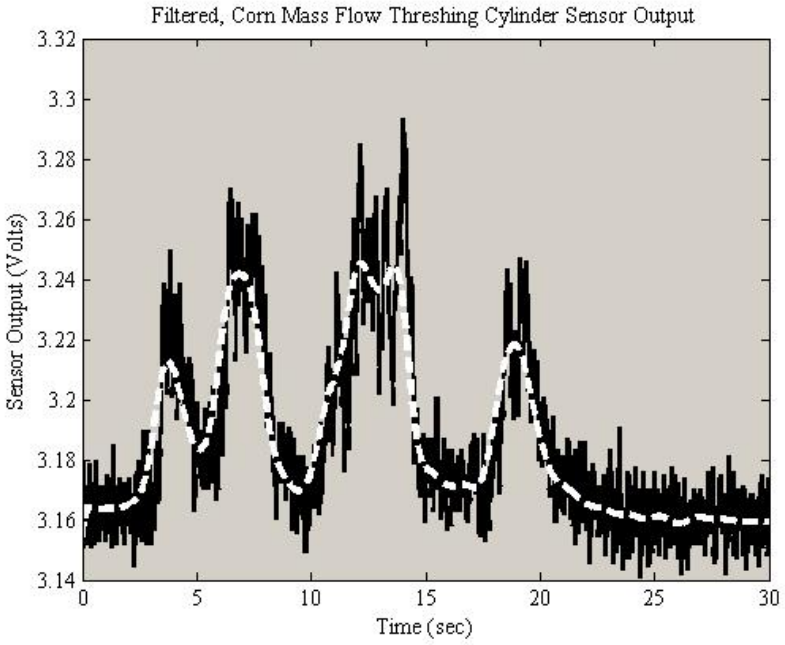

Figure 4.7. Filtered threshing cylinder sensor output under corn interval plot mass flow conditions.

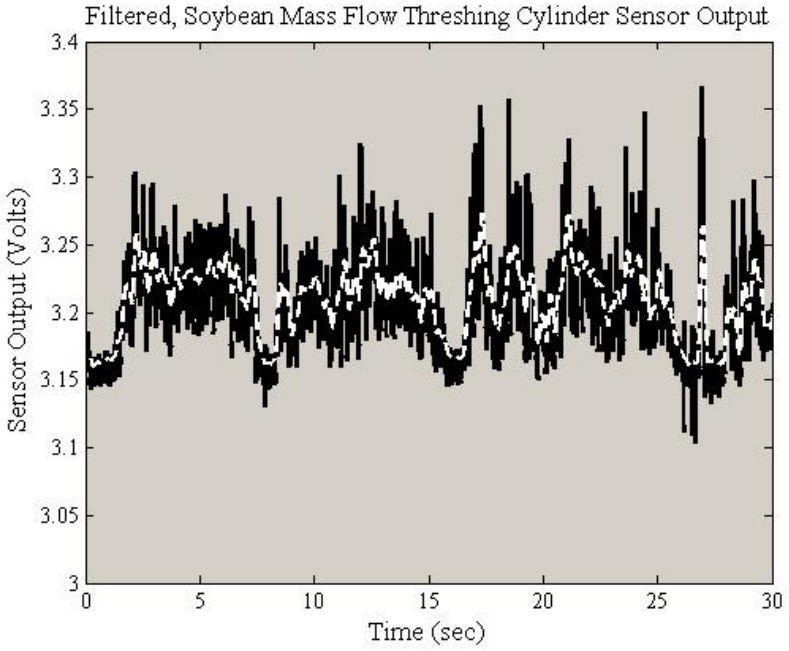

Figure 4.8. Filtered threshing cylinder sensor output under regular soybean flow conditions.

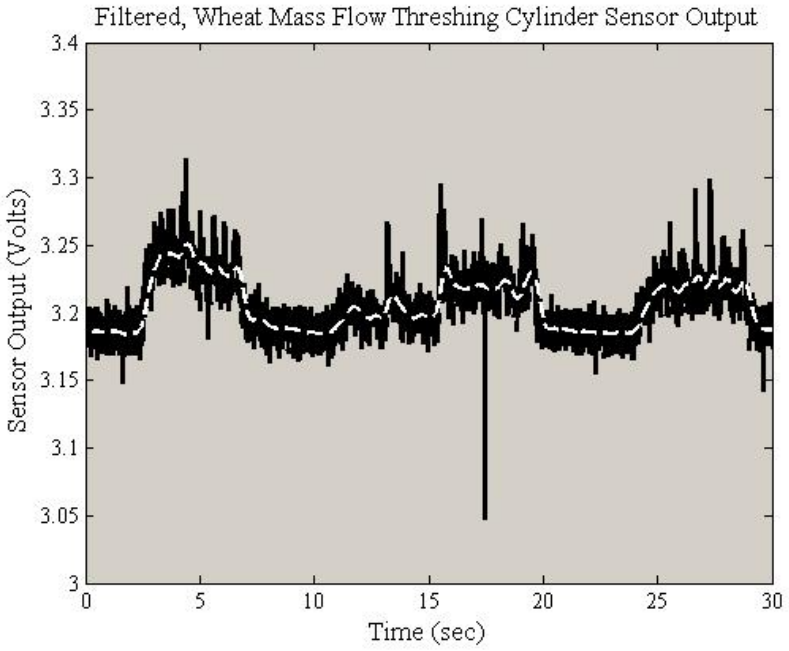

Figure 4.9. Filtered threshing cylinder sensor output under ASABE X579 wheat flow conditions.

Signal Delay Time

As with the feeder house data, it was critical to establish a value for signal delay time for the threshing cylinder data. The transitions from zero mass flow to typical 100% mass flow values as well as the shift back to zero mass flow were studied for all three grain crops harvested. Again, a four parameter sigmoidal function (Equation 3.8) proved the best fit to describe the cylinder transition zones. Typically, the R^2 values associated with these sigmoidal fit equations was between 0.6 and 0.72, regardless of crop type. The sigmoidal fit equations are plotted alongside their respective raw data set for the three crop conditions in Figure 4.12. Also, these data sets were collected at the same instance as the data used to generate the feeder house filling/emptying plots.

On initial examination, the plots created from the hydraulic pressure sensor look very similar to those generated from the feeder house sensor. However, there are two minor differences. One of the more surprising aspects of the cylinder is the sudden increase in pressure that was recorded during the transitional period. In general, the transition from the time when a mass flow was first registered, until steady state was achieved was less than the feeder house sensor (2 s). This was true in all crops. It would appear that the feeding dynamics of the harvesting head auger were no longer present in the threshing cylinder data, as there is no clear distinction between the corn head and the small grain platform.

While transitions occurred faster, the overall delay time was about one second longer. This longer delay time was expected, as the material had to travel an additional 1.5 m to arrive at the cylinder from the time it entered the feeder house. This additional delay was prevalent in the region of the plot between the combine's first entry into the field and the sensor's initial registering of mass flow (i.e. the lower asymptotic tail). On average there was a 3.25 s lag, which was 1.25 s longer than the feeder house signal. The mass flow transition time averaged 1.75 s. There is also the additional 0.5-second delay that is induced by the Matlab filtering algorithm. Therefore, a given cylinder drive data point was assigned the geographic coordinates that were logged 5.5 s prior to the reading.

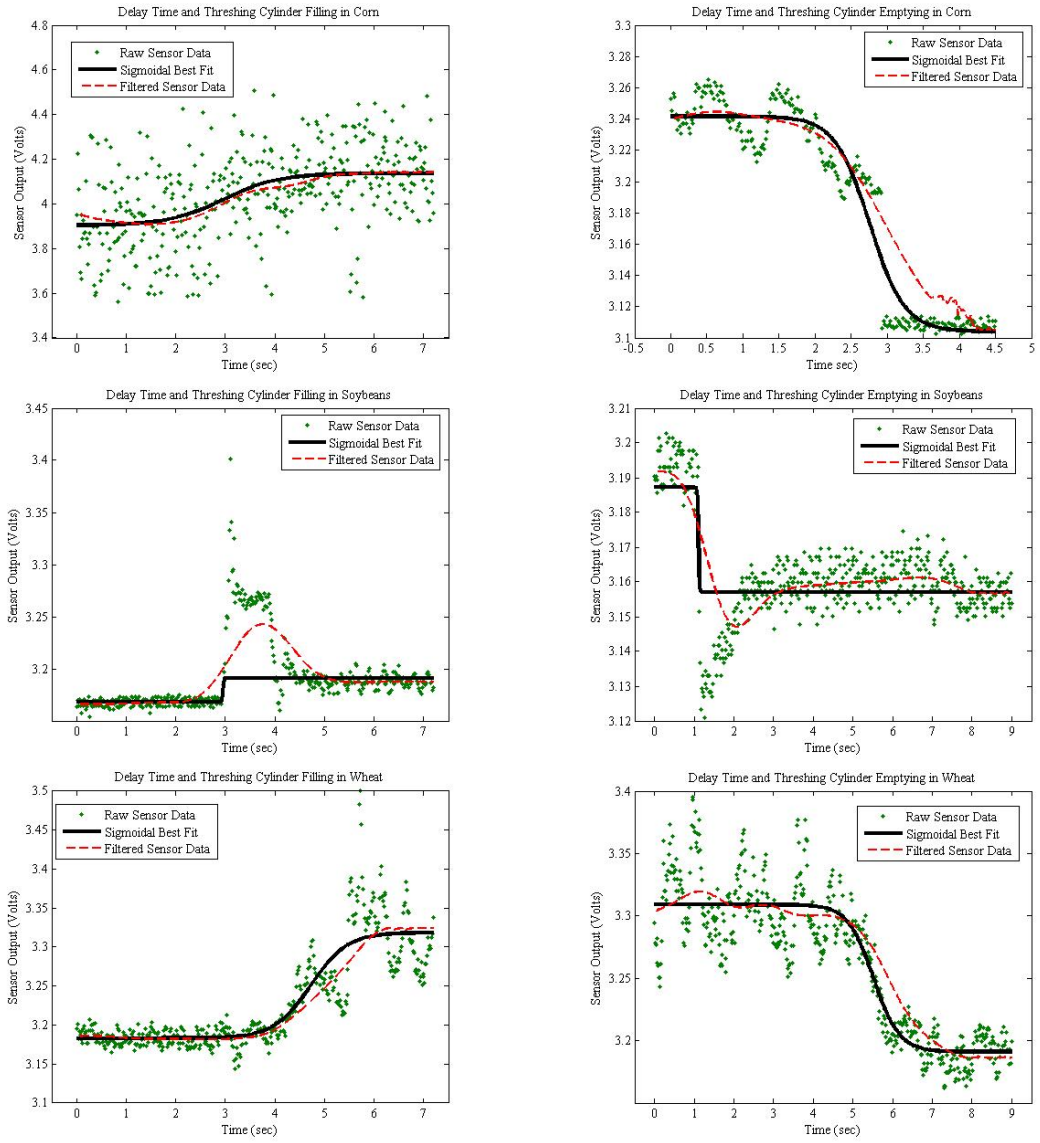

Figure 4.10. Examples of cylinder delay time and filling/emptying profiles for all three grain crop.

Sensitivity to Mass Flow Variations

Statistical analyses were carried out on both the traditional mass flow data as well as the data collected using the cylinder drive pressure sensor for corn (Table 4.1) and wheat harvests (Table 4.2). This analysis was completed to determine the effects of variable biomass levels incurred by varying the stripping plate spacing in corn or the cutter bar height in wheat. The results for the stripper plate spacing tests indicated that all passes had statistically similar grain yields. A similar analysis in wheat proved there was consistent grain yield regardless of the height of the cutter bar above the ground. Just as with the feeder house sensor, a test condition had been created where grain mass flow levels were held constant, while the amount of crop biomass introduced to the combine was varied. The cylinder sensor was able to detect the biomass flow variation induced by changing either stripper plate spacing in corn or cutting height in wheat. However, it appears the hydraulic drive pressure sensor does not have the same sensitivity as the chain tension sensor previously developed.

These initial results were somewhat assuring, since this test was designed to investigate the ability of the hydraulic pressure sensor to detect variations in the biomass flow. Reducing the stripper plate spacing or lowering the cutter bar will increase the amount of crop biomass fed into the harvester. This fact was evident as the 5 cm cutter bar height and the 2.5 cm stripper plate width always lead to the greatest amount of biomass being passed through the combine. The threshing cylinder hydraulic pressure sensor indicated there was also a significant difference in the narrowest stripping plate plots and the remaining plots about 67% of the time. The hydraulic pressure sensor succeeded in making a clear delineation between the 3.2 cm and 3.8 cm stripper plate settings. This delineation existed, although there was no apparent demarcation in the actual mass collected from the combine for the 3.2 cm and 3.8 cm plots. There was little variability in the signal coming out of this sensor, as it was even less than what was reported for the feeder house sensor.

During wheat harvest, the performance of the hydraulic pressure sensor was even more convoluted. The difference in biomass flow rates was evident in the samples that were collected after passing through the combine. By changing the cutter bar height, the biomass throughput increased by at least 800 kg/ha. The threshing cylinder sensor was able to detect a significant difference in the lowest cutter bar height. But the 20 cm and

35 cm values were essentially equal as far as this sensor is concerned. The key difference when lowering the cutter bar from 35 cm to 20 cm was a slight increase in the amount of wheat straw entering the combine. It appears that this additional amount of straw did not provide significant resistance to cause an increase in hydraulic pressure driving the threshing cylinder. On the positive side, the pressure sensor continued to output a stable, signal with low variability.

Based on this initial test, it appears the threshing cylinder required relatively large variations in biomass for a significant difference to register. It did not appear that this was a sensor issue, as improving the resolution of the sensor will not lead to better detection of crop mass flow changes. The sensitivity of hydraulic drive pressure variations to mass flow changes was less than that of the feeder house sensor. While this initial result is somewhat discouraging, it is important to verify these preliminarily findings with additional field testing. Also, there is still the possibility that this sensing methodology could still produce better results than the traditional mass flow sensor utilized by modern yield monitors.

Comparison to Yield Monitor Performance

A comparative examination was performed on the data collected during a corn field trial where the combine based through strips that alternated between maximum and minimum amounts of biomass (interval plots), and a second wheat test consisting of concurrent blocks of varying yield (ASABE X579 plots). The filtered cylinder drive pressure data were plotted along with yield data collected by the traditional mass flow sensor to determine if the sensor output tracked the variations of the blocking pattern. The sensor data were plotted against distance. The boundaries that divided the blocks of different crop biomass densities were added to the plot to establish the ability of both the hydraulic pressure sensor and yield monitor to detect changes in material throughput. Plots for the 2.5 km/hr, 5.0 km/hr, and 6.5 km/hr trials for both corn and wheat are shown in Figures 4.11 and 4.12.

Table 4.1. Comparison of cylinder drive sensor output at varying stripping plate widths in corn.

Threshing Cylinder Hydraulic Drive Pressure Sensor				
Stripping Plate Width (cm)	Replication	Avg. Reading (volts)	Std. Deviation (volts)	Significantly Different From*
2.5 cm	1 2 3	3.35 3.34 3.30	0.06 0.08 0.07	3.2(1), 3.8
3.2 cm	1 2 3	3.25 3.28 3.27	0.07 0.06 0.07	2.5(1,2)**, 3.8
3.8 cm	1 2 3	3.20 3.19 3.20	0.05 0.07 0.07	ALL
Traditional Grain Mass Flow Sensor				
Stripping Plate Width (cm)	Replication	Avg. Reading (kg/s)	Std. Deviation (kg/s)	Significantly Different From*
2.5 cm	1 2 3	5.74 5.32 5.55	0.63 0.61 0.60	None
3.2 cm	1 2 3	5.50 5.48 5.63	0.58 0.65 0.62	None
3.8 cm	1 2 3	5.37 5.68 5.48	0.58 0.61 0.54	None
Field Collected Samples				
Stripping Plate Width (cm)	Replication	Amount of Biomass (kg)	Normalized Biomass (Mt/ha)	Significantly Different From*
2.5 cm	1 2 3	53.82 53.63 54.27	3.05 3.04 3.07	3.2, 3.8
3.2 cm	1 2 3	44.14 37.66 45.62	2.50 2.13 2.58	2.5, 3.8(2,3)**
3.8 cm	1 2 3	43.21 40.28 38.64	2.45 2.28 2.19	2.5, 3.2(1,3)

* Significance tested at $\alpha = 0.05$; ** refers to a specific replicate

Table 4.2. Comparison of threshing cylinder sensor output at varying cutter bar heights in wheat.

Threshing Cylinder Hydraulic Drive Pressure Sensor				
Cutting Platform Height (cm)	Replication	Avg. Reading (volts)	Std. Deviation (volts)	Significantly Different From*
5 cm	1 2 3	3.30 3.30 3.31	0.07 0.08 0.05	20 cm, 35 cm
20 cm	1 2 3	3.25 3.23 3.25	0.03 0.06 0.08	5 cm
35 cm	1 2 3	3.24 3.23 3.26	0.10 0.05 0.09	5 cm
Traditional Grain Mass Flow Sensor				
Cutting Platform Height (cm	Replication	Avg. Reading (kg/s)	Std. Deviation (kg/s)	Significantly Different From*
5 cm	1 2 3	3.39 3.51 3.42	0.31 0.37 0.29	None
20 cm	1 2 3	3.43 3.41 3.37	0.33 0.26 0.26	None
35 cm	1 2 3	3.39 3.42 3.48	0.29 0.28 0.30	None
Field Collected Samples				
Cutting Platform Height (cm	Replication	Amount of Biomass (kg)	Normalized Biomass (Mt/ha)	Significantly Different From*
5 cm	1 2 3	48.65 62.47 36.54	2.62 2.74 2.67	20 cm, 35 cm
20 cm	1 2 3	51.78 50.87 49.20	2.15 2.27 2.24	5 cm, 35 cm
35 cm	1 2 3	34.10 33.52 34.99	1.49 1.47 1.53	5 cm, 20 cm

* Significance tested at $\alpha = 0.05$; ** refers to a specific replicate

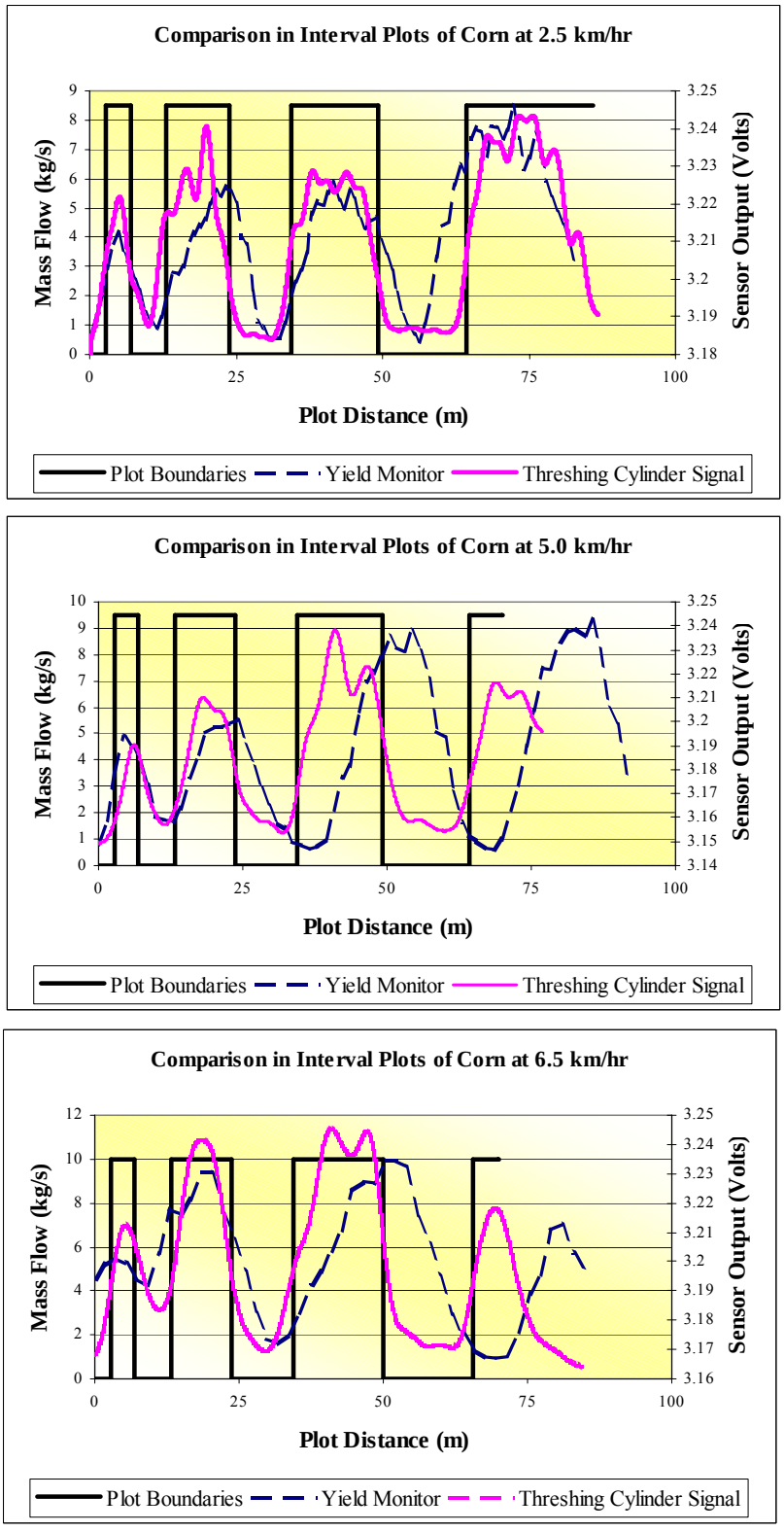

Figure 4.11. Comparison of yield monitor and threshing cylinder sensor performance in interval plots of corn at varying ground speeds.

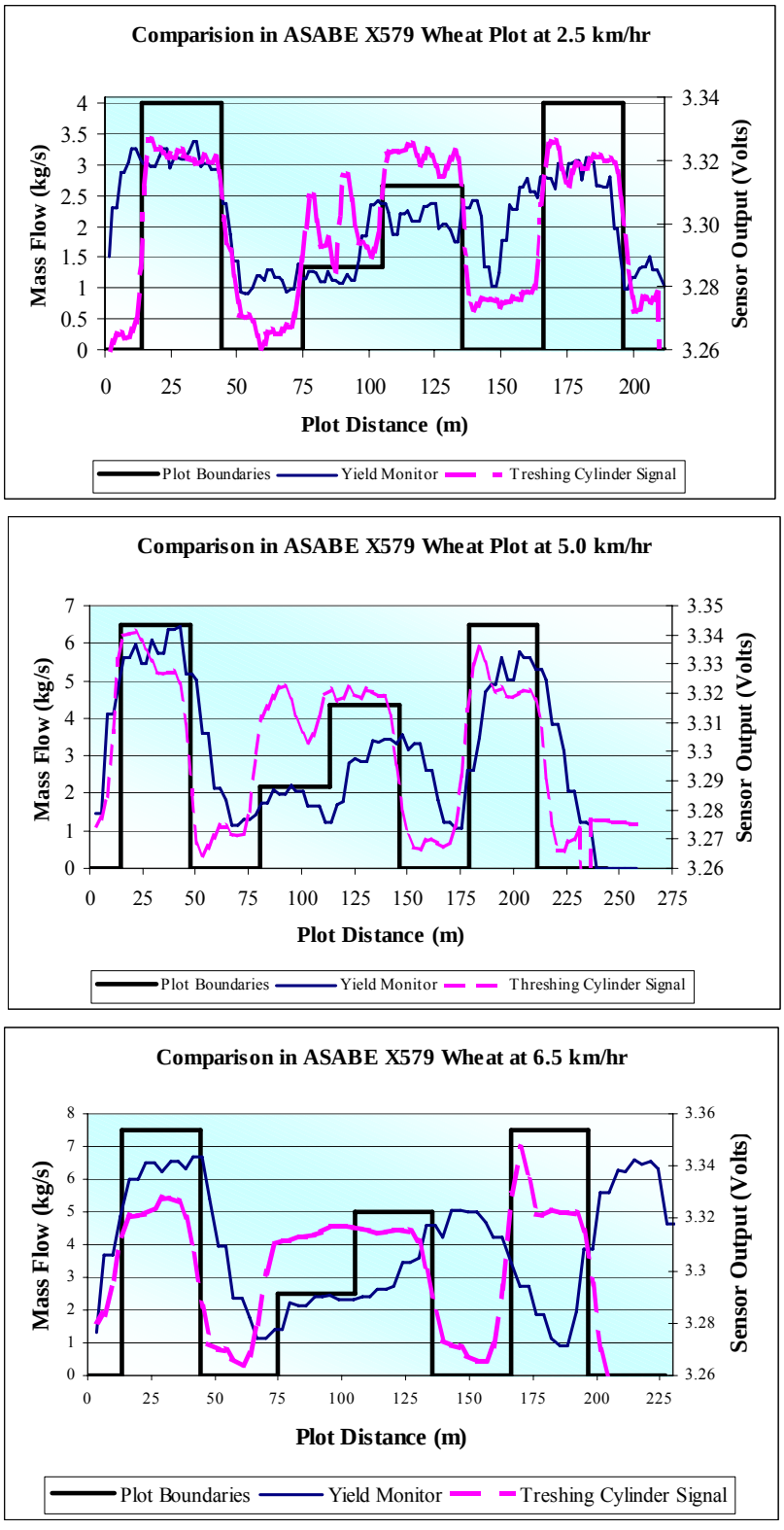

Figure 4.12. Comparison of yield monitor and threshing cylinder sensor performance in ASABE X579 wheat plots at varying ground speeds.

Initial observation of Figures 4.11 and 4.12 show a number of trends that were also apparent in the feeder house data analysis. This is especially true for the yield monitor data, as there is still an increase in mass flow when the machine velocity increases. Also, the lag in transition between full and empty corn blocks in the interval plots increases as the combine moves through the plot. By the end of the intervals plots, the yield monitor data suggests an empty block is full of grain and a full block is empty. This effect is more pronounced at higher ground speeds. The ability for the yield monitor to consistently produce the same mass flow value in blocks of equal biomass is questionable at best. The middle illustration in Figure 3.11 shows maximum grain flow rates of 5, 5.5, 9, and 9.5 kg/s in the 100% blocks. This field trial was set up so that these flow rates would be equal.

The hydraulic drive pressure sensor is an improvement over the yield monitor signal. Again, the alternative sensor produces much quicker transitions between the blocks and as a result it is able to follow the mass flow pattern induced by the field trial. One interesting aspect of the hydraulic data is the fact that it appears to act independent of combine velocity. This is another instance where the sensitivity of the hydraulic pressure as a crop mass flow detection method can be called into question. As speed increases, feed rate into the machine increases, yet at best there is a negligible change in the sensor output. The hydraulic pressure sensor displays analogous values for the 33% and 67% blocks in the ASABE X579 wheat plots. The threshing cylinder acts like a device that operates in a few discrete states. Based on this data it would appear the threshing cylinder is either full, empty, or somewhere in the middle.

Notched box plots were developed within Matlab to show how the variability of the two data streams varied while harvesting the plots. Typical box plots associated with corn and wheat harvests are provided in Figures 4.13 and 4.14. In the first series of box plots (Figure 4.13), the data were collected in corn interval plots. This yield monitor data suffers from severe inconsistency, and an inability to distinguish the blocking pattern used to establish the plot. The notches indicate the median value for many of the 100% blocks and 0% blocks are statistically similar ($\alpha = 0.05$). Unlike the yield monitor box plot, the threshing cylinder plot had a clearly discernable pattern of alternating blocks. Also, the threshing cylinder sensor produced less variation and had a reproducible signal in the plots with no biomass present. However, the median cylinder drive sensor value wass inconsistent when it comes to the 100% blocks. The

pre- and post- sections of the hydraulic pressure sensor data were more conforming to the actual test situation.

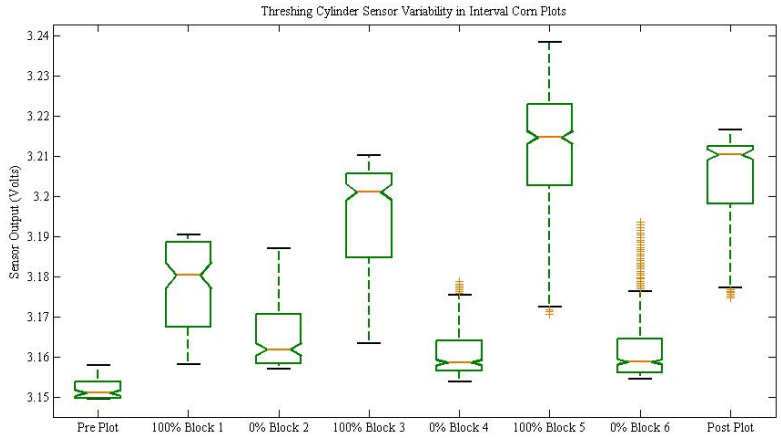

a) Cylinder Drive Pressure Sensor

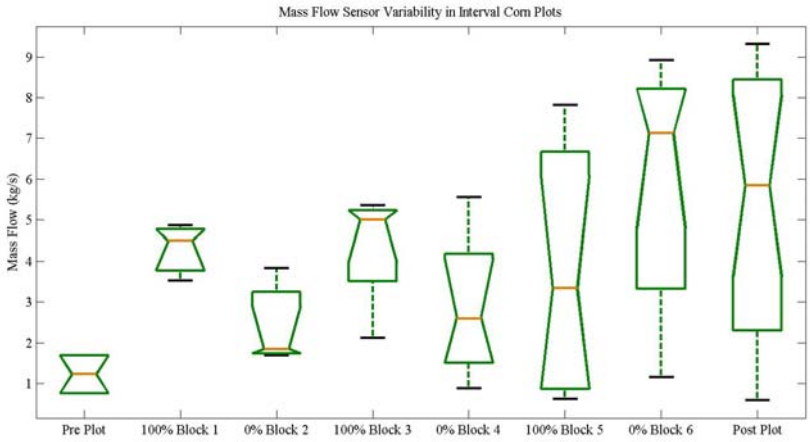

b) Grain Mass Flow Sensor

Figure 4.13. Boxplots of yield monitor and threshing cylinder sensor performance in interval corn plots.

In the second set of box plots (Figure 4.14), the data were collected while harvesting ASABE X579 wheat plots. The yield monitor data still had the problem of too much variability and the ability to easily determine the mass flow pattern established in the field was absent. The repeatability of the signal in blocks of equal biomass was also questionable in the yield monitor data as was the extreme variability in block 5, a block with no biomass flowing through the combine. The pre-plot block also exhibited noteworthy signal variability although no grain was present as the combine initially entered the plot.

The cylinder drive pressure sensor data was superior for reduced variability and better signal reproducibility given equivalent crop biomass feed rates. This point was particularly true at the zero flow rate, where the sensor always goes below 3.28 V. The main concern was this idea of the finite, discrete operating states. There are only three levels present in the box plot. The 67% block was clearly similar to the 100% blocks. The 33% block's media value appeared to fall in between the two extreme values. This reinforced the concern that the drive pressure required to turn the threshing cylinder can only determine if the cylinder was empty, partially full, or completely full. The reduced sensitivity compared to the feeder house sensor continues to be a major theme of this investigation. Although this sensitivity was a critical issue, the pressure sensor still had the advantage of generating relatively quick and definitive transitions between the blocks.

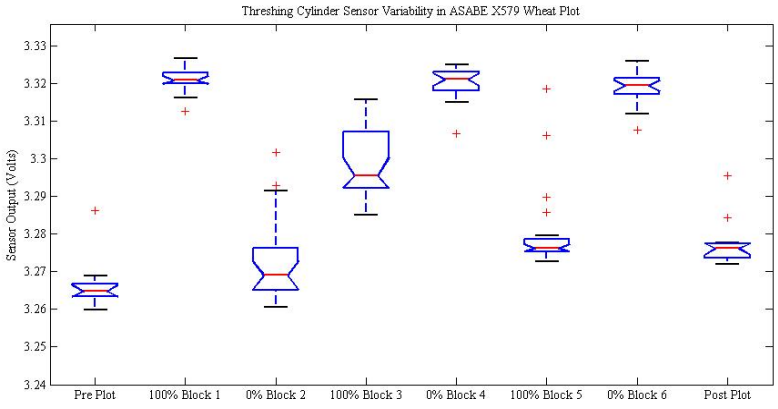

a) Cylinder Drive Pressure Sensor

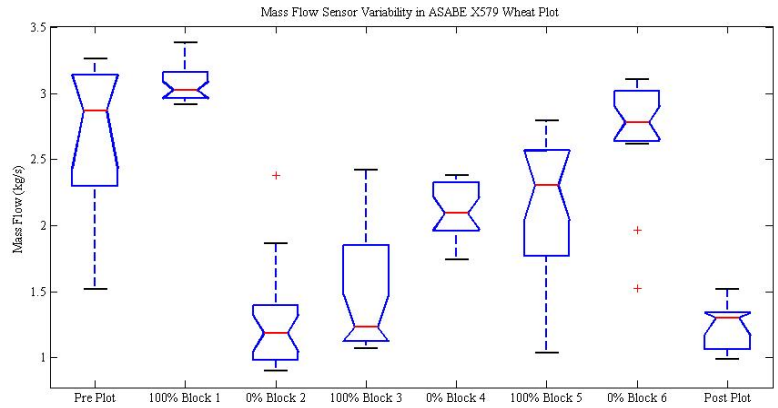

b) Grain Mass Flow Sensor

Figure 4.14. Boxplots of yield monitor and threshing cylinder sensor performance in ASABE X579 wheat plots.

Additional statistical analysis of the data was conducted to determine if significant differences existed between the blocks of ASABE X579 wheat plots as well as the different combine ground speeds. This same statistical analysis was also carried out on data collected while harvesting corn interval plots. This analysis was conducted on both the cylinder drive pressure and impact plate data sets. The results of these tests are presented in Table 4.3 (corn) and Table 4.4 (wheat). Included in these tables are the results of a Fisher's Least Significant Difference (Devore, 1999) test to determine how well each sensor was able to detect differences in the blocking scheme. Not shown in the table are the results from a speed comparison test. While machine velocity was a significant factor affecting the mass flow rate for the yield monitor data, the cylinder drive pressure did not appear to vary significantly with machine speed. This was the first statistical test that has proven the much discussed lack of sensitivity that is apparent when using hydraulic pressure to determine crop biomass feed rate.

The results of the analysis on the interval plot corn data were very surprising. When alternating between minimum and maximum plots of crop biomass, the grain mass flow data showed similarity between each block and at least one block that had the exact opposite field condition. Blocks 1, 3, and 5 had 100% crop biomass levels, however a significant statistical difference between these blocks and block with zero biomass present could not be determined. The other concerning fact, was that there are yield monitor blocks whose mean mass flow were statistically different even though the field trial was set up with zero grain or biomass in the block. Another recurring theme in this manuscript is the inability for the yield monitor to achieve a zero grain mass flow value in zones with a zero crop feed rate. There were three zero zones developed in these interval plots, and the lowest recorded yield monitor mass flow rate was 2.44 kg/s.

Unlike the traditional impact plate sensor, the cylinder drive pressure sensor was capable of sensing transitions from a block of no biomass and a block of maximum biomass. Also, the signal from the cylinder drive pressure sensor had very little variability compared to the yield monitor signal. The ability of the threshing cylinder drive to return to the same pressure for each zero flow or high flow block is also evident when viewing the data in Table 4.3. It appears that cylinder drive pressure can be an indicator of relatively large scale variations in crop feed rate into the combine. The main concern at that point was whether or not the sensitivity was present to detect smaller scale variations.

Table 4.3. Statistical comparison of traditional impact plate sensor and threshing cylinder hydraulic pressure sensor performance in interval corn plots.

Portion of Block Covered with Crop	Traditional Impact Plate Sensor			Threshing Cylinder Drive Pressure Sensor		
	Mean Mass Flow (kg/s)	C.V. (%)	Different from Blocks	Mean Output (Volts)	C.V. (%)	Different from Blocks
100 %	4.30	16 %	None	3.21	9 %	0%
0%	2.44	39 %	0% (3)*	3.16	14 %	100%
100 %	4.30	29 %	None	3.22	11 %	0%
0%	2.80	57 %	0% (3)*	3.15	10 %	100%
100 %	3.65	78 %	None	3.22	13 %	0%
0%	5.88	50 %	0 % (2,4), 100%(3)	3.16	11 %	100%
	LSD = 2.11 kg/s at $\alpha = 0.05$			LSD = 55 mV at $\alpha = 0.05$		

* A value in parenthesis refers to a specific 0% or 100% block, if no parenthesis is present then the value is significantly different from both occurrences.

Data collected during harvest of the ASABE X579 wheat plots allowed for a closer look at smaller changes in crop feed rates. Upon inspection of the wheat data analysis in Table 4.4, it was obvious that the yield monitor still had difficulty when it came to the measurement precision. The two instances of 100% blocks and 0% blocks are statistically different when the yield monitor data was considered. The traditional grain mass flow signal did detect a change from the 33% block to the 67% block, but closer observation revealed the 33% block had nearly the same mean grain mass flow value as the first 0% block. The yield monitor continued its tendency of operating with considerable variation within the blocks compared to the hydraulic pressure data.

The threshing cylinder drive pressure sensor correctly identified both 0% blocks and both 100% blocks as not being statistically different. Also, the 0% blocks were statistically different from all the other blocks making up the ASABE X579 wheat plot. The remaining plots, the 33% and 67% plots, are similar with each other and the 100% blocks. This evidence represented firm, statistical proof that threshing cylinder pressure cannot be used to sense minor variations in crop biomass feed rate. Measurement precision does not appear to be a factor and neither does the sensitivity of the pressure transducer. The underlying issue was that the threshing cylinder

requires a minimal amount of crop biomass feed rate to increase the hydraulic pressure drive at the cylinder. This threshold level seemed to be more than the typical variation that may be seen in the field. Therefore, the use of cylinder drive pressure as a means to detect crop biomass feed rate variations was at best marginal, especially compared to the performance of the feeder house chain tension sensor.

Table 4.4. Statistical comparison of traditional impact plate sensor and threshing cylinder hydraulic pressure sensor performance in ASABE X579 wheat plots.

Portion of Block Covered with Crop	Traditional Impact Plate Sensor			Threshing Cylinder Drive Pressure Sensor		
	Mean Mass Flow (kg/s)	C.V. (%)	Different from Blocks	Mean Output (Volts)	C.V. (%)	Different from Blocks
100 %	3.08	14 %	ALL	3.34	11 %	0%, 33%
0%	1.29	32 %	67%, 0% (2)*, 100%	3.23	4 %	33%, 67%, 100%
33 %	1.48	35 %	67%, 0% (2), 100%	3.28	3 %	0%, 100%
67 %	2.13	19 %	0%(1), 33%, 100%	3.31	7 %	0%, 100% (1)
0 %	2.17	26 %	0%(1), 33%, 100%	3.24	9 %	33%, 67%, 100%
100 %	2.67	17 %	0%, 33%, 67%, 100%(1)	3.33	6 %	0%, 33%
	LSD = 0.45 kg/s at $\alpha = 0.05$			LSD = 30 mV at $\alpha = 0.05$		

* A value in parenthesis refers to a specific 0% or 100% block, if no parenthesis is present then the value is significantly different from both occurrences.

Yield Monitor – Threshing Cylinder Signal Correlation

Further investigation was completed to determine if there was any type of relationship between the hydraulic pressure data and the traditional mass flow data. Figure 4.15 illustrates the relationship between cylinder drive pressure sensor and the grain mass flow data collected during the various field activities associated with this project. As before, randomly selected, steady-state flow data were selected for analysis. Both combine velocity and the type of crop that was being harvested were considered when developing this analysis.

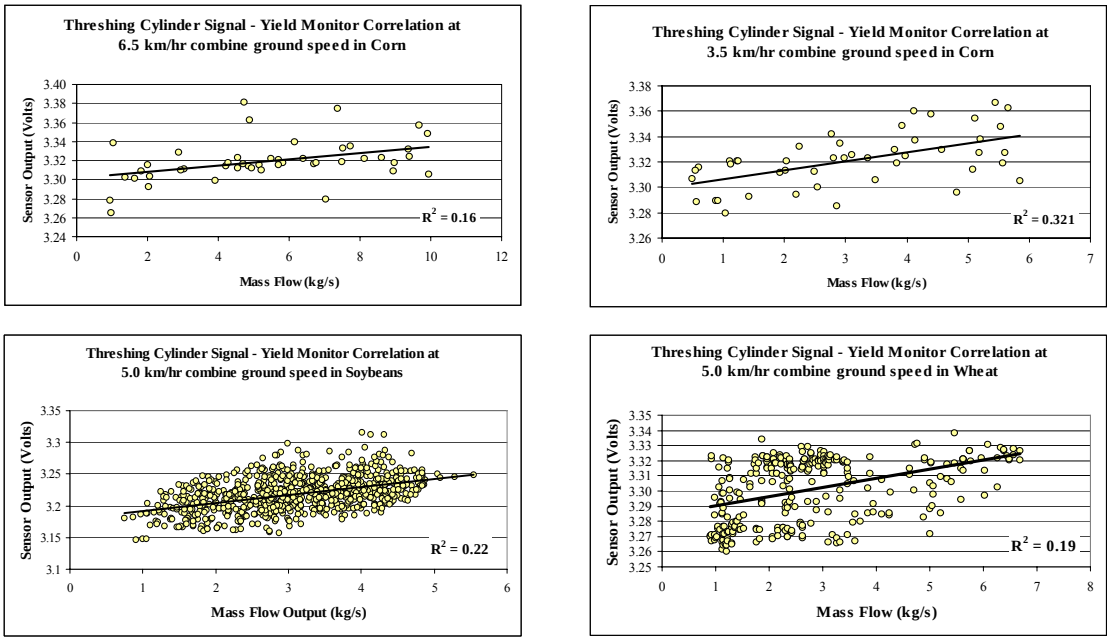

Figure 4.15. Crop biomass and grain mass flow relationship in three grain crops as interpreted by the threshing cylinder pressure sensor.

The figure does suggest a weak linear relationship between two data sets, however with R^2 values ranging between 0.16 and 0.32 there is very little correlation. This is an even weaker relationship than the indefinite relationship between grain mass flow and the feeder house signal. Part of the fault lies in comparing or attempting to develop a relationship between two imperfect measurements. But this result may also be attributed to the threshing cylinder operation at near constant drive pressure levels under varying grain mass flow conditions.

Comparison to Feeder-House Sensor Performance

The cylinder drive pressure sensor was developed as an alternative to the feeder-house-based sensor discussed in Chapter Three. For the purposes of directing future research efforts, it was necessary to compare the performance of these two sensing methods to determine if one method is superior. There were indications that the cylinder drive pressure sensor did not possess the same degree of sensitivity to crop mass flow changes as the feeder house based sensor. Data compiled from Chapters 3 and 4 are presented to further support this claim by means of a more direct comparison. Figure 4.16 provides box plots representing cylinder drive pressure sensor and feeder house sensor data collected simultaneously from an ASABE X579

wheat trial. From observation, the feeder house data represents the actual X579 blocking scheme. The most important box plots to note are Blocks 3 and 4. These two blocks represent crop biomass levels that are between the extreme values. The cylinder drive pressure data shows increased variability and Block 4 with 67% crop biomass has a reading similar to Blocks 1 and 6 with 100% crop biomass.

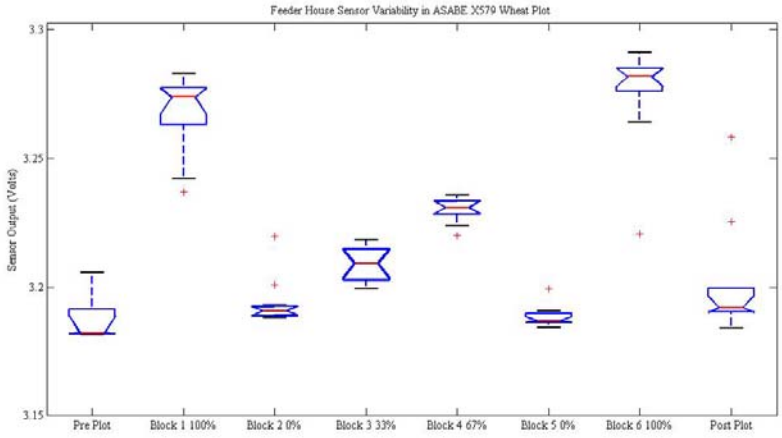

a) Feeder House Chain Tension Sensor

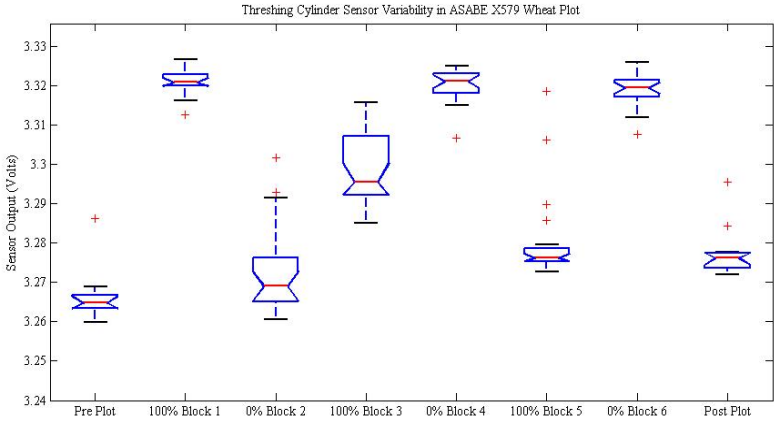

b) Cylinder Drive Pressure Sensor

Figure 4.16. Boxplots of feeder house and threshing cylinder sensor performance in ASABE X579 wheat plots.

The variability of the signal within a particular test block was nearly identical to the feeder house sensor. Furthermore, the transition from minimal flow to maximum flow was crisper with the hydraulic pressure senor. However, while there are positives to hydraulic pressure sensing, the inability for the cylinder drive pressure signal to consistently delineate

between these intermediate crop biomass blocks was ultimately its downfall. Therefore, when grain mass flow data correction was considered, it will be based off the feeder house signal.

Summary

This component of the research project was designed to find a second supplemental sensor that measures crop material mass flow through a grain combine in the hopes that the sensor's output could be used to correct grain mass flow rates collected by a yield monitor. The motivation behind the threshing cylinder drive pressure sensing was the fact that this sensing method is much easier to implement on a wide range of grain combines compared to the feeder house sensor. Tests to evaluate the sensitivity of the cylinder drive pressure sensor were developed and comparisons between this sensor, the feeder house-based sensor, and the traditional mass-flow sensor were completed. Based on the testing completed during this study, the following conclusions were made:

- Relatively large variations in crop biomass throughput were detected by the cylinder drive pressure sensor, but because of the magnitude of the detectable variations, the sensitivity of hydraulic pressure to biomass fluctuations must be questioned.
- When detected, the transitions between blocks were faster and more stable for the threshing cylinder sensor versus traditional grain mass flow data.
- The cylinder drive pressure sensor operates with 25 to 40% reduced variability when compared to traditional grain mass flow data.
- The cylinder drive pressure sensor did perform better than feeder house sensor in the area of feed spike rejection. The cylinder drive pressure did not exhibit sudden, unexplainable spikes for any of the data sets collected.
- Evidence from this study reinforces the positive aspects of the feeder house sensor as it can detect smaller variations in crop biomass feed rate and is obviously the superior sensing method.

Chapter Five

Redistribution of Yield Monitor Mass Flow Using Sensor Fusion

Introduction

Thus far the main focus of this dissertation has been the development of two mass flow sensing alternatives that can detect variations of crop material feed rate into a grain combine while avoiding many of the errors that plague current yield monitoring technology. Both the feeder house-based drive chain tension sensor and the threshing cylinder drive pressure sensor have shown the potential to sense changes in biomass flow through the combine. Performance deficiencies associated with the yield monitor were also highlighted, as the yield monitor's signal rarely matched the flow characteristics of the associated test profile. Although yield monitor problems are well documented, the data generated by the mass flow sensor is the most accurate source for the true grain mass flow. The sensors developed in the preceding chapters are sensing both grain and MOG flow. The focus then shifted to how the crop mass flow rate data can be used to adjust or redistribute the grain mass flow data to improve the spatial accuracy of yield monitor data.

Most current yield monitor correction procedures use simple limit filters, which delete errant data points exceeding threshold limits and arbitrary delay time shifts are applied until the map "looks right." Usually, these delay shifts are applied to individual combine passes until features like waterway boundaries or driveways align. While these methods may produce yield maps that are more visually appealing, they do not account for how these variable delay times or excessive data point values affect the grain distribution the yield map is intending to exhibit. At this time, it would appear that the feeder house sensor provided the best source of data for correction of yield monitor data. The feeder house chain tension sensor could be used to determine if a grain mass flow rate value appears excessive and correct the combine's variable delay time. Also, the tension on the feeder housing drive chain was more sensitive to biomass rate variations than the cylinder drive pressure measurement.

It seems that integrating the data collected by the alternative crop feed rate sensor and the traditional grain mass flow sensor would produce a more complete, accurate representation of the

grain mass flow profile. These sensory methodologies have a complimentary relationship. This relationship allows multiple sensors to operate independently, yet the sensor data can be fused to improve overall system accuracy. The purpose of this chapter is to investigate the utility of fusing data from the various mass flow sensors on the combine to produce accurate mass flow data.

Sub-Objectives

The feeder house-based sensor developed in Chapter Three produced stable, accurate data that has the ability to distinguish zones of differing crop biomass throughput better than the traditional grain mass flow and cylinder drive pressure sensors tested in this manuscript. It seemed that these data could be used to correct spatial distribution flaws in traditional grain mass flow data by redistributing grain mass flow data to mimic biomass flow patterns. The specific objectives for this portion of this project were:

1) Investigate sensor fusion methods that could be used to improve the spatial accuracy of grain mass flow data,
2) Develop an algorithm that uses crop biomass feed rate data collected by the feeder house sensor to redistribute the grain mass flow data more accurately, and;
3) Evaluate this correction under both field plot trials and regular full field harvests.

Methodology

A total of three mass flow redistribution methods using sensor fusion were studied. The underlying process, the justification, and an example illustrating the correction will be provided as the methodology is discussed. The three mass flow redistribution methods investigated were: variable delay time, Kalman filtering, and a relative comparison method. The specifics for each method will be discussed as each one represents an evolutionary step towards the final correction method.

The initial correction development focused on a post-processing algorithm to achieve the grain mass flow redistribution. The main reason for selecting the post-processing method was the availability of the data sets. The crop mass flow data generated by the sensors developed in Chapters Three and Four were archived in a separate file scheme and need to be merged with the

traditional mass flow data following harvest. The preliminary decision was to develop a platform independent correction algorithm to combine the two data sets. By using this approach, the end-user should be able to use a common software package such as Microsoft Excel, ESRI ArcGIS, or Matlab to redistribute the mass flow. Matlab was selected as the development environment for this code. The sensor fusion process would ideally occur real-time within the yield monitor; however, the proprietary nature of yield monitor data processing prevented this form of correction.

Besides the selection of a correction philosophy, there was a series of initial ground rules established to serve as the foundation of the correction algorithm. The first two assumptions focused on the data collected by the traditional mass flow sensor. These assumptions are:

1) Any mass recorded by the yield monitor exists and should not be deleted for simplicity's sake (i.e. conservation of mass), and;
2) Proper yield monitor calibration has occurred, insuring the grain mass flow measurement is accurate (as specified in manufacturer's literature).

Often, traditional mass flow processing programs, such as Ag Leader Technology's Spatial Management System (SMS), utilizes a filter to eliminate mass flow data that occurs beyond certain threshold values. This type of filtering is typically used when the combine is emptying after crop intake has ceased and the grain stream begins a slow decline. There is still value in this mass flow data as it is a measurement of grain produced in the field. Because of the combine's throughput lag, this trailing off grain stream is not indicative of the grain yield at a given point. Somehow, low mass flow values occurring as the combine empties must be reassigned to data point locations where the grain entered the combine.

Variable Delay Time

The first correction method was inspired through visual inspection of plots comparing the traditional mass flow profile to the feeder housing feed rate profile. An example of this plot is shown in Figure 5.1. The variable delay that is evident in the yield monitor data has been described by numerous researchers (Searcy et. al, 1989, Birrell et al., 1995, Whelan and McBratney, 1997, 2002, and Arslan and Colvin, 2002a, 2002b). Basically, the delay time on the initial filling (yield data points at distances less than
13 m) is too long and should be shortened to place the mass data farther into the test plot. While

emptying (red arrows), the delay time needs to be lengthened to place the mass flow data within the preceding block. Because of variable delay times while emptying, the yield monitor data appears to continue well past the end of the test plot. The test plot ends at 212 m; however, yield monitor mass flow data is collected up to 235 m. Excessive delay time causes the yield monitor to log data prior to the start of the plot. Because of the combine initially filling, the initial mass flow readings are assigned to GPS positions logged prior to the combine entering the plot.

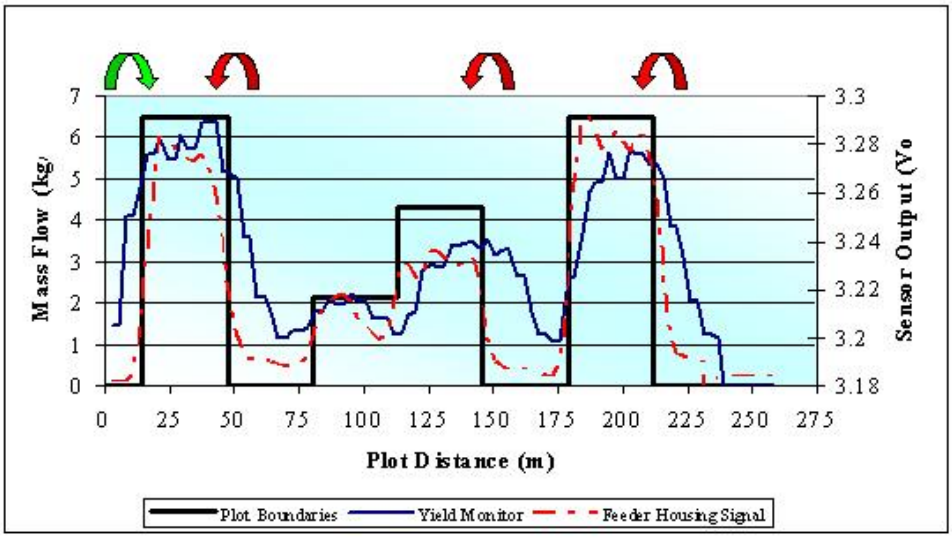

Figure 5.1. Effects of delay time variability on grain mass flow profile.

Current yield data processing software uses different transport delay times at the beginning and end of harvest segments to account for delay variations associated with the combine's threshing and separating mechanisms filling and emptying. The basic idea behind this method was to apply this same data processing scheme to points within the pass that are associated with the combine transitioning between emptying, filling, and steady-state mass flow. The feeder house rate data played an important role in the application of a variable delay time. The crop mass feed rate was used to delineate a transition to a filling, emptying, or steady-state crop mass flow within the combine. Therefore, while under steady-state conditions, the default 12 s delay time was used. Once a filling profile is identified the delay time is reduced to 7 s and for emptying profiles a 20 s delay time was applied to the data set. Figure 5.2 shows that application of the variable delay time correction in wheat.

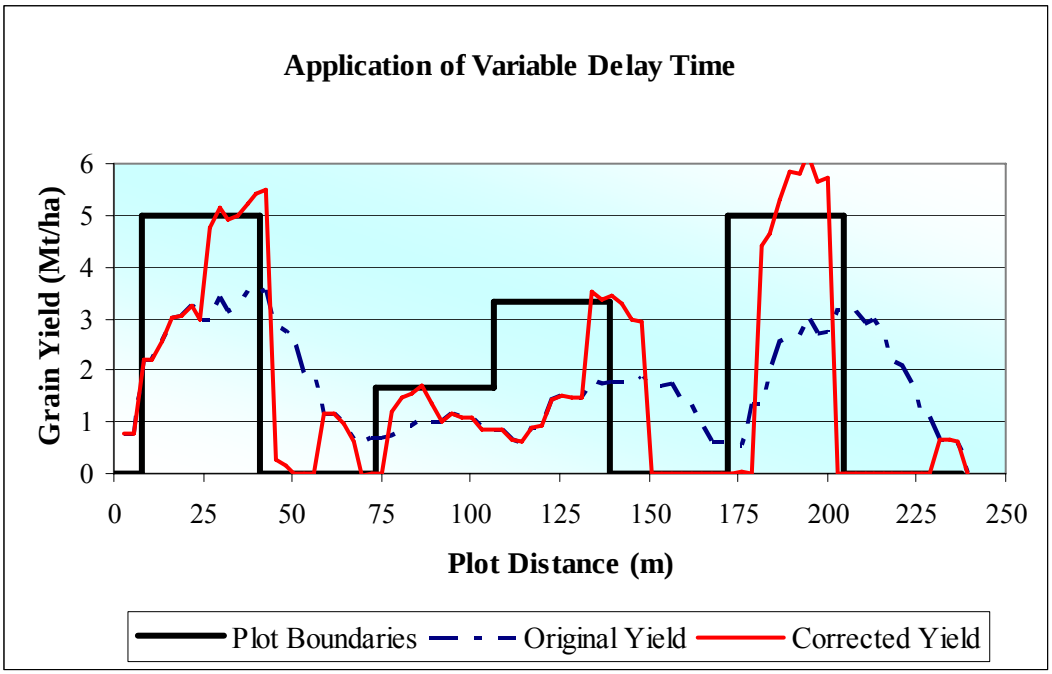

Figure 5.2. Using variable delay times to redistribute mass flow data in a ASABE X579 wheat plot.

Development of this correction approach, variable delay time, was terminated when it became apparent the approach did not produce acceptable results. The main reason was the variability of delay time is too great to apply constant values while the combine is at steady-state flow or filling or emptying. While the yield data could be somewhat rearranged to conform to the plot boundaries, there are too many errors with the actual movement of the mass. Primarily, there is no feedback with regard to how this mass is being redistributed. If this delay time approximation is erroneous, then mass is shifted into blocks with zero biomass present. There is also the question of how much mass should be moved. This method only focuses on shifting mass in the transitional area. Therefore, mass flow anomalies in the middle of a block are not addressed. Also, this method does correct baseline mass flow errors, such as the inability for the yield monitor to measure zero mass flow in the blocks with no biomass present.

To improve on the idea of using variable delay times, a more intensive comparison between grain mass flow and feeder house material throughput was needed. The next method utilized Kalman filtering. The Kalman filter should allow improved transition accuracy as well as better overall mass distribution because it will compare the two signals more intensely. This correction routine represents a classic approach to sensor fusion.

Kalman Filter Correction

A Kalman filter is a recursive algorithm that attempts to describe the current state of a system based on previous measurements that are subject to noise (Welch and Bishop, 2002). Two sets of equations are required to implement a Kalman filter: (1) time update equations, and (2) measurement update equations. The time update equations are used to update predictions about the future state of the system and the associated covariance. The measurement equations provide feedback regarding the status of the system which is the basis for revised predictions. For each measurement at a time step, k, the projected system state and covariance are updated.

The optimal setting for Kalman filter use occurs when the noise for both the process and measurement is white and normally distributed. When using a Kalman filter the goal is to estimate the state of the process while reducing the mean of the squared error. This can be done for most systems even if the nature of the system is unknown. Another key element for this filter is that it can be used to assess the past, present, and future states of the process in question. The Kalman filter presented below is for linear systems, $f(a+b) = f(a) + f(b)$.

For this correction method, the feeder house crop mass flow signal will be used to project the future grain mass flow values between yield monitor points. The yield monitor points will be used as the measurement update equation to assess the true grain mass flow condition. The discrete time process that the Kalman filter attempts to estimate is described as:

$$x_k = Ax_{k-1} + Bu_{k-1} + w_{k-1}$$

Equation 5.1

$$z_k = Hx_k + v_k$$

"A" represents the relationship between the current state and the previously occurring state of the process, "B" represents the relationship between an optional control input and the current state output, H is a term for the relationship between the measurement and the process state, and "w" and "v" are the normally distributed noise functions with covariance's Q and R respectively.

Equation 5.1 is the initial framework from which all necessary equations for the Kalman filter are derived. Typically the actual filter is expressed as

$$x_{k+1} = x_{k-1} + K(z_k - Hx_{k-1}) \quad \textbf{Equation.5.2}$$

Equation 5.3 describes how the Kalman filter works. It attempts to estimate the future status of a process by using previous state values and the current measurement information. The ($z_k - Hx_{k-1}$) term is known as the residual and is defined as the difference between the actual and predicted measurements. K represents the gain. The K value is selected in a manor to minimize the *a posteriori* (future predicted value) estimate error covariance. This covariance term is a function of the difference between the estimated and true values of the predicted term, x_k. The Kalman gain is calculated using the following term:

$$K = \overline{P}_k H^T (H\overline{P}_k H^T + R)^{-1} \quad \textbf{Equation.5.3}$$

Within the Kalman gain there is a new term, P_k. This term is estimate error covariance. In the Kalman filter the gain is calculated from the preceding estimate error covariance, then a new error covariance is calculated from the following.

$$P_k = (1 - KH)\overline{P}_K \quad \textbf{Equation.5.4}$$

The key to using this filter is that the designer has to estimate the initial values for the covariances associated with the system noise (Q), measurement noise (R), and the error estimate (P). In real-life applications, the covariance of the noise, R, is usually known or estimated prior to the filter being used. As the measure covariance is better understood, the algorithm performance also improves. This may be the easiest of all parameters to collect and analyze so a thorough investigation is necessary. The process covariance is usually hard to estimate, so a designer has to use discretion in the selection of a "Q" value. This is essentially the only place that filter tuning can occur.

In a Kalman algorithm there are two updates to the model, a prediction update and a measurement update. Using a feedback control scheme, a Kalman filter makes a prediction then uses a "noisy" measurement to correct the prediction. In this instance, the Kalman filter is used to project the future grain yield based on biomass flow rates collected in a noisy environment. The model assumes future yield is a function of the previous yield measurement.

Once these matrices have been established, the user has to define the values for the process and measurement error covariances as well as form an initial estimate error covariance matrix. Note that the degree to which these terms are known is highly questionable and often the designer uses trial and error to establish the proper values. There is a process of system identification that utilizes a secondary Kalman filter to assist with these estimates. This process is highly complex but Matlab has tools capable of setting up a system identification protocol and establishing the initial values. Once these terms are established it is time to calculate the Kalman Gain, K_k using Eqn. 5.3. Next Eqn 5.2 is used to update the estimate and a new error covariance, P_k, is calculated using Eqn 5.4. Finally a new projection is made along with a new projection error estimate. Figure 5.3 shows the corrected grain mass flow profile that is the result of Kalman filtering.

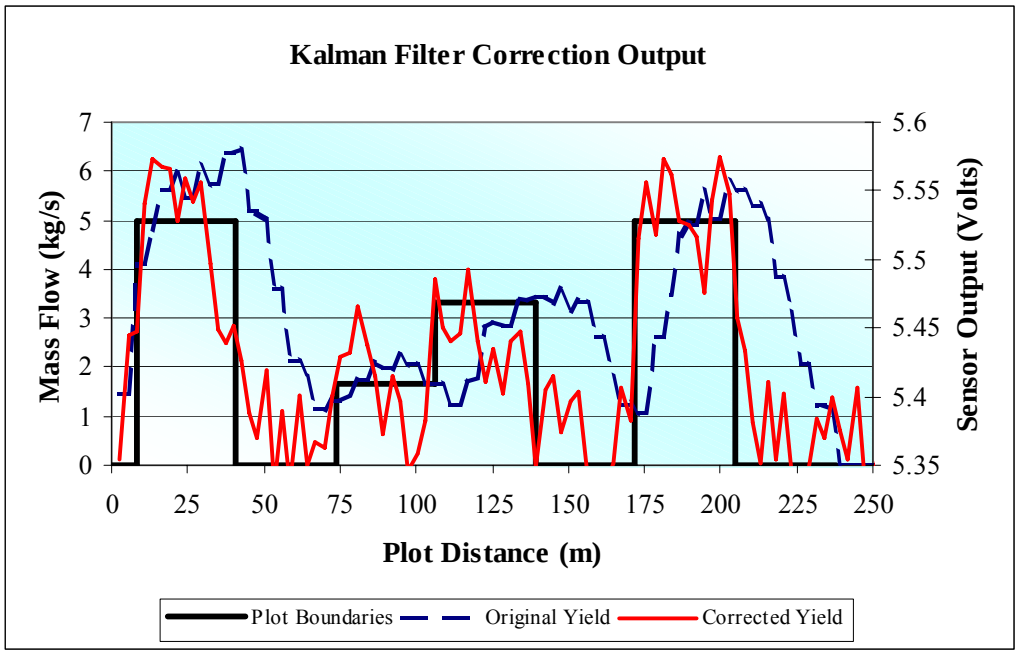

Figure 5.3. Using the Kalman filter to redistribute mass flow data in a ASABE X579 wheat plot.

Figure 5.3 shows an initial correction that occurs after applying the Kalman correction to yield monitor data collected while harvesting an ASABE X579 wheat plot. There is an obvious problem with this type of correction. Essentially, this filter arbitrarily forces the grain mass flow data to follow the profile of the crop biomass flow profile. At the end of Chapters 3 and 4 the

relationship between the grain mass flow and biomass flow was discussed in detail. At best this relationship is suspect and under certain harvest conditions it is virtually non-existent. The other Kalman filter problem is violation of the conservation of mass principle. To shape the grain mass flow profile, this filter is arbitrarily varying mass flow rates with no regard for mass balance. There is no accumulation of excess mass for later distribution to areas that are in need of additional mass. More simply, mass redistribution is non-existent.

The failure of the Kalman filter can be attributed to the use of a measurement that is not truly indicative of grain mass flow. The filter would perform better if the two data sets were obtained from two different types of grain mass flow sensors located in the clean grain elevator. Crop biomass flow and grain mass flow are simply too dissimilar to be effectively utilized in a Kalman filtering routine. Value in using biomass and grain mass flow rate comparison for correction purposes remains, but the Kalman filter happens to be a poor comparison method to use.

One of the correction routine improvements needed is the ability to accumulate excessive mass and redistribute this mass in areas that are grain deficient. The second improvement would be a comparison that does not attempt to force grain mass flow into the biomass flow profile. This could be accomplished by using relative differences between shifts if crop biomass flow to redirect grain mass flow. For example consider 60% of the maximum expected biomass is entering the combine in one block then as the combine enters the next block the crop biomass input drops to 40% of the maximum expected value. Instead of forcing each block to have 60% and 40% levels of grain mass flow (i.e. the result of the Kalman filter), this method ignores relative levels, rather it would make sure a 20% drop in grain mass flow occurs between the two blocks.

Relative Comparison Correction

This relative comparison method has been developed to compare the level of grain flow in a particular zone in a field to the biomass throughput measured in the feeder housing in the same vicinity. Essentially, a set of rules was established based on what the expected reaction of the traditional mass flow sensor should be to a variation in biomass flow. If the feeder house sensor indicates that material uptake has ceased, then grain mass flow should also stop. More generally, decreases in biomass flow should correlate well with decreases in grain mass flow.

Biomass flow increases are more likely to occur without a substantial variation in grain mass flow. To illustrate the uncertainty associated with biomass flow increases, imagine a combine entering a weedy patch in the field. In this scenario, the grain production may drop as a result of plant competition, but the biomass flow may increase given the uptake of crop and weed biomass.

To insure that an increase in biomass flow is an indicator of increased grain yield, two assessments are used in the correction algorithm. First, the travel distance over which the mass flow increase occurred is calculated. If there is a sudden, short duration increase in biomass uptake, this is most likely the result of erratic feeding (i.e. feeding irregular clumps of material into the combine during soybean harvest), the combine entering a spot of weeds, or some threshing/separating adjustment has been completed on the combine. Therefore, these biomass flow variations occurring over short distances are ignored. Secondly, this correction procedure is focused on varying throughput lag values to achieve grain mass redistribution. Therefore, an increase in crop biomass flow must be accompanied by a corresponding increase in grain biomass flow within a given period of time (i.e. 30 s) or grain redistribution will not occur. Again, the objective is not to artificially recreate a grain mass flow profile, rather the objective is the correct spatial placement of a mass flow increase determined by a variation measured by the feeder house chain tension sensor.

At this time, it would be best to use an example correction to discuss how the correction algorithm redistributes the mass flow data. To illustrate how this correction scheme works, a step-by-step example will be shown using the six block ASABE X579 test scheme. Also, the series of rules used to redistribute mass flow will be listed. First, the filtered feeder-house signal data is analyzed to find areas of significant difference (i.e. sudden increases or decreases in mass flow).

Rule 1: A significant change in mass flow is indicated by a sensor readout change of more than 10% in a 1 s time span.

Rule 2: If three or more consecutive significant changes are identified, then a location marking the change in mass flow is recognized.

Rule 3: The location where the crop material mass flow change takes places is the average geographic coordinate value of the points used to define the change.

Rule 4: At each location of change, boundaries are created to delineate areas of differing mass flow. The area between two boundaries will be referred to as a block.

Rule 5: The length covered by each block is checked to insure it is greater than some minimal value (8 meters for this example). This distance checking deletes blocks that were created because of a sudden surge in material uptake that results from irregular header feeding or a sudden weed patch.

If a "short" block is found, the boundaries are deleted and the block is reconfigured to account for the removal of the "short" block. For each block the average crop material mass flow signal was determined. Figure 5.4 below shows how the filtered feeder house signal data was regrouped into eight block of similar mass flow (Note: The test plot was set up with 6 true blocks, however this scheme actually split test blocks 4 and 6, resulting in the feeder house data implying eight blocks were present). The sudden spike seen in the seventh block might appear to be an anomaly, but this sharp increase consists of several data points and occurs over a distance of 17 meters. In the actual analysis, two additional blocks are added to incorporate pre- and post- test block mass flow profiles into the analysis.

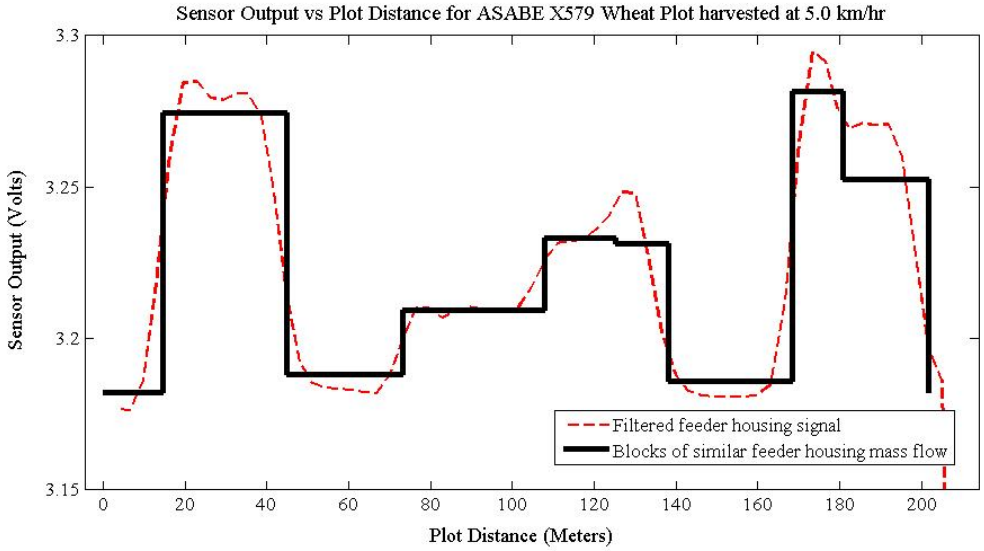

Figure 5.4. The results of breaking the feeder house sensor data down into blocks of similar plant material mass flow.

Once the feeder house data have are segregated into blocks representing similar biomass feed rates, the yield monitor data are studied to determine how well it fits the flow of material into the combine. Figure 5.5 shows how the averaged and blocked feeder house signal data compares to the grain mass flow data generated by the yield monitor. Similar to the results reported in Chapters Three and Four, the data collected by the yield monitor exaggerates the true nature layout of the plot (in reality each of the six blocks is 33 m in length) and the yield monitor data has a tendency to indicate a significantly different yield condition compared to true condition present in the block.

At this point, a series of comparisons between the two data sets are completed in an attempt to determine how the mass flow data should be redistributed.

Rule 6: The first step in the correction process is to identify which feeder house signal blocks indicate zero material throughput into the combine.

A zero mass flow threshold voltage was set at 3.19 V. This voltage level was chosen after scrutinizing the complete data set collected for this research project. Looking at the signal levels represented in Figure 5.5 reveals that Blocks 1, 3, 7, and 10 meet the criteria for zero mass input into the combine. This logic is correct as the actual test plot was established with these blocks being void of any crop material. With the zero biomass flow blocks established, decisions regarding the redistribution of the grain mass flow can commence.

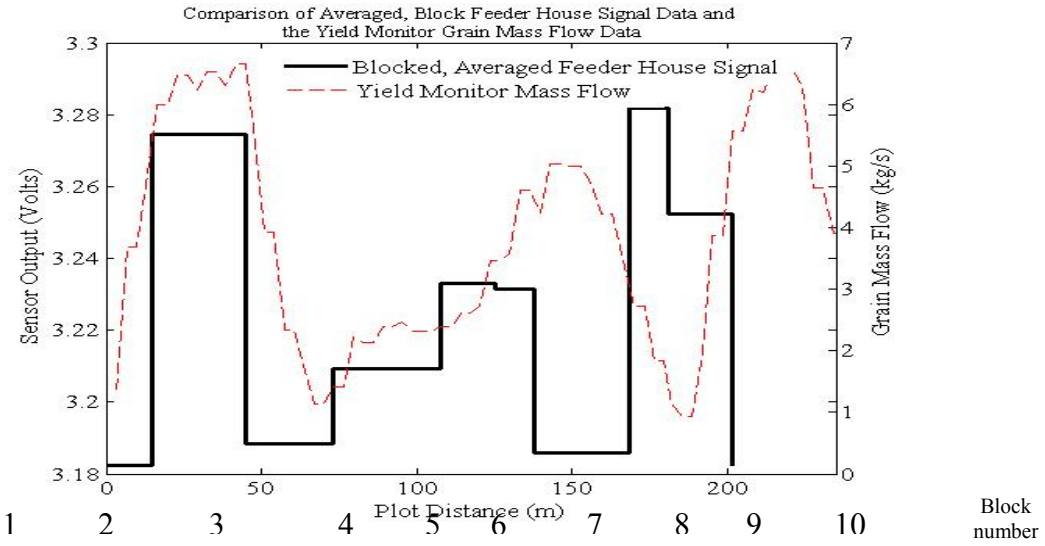

Figure 5.5. Comparison of blocked and averaged feeder house signal data with yield monitor mass flow data for an ASABE X579 field plot.

When applying the mass flow redistribution technique, it is important to note the quantity that is being redistributed. The mass flow rate (kg/s) is not the quantity being reallocated in this correction scheme. The actual grain mass is the quantity being moved between the blocks. The grain mass (kg) can be obtained from integrating the mass flow signal over some finite length of time. For this correction routine, the integration limits are equal to the boundaries that establish the blocks of equivalent mass flow feed rate. Using this integration technique, the weight of grain produced in each block is established. This mass is then assigned for redistribution. Based on integration Blocks 2, 3, 4 and 7 produced 126.12 kg, 63.15 kg, 51.86 kg, and 90.17 kg of wheat, respectively.

Initial grain mass reassignment is applied to the blocks whose feeder house signals indicate the feeder house was empty. Therefore, the grain mass flow should be zero. With that statement in mind, the grain mass associated with Blocks 1, 3, 7, and 10 must be moved to the neighboring blocks. There are three conditions that can lead to immediate grain mass reassignment: 1) If the first block is a zero biomass flow block. If all the mass is removed from the first block, it can only be applied to the next block ahead of it. So in the example, all of the mass from Block 1 (29.87 kg) is assigned to Block 2. 2) If the data for the last block indicates an empty feeder house, then all of its accumulated mass is assigned to the next to last block. In the example, all of the grain mass in Block 10 (194.62 kg) is removed to produce a zero grain mass flow condition and the mass is reassigned to Block 9. 3) A zero flow block is sandwiched between two blocks of significant mass flow. This third zero mass flow reassignment case is not readily apparent in Figure 5.5. To help illustrate this more complicated mass reassignment, Figure 5.6 has been created. In the figure, the feeder house signal for the center block is low enough to indicate the feeder house is empty and there should be no grain mass in this block. The yield monitor signal indicates that the combine switched from an emptying posture to a filling posture, the transition occurring at the minimal mass flow point in this block. Using this minimal mass flow point as a guide, all of the excessive mass logged prior to this point is assigned to the preceding block while all of the mass logged after this point is assigned to the following block. The similar situation could also occur when the combine switches postures from filling to emptying. In that instance, the maximum yield value is calculated and used as the dividing point.

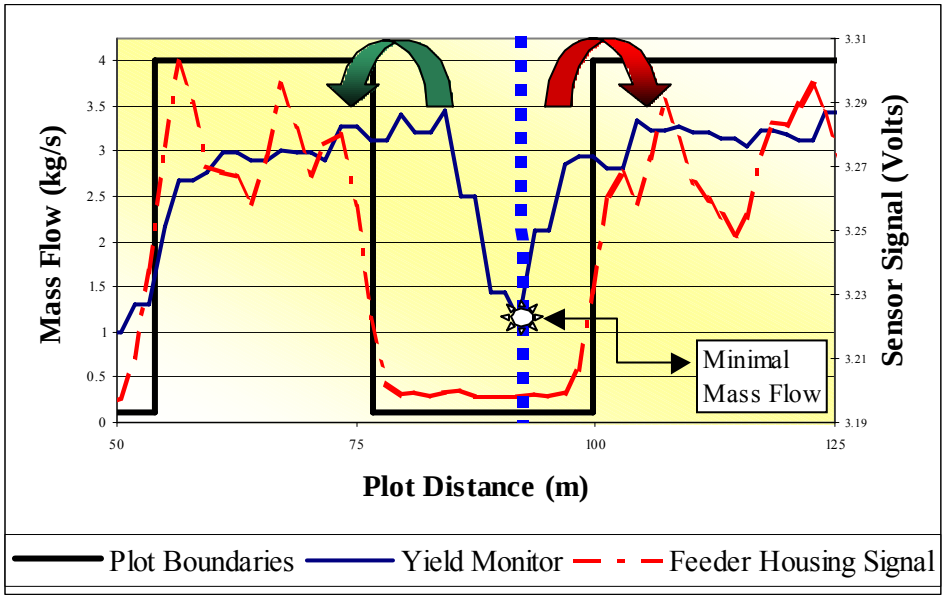

Figure 5.6. Dividing grain mass flow between two adjoining blocks requiring additional grain mass

The terminology used to describe the process is critical. The term reassignment has been used repeatedly up to this point because this reassigned mass is not simply added to the total mass of the new block. A systematic mass redistribution will be used when the mass is transferred to different blocks. This redistribution approach places emphasis on the data points closest to the block being purged of mass flow. For instance, when mass is subtracted from Block 1 and reassigned to Block 2, the data points in Block 2 closest to the Block 1 boundary will receive the majority of the weight. The Block 2 data points closest to the boundary with Block 3 will experience a marginal increase in biomass flow. This reassignment term is used to indicate the amount of mass being moved into a block and the direction of the transfer (i.e. to the preceding or to the following block).

Once the appropriate grain mass reassignment from the zero crop mass flow blocks has occurred, the relative level of grain mass for each block is determined. For this step the reassigned mass is added to the total mass of the block to which it is designated. This is a temporary step and the mass flow rate for individual points is not adjusted. The mass of grain in each block is divided by the mass of the block associated with the greatest grain weight. The relative level of biomass in each block is calculated using the same procedure. These relative

values are then compared to determine how the remaining non-zero mass flow blocks should be adjusted to better reflect the true spatial distribution of the grain production in the field.

For the remaining non-zero biomass flow blocks the difference between the relative biomass levels in consecutive blocks is used to redistribute grain mass flow. This comparison determines if the block needs more grain mass, has ample grain mass, or possess excess grain mass. If the relative biomass difference is greater than the relative grain difference for consecutive blocks, then more grain is required. If the grain difference is greater than the biomass difference, then too much grain is present in second block. If the difference in biomass and grain levels for consecutive blocks is within 10%, the amount of grain in the block is considered to be adequate.

Figure 5.7 provides a bar plot comparison of material levels for each of the blocks developed for this example. The sign above each block indicates how grain should be moved with relationship to the particular block. A question mark denotes little or no movement is needed. The question mark over the maximum yield block (Block 2) is placed there because all indications are this block should have grain mass removed. In reality, the maximum yield block can still accept more grain in a redistribution scheme. As the mass is redistributed throughout the block, especially when the mass is removed from the zero throughput areas, the amount of grain in all the non-zero throughput blocks will rise. Therefore, it would not be appropriate to cap the grain mass in a given block in the initial stages of this correction.

The other point to note is this method is not attempting to force the grain flow profile to match the biomass throughput profile. Biomass flow measurement is not a surrogate for grain mass flow measurement. The relative level comparison provides a basis for initial redistribution of mass flow. The true redistribution is focused on maintaining the difference in relative values between blocks. If the relative biomass level drops from 80% to 20% between successive blocks, the correction method tries to redistribute mass so the relative grain level will also drop sixty percentage points. It is not important that the grain level drops from the same levels, just that the difference is maintained.

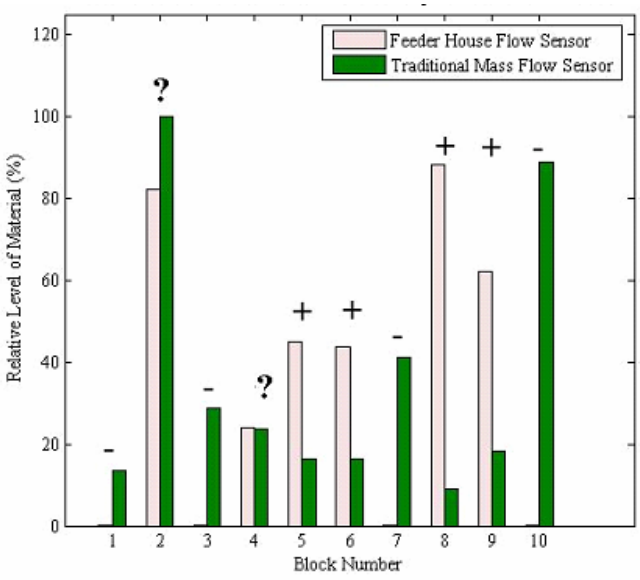

Figure 5.7. Comparison of relative material levels for an ASABE X579 plot.

The difference in relative levels of material in the blocks then multiplied by the distance covered by the combine within the block. This multiplication helps normalize the data in the event there are consecutive blocks requiring additional grain. For instance, consider the case of two successive blocks requiring additional grain mass and there is 100 kg available for reassignment from an adjoining block. The first block is 22 m long with a biomass relative difference of 20%. The second block is 10 m long yield monitor data points with a biomass relative difference of 27%. Multiplication of the relative difference and the number of yield monitor points will produce a value of 440 for the first block and 270 for the second block. Dividing these two values by their sum dictates how the 100 kg of extra mass will be split between the two blocks. Using this logic, the first block will receive 62% or 62 kg of the mass and the second block will be reassigned the remaining 38% or 38 kg.

At this point, the mass flow redistribution is 90% complete, since the grain mass that needed to be moved about has been reassigned to the correct block. The one step still needed is the division of this total mass value into mass flow rate values for individual points. On one hand, the easiest thing to do would be to simply add the total reassigned mass value to the total mass in a block and divide by the number of data points collected by the yield monitor in the block. The result would produce a constant average mass flow value for every data point in the block. This type of correction would probably be sufficient if the block size was small, which is

the case for the field plots. However, under regular harvest conditions, the size of the redistribution blocks will be much bigger and most likely mass flow correction will only be required near the boundaries used to define transition in mass flow. Therefore, a redistribution method that places emphasis on the yield monitor data points closest to the mass transition is necessary.

Inspection of an average feeder house mass flow profile, similar to Figure 5.1, reveals that the changes in mass flow can best be described as a series of step input changes. This realization is very important because researchers have completed projects that attempt to describe the response of the mass flow sensor to a step input. Searcy et al. (1989) provides the classic solution using a first-order exponential decay model to describe the flow of material from the header to the mass flow-sensing device. In the time domain this model is expressed as:

$$v(t) = r\left(1 - e^{\frac{-(t-p-t_o)}{q}}\right) \qquad \textbf{Equation 5.5}$$

where:

v(t)	=	output grain flow rate (as measured by the mass flow sensor)
r	=	magnitude of the flow rate step input
p	=	transportation delay
q	=	time constant of first-order lag
t_o	=	time of step input

The most interesting feature of this expression is the variability associated with the first-order lag term, q. Searcy set q equal to 2 s when the combine experienced an increase step input. These values were confirmed by Birrell et. al (1995) and Whelan and McBratney (2002).

Using the exponential decay to redistribute the mass flow within the blocks is followed with recursive correction. The redistribution procedure is repeated multiple times until a stable correction is reached. Stability was achieved when grain mass was no longer redistributed between blocks. Typically, the removal of all mass from zero throughput areas denotes a stable solution. The recursive aspect of this program was rarely used; usually one or two iterations provided the maximum grain mass redistribution possible. Figure 5.6 provides an example of the final solution. While the results of this method will be discussed in greater detail later, the plot

does show noticeable improvement in the yield profile. The transitions between blocks are sharper and the mass profile appears to match the actual distribution that should be created by the field trial.

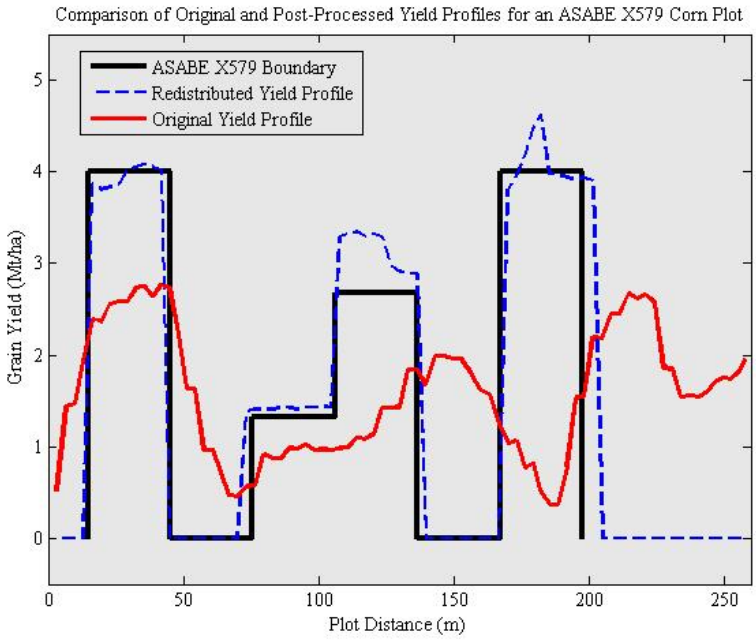

Figure 5.8. Relative comparison corrected yield measurements.

Algorithm Evaluations

With the successful development of the correction algorithm, it was time to commence an assessment of this correction routine's value as a yield monitor correction utility. The evaluation started by looking at how well the redistribution program could process the data collected in the interval and ASABE X579 field trials. These field trials should be a test of the precision and robustness of this correction procedure. The field trials are set up to mimic mass flow changes at a more severe rate than the variations experienced under regular grain harvest conditions. Each field trial was filtered using methods developed in Chapter Three and used to redistribute the corresponding yield monitor data. Statistical analysis including box plots, descriptive statistics, significant difference tests, and linear regression were conducted to determine if the corrected mass flow profile resembled the mass flow profile that should occur based on the nature of the plot layout. When errors in the Matlab script were discovered corrective measures were taken to improve the accuracy of the correction. The vast majority of the problems with the script were

concerned with indexing and array management and very few adjustments were required for the final correction routine.

Besides looking at the performance of the correction routine in the field trials, data collected under regular harvest conditions were also studied. The variations in mass flow experience in regular harvesting conditions are moderate compared to the field plots. The regular harvest data will test the correction routine's ability to redistribute mass flow rates when there are slight changes in flow rates over long distances. The assessment of the correction routine's accuracy is much harder in the full fields. Essentially, the assessment was based on observation and intuition, as the true nature of the mass flow profile in the field is almost impossible to quantify. Field boundary maps offer one potential data set that could be used to indicate areas where grain production should not occur (i.e. waterways). One area to note within the corrected fields will be the starting and finishing points of each combine pass. Also, the position of yield monitor data points that occur as the combine enters or exits waterways and driveways is of interest. These key points represent a break in steady-state material flow into the combine resulting in variable delay times. If this correction routine operates properly, then there should be significant mass flow redistribution within these areas.

Results and Discussion

Relative Comparison in Field Plots

To illustrate the performance of the relative comparison correction in the field, a series of figures (Figures 5.9 – 5.11) have been prepared. These figures reflect the performance of the correction for ASABE X579 test plots and interval plots in both corn and wheat. Within each figure, the uncorrected mass flow profile is provided for comparison. Visual examination of these figures will reveal the robustness and relative success of this correction method. The key feature to note after the correction has been applied is agreement between yield estimate changes and the plot boundaries. Also, the consistency of the yield estimates for the blocks that should produce equivalent mass flow values.

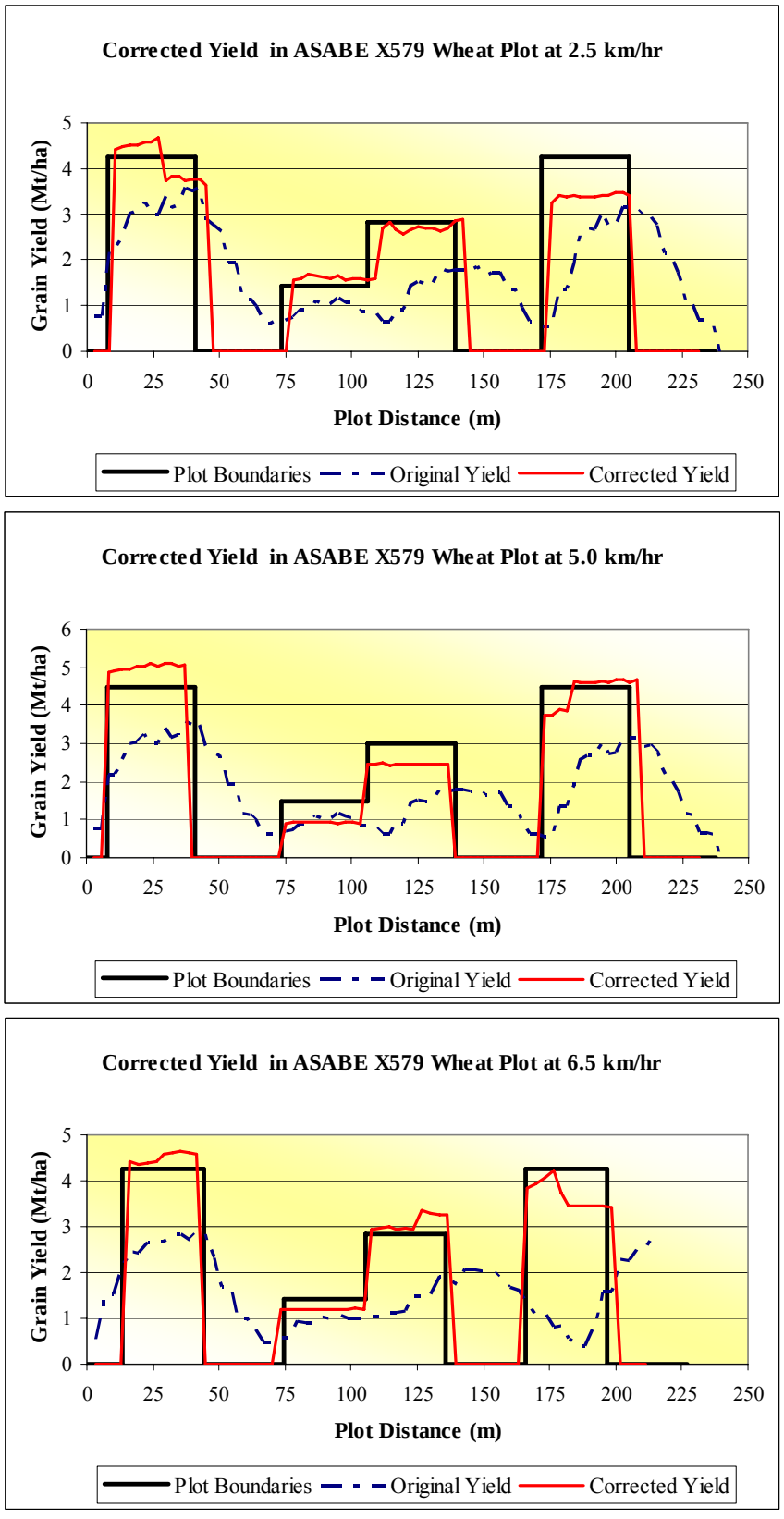

Figure 5.9. Relative difference correction applied to ASABE X579 wheat plots.

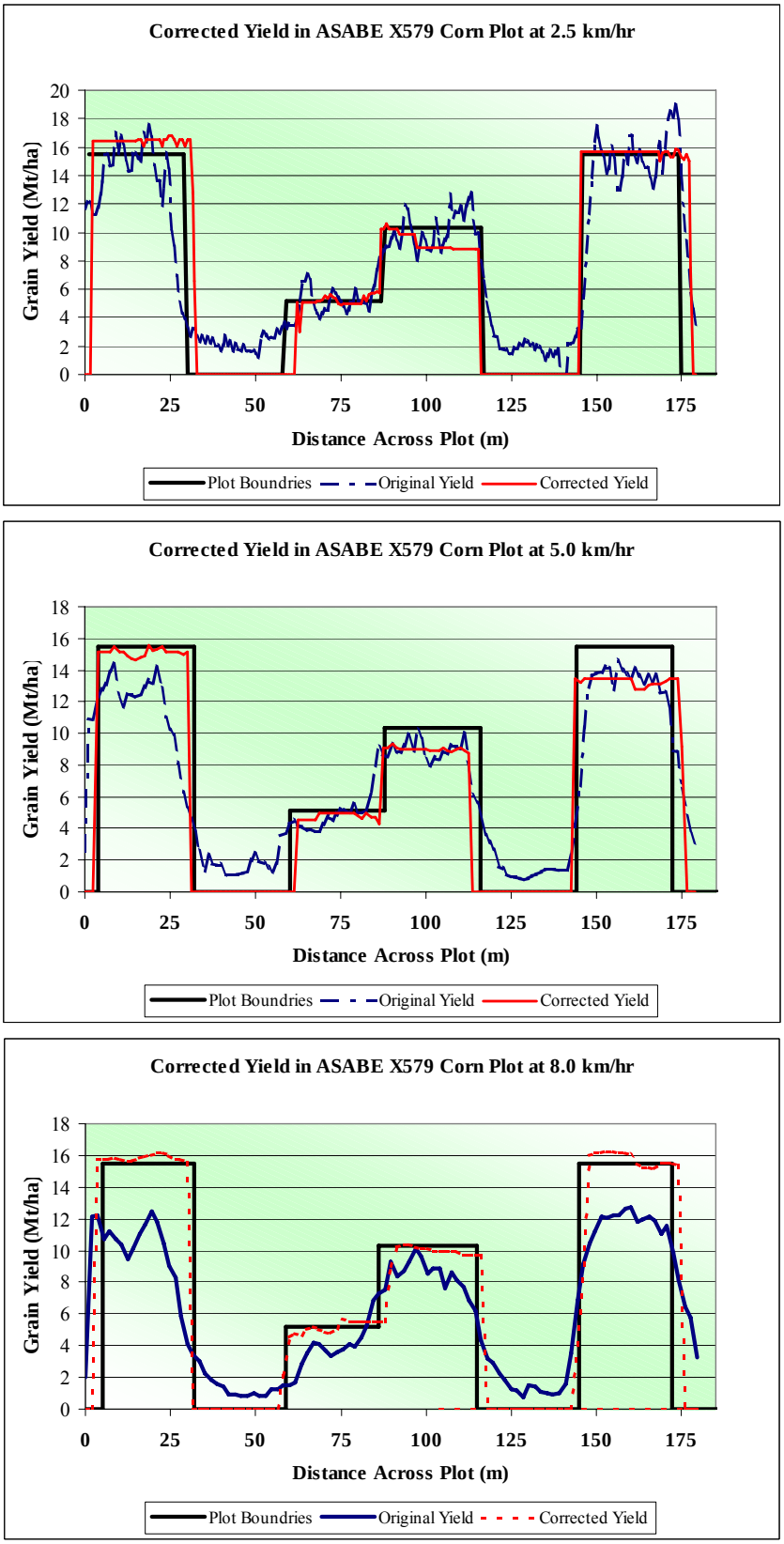

Figure 5.10. Relative difference correction applied to ASABE X579 corn plots.

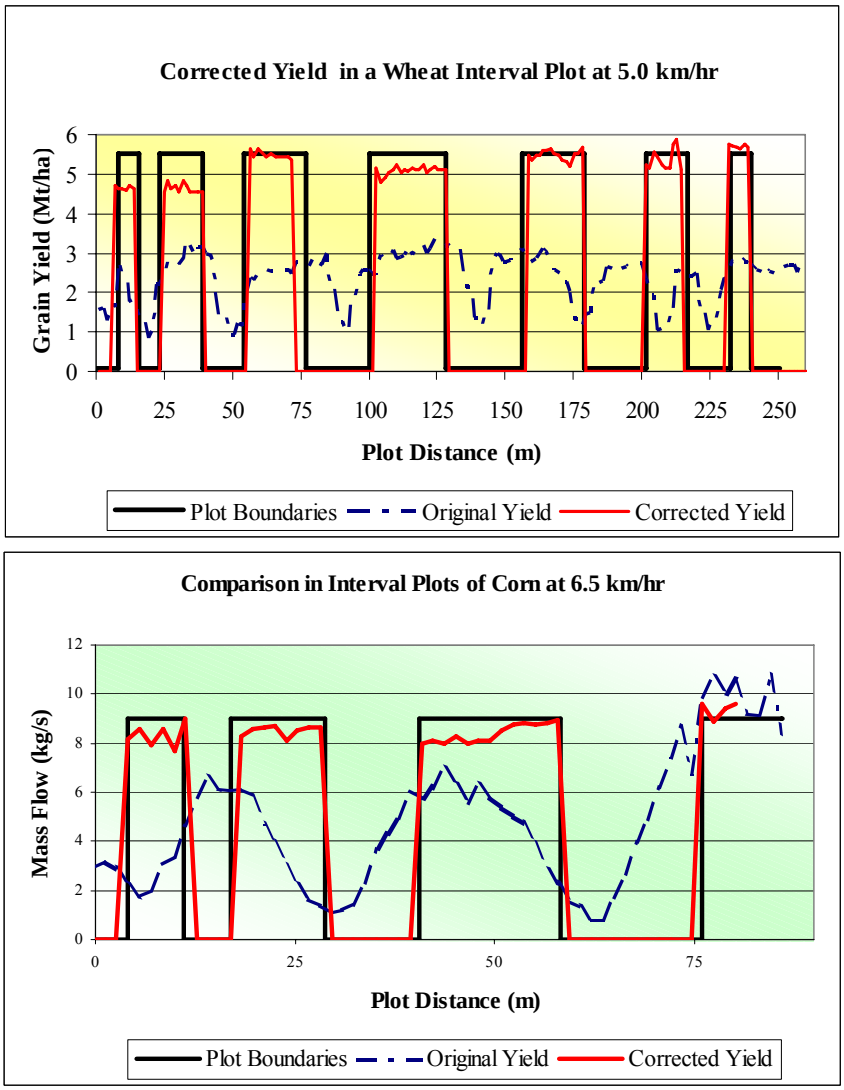

Figure 5.11. Relative difference correction applied to various interval plots.

By fusing the information contained in the feeder house data with the data collected by the yield monitor, it seems yield values that correctly mimic the profile induced by the field plots are created. However, this analysis cannot be limited to visual judgments. A series of statistical analyses were conducted to determine if this improvement was significant. Included in the analyses were box plot development, descriptive statistics, and significant difference tests. These tests provide a means to compare the results of the mass redistribution to the original data set. The results section will provide representative examples of field plot trials when discussing the improvement in yield estimates provided by this correction procedure.

Box plots have been developed to show the effectiveness of the relative difference method in redistributing grain mass flow. These notched box plots compare uncorrected and corrected yield estimates. Figure 5.12 contains example data from an ASABE X579 wheat plot. The main points to note in the uncorrected data are the statistical similarity between many of the plots that had significantly different grain volumes at the time of harvest and the inability to reflect the zero yield condition in the plots with no grain present. One of the more concerning features of the box plot is that the uncorrected data indicates that Block 2 having no biomass present produced 3 Mt/ha of wheat just like Block 1, which had 100% of the crop material present.

The yield profile for the plot shows a great deal of improvement when the corrected yield measurement is considered. One of the most noticeable elements of the corrected plot is the zero yield values in the pre plot, post plot, Block 2 and Block 5 zones. Obviously, the strength of the relative difference correction method is the identification and redistribution of mass in block that had no material entering the feeder housing. The second impression is the relatively low variability shown within the various blocks. All of the box plots are extremely flat which indicates the majority the data set for the block is very close to the median value. Also, the increase in yield for the 100% blocks should be noted. This is simply the result of redistributing grain from the area with no crop material present at harvest.

The only flaw on the corrected yield profile is the inability to have equivalent yield values in the two 100% biomass blocks. Unfortunately, the corrected yield calculation for Block 6 is significantly lower than the calculation for Block 1. This is by no means a trend for all corrected data sets; rather this is just how the feeder house chain tension signal directed mass flow redistribution for this particular example. Also, there is always the possibility that the various 100% plots differ due to field position and yield potential in a particular location. Although efforts were taken to ensure uniform yield across a field plot, there were slight (not readily seen on visual inspection) differences present.

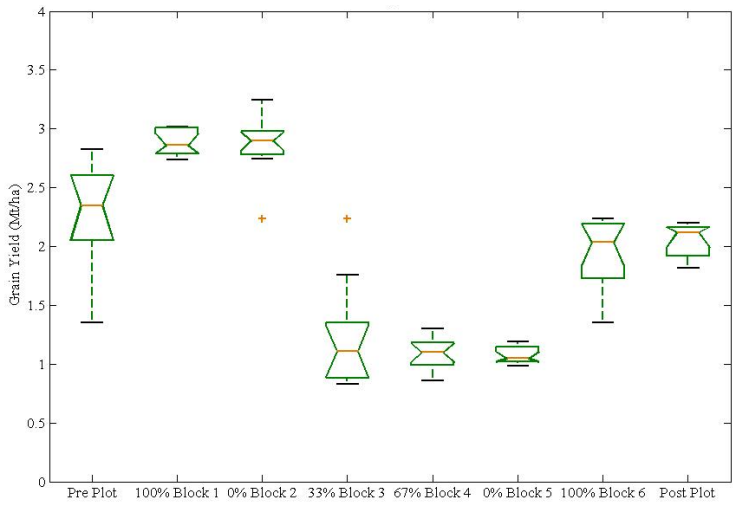

a) Uncorrected Yield Estimates

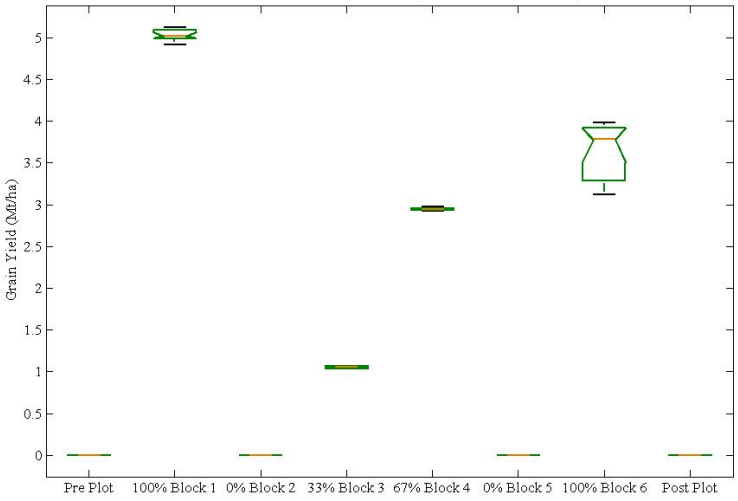

b) Corrected Yield Estimates

Figure 5.12. Boxplots of original and corrected yield estimates in an ASABE X579 wheat plot.

Besides the ASABE X579 trial, box plots were developed for data collected while harvesting corn interval plots. These box plots are presented in Figure 5.13. When moving across the plot there should be a clear alternating pattern between blocks of zero yield and blocks with some arbitrary maximum yield value. Obviously, this pattern is indistinguishable for the uncorrected data set. The variability of yield estimates within the uncorrected blocks appears to be excessive as well. When mass flow redistribution is applied, the true yield pattern is perceptible. All of the maximum yield blocks have statistically similar median values once correction is complete.

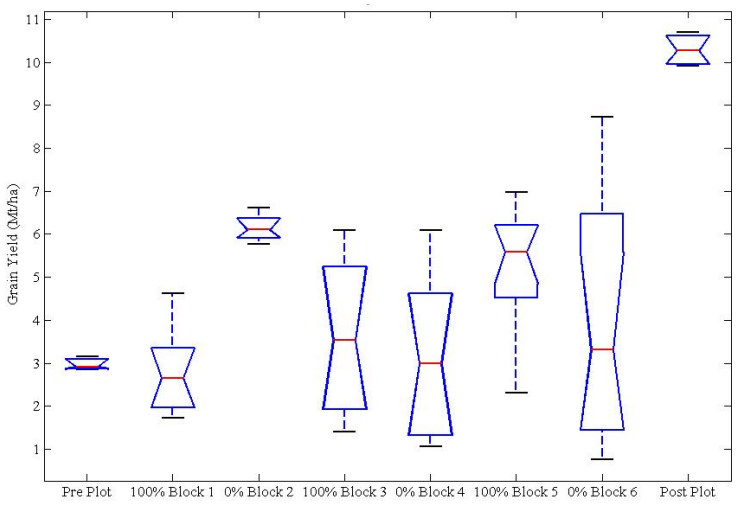

a) Uncorrected Yield Estimates

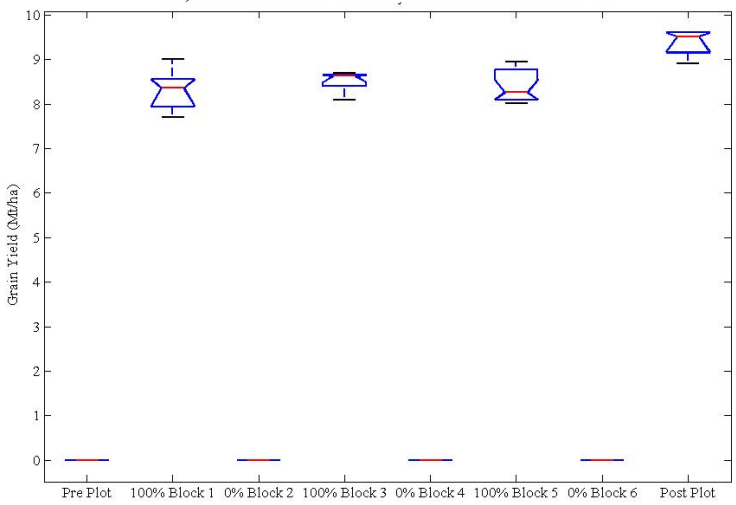

b) Corrected Yield Estimates

Figure 5.13. Boxplots of original and corrected yield estimates in an interval corn plot.

A more traditional statistical analysis is proven in Table 5.1. The mean yield values for each ASABE X579 block are available for inspection. Also, a Fischer's Least Significant Difference test (Devore, 1999) was completed to determine how these values differed Prior to correction, the yield values in the various blocks show inconsistency. There are yield differences blocks of similar biomass levels and there are similarities in blocks with significantly different crop material levels. The first block with all the biomass present at harvest has a yield value

nearly identical to the yield calculated for the second block which had no crop material present at harvest.

Table 5.1. Statistical comparison of corrected and uncorrected yield estimates in a ASABE X579 wheat plot.

Portion of Block Covered with Crop	Original Yield Profile			Corrected Yield Profile		
	Mean Yield (Mt/ha)	C.V. (%)	Different from Blocks	Mean Yield(Mt/ha)	C.V. (%)	Different from Blocks
100 %	2.89	10 %	0% (2), 33%, 67%, 100%(2)	4.67	4 %	0%, 33%, 67 %
0%	2.93	16 %	0% (2), 33%, 67%, 100%(2)	0.00	0 %	33 %, 67 %, 100%
33 %	1.23	25 %	0% (1), 100 %	1.35	3 %	0 %, 67%, 100 %
67 %	1.07	12 %	0% (1), 100 %	2.94	3 %	0 %, 33 %, 100 %
0 %	1.06	6 %	0 % (1), 100%	0.00	0 %	33%, 67 %, 100%
100 %	1.94	15 %	All Blocks	4.59	8 %	0%, 33%, 67%
	LSD = 0.45 Mt/ha at $\alpha = 0.05$			LSD = 0.81 Mt/ha at $\alpha = 0.05$		

After applying the correction routine, much of this irregularity in the yield values has been removed. The yield values in plots of similar biomass levels are more consistent and the overall variability has been reduced. Individual blocks are significantly different from all the other blocks possessing dissimilar crop material levels at the time of harvest. Note the improvement in consistency between the two 100% crop coverage blocks once the correction is applied. These results are typical of all corrections applied to X579 plots as well as interval plots.

A final method employed to investigate the effectiveness of the grain mass redistribution was the comparison of pre- and post-corrected correlation coefficients, R^2-values. To implement this comparison, it was assumed that the line of best fit for each plot trial could be defined by the curve indicating plot's blocking scheme. The plot's blocking scheme has been designated with the term "block boundaries" in preceding figures. Figure 5.14 shows how a comparison between individual points and the line denoting the block boundary.

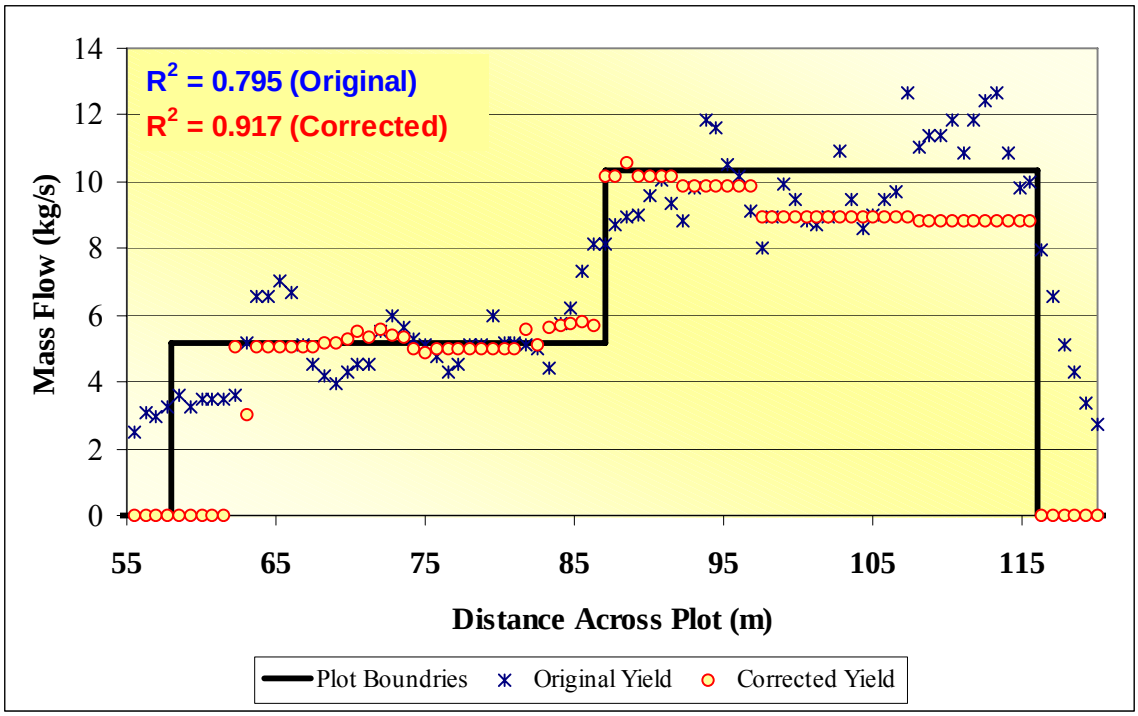

Figure 5.14. Correlation between plot boundaries and yield data points pre- and post-grain mass redistribution (zoomed in to highlight residual calculation).

For each data point, the residual value is calculated, and then the R^2-value for both data sets is then determined. Using this analysis, it was shown that for the ASABE X579 plots the R^2-value increased from between 0.44 – 0.61 to 0.87-0.92 when the mass redistribution was applied. For interval plots, R^2-values increased from 0.42 – 0.57 to 0.82 – 0.90 after mass redistribution. The analysis indicates that the mass flow data is more representative of the blocking scheme after correction. By comparing the correlation between the blocking scheme and yield data points, it can be seen that relative-comparison mass redistribution is an effective method of yield monitor data correction.

Based on all the information presented so far, the relative comparison method produces what appear to be corrected mass flow profiles that provide improved spatial and yield estimate accuracy. The spatial accuracy is indicated by the sharper yield transitions and the yield data fits into the confines of the plot boundaries after correction. The accuracy improvement is the result of redistributing the mass which tends increase maximum values while removing grain mass from any areas associated with no material entering the feeder housing. Both the interval and

ASABE X579 plots highlight the strengths of this correction method; however, there are instances that the relative correction method will produce marginal results.

The main drawback to the relative comparison method is that it does not adapt well to situations where mass flow rates gradually change over relatively long distances. An example of this type of flow characteristic is a ramp flow profile. Figure 5.14 demonstrates the failure of the relative comparison method to adequately redistribute the yield monitor mass flow data to the correct mass flow profile. The primary reason for the error is the underlying approach taken by this correction method. Basically, it attempts to locate step inputs and make decisions about the relative difference in magnitude between successive zones.

Applying this correction method to the ramp flow curve causes the linear variations in mass flow to be divided into various steps. This is similar to what happens to an analog signal when analog-to-digital conversion is applied. To minimize the stepping, the minimum block size value was lowered to 0.5 meters (used in Figure 5.14). When this algorithm was initially developed, it was designed to ignore sudden surges in feed rate. Any change in feed rate had to be sustained over a distance of 8 m for it to be considered (this is typically equivalent to three or more consecutive yield monitor data points).

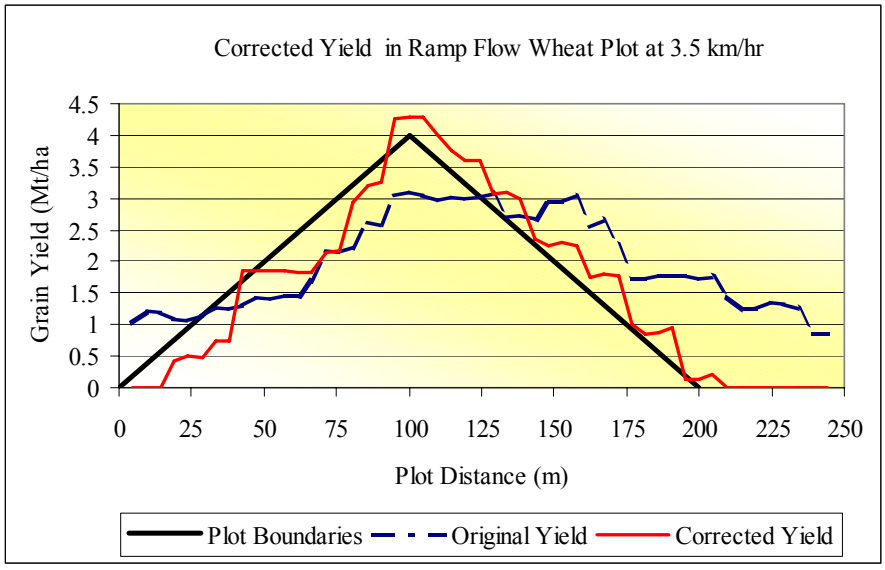

Figure 5.15. Relative difference correction applied to a ramp flow wheat plot.

The mass flow profile has improved after correction. The maximum yield estimate is much closer to the true field condition and the mass flow data now fits within the confines of the plot boundary. But more improvement is needed. The main issue is the inability to reproduce the smooth linear line. Even the application of data smoothing or curve fitting would correct the problem because the triangular shape would be unbalanced (too steep left of the maximum value and too flat on the right side). Delay appears to be a concern as the corrected yield estimates to the left of the maximum is running behind the yield value present in the field.

Some of the blame for this delay issue lies squarely with the feeding mechanisms on the small grain platform. As the combine enters a ramp flow plot it is only cutting material with a small portion of the head (less than 1 m). It takes a few seconds for enough material to build up on the head before it travels across the feed auger to the feeder house opening. Also, the initial grain has to travel one-half the length of the feeding auger on the head and this represents the maximum distance crop material has to travel on the cutting platform. Besides mechanical delay time, the other issue is that this very low volume of material initially entering the feeder house does not cause a perceptible change in chain tension, causing some additional delay.

In the end, this ramp flow test questions the ability to use the relative difference method for slower, more gradual changes in material flow rates. This method works well for the detection and redistribution of grain when sharp transitions are present. For linear variations occurring over long distances the method attempts to create a long series of step transitions that does improve yield monitor mass flow distribution. However, refinement is needed to identify when these gradual variations are present and some form of data smoothing is required to improve the appearance of the corrected profile. The application of a linear regression line would improve the appearance of the yield profile when gradual variations are identified.

Hydraulic Pressure Correction

Thus far the grain mass redistribution procedure has focused using the feeder house chain tension sensor as the correction signal. Previously, there was a great deal of effort placed in the evaluation of a hydraulic pressure on the threshing cylinder as a mechanism to monitor feed rate into the combine. The conclusion of this investigation was the sensitivity of this sensor was not sufficient to warrant its use in the correction of traditional mass flow data. All of the correction procedures were redirected to look at the use of the hydraulic pressure signal as the basis for

mass redistribution. Similar trends were evident for all of the correction procedures, thereby justifying use of relative comparison correction.

Figure 5.16 provides a visual comparison of the corrected mass flow profiles that resulted from using the feeder house sensor and the threshing cylinder signal on data collected in a corn interval plot. From visual inspection of these plots, the hydraulic sensor is almost as accurate as the feeder housing drive sensor in the definition of the blocking scheme. The corrected yield levels are very similar in both plots as well. The blocks are slightly expanded for the hydraulic sensor correction, but this error is not a great concern. This test plot reinforces the idea that threshing cylinder pressure can be used to delineate between large swings in mass flow, but it was not clear how this correction method would work for plots with smaller variations in yield.

Figure 5.17 provides a visual comparison of the corrections resulting from using the two signals on data collected in an ASABE X597 plot. The concern in this test setup is the inability for the hydraulic pressure sensor to identify a true difference between the 33% and 67% biomass block. The pressure corrected data generates equivalent yield estimates for both of these blocks. This trend was seen in the correction of numerous field trials. This is simply the result of the three-state threshing cylinder response. The threshing cylinder response to biomass feed rates appears to be limited to empty, full or somewhere in the middle. This response is carried over to the corrected yield monitor data as there are only three distinct yield values within the plot following correction.

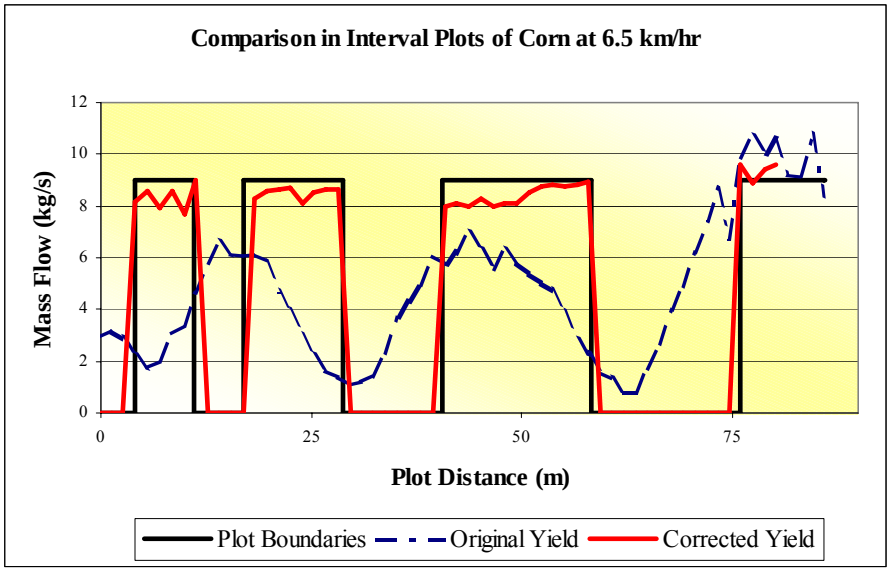

a) Corrected via Feeder Housing Signal

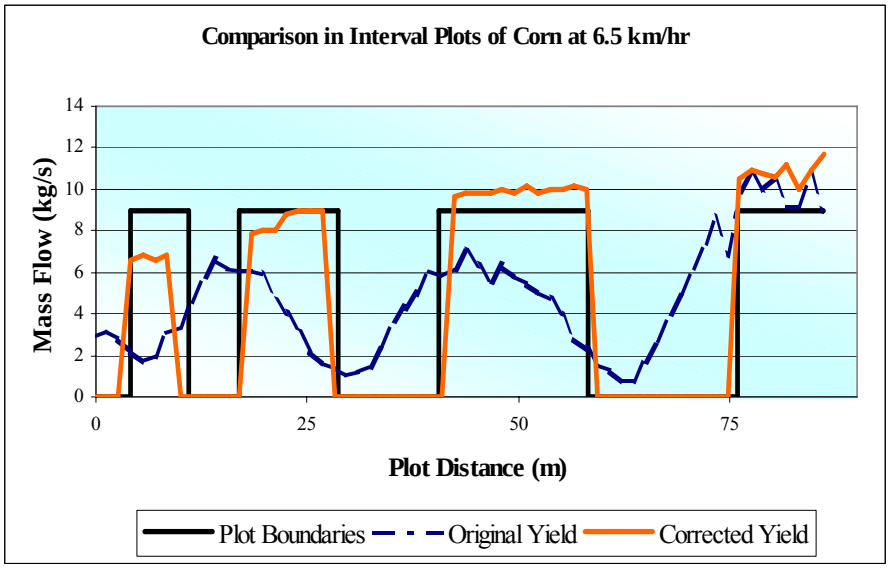

b) Corrected via Threshing Cylinder Signal

Figure 5.16. Comparison of feeder housing and threshing cylinder corrected interval mass flow profiles in corn.

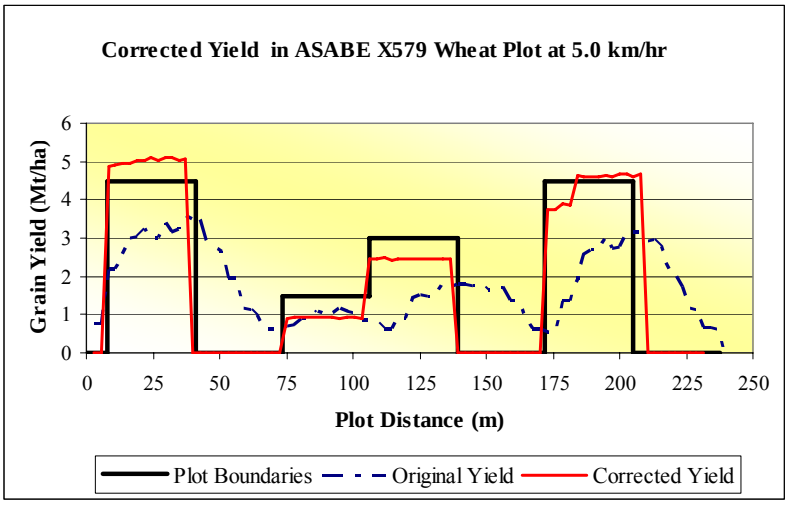

a) Corrected via Feeder Housing Signal

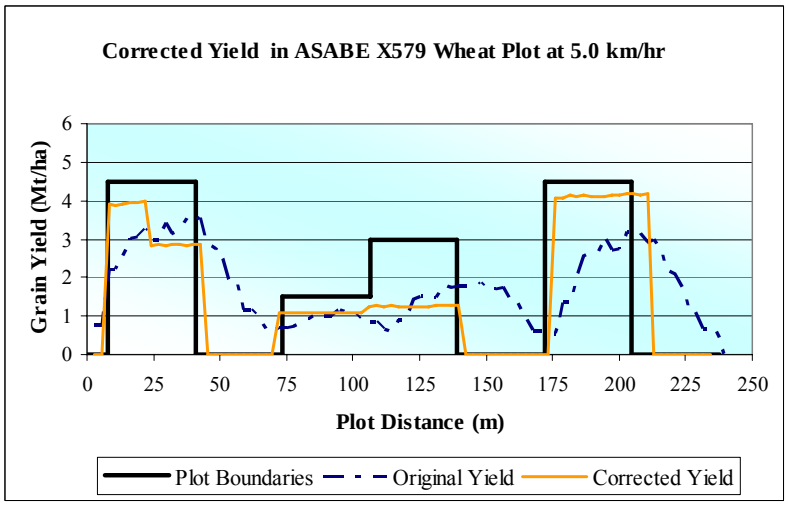

b) Corrected via Threshing Cylinder Signal

Figure 5.17. Comparison of feeder housing and threshing cylinder corrected ASABE X579 mass flow profiles in wheat.

It would appear that focusing on the feeder house-based sensing was the better choice. There were only a handful of test cases where the hydraulic pressure sensor data generated corrected mass flow profiles that were equivalent to the feeder house data profiles. The hydraulic pressure could correct the interval plots with similar levels of improvement, but this would be expected because only the zero and maximum flow states are present. The threshing cylinder also has a slightly slower transition to an empty state than the feeder house, particularly in high flow conditions. Most likely this can be attributed in part to tailings return.

Mass Flow Redistribution in Whole Fields

The relative comparison method appears to be a robust and accurate mass flow redistribution scheme based on results of field plot trials. Because this method proved the most beneficial in the field plot trials, it was decided that this method should be use to correct the mass flow distribution for an entire field. Figure 5.18 shows how the yield distribution within an example wheat field changes with correction.

The most obvious difference in the yield map is the removal of grain from the waterway. The feeder house signal indicated the lack of crop presence within this area, which would be expected in a waterway. The mass was removed and the majority of the mass was relocated along the ends of the combine passes. Inadequate combine filling delay time caused the majority of the passes to appear to be too short on one end of the pass. At the ends of the passes, the chain tension sensor indicates material is flowing through the feeder house. Therefore, it can be concluded that grain was produced in this area.

The remaining mass movement is typically associated with combine velocity fluctuations. The forward velocity of the combine has a direct effect on the rate at which material enters the grain combine. As the speed varies, there are short periods of time that the material transport will revert to a filling or emptying characteristic. Although the deviation in the transport profile is brief, it causes variability in the transportation lag time. Slowing and then speeding up the forward combine speed causes a momentary dip in the yield value to occur. The combine will have a brief discontinuity in the grain mass flow profile and a low yield calculation will result. This yield value is not indicative of the amount of grain produced in the field; rather it is an operator induced anomaly. Fortunately, the feeder sensor data is not quite as susceptible to momentary discontinuities in crop material flow. This is most likely due to the filtering and averaging that has manipulated the signal.

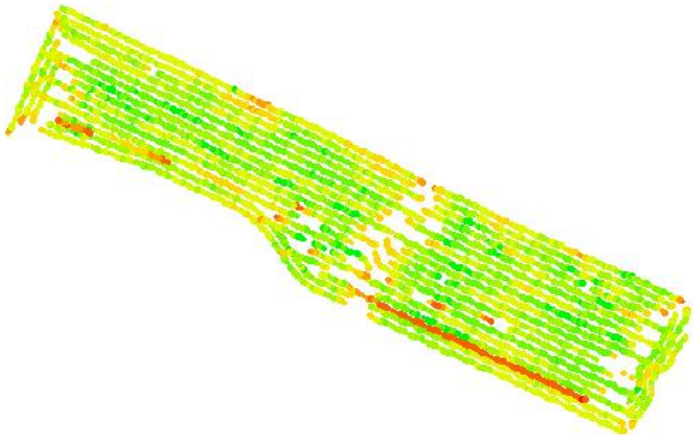

a) Uncorrected Yield Map

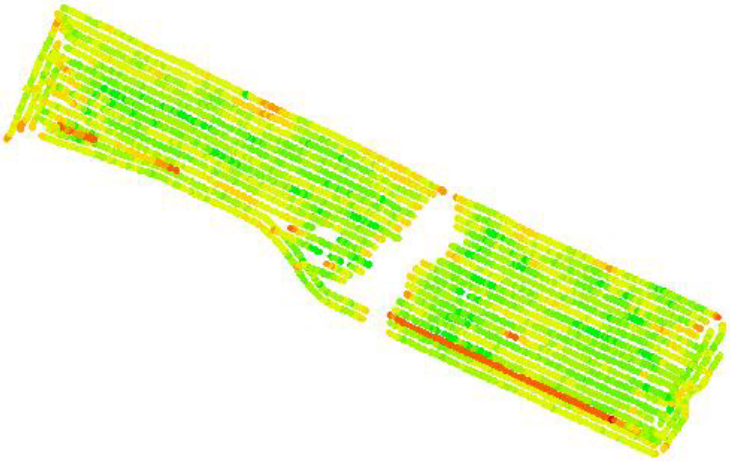

b) Corrected Yield Map

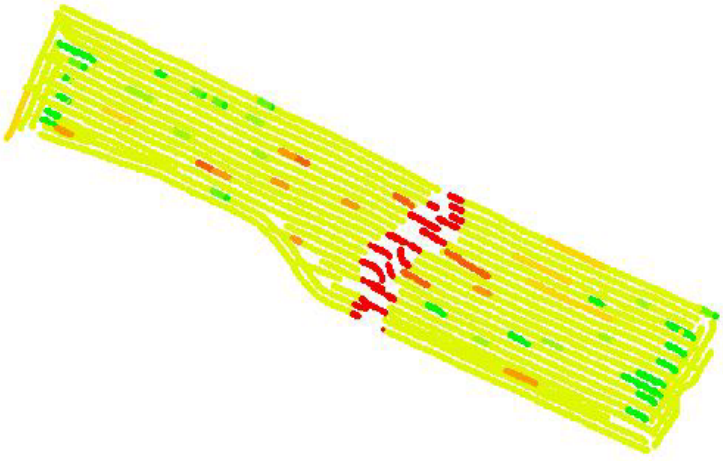

c) Net Mass Redistribution (expressed as a percent of the original)

Figure 5.18. Comparison of corrected and original yield maps for a 10 ha wheat field.

Summary

A yield monitor mass flow redistribution algorithm was developed. This algorithm fuses data from the mass flow sensor with crop material flow rates sensed by the chain tension sensor located in the feeder housing. Comparison of relative levels of crop material and grain in various zones provides the basis of the redistribution. The underlying theme driving the development of this algorithm is there cannot be grain produced in areas that produce zero crop feed rates. Based on the corrections completed during this study, the following conclusions were made:

- Monitoring relative differences between grain and crop biomass throughput levels redistributes mass flow data in a pattern consistent with field plot layouts.
- After correction, yield profiles have sharper transitions and reduced variability within areas of similar yield. Also, maximum yield values are closer to the yield values estimated in the field via truck scales.
- This routine has difficulty handling corrections associated with long, gradual variations in mass flow.
- Feeder house signal data is better for grain mass flow correction than the cylinder drive pressure data based on evaluation using the relative comparison method.

Chapter Six

Spatial Data Model for Correction of Combine Cutting Swath Errors

Introduction

Besides correction of grain mass flow data, the other improvement technique needed is a means to correct the recorded cutting width. Cutting width is a user entered variable, and the majority of the time a single value is keyed in by the operator for an entire field. The cutting width will change as variations in the combine's path cause the cutting head to cross over ground that has previously been harvested. Therefore, only a portion of the cutting head is engaged in harvesting crop. In the literature review, a number of swath width correction procedures were discussed and this resulted in the decision to proceed with the development of a post-processing algorithm to correct erroneous cutting width records. Developing a low-cost, effective real-time distance measurement system would be the ideal solution. However, real-time measurement systems are currently cost prohibited and often the data generated by these devices is prone to error.

In recent years, most crop producers have become familiar with GPS positioning, GIS, and the software packages required to process and archive data associated with these sources. This familiarity with technology provides the opportunity to use post-processing of spatial information to achieve the desired cutting width correction. The most promising post-processing method was the vector-based solution developed by Drummond et. al (1999). The main drawbacks to this method were the computing/software requirements as well as the need to utilize two extremely accurate positioning systems. To improve upon this vector analysis approach, this project focused on the feasibility of using lower grade position systems, reducing the total number of required positioning systems to one, and developing software that can be used on any computer running ESRI (Environmental Systems Research Institute, Inc., Redlands, CA) ArcGIS. GIS packages are designed to manage and analyze large spatial data sets. ESRI produces one of the more popular GIS packages, ArcGIS. This program was selected because of its popularity and flexibility.

Sub-Objectives

In general, incorrect yield calculations resulting from erroneous cutting width entries plague yield monitor data sets. To improve cutting width estimates, a post-processing algorithm was developed to determine cutting width from GPS position information previously. The specific objectives are:

1) Develop a GIS-based post-processing algorithm that will generate actual harvest area polygons for each position fix in a yield monitor data file, and;
2) Evaluate the algorithm for harvests using a variety of grain platform sizes.

Methodology

Post-Processing Algorithm Development

The fundamental assumption for post-process determination of actual cutting width (ultimately actual harvest area) is that GPS positioning information has high relative accuracy for a period of time that coincides with the time between adjacent passes within a field. To test this assumption, an agricultural grade receiver (Trimble Ag132 DGPS receiver with Coast Guard Beacon correction) was placed in a static location and data were recorded for approximately 30 minutes. The GPS coordinates were project into UTM Zone 16 Cartesian coordinates with metric units. Assuming that adjacent passes within the field occur within 5 minute intervals, the relative accuracy of the receiver output were compared for the 5 minute versus 30 minute intervals. Mean circular error and measurement standard deviation provide the basis for the comparison appearing later in this chapter.

The post-processing algorithm developed to determine true harvested areas for each GPS fix in the yield data file is an Avenue script developed within ArcView GIS (Appendix D). This script is a modification of an algorithm developed by Fulton et al. (2003) that was used to develop application polygons from GPS points generated as a fertilizer applicator traversed a field. These polygons were used to indicate the distribution of granular fertilizer in the field after application was completed. The true harvest area script is similar from the standpoint of polygon generation, but the processing has been modified for this unique case. Figure 6.1 provides an illustration indicating the GIS features used to correct harvest area errors. The processing

algorithm requires the "advanced format" ASCII text file created by Ag Leader Technology's SMS yield data processing program. This file writes WGS84 latitude and longitude coordinates, which were projected into UTM (NAD 83 Zone 16N) coordinates to facilitate processing. This projection converts the spatial coordinates from degree-minute-seconds format into X-Y Cartesian coordinate system to enable further processing. The process then identifies the heading of the combine as the trajectory between the GPS position fix of the point in question and the next fix. The heading is the azimuth between these two locations.

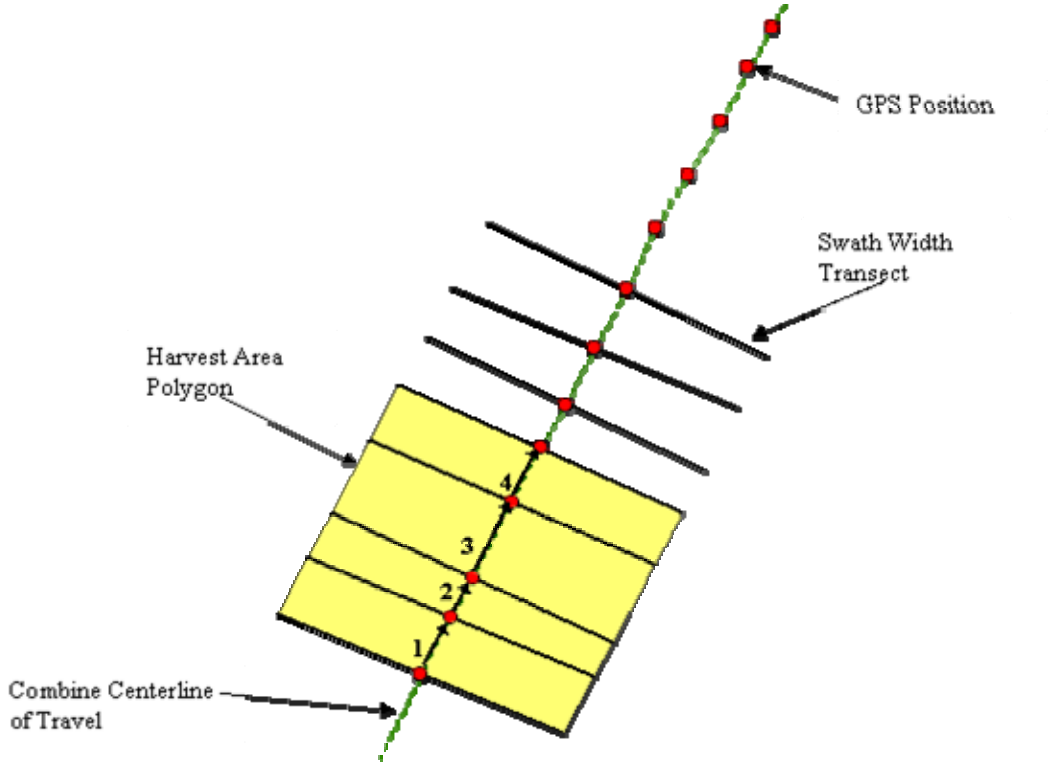

Figure 6.1. Harvest area polygon construction approach.

The correction script then connects the position fixes to form a spline feature, which indicates the centerline of travel for the grain combine. If there is a sharp change in the combine's heading, the spline is divided to create a new pass. These breaks prevent the script from creating a polygon between the points that denote the end of one pass and the beginning of the next pass. The centerline feature also directs creation of transects. At each position fix a transect is created normal to the centerline. The length of the transect equals the full cutting width of the platform used by a combine, and this transect is centered along the centerline. The

user enters the value for the cutting width when this correction script is executed. The user can also enter an offset value in the event that the GPS receiver was not centered on the combine. This offset value is used to properly place the transcet on the centerline.

After completing the construction of these transect lines for the entire field, a series of polygons is constructed. Polygon construction results when the normal lines are connected to the terminus of consecutive transects. Each polygon now represents the actual area traversed by the combine head between GPS fixes, and this area is assigned to the most recent fix. The final and most computationally complex processing step is to determine the actual harvested area for each fix by looking for overlapping polygons. Overlapping, or intersecting polygons, are indicative of a reduction in actual harvest width. The Avenue script uses a graphical method to determine if there are instances of overlapping harvested area polygons in the field. As polygons are created, the areas of two or more polygons will overlap if the combine operator did a poor job of entering the actual cutting width of the combine. When overlap occurs, the area of the first polygon to occur (based on time) will be left unchanged. The areas of polygons that intersect this first polygon will be adjusted through subtraction of the overlapping area. Figure 6.2 demonstrates this correction strategy as the first polygon (A1) is not edited, but the area of polygon A2 is reduced by the amount of overlap between itself and A1. The area of the third polygon is reduced by the area of overlap between itself and A1 and A2.

After the actual harvest area polygons were created for each position fix, the area of each polygon was determined using a second Avenue script. Polygon areas were calculated in square meters and converted to hectares. Both of these area values are merged with the yield monitor data file. Proper alignment between the two datasets is insured by the use of a feature indexing system that is part of the ArcView engine. Figure 6.3 below shows a sample of the graphical output from the ArcView correction script. The graphic on the right has had some adjoining polygons deleted from a select number of adjacent passes to illustrate the polygon clipping.

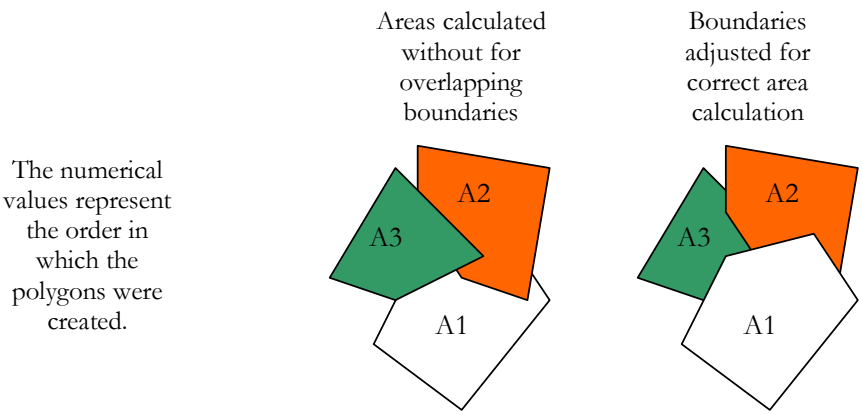

Figure 6.2. Example of polygon coverage correction routine.

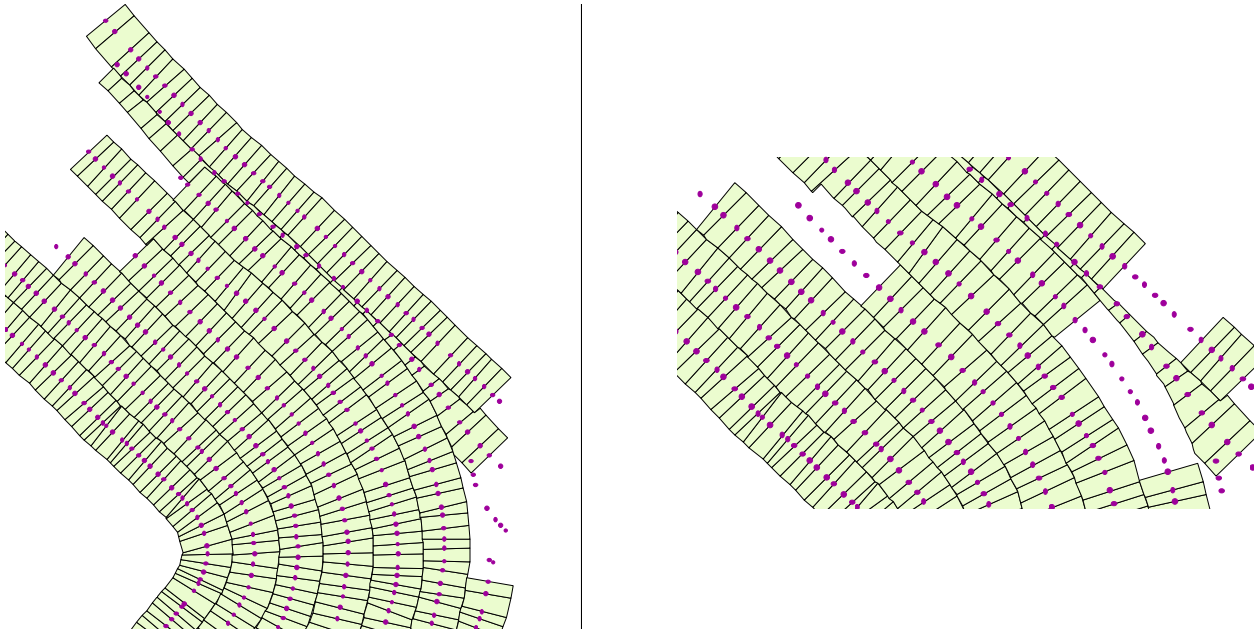

Figure 6.3. Post-processed harvest area polygon for a representative section of a harvested wheat field.

Data Acquisition

The collection of data for this chapter extended beyond the field experiments conducted for this investigation. Additional solid-sown crop harvest data were requested from cooperating crop producers so that a wide variety of data could be studied. Additional soybean harvest files were acquired from University of Kentucky's Animal Research Center (ARC) located in Woodford County, Kentucky. At the time of this harvest, the University farm owned and

operated a John Deere 7720 combine with 5.5 m small grain platform. Worth and Dee Ellis Farms located in Shelby County, Kentucky also provided soybean and wheat harvest data. The Ellis Farm data were collected using a John Deere 9610 combine equipped with a 6 m head. The remaining data analyzed in this Chapter were collected using the University of Kentucky Biosystems and Agricultural Engineering Department's John Deere 9500 equipped with a 7.33 m small grain platform. The UK-BAE combine conducted wheat and soybean harvests at both the ARC and Ellis Farms. Using an assortment of small grain platform widths allowed the processing algorithm to be adequately tested under a variety of harvest conditions.

The two University-owned combines were equipped with Ag Leader AL2000 yield monitors and a Trimble Ag 132 GPS receivers operated with U.S. Coast Guard correction. The Ellis Farms combine was equipped with a John Deere AMS Greenstar yield monitor system and a Starfire GPS receiver with WAAS correction. All yield monitor data were downloaded via PCMCIA cards to a laptop computer, and exported using SMS Basic (Ag Leader, Inc.) in advanced file formats. Parameters of interest included grain mass flow rate and distance traveled per cycle, moisture contents, swath or header width, latitude, and longitude. These data were replicated for each cycle. Data were logged at cycle times of 1 s. All data files were imported into ESRI ArcGIS to verify that data were contained within the boundary of the field. In all, there were full data sets for six soybean and six wheat fields, representing over 280 solid-sown crop hectares.

In addition to these regular field data sets, additional field data were collected to verify the accuracy of correction methods. Because this correction procedure is focused on adjusting the effective cutting width, the actual cutting swath in the field has to be documented to confirm the amended cutting width is a more accurate reflection of the true width. To verify the accuracy of the GIS correction procedure, the small grain platform was equipped with RTK-GPS receivers on each of the crop dividers. The cutter bar spans the distance within the two dividers and is equivalent to the maximum cutting width. RTK-GPS positioning allows the location of each end of the grain platform to be known within a few centimeters of the actual location. The crop divider positions were logged at 10 Hz during summer wheat harvests in 2005 and 2006. The data were archived using a Microsoft Visual Basic program that wrote each of the incoming GPS NEMA GGA text strings to a text file. The NEMA GGA string is a standardized RS-232 serial communication message that contains basic GPS position information such as time, latitude,

longitude, and signal quality. The time stamping is critical to allow proper alignment with yield data in future analysis.

Because the mass flow sensing alternatives developed in Chapters Three and Four were tested in conjunction with the summer wheat harvests, there are two separate sets of positioning data available for this test. The yield monitor data was georeferenced using a 1 Hz DGPS signal using U.S. Coast Guard correction. The mass flow alternative data were georeferenced using a 10 Hz RTK-GPS signal. Both the DGPS and RTK-GPS antenna were placed along the centerline of the combine simultaneously. Therefore, there are two adequate GPS data sets that could be used to determine the location of the combine in the field. Each of these data sets will be used in future analyses to determine how the relative accuracy of a GPS receiver position affect output from a swath width correction algorithm.

Accuracy Evaluation

A single field was divided into two parts and the GIS polygon coverages were generated for each yield monitor data point. The polygons were not clipped. This allows each polygon to represent the harvest that would occur if the full cutting width were utilized. The polygons were plotted along side the lines representing the path traveled by each end of the small grain platform. Discrepancies between the edges of the polygons and the true path were quantified and studied. Depending on the severity of these discrepancies, measures were taken to improve the accuracy of the system.

The use of vector analysis to correct harvest area is not a new idea, but previous iterations of this method used RTK-GPS positioning from two receivers on the grain platform. To acquire this level of positioning accuracy requires a significant capital investment. With the adoption of automatic guidance systems in agriculture for both tractors and grain combines, today there are machines equipped with a single RTK-GPS antenna that tracks the centerline of the machine. Because the method developed for this dissertation requires the use of a single GPS signal, the highly accurate RTK-corrected signal is desired. The GIS polygon coverage will use RTK-GPS position solutions and generate new harvest areas.

Results and Discussion

Relative GPS Accuracy

One of the assumptions used in the development of this correction procedure was the belief that DGPS positioning can be used to establish the relative position of two points with confidence. To investigate this claim, a Trimble Ag132 DGPS receiver was placed over a known location and collected data over the span of 30 minutes. These data were averaged in 5-minute increments. A statistical analysis (Table 6.1) was completed to determine the variation in the GPS data for each increment. The first 5-minute increment represents the receiver start up, hence the increased average error. The standard deviations for all intervals are less than 6 cm and the greatest average error recorded for a single interval (beyond system start up) was 11 cm. This error values was less than 2% of the width of typical small grain platforms. The most noteworthy point in the analysis is that in 80% of the intervals the incremental standard deviation is significantly less than the standard deviation for the full 30 min period.

Table 6.1. Comparison of Relative GPS Errors

Interval	Time Interval (min)	Circular Error	
		Average (m)	Std. Dev. (m)
1	5.0	0.155	0.0483*
2	5.0	0.090	0.0574
3	5.0	0.068	0.0277*
4	5.0	0.115	0.0389*
5	5.0	0.090	0.0497*
6	5.0	0.077	0.0316*
All	30.0	0.104	0.0544

* A comparison of variances revealed the 30 minute interval variance was significantly greater than the 5 minute interval variance at an alpha of 0.025.

From the previous analysis, it is reasonable to assume that while the absolute error of an agricultural grade GPS receiver is at a level that some may consider to be unacceptable for determining actual header cut width, when considering the relative accuracy of the receiver, and the fact that most adjacent passes within a field will be made within a few minutes of one another, this situation, while not totally resolved, is improved. There is evidence that errors due to GPS position drift occurring when extreme time differences exist between consecutive field passes can be considerable. Typically this occurs if a combine breaks down or harvesting

operations cease due to weather or darkness. The absolute distance between the consecutive passes would no longer equal the approximate platform cut width. In general, the newest cutting path will be too close to a previous pass on one side and too far away from the previous pass on the other side.

Accuracy of Polygon Generation

After the initial field data were processed, the correction program assessed the spatial accuracy of the polygons. Accuracy was defined as the difference between the location of the algorithm's polygon ends (the non-transect sides) and the position of the ends of the cutting platform defined by RTK-GPS data. The clipping feature of the correction script was disabled, thereby allowing the script to continuously generate harvest area polygons that would result from harvesting with the maximum cutting width. Figure 6.4 illustrates the RTK-GPS data plotted alongside the unclipped polygons. The coordinates for the four corners of the polygon (a.k.a. the transect ends) were recorded for each point. Using these coordinates, the error term was calculated as the distance from the transect terminus to the RTK-GPS defined line denoting the path of the cutting platform.

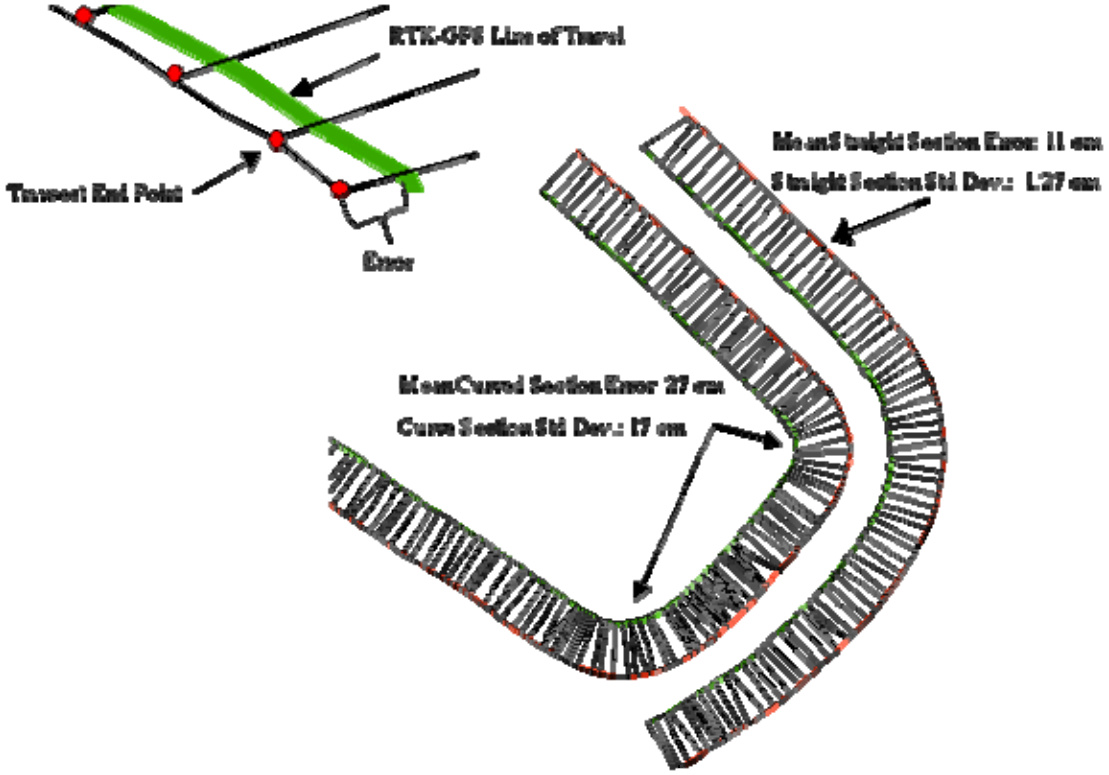

Figure 6.4. Illustrating the errors associated with harvest area polygon generation.

Based on this error calculation method, there were a number of trends that became apparent. First, there is an obvious problem with the performance of the correction in turns or tight curves. In Figure 6.4, values for the mean error are provided as a means of comparison. In the straight passes, the average error is 11 cm with a modest standard deviation (1.27 cm). Both inaccuracy and variability increase in the curved sections, as the error increases to 27.10 cm with a standard deviation of 17.36 cm. At first glance this may be cause for concern, but the reality of the situation is only the data associated with the inside GPS receiver indicates this trend. The outside receiver produces mean errors of 13.44 cm with a standard deviation of 3.70 cm. It is quite possible that the dynamics associated with the header pivoting around the corner may affect the accuracy of the GPS system against which the correction algorithm's accuracy is being judged.

Other reasons suggesting this error term may not be excessive are the scale of this operation as well as performance of the correction algorithm itself. A 7.5-meter small grain platform was used in this harvest, so the curved section average error term represents 3.6% of the cutting width. It seems unlikely that an operator in the field would estimate the cutting width of the combine to within 3.6% of the true cutting width. Also, in the case of the most severe error in the curved section, the polygon is overestimating the cutting width. Because this is an overestimate, there is the strong likelihood that the polygon will be clipped during the correction and this error will be removed.

While there is error associated with the polygon generation, the magnitude of the error is relatively low given the cutting width of the machine and the errors are very stable when straight sections of a field are considered. A field with a large number of sharp turns may be a cause for concern when using this correction methodology. But given the typical error value (approximately 12 cm) it is unlikely that an operator could estimate cutting widths to this tolerance, much less take the time to key these highly variable values into the yield monitor.

Actual Cutting Width Determination

After processing the yield data, the Avenue script assigns the polygon area associated with the yield point to a new column in the spatial database file (a .dbf file). Because the yield monitor measures and records the distance between mass flow readings, it is possible to calculate the effective cutting width for each yield point through division of the ArcView derived harvest

area by this cycle distance. Figure 6.5a illustrates the effective cutting width distribution for a 7.5 m small grain platform harvesting wheat in the curved section of a field. Figure 6.5b provides the same data for a 7.5 m platform harvesting in straight portions of a field. There are two points to note. First, the mean effective cutting width for the curved portion of the field was 5.62 meters, which shows a considerable reduction over the maximum cutting width of 7.5 meters. However, this result was common to all data sets analyzed. It seems most operators allow one end of the cutting platform to swing out wide while harvesting in turns to insure all of the crop is gathered. To an operator, it is more important to make sure all the grain gets cut during the turn; effective utilization of the head is not nearly as important. If an attempt to use the full cutting width fails, then the operator is forced into an even more unproductive set of maneuvers to turn around and harvest any crops left standing. Also the pivot point of the combine while turning is between the drive wheels, therefore, because of geometric relationships it is nearly impossible to utilize a full cut width. Turning is a special case, and is not indicative of the true relationship between the effective cut width and the maximum cut width. On average, the effective cutting widths were within 1 meter of maximum cutting width in 10 of the 12 fields analyzed. Figure 6.5b is more indicative of an effective harvest width correction. In rectangular fields, it seems the operator is able to make more efficient use of the cutting platform.

The interesting feature in Figure 6.5 is the evidence of effective cutting widths that are greater than the grain platform is capable of covering. There are approximately 400 points or 2% of the data that have effective cutting width values of 6.5 meters or greater in Figure 6.5a. This error is attributed in part to the correction procedure used by the Avenue ArcScript. The script creates polygons by connecting consecutive transects defined at the yield data points. In previous discussions regarding the correction algorithm, the transects were determined by combine's heading between two consecutive GPS position fixes. If the heading between two points exceeds 70 degrees, then the correction algorithm will not connect the two points. This feature insures harvest area polygons are not generated between the points defining the stopping point of one pass and the start of the next. However, when the combine passes through a waterway in the field and data points are logged, the correction algorithm will simply connect the dots to produce a large polygon spanning the waterway. Figure 6.10a contains evidence of harvested area polygon generation through a waterway.

When the area of these large polygons is divided by the cycle distance logged on the yield monitor, the result is an excessive cutting width value. Ideally, there would be a feature that would prevent the polygons from being generated if the distance between points exceeds a threshold value. However, this would not be a good idea, since many crop producers use logging at intervals greater than 1 Hz to store more data on a single PCMCIA card. As logging rates decrease, cycle distance increases. Calculating the effective cutting width is a form of data filtering, because these data points, whose corrected harvest areas correspond to cutting widths greater than the full cutting width of the platform, should be deleted.

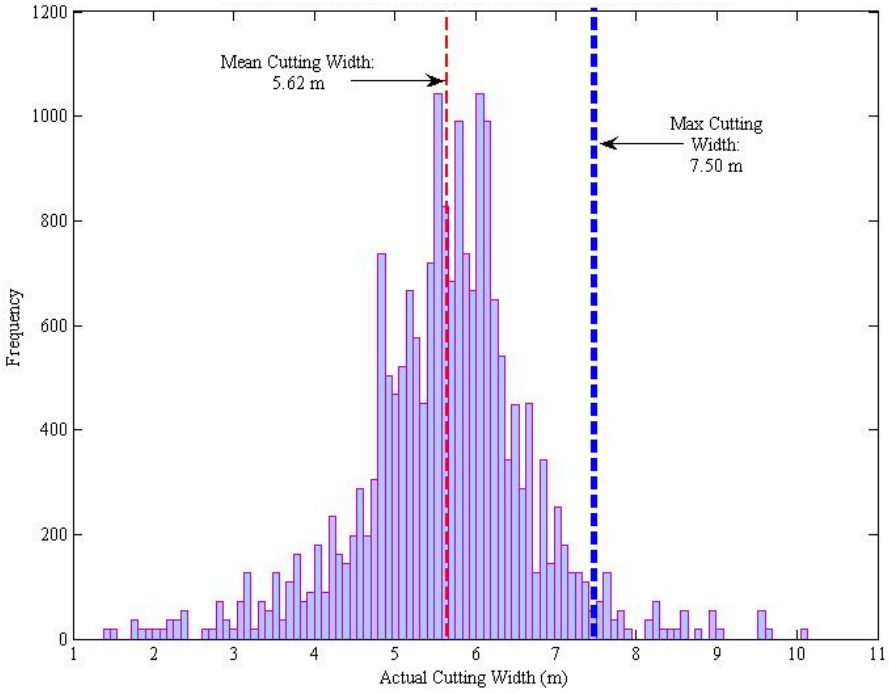

a) Cutting Width Distribution in Curved Passes

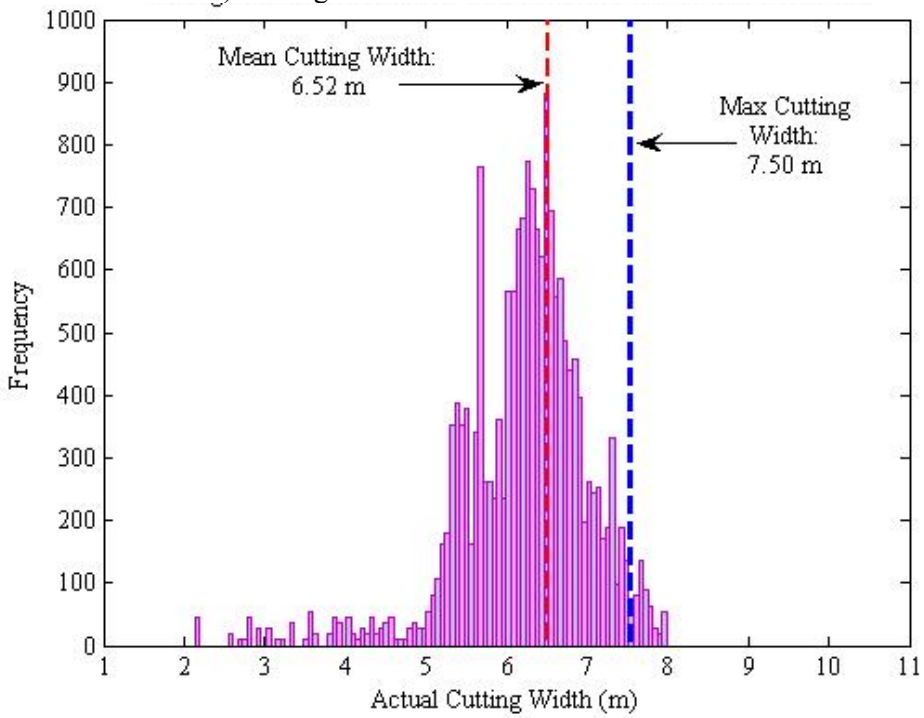

b) Cutting Width Distribution in Straight Passes

Figure 6.5. Comparison of actual cutting width distributions on straight and curved passes in a wheat field harvest with a 7.5 m small grain platform.

Total Field Area

Another method that can be used to verify the accuracy of the cutting width value logged within the yield file is to integrate the harvested area for all of the yield data points. Multiplying cycle distance by cutting swath width and summing these results should produce a value very close to the total area of the field. If the summed result is larger than the true field area, then this result signifies that the combine covered more ground than is present in the field. For each of the three wheat fields harvested for this experiment the summed harvested areas values were considerably larger than the true field area.

As an example, consider the 9.00 ha wheat field harvested in July 2005 pictured in Figure 6.10a and Figure B.9. When the harvested area for each point was calculated using the yield data file values and the summed the total field area added up to 9.83 ha. Summing the areas associated with the GIS-created harvested area polygons resulted in a total field area of 8.14 ha. The 9.00 ha field value is based on a GPS collected field boundary, which does not take into account the waterway running through the middle of the field. Therefore, it is obvious that the harvested area polygons are a more accurate reflection of the total harvested area than the summed area results from the yield monitor data. This quick comparison of total field area versus the area covered by the combine is a good indicator of the presence and magnitude of the incorrect cutting width entry.

Grain Yield Recalculation

Thus far the accuracy of the harvest area correction script has been discussed. The Avenue script appears to create polygons that represent the path of the cutting platform with reasonable accuracy, and the effective cutting widths that can be calculated from the harvest area values are realistic. Because this appears to be a potentially valuable tool for the correction of yield monitor data, it is time to take a closer look at how grain yield estimates are recalculated and determine if the corrected values are an improvement over the yield monitor estimated values. Both graphical and statistical analyses of the data sets were conducted to learn how the correction routine affected grain yield estimates.

A total of three data sets were examined. Uncorrected yield monitor data and ArcView post-processed data were studied. The third data set is comprised of yield monitor data corrected by using a constant effective cutting width value for the entire data set. This average effective

cutting width is based on the average harvested polygon area and the average speed of the combine in the field. This third method was implemented due to the extreme computational complexity and time required to run the ArcView Script. Using the third correction routine, a smaller section of the field would be processed to determine the average effective cutting width. This value is then applied to the remaining yield monitor points. The points not processed in ArcView rely on logged cycle distance and the average effective cutting width value harvest area determination.

The initial investigation into yield estimate recalculation is limited to a graphical approach. Using Matlab, histograms were created for all three yield estimate data sets. Figures 6.6 and 6.7 show the results for wheat harvested using 7.5 m and 6.5 m grain platforms, respectively. Figure 6.8 shows the results of a soybean harvest using a 5.5 m small grain platform. For both wheat examples, the mean yield value is increased significantly when the GIS correction routine is applied. In the case of the 7.5 m platform in wheat, the yield estimate increased 28% from 2.47 Mt/ha to 3.18 Mt/ha after the correction was applied. Similarly, the yield estimate increased 24% from 2.75 Mt/ha to 3.41 Mt/ha after the correction was applied to wheat field harvested with the 6.5 m platform.

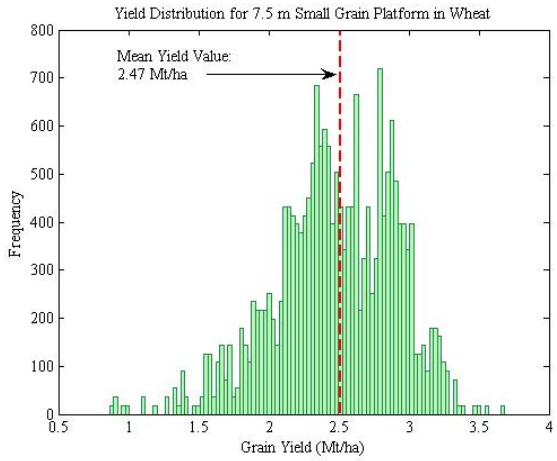

a) Uncorrected yield estimate distribution

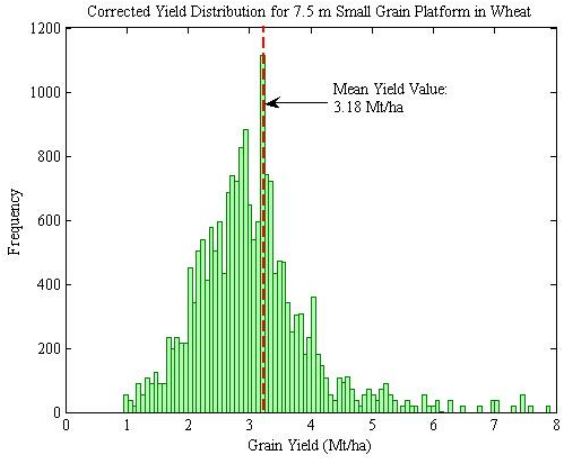

b) ArcView script corrected yield estimate distribution

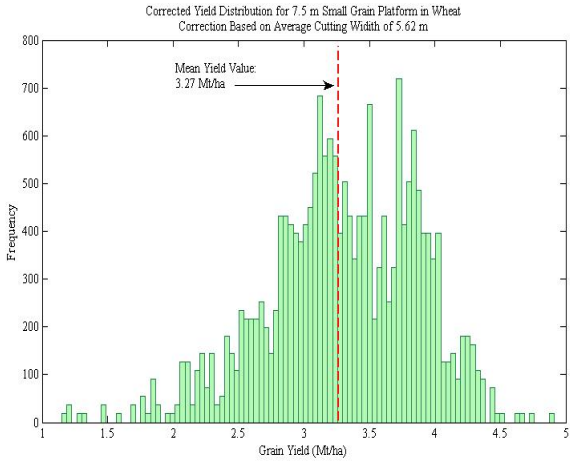

c) Average effective cutting width corrected yield estimate distribution

Figure 6.6. Comparison of grain yield distributions using uncorrected and corrected yield monitor data for wheat harvested with a 7.5 m grain platform.

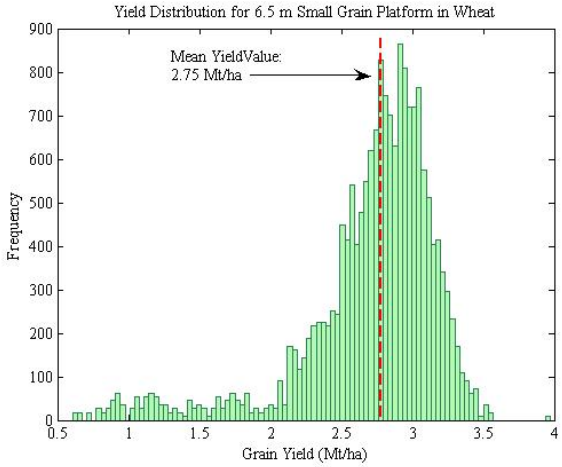

a) Uncorrected yield estimate distribution

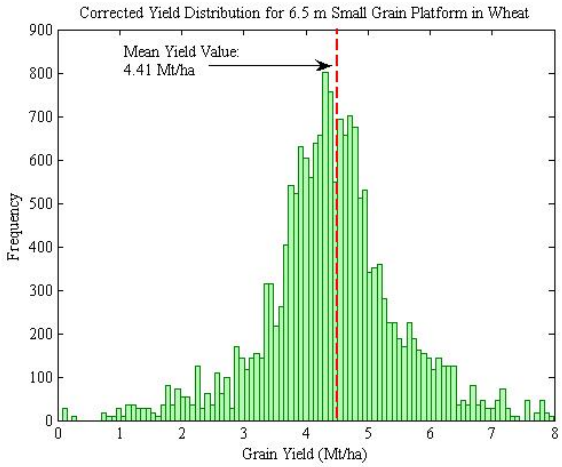

b) ArcView script corrected yield estimate distribution

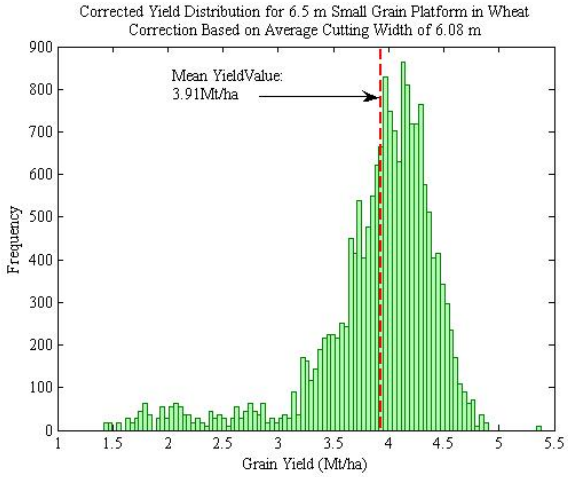

c) Average effective cutting width corrected yield estimate distribution

Figure 6.7. Comparison of grain yield distributions using uncorrected and corrected yield monitor data for wheat harvested with a 6.5 m grain platform.

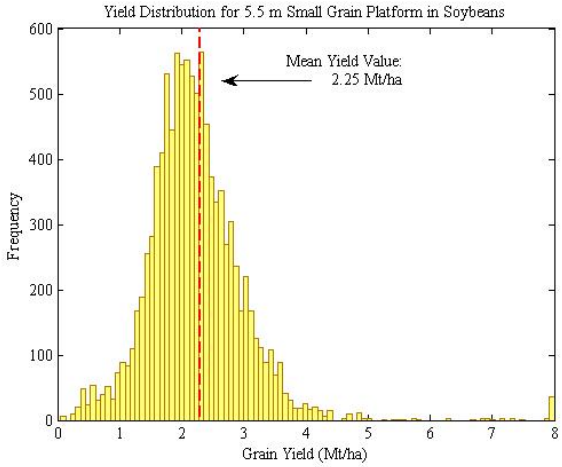

a) Uncorrected yield estimate distribution

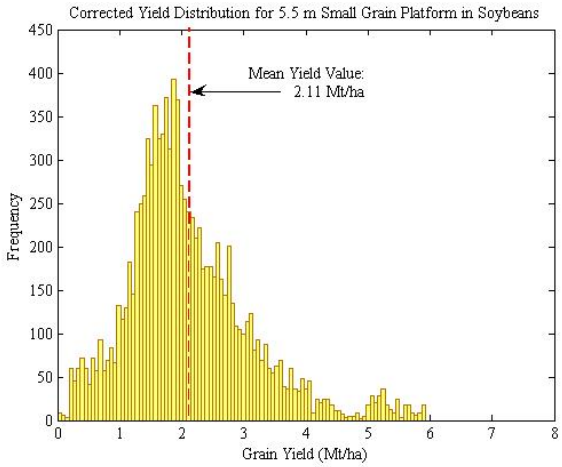

b) ArcView script corrected yield estimate distribution

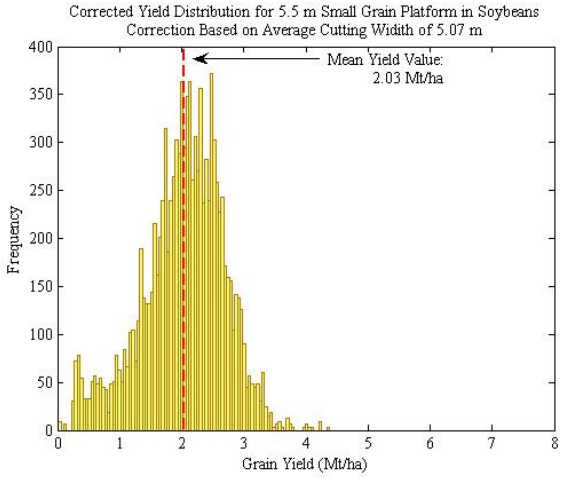

c) Average effective cutting width corrected yield estimate distribution

Figure 6.8. Comparison of grain yield distributions using uncorrected and corrected yield monitor data for soybeans harvested with a 5.5 m grain platform.

The third correction method produced average yield estimates for the field that were much closer to the value determined with the ArcView program. This would be the expected result, since the third correction procedure applies a constant effective cutting width value determined by the ArcView Avenue script to the entire data set. The main difference between the full GIS correction and the application of an average effective cutting width value is the variation in the data is reduced with the latter. Careful examination of the wheat harvest histograms shows the yield variation increases for the ArcView corrected script. The most apparent feature is how the data tails off towards relatively high grain yield values. These extreme values are the result of grain mass flow values being assigned to exceptionally small harvest area polygons.

Figure 6.9 provides an illustration of how these small harvest area polygons are generated. These polygons occur in field locations where the combine has stopped with the feeder housing down, in a harvest position. Most yield monitors use the feeder house position to determine whether or not the machine is harvesting crop. As long as the feeder housing is down the yield monitor will log data. As a result of variations in the GPS position fixes, it would appear that the combine is moving very short, erratic distances. Because the correction script calculates a heading between each GPS position and draws a transect normal to the heading, small pinwheel shaped clusters of transects are produced. The distance between the transects is so small that the resulting harvest polygons have associated areas of less than 1 m^2.

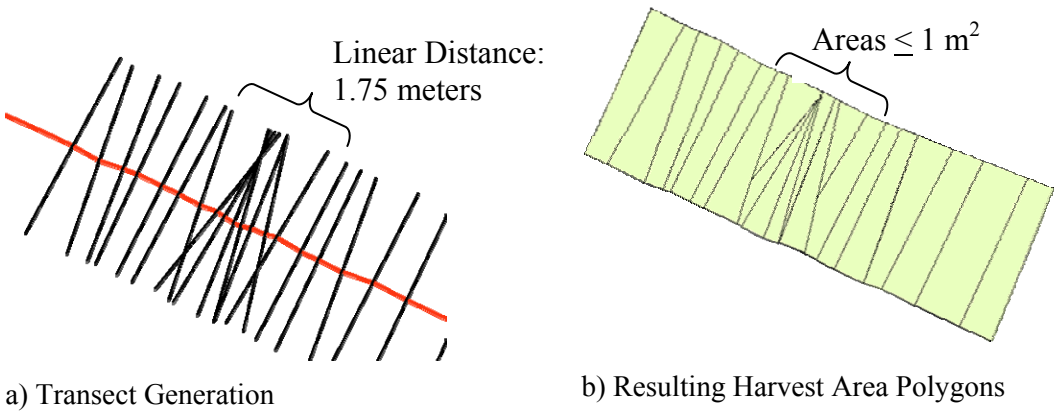

Figure 6.9. Generation of erroneous harvested area polygons due to a substantial reduction in machine velocity

The generation of the excessively small harvested area polygons can be avoided by pre-filtering the data to remove cycle distances below a given threshold. This type of threshold filtering has value and has been discussed in detail in Chapter Two. The USDA ARS Cropping Systems Laboratory in Columbia, Missouri has developed a yield monitor data editor that will provide these filtering capabilities (USDA, 2006). For the remainder of the analysis in this chapter, all data sets were filtered using the USDA-ARS Yield Editor. These histograms were developed to provide insight into errors associated with the GIS correction method.

The typical yield correction that occurs after processing yield monitor data through the ArcView program can be seen in Figures 6.6 and 6.7. The most typical operator error is to use the maximum cutting width value for the entire harvest. This error will underestimate grain yield because the mass flow value is being divided by a disproportionate harvest area. Using the true cutting width will decrease the harvested area associated with a mass flow reading and increase the yield estimate for the point.

Figure 6.8 appears to illustrate an errant field correction as the yield calculated for the corrected areas actual drops by 8% from 2.25 Mt/ha to 2.11 Mt/ha. This is an accurate correction and this figure shows an unexpected benefit provided by this correction routine. A 5.65 m cutting platform was used in the harvest of this field, but because of an operator error/oversight, the cutting width entered into the yield monitor was 4.74 m. This operator error was not discovered until after an initial correction was applied to the original data set. The output from this first correction showed obvious gaps between the polygons created for consecutive passes. These gaps would indicate either wayward GPS positioning, missing combine passes, or an excessive amount of crop was left unharvested in the field. Through a process of elimination, all of these error sources were eliminated from consideration and the cutting width recorded by the yield monitor was checked. The yield file showed that the operator had reduced cutting width after 117 points were collected, but never changed the cutting width back to the original, correct full width for this particular combine. In addition to the correction of overlapping passes, this program will correct for instances when the cutting width is greater than the cutting swath recorded by the yield monitor.

The traditional method of displaying grain yield estimates across a field is to use a yield map. Yield maps have been developed to show yield estimates for both the uncorrected and corrected yield monitor data. A difference map has also been created to indicate the percent

yield difference between the original, uncorrected data set and the post-processed data set. Figures 6.10 and 6.11 present these yield maps for a wheat harvest using a 7.5 m cutting platform and a soybean harvest using a 5.5 m platform. These are the same data sets that were used to develop the histograms in Figures 6.6 and 6.8. The yield maps show the same trends as the histograms for both grain harvests.

The wheat field yield maps show an increase in yield in the post-processed map versus the original data set. The difference map provides some interesting new insight. It appears that the difference in yields is fairly constant across the entire field. It is impossible to select discrete zones where the yield differences vary from the yield differences displayed in the remainder of the field. This supports the notion that the amount of the header width used while harvesting grain is a characteristic of the operator. A particular combine operator may allow 0.67 m of the header to pass over previously harvested ground and this overlap will remain fairly constant throughout the harvest. This difference map also supports the idea of processing a small portion of the field to establish a correction factor that could be applied to the entire field. Another feature discussed earlier and visible in this wheat field, is the large polygons that were generated when the combine passed through the waterway in the center of the field.

The soybean field yield maps show a decrease in yield in the post-processed map versus the original data set. Recall, this is the field that the operator entered a cutting width that was much smaller than the full cutting width of the machine, so the correction methods have increased the effective harvest width. The difference map associated with this field does show some patterns that are an indication of an inconsistent combine operator. Careful inspection of the difference map will show that the largest increase in yield occurs along the passes that are very close in proximity to other passes. This indicates the operator is making an additional pass through the field to harvest narrow strips of standing crop. The GIS correction program recognizes that the majority of the area on both sides of these passes has been previously harvested and dramatically reduces the harvest area, thus increasing the yield estimate substantially.

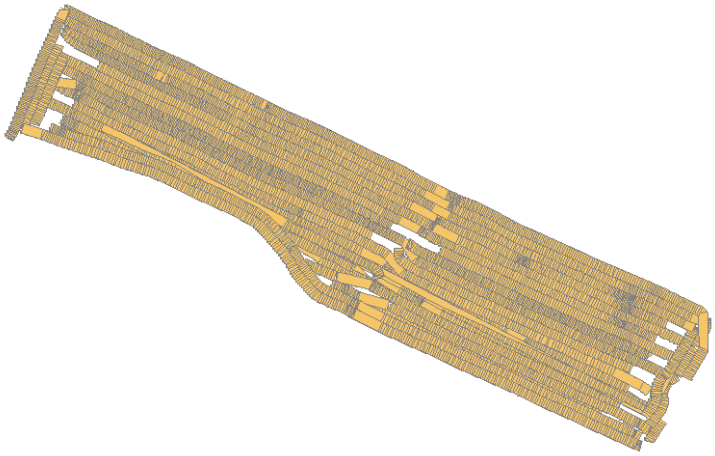

a) Harvest Area Polygon Generation

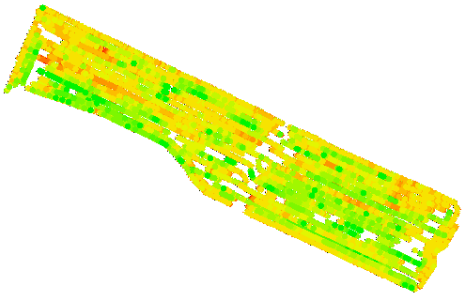

b) Uncorrected Yield Map

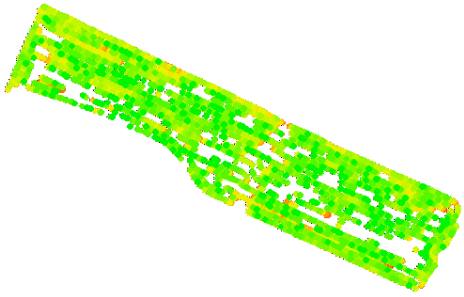

c) Post-Processed Yield Map

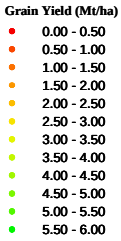

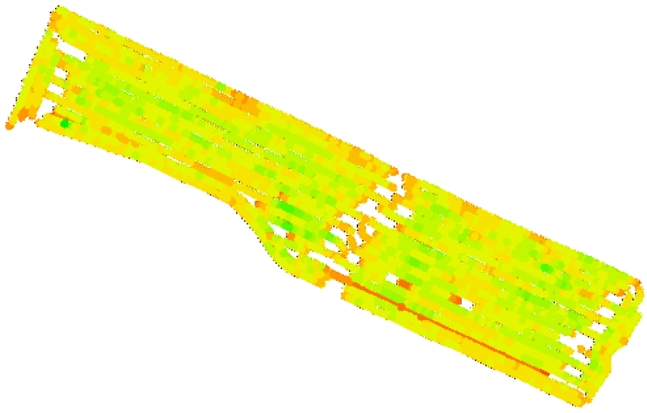

d) Percent Difference in Uncorrected and Post-Processed Yield Maps

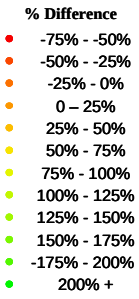

Figure 6.10. Comparison of uncorrected and post-processed yield estimates in wheat.

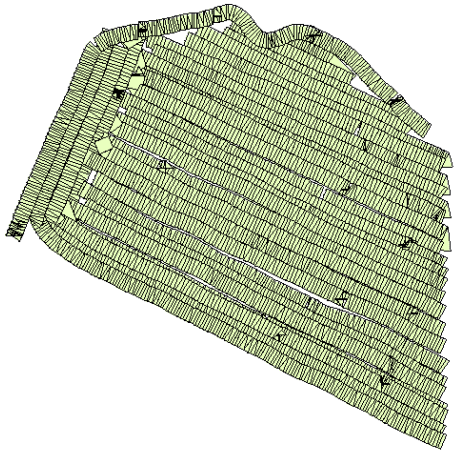

a) Harvest Area Polygon Generation

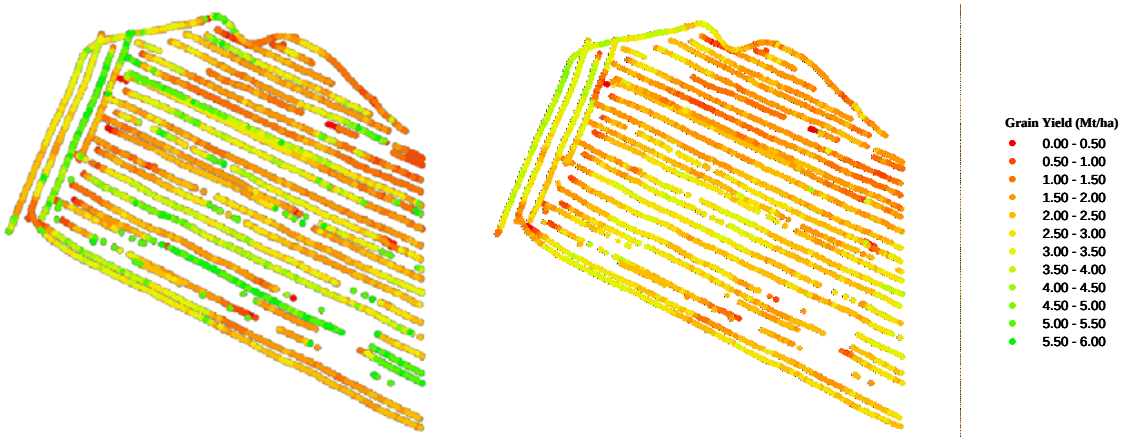

b) Uncorrected Yield Map c) Post-Processed Yield Map

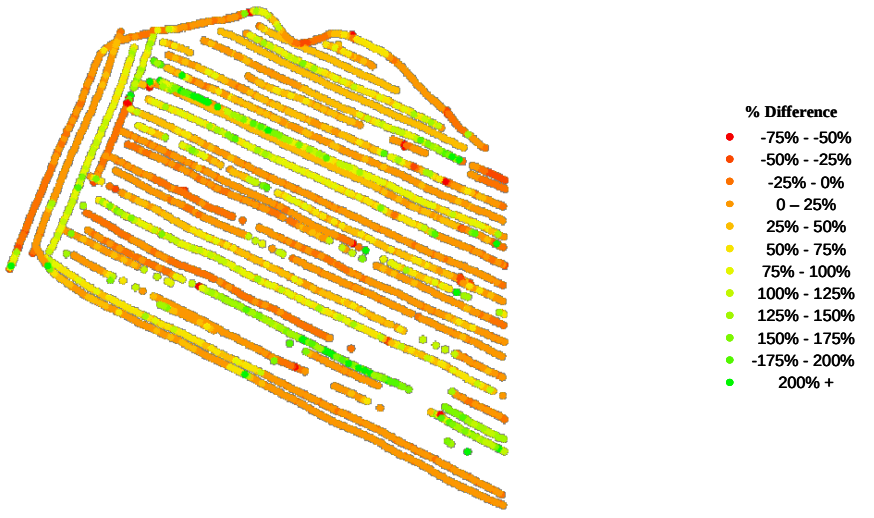

d) Percent Difference in Uncorrected and Post-Processed Yield Maps

Figure 6.11. Comparison of uncorrected and post-processed yield estimates in soybeans.

Yield monitor data from three soybean fields and three wheat fields were processed to quantify the potential effect of post-processing correction. Presented in Table 6.2 are summary statistics for the grain yield from the raw yield, the post-processed data, and the average effective cutting width correction. The mean yield determined from scale values is provided. The scale yield was calculated by dividing the total mass of grain harvest from the field by the total area of the field. This mass per unit area value was then converted to a volume per unit area using the appropriate grain test weight value. The data shown in the table suggests the propagated difference between corrected and uncorrected data may even be greater than originally thought. On average, the corrected estimated yield is 18% greater than the yield estimate for the original data set. If a single mean effective cutting width value is used as the correction factor, the estimated yield increases 15% over the original yield data. The only field where an increase in yield is not seen is the second 5.5 m soybean field. This is the field where the operator entered an excessively narrow cutting width for the majority of the harvest.

Perhaps the more noteworthy trend is the 79% increase in the standard deviation of the yield estimate after using the GIS correction method. This tendency suggests there is significantly greater yield variation within the field than many yield monitors indicate. This conclusion is similar to the findings of Whelan and McBratney (2000) who proposed a 1^{st} order model for mass flow correction. This 1^{st} order model had the effect of increasing yield estimate variability and subsequent field sampling proved that in-field yield estimates are significantly more variable than the estimates provided by yield monitors. Perhaps the difference in variation is created within the grain combine as a result of transportation delay and throughput lag. What this evidence suggests is that in some cases, as is often the case when harvesting soybeans and small grains, the errors associated with the current methods used to estimate harvested area may be more significant than at first thought.

While the increased variability can be justified, it still seems a bit excessive. The reason for this is most likely harvest area polygon generation errors that are the result of using an imperfect measurement. The heading between two consecutive GPS fixes is crucial in the development of the swath width transects. Slight deviations in the generation of this transect can radically alter the harvested area determination. This shows the difficulty of applying a systematic correction to an error-prone, irregular data set. So returning to the average effective cutting width correction, it seems it is possible to perform a similar correction on the data set and

reduce the variability. When the average effective cutting width is applied to the yield monitor data, the yield estimate variability increases an average of 22%.

Table 6.2. Summary statistics for estimated yields.

Crop & Platform Width	Correction	Mean Yield (Mt/ha)	Minimum Yield (Mt/ha)	Maximum Yield (Mt/ha)	Standard Deviation (Mt/ha)	Scale Yield (Mt/ha)
Soybeans 5.5 m - 1	Original	2.51	0.28	3.27	0.499	2.81
	Post-Processed	2.83	0.16	4.98	0.813	
	Avg. Width	2.77	0.20	4.65	0.651	
Soybeans 5.5 m - 2	Original	2.25	0.31	3.15	0.501	2.07
	Post-Processed	2.11	0.12	4.59	1.081	
	Avg. Width	2.03	0.08	4.27	0.795	
Soybeans 6.5 m	Original	3.17	0.13	5.17	0.647	4.05
	Post-Processed	3.95	0.12	5.69	0.894	
	Avg. Width	3.97	0.17	5.13	0.705	
Wheat 7.5 m - 1	Original	3.04	0.27	4.78	0.571	3.91
	Post-Processed	3.99	0.12	5.93	1.264	
	Avg. Width	3.83	0.21	5.07	0.612	
Wheat 7.5 m - 2	Original	2.47	0.16	4.06	0.736	3.00
	Post-Processed	3.01	0.09	6.17	1.173	
	Avg. Width	2.96	0.10	5.16	0.701	
Wheat 6.5 m	Original	2.75	0.23	4.26	0.518	3.46
	Post-Processed	3.41	0.14	5.15	0.915	
	Avg. Width	3.30	0.18	4.97	0.695	

Further analysis regarding the normality of yield data, in both the unprocessed and post-processed states, shows some interesting trends. Normal probability plots for both data sets illustrate some changes in the distribution of yields. In Figure 6.12a, the central portion of the plot is nearly linear, suggesting the data is normally distributed. The major deviation is at the

non-linear nature of the tails of this plot. After processing the data using GIS correction (Figure 6.12b) the central portion of the normal probability plot appear less linear suggesting that yield is not normally distributed. However, in the latter plot the tail appear to be more normally distributed than for the unprocessed data. Comparison of these results to the general shape of the histograms developed earlier supports this conclusion.

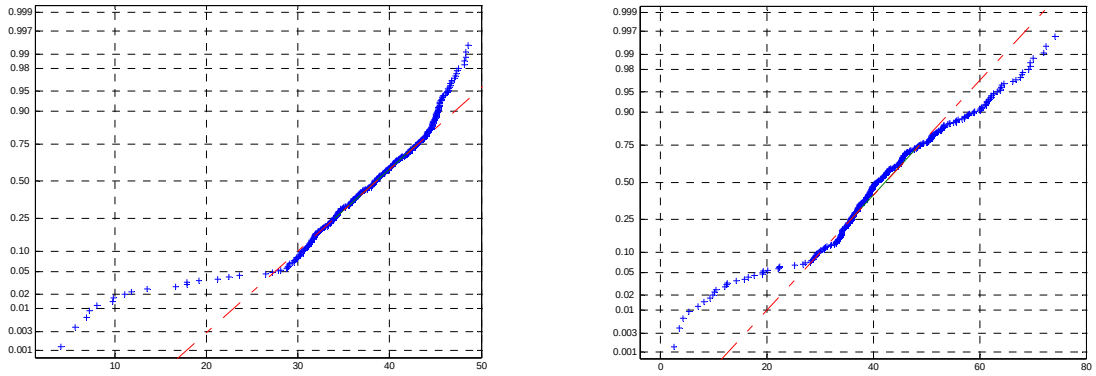

a) Original Yield Estimate

b) Corrected Yield Estimate

Figure 6.12. Normal probability plots for a) original yield estimates, and b) post-processed yield estimates.

Summary

At a minimum, the findings of this investigation suggest that further efforts are needed to fully assess the accuracy of area determinations methods used in most commercially available yield monitors. The feasibility of the GIS correction method is dependant on GPS receiver accuracy. Errant GPS data will cause errors in the correction routine. Also, yield monitor data points that contain ambiguous data, such as extremely short cycle distances or extreme mass flow readings, will lead to poor yield estimates for both the yield monitor and post-processed data sets. Based on the testing completed during this study, the following conclusions were made:

- The GIS algorithm (ArcView Avenue Script) developed to correct combine cutting swath errors generated harvested area polygons that appear to represent the true harvest area that occurred in the field.
- The value keyed in to a yield monitor for cutting width is generally excessive. The GIS algorithm corrected the cutting width value, thereby increasing in grain yield estimates by an average of 18%.
- The correction method tends to increase yield estimate variability across the field by as much as 120%.
- Because of computing complexity issues and the time required to process an entire field with the GIS correction routine, an alternative correction method was developed. This alternative method applied the average effective cutting width found for a small section of the field to the entire data set and produced adequate yield estimate corrections with moderate variability. While better than operator entry, this method is not as exact as the full field application of the Avenue script.

Chapter Seven
Conclusion

Concluding Remarks

Yield monitoring is a revolutionary technology from the viewpoint that it gives grain producers an opportunity to quantify infield crop production variability with relative ease. However, the errors that plague these systems can lead to inaccurate information affecting management decisions. A review of previous research as identified the many sources of yield monitor error and discussed a variety of methodologies that could be used to enhance yield monitor data. The variability of material transport time through the cleaning and separating mechanisms within a grain combine and incorrect cut-width values are two of the most prominent yield monitor error sources. This research project intended to improve yield monitor accuracy by limiting the effects of these errors through the use of sensor fusion and post-processing algorithms.

Objective 1 of this research was addressed with the development of two crop mass flow sensing devices. A chain tension sensor attached to the feeder-house drive chain was evaluated along with a hydraulic pressure sensor attached the piston responsible for adjusting the threshing cylinder's variable-speed drive. Both of these sensing methods were capable of distinguishing variations in crop biomass throughput better than the traditional grain mass flow sensor used by a yield monitor. The key improvements observed in the alternative mass flow sensor data was the detection of areas absent of grain production and delineation of the start and end of harvest segments. Typically, the feeder-house based sensor was more sensitive to variations in crop throughput than the cylinder drive pressure sensor.

The relationship between grain mass flow and crop mass flow was determined to be relatively weak ($R^2 < 0.60$). Because of this marginal relationship, it seems crop mass flow readings are not a suitable replacement for grain mass flow measurements. However, variations in crop throughput into the combine provide a reasonable expectation of an impending variation in grain mass flow. For instance, if there is no crop material entering the feeder housing, the grain mass flow for this area should be zero. Similarly, if a 50% decrease in crop throughput is

determined, then there should be a grain mass flow decrease of similar magnitude in the vicinity of this reading.

Objective 2 was completed by incorporating the results of Objective 1 into a correction routine to redistribute the grain mass flow measured by the yield monitor. Using the feeder-house chain tension sensor, the location and magnitude of variations in crop throughput were noted and then used to redirect the mass flow data. The features unique to this correction routine were the conservation of grain mass and feedback regarding the redirection of grain mass. The correction method was especially successful at grain redistribution when variations could be described as a step input. There were significant improvements ($\alpha = 0.05$) in the grain mass flow distribution compared to the field plot boundaries after the correction was applied. When field trial plot boundaries are used as lines of best fit, the correlation between corrected yield points and the blocking scheme improve by 50%.

For yield maps created of entire fields, the errors associated with transport delay are often reflected in loosely defined waterway boundaries or ill-defined start/end points of combine passes. The start/end points of combine passes should be in close proximity to border rows which clearly define the harvest area. After applying the mass redistribution, there is visual evidence that indicates improvement in mass flow redistribution has occurred. Typically, the end points of passes are more consistent and the waterway boundaries are clearly delineated.

Objective 3 was met by developing a GIS-based approach (Avenue script within ESRI's ArcView GIS package)e to determine the true harvest area for each yield monitor position fix. These harvest area polygons usually indicate an effective cut-width that is smaller than the full cut-width of the grain platform. Typically, an operator overestimates cut-width by 10-15% when the full cut-width is used for an entire field. This overestimation causes yield values reflected in a yield map to be below actual field levels. The variability of yield estimates increases after the harvest area correction is applied and this result is similar to yield variable levels found in fields harvested by hand.

The final objective was evaluated throughout this investigation. Data from harvests of corn, soybeans, and wheat were used to evaluated the performance of systems developed in the preceding objectives. The performance of the alternative mass flow sensors and the post-processing algorithms was equal for the entire data set regardless of crop species. The few differences between crop systems that could be inferred from this study are the result of

characteristics associated with the equipment used in this study and do not represent a universal attribute. The feed difficulties associated with the soybean harvest being the prime example.

In conclusion, the research presented in this dissertation introduces correction methods that can be used to improve two of the greatest sources of yield monitor error. Time delay variations can cause serious spatial inaccuracies in the grain mass flow profile. In order to use yield maps to make decisions at the resolution that crop producers desire, it is critical that these errors are addressed. The time delay variations represent a type of random noise, whose correction is non-trivial for the standpoint that simple threshold filters or constant time shift values do not address adequately. A more systematic source of error is the entry of an incorrect combine-cut width. Typically, combine cut-width errors under estimate crop yield by 10-15% for the entire field. This error does not effect the distribution of crop production variability; rather it is more of a constant shift in yield magnitudes.

Suggestions for Future Work

This project was somewhat limited in the field trials attempted from a cropping system and machinery standpoint. While the three major grain crops grown in the United States were tested, it would be interesting to see how these mass flow sensing devices respond when harvesting more exotic crops such as grass seed, sunflower seeds, and eatable peas. From a machinery perspective, the major omission from this study is the lack of testing on a rotary combine. Due to accessibility, modification concerns, and time constraints, it was not possible to test using a combine that was not controlled by the University of Kentucky. The function of the feeder house sensor in all likelihood would not differ from operation on a straw walker combine. Rather the two concerns are how would the hydraulic pressure on the rotor vary in field conditions and how well can mass flow be redistributed in a rotary machine. Because a rotary combine is not equipped with straw walkers, there is a considerable difference in the mass flow path and the resulting delay time variability.

Also from the machinery standpoint, a modern small grain platform would improve crop feeding into the feeder house, particularly in soybeans. Along the same lines as an improved small grain platform, other harvesting heads should be tested. Draper heads, which use a wide belt to pull material towards the center of the feeder house, are known for smoother feeding than

their auger driven counterparts. Also, a stripper head in wheat would dramatically influence both the alternative sensing methods discussed in this project because only the wheat head is fed into the machine. Currently, it is unknown how these harvest system variations would impact both the correction and sensing routines developed thus far.

Another research project that should be developed based on this project is the use of similar sensing mechanisms to measure mass flow in crops where biomass represents the actual crop. Forages and silage are two excellent opportunities to apply this technology. Because forage choppers and balers have plant material feeding mechanisms similar to the feeder house on a combine, it would be possible to measure feed rates using similar techniques as the ones developed in this project. Forage crops have lagged behind in the development and adoption of site-specific technologies. This research may provide the justification for the development of a cost-effective yield monitor for these crops. Another forage crop application would be using these crop mass flow measurements to control the speed of the prime mover to keep feed rates at optimal levels. This has been attempted in combine harvesters, but the complexity of the harvest mechanisms have lead to marginal results. Because the material pathway is shorter and less complex in hay balers or forage choppers, feed rate control seems to be feasible.

The final suggested area for future work is the development of a real-time cut-width correction mechanism. The post-processing algorithm discussed in this manuscript works well, but the computational requirements will limit its effective use and distribution. There would be ample time to correct the yield maps because there is significant downtime between crop harvest and planting. However, the greater concern is this correction procedure is another step in a long line of additional tasks required of a crop producer subscribing to precision agriculture management. To simplify data collection and processing, it would be much easier to use a real-time cut-width measurement method. To justify expense, a real-time correction cut-width measuring device should provide a farmer with additional benefits besides improved yield measurements. Vehicle guidance would be tied into this technology

Appendix A:
ASABE X579 Draft Standard

X579 Yield Monitor Field Test Engineering Procedure

Developed by the ASAE Precision Farming Committee PM-54/01 Workgroup; approved by the …..

1. Purpose and Scope

1.1. This standard provides the basic requirements for field evaluating the accuracy of the yield monitor.
1.2. The standard defines the methods to determine time delay through the harvester
1.3. This standard tests yield measurement location accuracy and to evaluate machine and ground speed variation induced error.
1.4. This standard outlines the method to prepare a field for testing to simulate changing yield conditions.

2. Terminology

2.1. **Yield Monitor:** A system of sensors and electronics mounted on a harvester and used to quantify the yield for the crop being harvested on an instantaneous and averaging basis. This includes all sensors necessary to accurately calculate a dry yield for a given location within a field .
2.2. **Flow Sensor:** The sensor(s) that directly measure the mass or volume flow of the crop in a short time sample.
2.3. **Test monitor:** The yield monitor to be evaluated.
2.4. **Test run:** The events necessary to record a single set of measurements.
2.5. **Test:** All the events and data of several test runs and the test stand qualification information.
2.6. **Sample Reference System:** A high precision weighing system used to determine actual weight of each test run. The reference system includes a moisture test to correct weight to dry basis for crops that require it.
2.7. **Blank Area:** Field area where crop has been removed to achieve 0 yield.
2.8. **Half Head Area:** Field trial area where crop has been manually removed to result in harvest occurring across only 1/2 of the harvester header width.
2.9. **MFD:** Mass Flow Delay is the time required for the crop to travel from harvest point of the harvester to contact the flow sensor when modeled as a first order system with a transport delay. Figure A.1 shows the transport delay labeled as t_d.

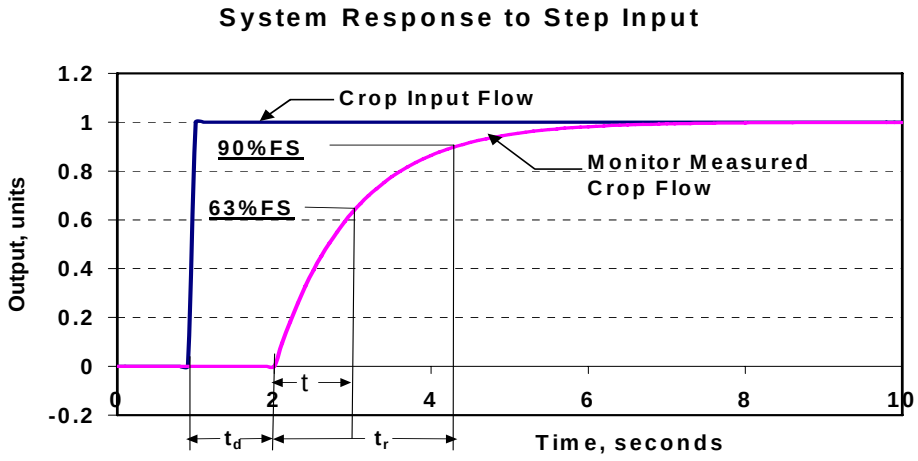

Figure A.1. Actual and Measured Mass Flow through a Harvester for MFD Determination

2.10. **STC:** System Time Constant is either:

2.10.1. The time (t) required for the sensor to reach 63% of the steady state grain flow after the initial mass flow is recorded.

2.10.2. The time (t_r) required to reach 90% of the steady state grain flow divided by 2.3. (t_r / 2.3)

2.11. **HW:** Harvest Width is the maximum width of crop harvested for a single harvester pass.

2.12. **BL:** Block Length is the plot length required for one yield monitor test. It is (MFD + 6 x STC) x standard Harvester speed during harvest. For harvesters with no MFD or STC use 50 meters for a minimum BL.

3. **Field Selection and Preparation**

3.1. Choose a field large enough to run the planned trials in a scientifically and statistically sound manner.

3.2. Choose a field with as uniform visual crop characteristics (height, color, population) as possible with any variations documented and consistent through out all BL's.

3.3. Select a harvest area with relatively uniform crop and free of obstacles, providing straight line harvesting with maximum harvesting width and no edge of field or field borders within the BL

3.4. Measure and record field slope. If the yield monitor test results from ASAE X578 identified variation with slope changes, select a field with slopes of at least 5% and orient test blocks for uphill and downhill harvesting.

3.5. Select test block areas in the center of a field. Minimum distance to the headlands or borders is 2 harvester header widths.

3.6. Use blank areas before and after the test blocks no shorter than the harvester travels during the MFD moving at normal harvest speed. Use blank width equal to the header width. Make each step in the test block to be harvested no less than twice the MFD.

3.6.1. Determine the MFD as defined in section 2.9 using a stopwatch. Start recording time as crop enters the header and stop when the first indication of flow is measured. If adjustments are made to improve harvester performance, measure the MFD again.

3.6.2. Before determining the STC, harvest with crop flowing past the sensor for 10 minutes to condition all crop contact surfaces. Harvest a path in the vicinity of the test area at the desired harvest speed and record the average crop flow rate. Calculate the STC flow as defined in section 2.10. Harvest an adjacent pass and record the time required to reach the STC flow.

3.6.3. Empty the harvester crop flow path. Stop harvesting but keep the harvest functions operating until measured crop flow reported the yield monitor reports less than 0.5% of the flow during normal harvesting.

3.6.4. In a non-test area and moving at normal harvest speed, enter the crop while recording time from start of harvest and flow or weight at yield monitor sensor.

3.6.5. Determine STC by fitting data to STC definition in 2.11.

3.7. Determine test BL as the distance the harvester will travel at steady speed through the MFD period + 6 x STC.

3.8. Determine the latitude and longitude location for start and end of blank area using the same GPS receiver but not reported through the yield monitor. Use a 3 second average of the location as reported by the GPS receiver.

3.9. Identify a minimum of 3 non-adjacent test block areas prepared with crop removed as described below.

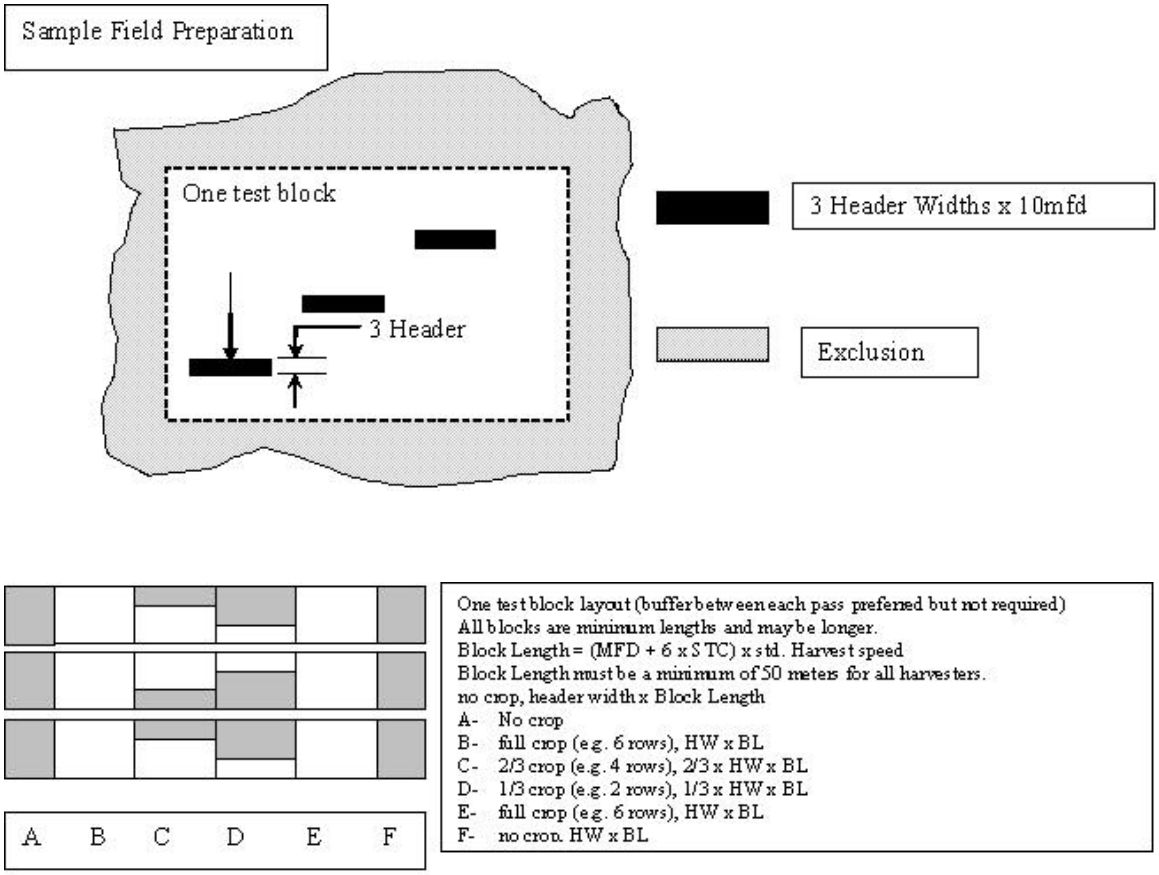

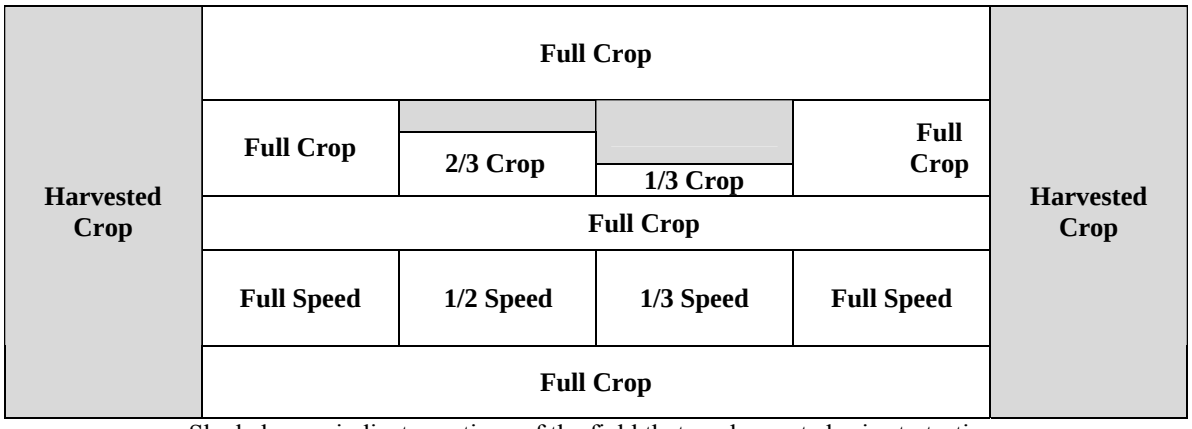

Shaded areas indicate portions of the field that are harvested prior to testing.

4. Harvest Location Accuracy Test

4.1. This test verifies the accuracy of the location where a yield sample is harvested. The test does NOT verify the accuracy or repeatability of the GPS receiver. Refer to ASAE STD X xxxx for GPS receiver accuracy testing.

4.2. This test verifies the accuracy of the reported area harvested for varied head width, harvest width and harvest speed.

4.3. This test is based on field operation and requires the yield monitor installed on an applicable combine or harvester with a DGPS receiver.
4.4. Using the DGPS receiver, determine the latitude and longitude for the start and end of the predetermined test block. The GPS antenna must be located on the edge of the test block and latitude and longitude recorded as reported by the GPS receiver not the yield monitor. Use a 3 second average of the location as reported by the GPS receiver. The location of the center of the test block (anticipated harvester path) must also be recorded.
4.5. Harvest the test block with the GPS antenna mounted normally on the harvester. Record all yield data.
4.6. Map the location of each test block with both the manually recorded data from 4.4 and the yield monitor data from 4.5.
4.7. Determine the error in position for each end of the test block and the harvester path using the data from 3.4 as the reference position.
4.8. Repeat the test block location measurement as described in 3.4 after two days and plot on the same test block map to check for time variation in GPS location reading

.

5. Response Time and Weight Accuracy Test

5.1. Complete yield monitor calibration and tare operations per manufacturer specifications before harvesting in order to start each pass with an established "zero" point.
5.2. Set recording distance or time on the yield monitor to the minimum allowed (or recommended) to record the maximum number of data points to identify variation.
5.3. Complete any harvester setting adjustments and verify harvester and yield monitoring system are functioning properly
5.4. Maintain a constant ground speed before, during and after harvesting the test block areas.
5.5. Harvest through blank and stepped harvest areas while recording yield data, harvester speed and position. Do not stop between steps.
5.6. Weigh each test block separately on the sample reference system.
5.7. Record the mass flow delay -both manually timed and observed by flow rate shown on the yield monitor.
5.8. Repeat testing with ground speed varied as shown below.
5.9. For fields with slope greater than 1%, repeat testing with data recorded while harvesting in the opposite direction of travel through equivalent test blocks.

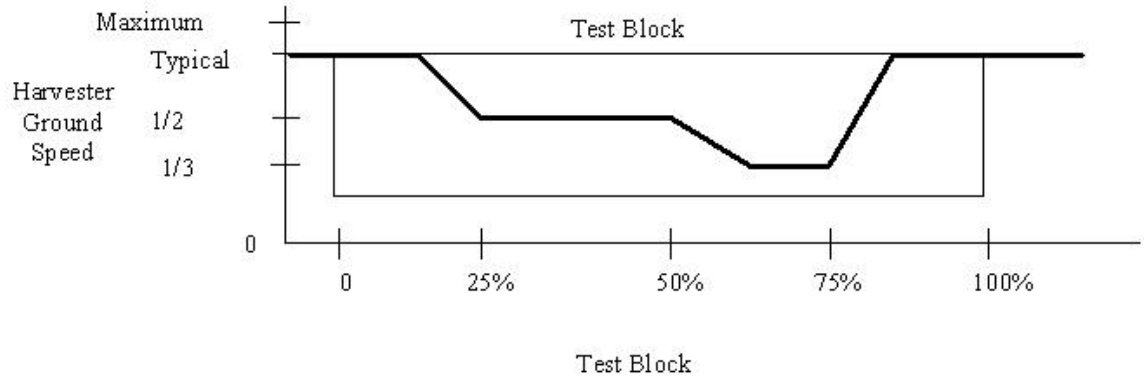

6. **Test Reporting**

6.1. Map test block location. Overlay static GPS measurement, yield monitor measurement and post test GPS measurement. Report location differences in meters (feet) for start, end and harvest path for each block.
6.2. Report mass flow delay determined by using the yield monitor and by operator observation.
6.3. Map the yield monitor yield data.
6.4. Calculate average reported yield for each test block area from yield monitor data.
6.5. Calculate total yield and report actual yield for each test block area.
6.6. Report actual total yield for each test block area.

6.7. Calculate yield monitor accumulated weight total deviation from actual weight data for test block. Repeat calculations for constant speed, varied speed and reverse slope tests. Weights are reported for as harvested and corrected to a dry weight basis to determine moisture sensor influence on weight determination.
6.8. Report harvester speed, field observations and any variation recorded.
6.9. Report harvester manufacturer, type, settings, head size, operating speeds including engine RPM, shaft speeds, ambient temperature, humidity, crop moisture and other test parameters.

Appendix B:
Test Field

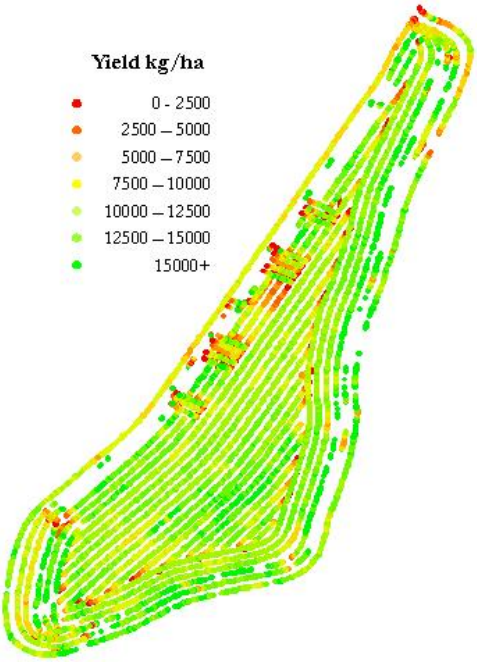

Figure B.1. Field C1, a 6.25 ha corn field in Shelby County, Kentucky with an average yield of 12.20 Mt/ha. Harvested November 2003.

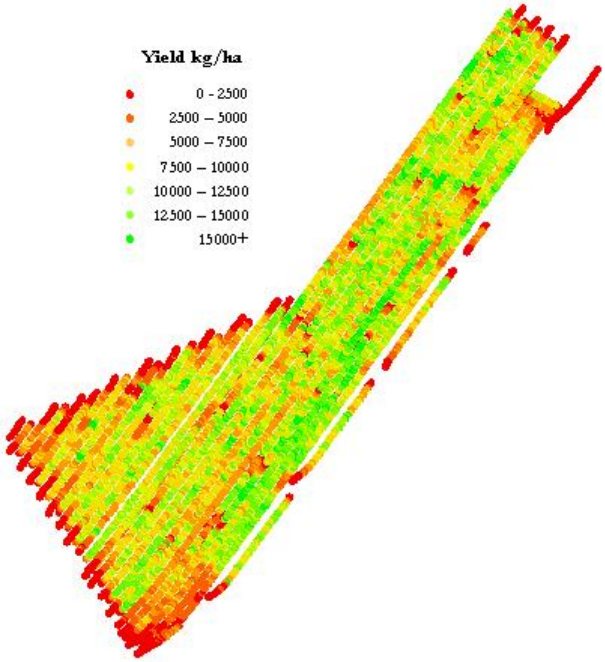

Figure B.2. Field C2, a 6.25 ha corn field in Woodford County, Kentucky with an average yield of 10.30 Mt/ha (164 bu/ac). Harvested September 2004.

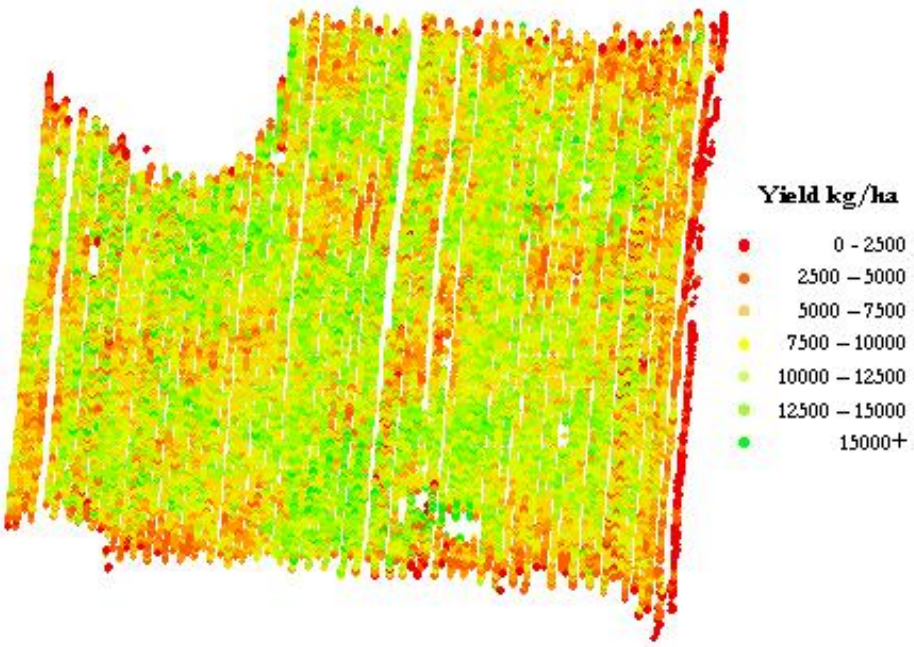

Figure B.3. Field C3, a 12.5 ha corn field in Hardin County, Kentucky with an average yield of 12.00 Mt/ha. Harvested September 2004.

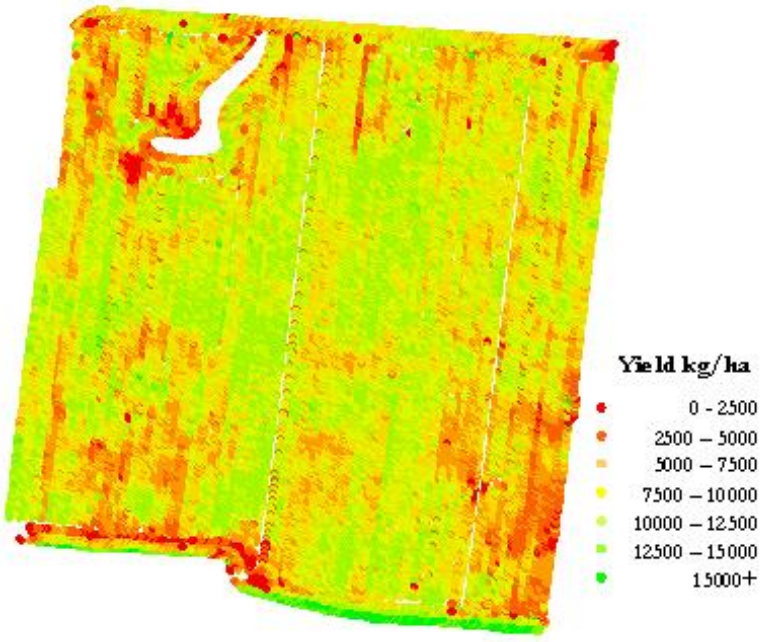

Figure B.4. Field C4, a 44 ha corn field in Hardin County, Kentucky with an average yield of 10.85 Mt/ha. Harvested October 2004.

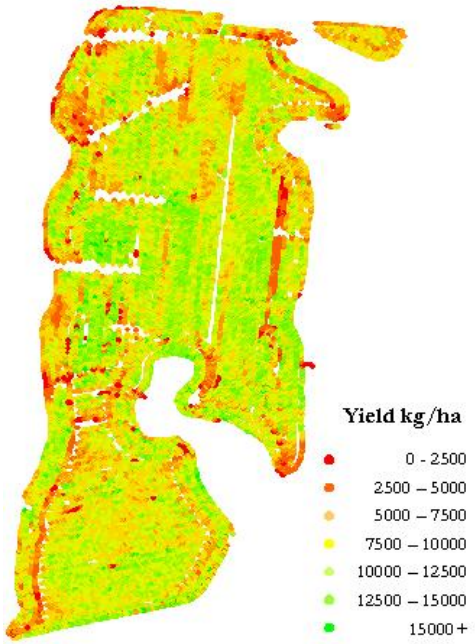

Figure B.5. Field C5, a 31.07 ha corn field in Shelby County, Kentucky with an average yield of 10.20 Mt/ha. Harvested November 2004.

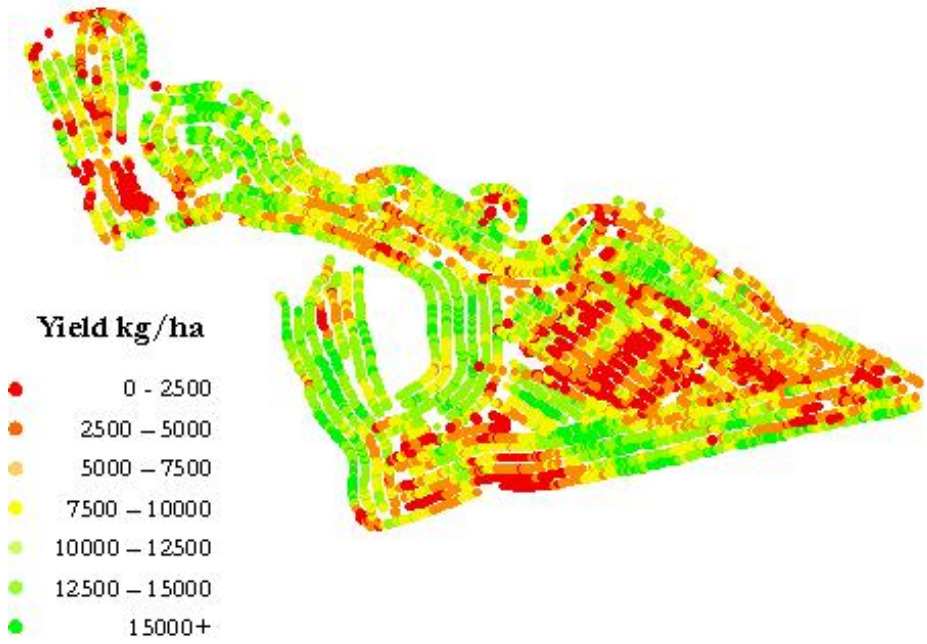

Figure B.6. Field C6, a 6.15 ha corn field in Henry County, Kentucky with an average yield of 7.90 Mt/ha (126 bu/ac). Harvested December 2004.

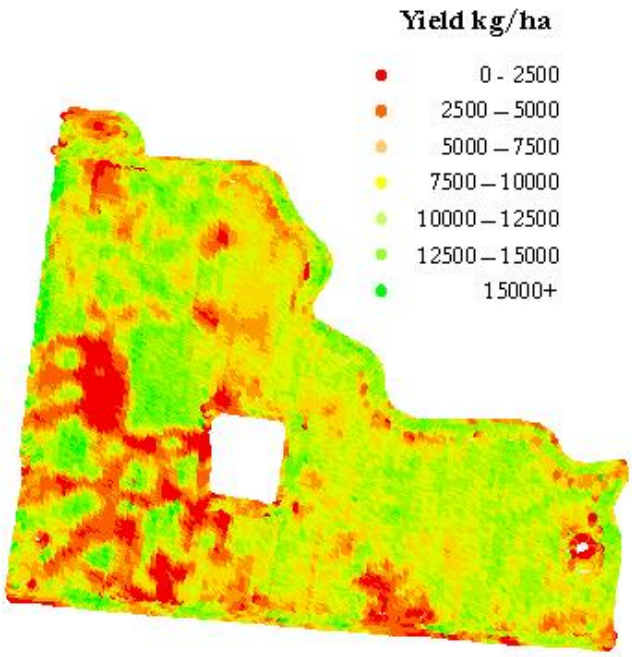

Figure B.7. Field C7, a 34.51 ha corn field in Henry County, Kentucky with an average yield of 7.70 Mt/ha. Harvested October 2005.

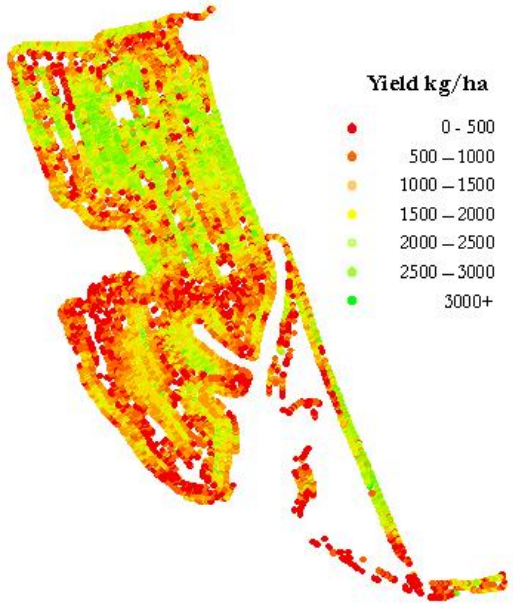

Figure B.8. Field SB1, a 16.5 ha soybean field in Henry County, Kentucky with an average yield of 1.45 Mt /ha. Harvested December 2004.

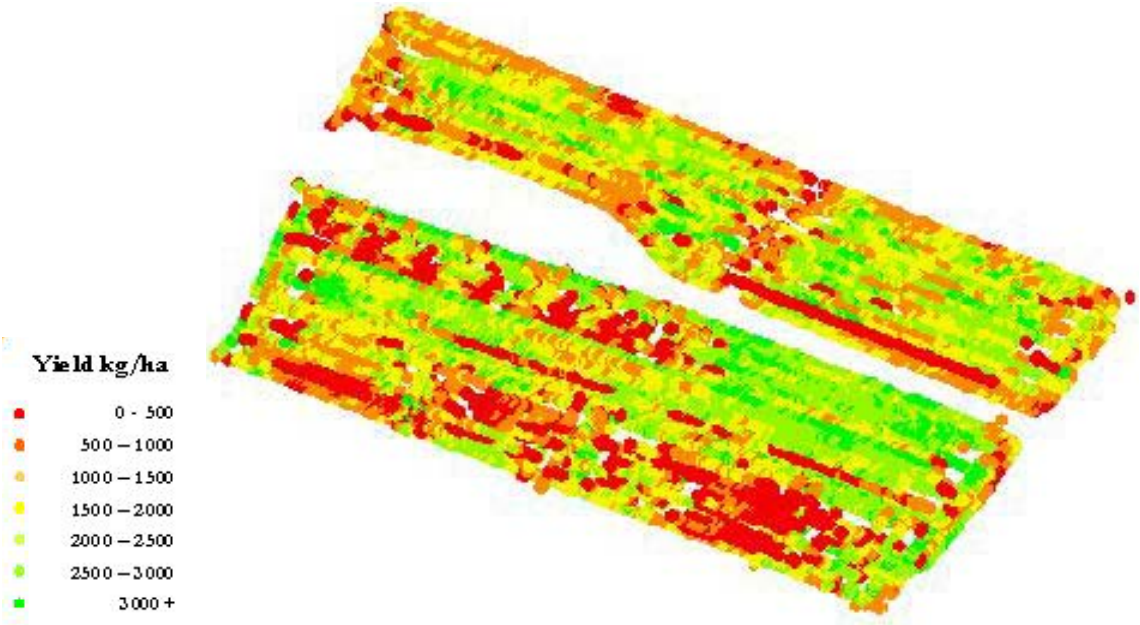

Figure B.9. Field W1, a 29 ha wheat field in Woodford County, Kentucky with an average yield of 2.15 Mt/ha. Harvested June 2005.

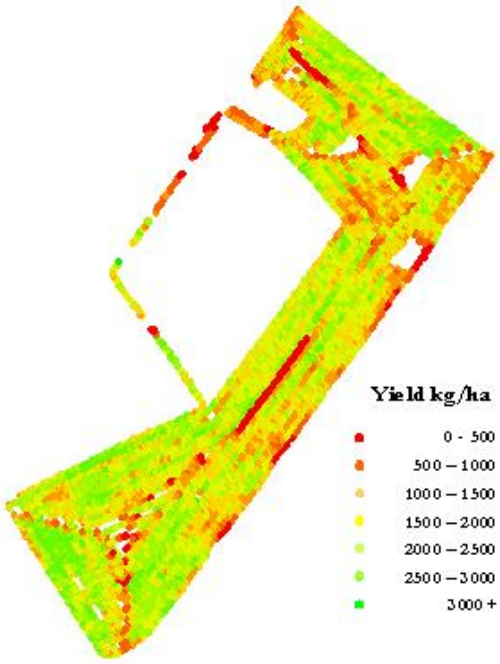

Figure B.10. Field W2, a 21.5 ha wheat field in Woodford County, Kentucky with an average yield of 2.10 Mt /ha. Harvested July 2005.

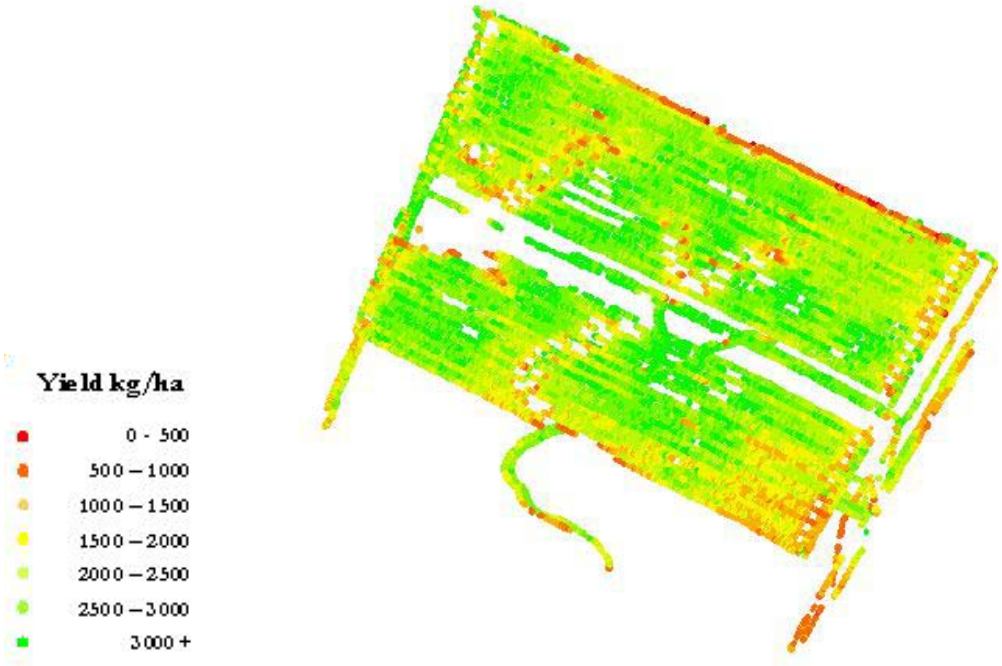

Figure B.11. Field W3, a 20.71 ha wheat field in Woodford County, Kentucky with an average yield of 2.10 Mt/ha. Harvested June 2006.

Table B.1. Field Tests Details.

Field	Date	Test[1]	Replicates	Variables Evaluated	Test Completed[2]
C1[2]	11/19/03	X579	2	Speed	2.4, 4.0, 5.6 km/h
		SS		Plate Width	2.6, 3.2, 3.6 cm
		MF			
C2[2]	9/9/04	MF	4	None	n/a
C3	9/23 – 9/25/04	FF	n/a	None	n/a
C4	10/8 – 10/11/04	FF	n/a	None	n/a
C5	11/1 – 11/8/04	FF	n/a	None	n/a
C6	12/4/04	IT	3	Speed	2.4, 4.0, 5.6 km/h
		RF	2		
C7	10/17 – 10/19/05	FF	n/a	None	n/a
SB1	12/2 – 12/4/04	FF	n/a	None	n/a
W1	6/28/05	FF	n/a	None	n/a
	6/29/05	IT	3	Speed	2.4, 4.0, 5.6 km/h
		X579	2		
	6/30/05	RF	2	None	n/a
		MF	6	Cutting Height	8, 15, 22 cm
W2	7/5/05	FF[3]	n/a	None	n/a
W3	6/30/06	FF	n/a	None	n/a

[1] X579 = ASABE X579 Field Evaluation, RF = Ramp Flow, IT = Intervals, FF = Full Field, SS = Stripping Plate, MF = Mass Flow Calibration

[2] The combine was not equipped to monitor hydraulic pressure for fields C1 and C2.

[3] The combine was equipped to with additional RTK-GPS receivers to log the position of the crop dividers on the grain platform to verify the performance of the GIS polygon coverage program

.

Appendix C:
Matlab Programs

```
%%%%%%%%%%%%%%%%%%%%%%%%%%%%%%%%%%%%%%%%%%%%%%%%%%%%%%%%%%%%%%
%                                                                                                    %
%   File:          YieldFilt.m                                                                       %
%                                                                                                    %
%   Description:        This file reads in the feeder house sensor data and performs the appropriate singal processing.         %
%                       The processing  removal of DC components, discrete Fourier transform, and a FIR filter.                %
%                                                                                                    %
%   Author:        Matt Veal                                                                         %
%                                                                                                    %
%   Date:          6 June 2006                                                                       %
%                                                                                                    %
%%%%%%%%%%%%%%%%%%%%%%%%%%%%%%%%%%%%%%%%%%%%%%%%%%%%%%%%%%%%%%

%Initial data formatting.  Proper time index is added, the analog-to-digital conversion count is converted to Volts, and the DC
%component in the signal is removed.

N = length(data);
interval = -1/400;
for i = 1:N
   data(i,4) = (data(i,2)/4096)*5;
   data(i,3) = interval + (1/400);
   interval = data(i,3);
end
avgval = mean(data(:,4));
x = data(:,3);
y = data(:,4)-avgval;

%The raw signal is plotted versus time
figure
plot(x,y);

%A 512-count discrete Fast Fourier analysis is completed on the signal and the magnitude of the analysis is plotted.
Y = fft(y,512);
Pyy = Y.* conj(Y) / 512;
f = 1000*(0:256)/512;
figure
stem(f,Pyy(1:257));
title('Frequency component of y')
xlabel('frequency (Hz)')


%The option of signal clipping is presented in the event the tails of the signal are not representative of the majority of the signal.
clipping = input('Is data clipping required? YES(1) or NO(2):   ');
if clipping == 1
   j = 1;
   Minclipping = input('What is the minimum clipping value?   ');
   Maxclipping = input('What is the maximum clipping value?   ');
   for i = 1:N
      if data(i,3) < Maxclipping
         if data(i,3) > Minclipping
            dataclip(j,1) = data(i,1);
            dataclip(j,2) = data(i,2);
            dataclip(j,3) = data(i,3)-Minclipping;
            dataclip(j,4) = data(i,4);
            j = j + 1;
         end
      end
   end
   avgvalclip = mean(dataclip(:,4));

%Once the clipping is carried out, the new signal is plotted versus time and the Fourier analysis is completed and plotted once again.
   xclip = dataclip(:,3);
   yclip = dataclip(:,4)-avgvalclip;
   figure
   plot(xclip,yclip)
   figure
   Yclip = fft(yclip,512);
   Pyyclip = Yclip.* conj(Yclip) / 512;
   f = 1000*(0:256)/512;
   stem(f,Pyyclip(1:257))
```

```
   title('Frequency content of y')
   xlabel('frequency (Hz)')
end

% A 128-tap FIR filter is now implemented to remove periodic elements from the feeder house sensor data.  This is a low-pass filter.  The
% resulting filter data is plotted on top of the original signal.

Nn = 128;
Wn = 1/400;
b = fir1(Nn,Wn);

if clipping == 1
   Filty = filter(b,1,dataclip(:,2));
   Filty = (Filty/4096)*5;
   yclip = yclip + avgval;
   figure
   plot(xclip,yclip,xclip,Filty);
else
   Filty = filter(b,1,data(:,2));
   Filty = (Filty/4096)*5;
   y = y + avgval;
   figure
   plot(x,y,x,Filty);
end

meansigval = mean(Filty);
stdsigval = std(Filty);
N = length(Filty);


%This portion of the program determines if there are an excessive number of spikes in the data (i.e. soybean signal), if spikes are still in the data
%a 20-point moving average filter is implemented to further filter the data.

maxcount = 0;
maxvalue = meansigval + 2.5*stdsigval;
for i = 1:N
   if Filty(:,1) > maxvalue
      maxcount = maxcount + 1
   end
end

if maxcount > 10
   M = 20;
   B = ones(M,1)/M;
   AvgFilty = filter(Hd,Filty);
   figure
   plot(x,y,x,AvgFilty)
end

clear Nn Wn b f Pyy Pyyclip Yclip Y N interval Minclipping Maxclipping
clear avgval avgvalclip M B
```

```
%%%%%%%%%%%%%%%%%%%%%%%%%%%%%%%%%%%%%%%%%%%%%%%%%%%%%%%%%%%%%%%%%
%                                                                                                               %
%                                                                                                               %
%                                                                                                               %
%   File:           YieldFix.m                                                                                  %
%                                                                                                               %
%   Description:        This file reads in the feeder house sensor data and defines the location of significant changes      %
%                       in mass flow.  The relative mass flow intake at each segment is defined and the yield monitor       %
%                       mass flow is corrected.                                                                 %
%                                                                                                               %
%   Author:         Matt Veal                                                                                   %
%                                                                                                               %
%   Date:           8 June 2006                                                                                 %
%                                                                                                               %
%%%%%%%%%%%%%%%%%%%%%%%%%%%%%%%%%%%%%%%%%%%%%%%%%%%%%%%%%%%%%%%%%

%Load initial feeder house signal properties into the program
N = length(DATA);
FH_Max = max(DATA(:,10));
FH_Min = 2625;
FH_Range = FH_Max - FH_Min;

%The minimum difference in signal that the program will note for deciding where to define boundaries between areas of significant mass flow
%differences
crit = input('Enter the value off significant difference:       ');

%Note:  Any single letter is simpling an indexing term
k = 0;
j = 1;
MarkTemp = 0; %Temp accumulator to set boundaries between flow differences

%Conversion from mass flow to yield - bu/ac
for i = 1:N
    DATA(i,12) = ((DATA(i,3)*((100-DATA(i,6))/(100-13.5)))/(60*DATA(i,5)*DATA(i,4)))*144*43560;
    DATA(i,13) = (DATA(i,10)/4096)*5;
    DATA(i,14) = (DATA(i,3)*0.4536);
end

% Used to located the location of a significant change in mass flow, at least 3 back to back significant readings are needed to denote
% a change in mass flow

for i = 2:N
        if abs(DATA(i,10) - DATA(i-1,10)) > crit
            MarkTemp = DATA(i,7) + MarkTemp;
            k = k + 1;
        else
            if MarkTemp > 0
                if k > 1
                    %Marker array notes the boundary location
                    MarkerHold(j,1) = MarkTemp/k;
                    j = j + 1;
                end
                MarkTemp = 0;
                k = 0;
            end
        end
end


j = length(MarkerHold);
r = 2;
MinimumPlotDist = 1;
Marker(1,1) = MarkerHold(1,1);
for i = 2:j
    if MarkerHold(i,1) - MarkerHold(i-1,1) > MinimumPlotDist
        Marker(r,1) = MarkerHold(i,1);
        r = r + 1;
    end
end
```

```
if MarkerHold(j,1) ~= Marker(r-1,1)
   Marker(r,1) = MarkerHold(j,1);
End

% The following section denotes the average sensor reading within each of the segments identified by the boundaries also the relative
% amounts of mass flow for each block are determined.
n = 0;
m = 0;
FH_Temp = 0;
FH_Val(1,1) = FH_Min;
FH_Val(1,2) = (FH_Min - FH_Min)/FH_Range;
FH_Val(1,3) = 1;
FH_Val(1,4) = 0;
j = length(Marker);

for k = 1:j-1;
   if Marker(k+1,1) - Marker(k,1) > 0;
      Start_Pt = Marker(k,1);
      Stop_Pt = Marker(k+1,1);
      for i = 1:N
         if DATA(i,7) >= Start_Pt
            if DATA(i,7) <= Stop_Pt
               FH_Temp =  FH_Temp + DATA(i,10);
               n = n + 1;
            end
         end
      end

      if n > 0
         FH_Val(k+1,1) = FH_Temp/n; %Average Value
         FH_Val(k+1,2) = (FH_Val(k+1,1) - FH_Min)/FH_Range; %Relative Value
         FH_Val(k+1,3) = n;  %No. of readings in a block
         FH_Val(k+1,4) = Start_Pt;   %Staring location of the block
         n = 0;
         FH_Temp = 0;
      end
   end
end

% Routine to plot the feederhouse data determined in the above sections of this program

Marker_plot(1,1) = 0;
for k = 2:j
   Marker_plot(k+m,1) = Marker(k-1,1);
   Marker_plot(k+m+1,1) = Marker(k-1,1);
   m = m + 1;
end
Marker_plot(j+m+1,1) = Marker(j,1);
Marker_plot(j+m+2,1) = Marker(j,1);
m = 0;
for k = 1:j
      Marker_plot(k+m,2) = (FH_Val(k,1)/4096)*5;
      Marker_plot(k+m+1,2) = (FH_Val(k,1)/4096)*5;
      m = m + 1;
end
Marker_plot(k+m+1,2) = (FH_Val(1,1)/4096)*5;

% plots feeder house data versus distance with plot boundaries included

plot(DATA(:,7),DATA(:,13),Marker_plot(:,1), Marker_plot(:,2))
figure

%plots feeder house and yield data versus plot distance

plotyy(DATA(:,7),DATA(:,10),DATA(:,7),DATA(:,12))



% Similar routine to the one above, but set up to determine how the yield monitor mass flow data has been distributed
```

```
% In the event that the yield file contains more data than the feeder house file this section of the program determines when the yield monitor data
% has concluded logging

k = 0;
m = 0;
n = 0;

j = length(Marker);

Speed = mean(DATA(:,4))*0.0254; %Average combine velocity (m/s)
YM_Max = max(DATA(:,3));
YM_Min = min(DATA(:,3));
YM_Range = YM_Max - YM_Min;
YM_Temp = 0;

% This routine is used to find the end of the yield file.  Often yield files have a constant value repeating at the end of the file.  If 5 consecutive
% equal values are encounter, the end of the file is noted, otherwise the full length of the file is utlizied.

FinalVal = 0;

if FinalVal == 0
   FinalVal = N;
End

% The following section denotes the average mass flow reading within each of the segments identified by the boundaries also the relative
% amounts of mass flow for each block are determined.

if FinalVal > 0
   Marker(j+1,1) = DATA(FinalVal,7);
end
NumMarkers = length(Marker);
YM_Val(1,1) = YM_Min;
YM_Val(1,2) = (YM_Min - YM_Min)/YM_Range;
YM_Val(1,3) = 1;
YM_Val(1,4) = 0;
m = 0;
for k = 1:NumMarkers-1;
   if Marker(k+1,1) - Marker(k,1) > 0;
      Start_Pt = Marker(k,1);
      Stop_Pt = Marker(k+1,1);
      for i = 1:N
         if DATA(i,7) >= Start_Pt
            if DATA(i,7) <= Stop_Pt
               YM_Temp =  YM_Temp + DATA(i,3);
               n = n + 1;
            end
         end
      end

      if n > 0
         YM_Val(k+1,1) = YM_Temp/n;
         YM_Val(k+1,2) = (YM_Val(k+1,1) - YM_Min)/YM_Range;
         YM_Val(k+1,3) = n;
         YM_Val(k+1,4) = Start_Pt;
         YM_Val(k+1,5) = YM_Temp;
         n = 0;
         YM_Temp = 0;
      end
   end
end

% Routine to plot the yield monitor data determined in the above sections of this program

Marker_plotYM(1,1) = 0;
for k = 2:NumMarkers
   Marker_plotYM(k+m,1) = Marker(k-1,1);
   Marker_plotYM(k+m+1,1) = Marker(k-1,1);
   m = m + 1;
end
```

```
Marker_plotYM(j+m+1,1) = Marker(j,1);
Marker_plotYM(j+m+2,1) = Marker(j,1);
m = 0;
for k = 1:NumMarkers
      Marker_plotYM(k+m,2) = YM_Val(k,1);
      Marker_plotYM(k+m+1,2) = YM_Val(k,1);
      m = m + 1;
end
Marker_plotYM(k+m+1,2) = YM_Val(1,1);
figure

%plots yield data versus distance with the boundaries defined by the plot boundary

plot(DATA(:,7),DATA(:,14),Marker_plotYM(:,1), Marker_plotYM(:,2))
figure

%plots yield data versus distance with the plot boundaries defined by the feeder housing data

[AX,H1,H2] = plotyy(Marker_plot(:,1), Marker_plot(:,2),DATA(:,7),DATA(:,14));
set(H1,'LineStyle','-')
set(H2,'LineStyle','--')
set(H1,'LineWidth',2.75)
set(H2,'Color',[1 0 0])
set(H1,'Color',[0 0 0])

% This section of the program marks the beginning of the correction routine. The plot boundaries defined by the feeder house are used to
% redistribute mass flow data collected by the yield monitor based on how the intake of crop material changes as the harvester moves
% through the plot.

for i = NumMarkers+1:-1:1
   if i == 1
      Marker(i,1) = 0;
   else
      Marker(i,1) = Marker(i-1,1);
   end
end
NumPlots = NumMarkers;
NumMarkers = length(Marker);
n = 0;
FH_Temp = 0;
YM_Temp = 0;
nocorrection = 0;
q = 1;
LookBack = 0;


%The plot summary array is used to determine how the grain mass flow should be redistributed based on the mass flow data.  Descriptions for the
array

%columns are as follows:
%    1 - Block Number           2 - Starting Point
%    3 - Ending Point           4 - Readings in Block
%    5 - Average FH Reading     6 - Relative FH Val
%    7 - Average YM Reading     8 - Total block weight
%    9 - Relative YM Val        10 - Should Block be Empty?
%   11 - Move Mass Forward      12 - Move Mass Back
%   13 - Add Weight to Block?   14 – Has Mass Been Moved?
%   11 - Move Mass Forward      12 - Move Back
%   13 - Add Weight to Block?   14 – Net Mass Movement

for k = 1:NumPlots
  PlotSummary(k,1) = k;
  PlotSummary(k,2) = Marker(k,1);
  PlotSummary(k,3) = Marker(k+1,1);
  n = 0;
  FH_Temp = 0;
  YM_Temp = 0;
  %Determine average values for first block
  for i = 1:N
        if DATA(i,7) >= PlotSummary(k,2)
```

```
            if DATA(i,7) <= PlotSummary(k,3)
               n = n + 1;
               FH_Temp =  FH_Temp + DATA(i,10);
               YM_Temp =  YM_Temp + DATA(i,3);
               YM_Store(n,2*q-1) = DATA(i,3);
               YM_Store(n,2*q) = DATA(i,7);
            end
         end
   end
   PlotSummary(k,4) = n;
   PlotSummary(k,5) = FH_Temp/n;
   PlotSummary(k,6) = (PlotSummary(k,5) - FH_Min)/FH_Range;
   PlotSummary(k,7) = YM_Temp/n;
   PlotSummary(k,8) = YM_Temp;
   PlotSummary(k,9) = PlotSummary(k,7)/YM_Max;
   if PlotSummary(k,6) < 0.08;
      PlotSummary(k,10) = -1;
   else
      PlotSummary(k,10) = 0;
   end

   q = q+1;
   n = 0;
   FH_Temp = 0;
   YM_Temp = 0;

end

%If a zero mass flow block is detected, all of the mass is moved out of the
%block to either the immediately preceding or following block depending of
%the case.

moveforward = 0;
movebackwards = 0;
for k = 1:NumPlots
   if k == 1
      if PlotSummary(k,10) == -1
         PlotSummary(k,11) = PlotSummary(k,8);
         PlotSummary(k,12) = 0;
      end
   elseif k == NumPlots
      if PlotSummary(k,10) == -1
         PlotSummary(k,11) = 0;
         PlotSummary(k,12) = PlotSummary(k,8);
      end
   else
      if PlotSummary(k,10) == -1
         n = PlotSummary(k,4);
         for i = 1:n
            tempYM(i,1) = YM_Store(i,2*k-1);
            tempYM(i,2) = YM_Store(i,2*k);
         end
         lowestmassflow = min(tempYM(:,1));
         for i = 1:n
            if tempYM(i,1) == lowestmassflow
               lowpt = tempYM(i,2);
            end
         end
         for i = 1:n
            if tempYM(i,2) <= lowpt
               movebackwards = tempYM(i,1) + movebackwards;
            else
               moveforward = tempYM(i,1) + moveforward;
            end
         end
         PlotSummary(k,11) = moveforward;
         PlotSummary(k,12) = movebackwards;
      end
   end
         moveforward = 0;
```

```
        movebackwards = 0;
end

%Initial mass movement for blocks that are required to recieve all of the
%mass from a zero mass block.  This can include the first or last block,
%plus any block that is "sandwiched" between two blocks.

PlotSummary(1,17) = 0;
for k = 1:NumPlots
   if k == 1
      if PlotSummary(k+1,12) > 0;
         PlotSummary(k,14) = PlotSummary(k+1,14);
         PlotSummary(k,10) = 1;
      end
   elseif k == NumPlots
      if PlotSummary(k-1,11) > 0;
         PlotSummary(k,13) = PlotSummary(k-1,11);
         PlotSummary(k,10) = 1;
      end
   else
      if PlotSummary(k-1,11) > 0
         if PlotSummary(k+1,12) > 0
            PlotSummary(k,13) = PlotSummary(k-1,11);
            PlotSummary(k,14) = PlotSummary(k+1,12);
            PlotSummary(k,10) = 1;
         end
      end
   end
end

%Recalculation of relative mass flow amounts in each block
PlotSummary(:,15) = PlotSummary(:,14) + PlotSummary(:,8) + PlotSummary(:,13);
MaxMF = max(PlotSummary(:,15));
PlotSummary(:,16) = PlotSummary(:,15) / MaxMF;

for k = 1:NumPlots
   if PlotSummary(k,10) ~= -1
      if PlotSummary(k,10) ~= 1
       PlotSummary(k,17) = (PlotSummary(k,6) - PlotSummary(k,16))*PlotSummary(k,4);
      end
   end
   if PlotSummary(k,17) > 0
      PlotSummary(k,10) = 1;
   elseif PlotSummary(k,17) < 0;
      PlotSummary(k,10) = -1;
   end
end

PlotSummary(:,15) = PlotSummary(:,11)+PlotSummary(:,12)+PlotSummary(:,13)+PlotSummary(:,14);
WeightTotal = 0;
kk = 0;
k = 1;
while k < NumPlots + 0.01;
   if PlotSummary(k,15) == 0
      if kk == 0
         WeightTotal = abs(PlotSummary(k,17));
         kk = kk + 1;
      elseif kk > 0
         if PlotSummary(k,17) > 0
            if PlotSummary(k-1,17) > 0
               WeightTotal = abs(PlotSummary(k,17))+WeightTotal;
               kk = kk + 1;
            elseif PlotSummary(k-1,17) < 0
               r = k-kk;
               for i = (k-1):-1:r
                  PlotSummary(i,18) = (abs(PlotSummary(i,17))/WeightTotal);
               end
               kk = 0;
               WeightTotal = 0;
               WeightTotal = abs(PlotSummary(k,17));
```

```
            kk = kk + 1;
        end
    elseif PlotSummary(k,17) < 0
        if PlotSummary(k-1,17) < 0
            WeightTotal = abs(PlotSummary(k,17))+WeightTotal;
            kk = kk + 1;
        elseif PlotSummary(k-1,17) > 0
            r = k-kk;
            for i = (k-1):-1:r
                PlotSummary(i,18) = (abs(PlotSummary(i,17))/WeightTotal);
            end
            kk = 0;
            WeightTotal = 0;
            WeightTotal = abs(PlotSummary(k,17));
            kk = kk + 1;
        end
    end
elseif WeightTotal > 0
    r = k-kk;
    for i = (k-1):-1:r
        PlotSummary(i,18) = (abs(PlotSummary(i,17))/WeightTotal);
    end
    kk = 0;
    WeightTotal = 0;
        end
k = k + 1;
end

for k = 1:NumPlots
if PlotSummary(k,17) < 0
    PlotSummary(k,17) = (PlotSummary(k,6) - PlotSummary(k,16));
    moved = 0;
    if PlotSummary(k-1,17) > 0
        if k > 1
            PlotSummary(k,12) = abs(PlotSummary(k,17))*PlotSummary(k,8);
            PlotSummary(k,15) = PlotSummary(k,11) + PlotSummary(k,12);
            moved = 1;
        end
    elseif moved < 1
        if k < NumPlots
            if PlotSummary(k+1,17) > 0
                PlotSummary(k,11) = abs(PlotSummary(k,17))*PlotSummary(k,8);
                PlotSummary(k,15) = PlotSummary(k,11) + PlotSummary(k,12);
                moved = 1;
            end
        end
    end
end
end

for k = 1:NumPlots
if PlotSummary(k,15) == 0
    if k > 1
        PlotSummary(k,13) = PlotSummary(k-1,11);
    end
    if k < NumPlots
        PlotSummary(k,14) = PlotSummary(k+1,12);
    end
end
end

TransferWeight = 0;
kk = 0;
k = 1;
while k < NumPlots + 0.01;
if PlotSummary(k,15) == 0
        TransferWeight = TransferWeight + PlotSummary(k,13)+PlotSummary(k,14);
        kk = kk + 1;
 elseif PlotSummary(k,15) > 0
```

```
      if TransferWeight > 0
         r = k-kk;
         for i = (k-1):-1:r
            PlotSummary(k,18)
            PlotSummary(i,15) = (TransferWeight*PlotSummary(i,18));
         end
         kk = 0;
         TransferWeight = 0;
      end
   end
   k = k + 1;
end

for k = 1:NumPlots
  PlotSummary(k,19) = (PlotSummary(k,8) + (PlotSummary(k,10)*PlotSummary(k,15)))/PlotSummary(k,4);
end


for k = 1:NumPlots
      StartPoint = PlotSummary(k,2);
      EndPoint = PlotSummary(k,3);

      for i = 1:N
         if DATA(i,7) >= StartPoint
            if DATA(i,7) <= EndPoint
               DATA(i,15) = PlotSummary(k,19);
               DATA(i,16) = (((DATA(i,15)*((100-DATA(i,6))/(100-13.5)))/(60*DATA(i,5)*DATA(i,4)))*144*43560)*0.0673;
            end
         end
      end
   end
figure
plotyy(Marker_plot(:,1), Marker_plot(:,2),DATA(:,7),DATA(:,16))
```

Appendix D:
ESRI Avenue Script

Start up – Sets project up for analysis for a particular field and combine

```
'-- Set project title
  av.SetName("UK BAE Yield Monitor Polygon Area Generator Application")

  '**** look into inserting UK logo in title bar
'-------------------------------------------------------------------------
'-- Open the project in the Data Overview document
  dView = av.GetProject.FindDoc("Yield Monitor Data")
  dView.GetWin.Open

  '**** Need to add code for the possibility of the view not existing
  '**** it may have been deleted in a previous run of the application
'-------------------------------------------------------------------------
'-- Identify the startup dialog and center it in the application
  theDlg = av.FindDialog("StartupDlog")

  avUpperLeft = av.ReturnOrigin
  avCenter = avUpperLeft + (av.ReturnExtent / (2@2))
  halfDialogWidthHeight = theDlg.ReturnExtent.ReturnSize / (2@2)
  movePoint = avCenter - halfDialogWidthHeight
  theDlg.MoveTo(movePoint.GetX, movePoint.GetY)
'-------------------------------------------------------------------
'-- Initialize dialog elements & set initial values
  wrkDir = av.GetProject.GetWorkDir.AsString

  offsetDist = theDlg.FindByName("txtOffsetDist").SetText("")

  unitsList = {"feet", "meters"}
  theUnits = theDlg.FindByName("lbUnits").DefineFromList(unitsList)

  addData = theDlg.FindByName("cbRawData").SetSelected(False)

  cancelBtn = theDlg.FindByName("btnCancel")
  helpBtn = theDlg.FindByName("btnHelp")
  goBtn = theDlg.FindByName("btnContinue")
'-------------------------------------------------------------------
'-- Open the dialog box
  theDlg.Open
'-------------------------------------------------------------------
```

Adds UTM x-y coordinates for each yield monitor point

```
'-- Begin Code
'-- Initialize view and get view's themes
  theProject = av.GetProject
  theView = av.GetActiveDoc
  theThemes = theView.GetThemes
'-- Make sure that the selected theme is a point theme
  if(ptTheme.GetFTab.GetShapeClass.GetClassName <> "Point") then
    MsgBox.Info("The theme is not a point theme.","Theme: " ++ptTheme.GetName)
    exit
  end
'-- Make sure that the selected theme is editable by checking FTab
  if((ptTheme.GetFTab.CanEdit).NOT) then
    MsgBox.Info("This theme cannot be edited.","Theme:"++ptTheme.GetName)
    exit
  end
'-- Set the theme editable
  ptFTab = ptTheme.GetFTab
  if(ptFTab.IsEditable) then
    alreadyOpen = TRUE
  else
    alreadyOpen = FALSE
  end
  ptFTab.SetEditable(TRUE)
'-- Create and add the new ID field
  idField = Field.Make("Pt_ID", #FIELD_LONG, 5,0)
  ptFTab.AddFields({idField})
'-- Add sequential ID to recordset
  idNum = 0
  for each rec in ptFTab
    idNum = idNum + 1
    ptFtab.SetValue(idField, rec, idNum)
  end
'-- Add X and Y Fields to FTab to receive output
  xField = Field.Make("X",#FIELD_FLOAT,18,6)
  yField = Field.Make("Y",#FIELD_FLOAT,18,6)
  if(ptFTab.FindField("X-coord") = NIL) then
    ptFTab.AddFields({xField})
  else
    xField = ptFTab.FindField("X")
  end
  if(ptFTab.FindField("Y-coord") = NIL) then
    ptFTab.AddFields({yField})
  else
    yField = ptFTab.FindField("Y")
  end
'-- Loop through point records and add the actual X & Y field values
  shpField = ptFTab.FindField("Shape")
  for each rec in ptFTab
    theShape = ptFTab.ReturnValue(shpField, rec)
    x = theShape.GetX
    y = theShape.GetY
    ptFTab.SetValue(xField,rec,x)
    ptFTab.SetValue(yField,rec,y)
  end
'-- Close the FTab
  if ((alreadyOpen = TRUE).NOT) then
    ptFTab.SetEditable(FALSE)
  end
'-- End of Script
```

Calculate bearing and distance between each yield data point

```
'-- Select the working theme and get the FTab
  theView = av.GetActiveDoc
  workTheme = theView.GetActiveThemes.Get(0)
'-------------------------------------------------------
'-- Make the FTab editable
  theFTab = workTheme.GetFTab
  theFTab.SetEditable(True)
'-------------------------------------------------------
'-- Determine the number of records in FTab
  numRecs = theFTab.GetNumRecords

  '-- remember numbering starts at zero, so actual number is one
  '--less than value returned...make adjustment
  numRecs = numRecs -1
'-------------------------------------------------------
'-- Select all records
  if (theFTab.GetSelection.Count = 0) then
    theFTab.GetSelection.SetAll
  end
'-------------------------------------------------------
'-- Initialize previous bearing variable
  prevBearing = 0
'-------------------------------------------------------
'-- Determine what names are used for X/Y coordinates
  xName = "None"
  yName = "None"
  fieldList = theFTab.GetFields
  for each n in fieldList
    fldName = n.AsString

    if ((fldName = "Longitude") or (fldName = "X") or
      (fldName = "X-Coordinate") or (fldName = "X-Coord")) then
        xName = fldName
    elseif ((fldName = "Latitude") or (fldName = "Y") or
      (fldName = "Y-Coordinate") or (fldName = "Y-Coord")) then
        yName = fldName
    end
  end

  if ((xName = "None") or (yName = "None")) then
    Msgbox.Error("Coordinates could not be identified","Coordinate Error")
    exit
  end
'-------------------------------------------------------
'-- For each point to the next point
  for each i in 0 .. (numRecs)
    X1 = theFTab.ReturnValue(theFTab.FindField(xName), i )

    If (i < (numRecs)) then
      X2 = theFTab.ReturnValue(theFTab.FindField(xName), i + 1)
    else
      X2 = theFTab.returnValue(theFTab.FindField(xName), 0)
    end

    Y1 = theFTab.returnValue(theFTab.FindField(yName), i )

    If (i < (numRecs)) then
      Y2 = theFTab.ReturnValue(theFTab.FindField(yName), i + 1)
```

```
    else
      Y2 = theFTab.ReturnValue(theFTab.FindField(yName), 0 )
    end

    pt1 = point.make(x1,y1)
    pt2 = point.make(x2,y2)

    '-- Calculate the hypotenuse (distance between the 2 points)
    h = pt1.distance(pt2)

    dX = (X2 - X1)
    dY = (Y2 - Y1)

    a = 90 - (( dX /h).ACos.AsDegrees)
    if (dX < 0) then
      if (dY < 0) then
        a = 180 + a.Negate
      else
        a = 360 + a
      end
    else
      if (dY < 0) then
        a = 180 - a
      end
    end


    '-- Record the value of the distance in the FTab
    theFTab.SetValue(theFTab.FindField("Distance"),i, h )

    '-- Record the value of the bearing in the FTab
    theFTab.SetValue(theFTab.FindField("Bearing"),i, a )

    '-- Compare bearing value to previous bearing
    if ((i = 0)  or (i = numRecs))then
      prevBearing = a
    else
      splitCheck = (a-prevBearing).abs

      if (splitCheck > 40) then
        '-- Make sure difference doesn't involve 360 vs small number
        if (splitCheck > 280) then
          theFTab.SetValue(theFTab.FindField("SpFlag"),i,2)
        else
          theFTab.SetValue(theFTab.FindField("SpFlag"),i,1)
        end
      end
      prevBearing = a
    end

    '-- Check for distance between points as split points
      if (h>(50/3.281)) then
        theFTab.SetValue(theFTab.FindField("SpFlag"), i,3)
      end
  end 'each i in 0 .. (numRecs)
'-----------------------------------------------------------
'-- Stop editing, save edits and refresh the view
  theFTab.SetEditable(False)
  theFTab.GetSelection.ClearAll
  theFTab.UpdateSelection
  theView.Invalidate
'---End of script
```

Develop combine's centerline of travel based on series of yield data points

```
'-- Get the view and its projection, if any
  theView = av.GetActiveDoc
  thePrj = theView.GetProjection
  if (thePrj.IsNull) then
    hasPrj = false
  else
    hasPrj = true
  end
'-----------------------------------------------------------------------
'-- Initialize Offset Table
  for each t in theView.GetActiveThemes
    if (t.HasTable) then
      ptTheme = t
      theTable = t.EditTable
    end
  end
  theTable = av.FindDoc("Attributes of Offset_UTM.shp")
  theTableWin = theTable.GetWin
  theTableWin.Close

  theVTab = theTable.GetVTab
  '-- Determine what names are used for X/Y coordinates
    xName = "None"
    yName = "None"
    fieldList = theVTab.GetFields
    for each n in fieldList
      fldName = n.AsString

      if ((fldName = "Longitude") or (fldName = "X") or
        (fldName = "X-Coordinate") or (fldName = "X-Coord")) then
          xName = fldName
      elseif ((fldName = "Latitude") or (fldName = "Y") or
        (fldName = "Y-Coordinate") or (fldName = "Y-Coord")) then
          yName = fldName
      end
    end

    if ((xName = "None") or (yName = "None")) then
      Msgbox.Error("Coordinates could not be identified","Coordinate Error")
      exit
    end
'-----------------------------------------------------------

  XField = theVTab.FindField(xName)
  YField = theVTab.FindField(yName)
  IDField = theVTab.FindField("LineID")
  VertField = theVTab.FindField("ID")

  _pCount = 0
  for each rec in theVTab.GetSelection
    _pCount = _pCount + 1
  end
'-----------------------------------------------------------------------
'-- Create new shapefile to receive line segments
  shpFileName = "Centerline.shp"
  def = FileDialog.Put(shpFileName.asFilename,"*.shp","Creating temporary shapefile...")

  if(def=nil) then exit end

  def.SetExtension("shp")
```

```
  outputFTab = FTab.MakeNew(def,Polyline)
  outputFTab.AddFields({Field.Make("ID",#FIELD_LONG,8,0)})
  outputShapeFld = outputFTab.FindField("Shape")
  outputIDFld = outputFTab.FindField("ID")
'-----------------------------------------------------------------
'-- Select all the points
  theBitmap = theVTab.GetSelection
  theBitmap.SetAll
  theVTab.SetSelection(theBitmap)
'-----------------------------------------------------------------
'-- Collect all the points into a list and make the line
  pointList= {}

  for each rec in theVTab.GetSelection
    aPoint = Point.Make(theVTab.ReturnValue(XField,rec), theVTab.ReturnValue(YField, rec))
    pointList.Add(aPoint)
  end

  newRec = outputFTab.AddRecord
  newLine = Polyline.Make({pointList})
  outputFTab.SetValue(outputShapeFld,newRec,newLine)'.AsPolyline

  theBitmap.ClearAll
  theVTab.UpdateSelection
'-----------------------------------------------------------------
'-- Add the new theme to the view
  newTheme = FTheme.Make(outputFTab)
  theView.AddTheme(newTheme)
'-----------------------------------------------------------------
'-- Add new lines to centerline shapefile
  outputFTab.SetValue(outputShapeFld,newRec,newLine)'.AsPolyline
'-----------------------------------------------------------------
'-- Calculate the centerline lengths
  newFTab = newTheme.GetFTab

  '-- Make the FTAB editable
  newFTab.SetEditable(TRUE)
  theLine = newFTab.ReturnValue(newFTab.FindField("Shape"),0)
  lenField = Field.Make("Length", #FIELD_DOUBLE,16,3)
  newFTab.AddFields({lenField})

  for each rec in newFTab
    theLength = theLine.ReturnLength
    newFTab.SetValue(lenField,rec,theLength)
  end

  newFTab.SetEditable(FALSE)

  theView.Invalidate

'--------------------------End of Script----------------------------
```

Generate transects normal to the centerline of travel at each yield data point

```
'-- Initialize the view and get the point theme for polygon generation
  theView = av.GetActiveDoc
  ptTheme = theView.FindTheme("Offset_UTM.shp")
  ptTheme.SetActive(True)
  ptFTab = ptTheme.GetFTab
  clTheme = theView.FindTheme("Centerline.shp")
  clFTab = clTheme.GetFTab
'-------------------------------------------------------------------------
'-- Get the transect length from spreader width global variable
  csLength = _swathWidth
'-------------------------------------------------------------------------
'-- Set the Distance variable from the spreader width global variable
  theDist = _swathWidth/2
'-- Create a new shapefile to accept new transects
    class = Polyline 'create polyline class
    shpFileName = "Transects.shp"    'make shapefile definition
    def = FileDialog.Put(shpFileName.asFileName, "*.shp", "Creating shapefile " +
      shpFileName)

    tbl = FTab.MakeNew(def, class)
'-------------------------------------------------------------------------
'-- Create attribute fields to accept transferred data
  idField = Field.Make("ID", #FIELD_DECIMAL, 8, 0)
  idField.SetVisible( TRUE )
  clIDField = Field.Make("CL_ID", #FIELD_DECIMAL,5,0)
  xField = Field.Make("PtX", #FIELD_DECIMAL, 16,5)
  yField = Field.Make("PtY", #FIELD_DECIMAL, 16, 5)
  'areaField = Field.Make("Area", #FIELD_DECIMAL,10,3)
  'acreField = Field.Make("Acres", #FIELD_DECIMAL, 10, 3)
  'v0Field = Field.Make("Val0", #FIELD_LONG, 5,0)
  'dateField = Field.Make("DateStamp", #FIELD_LONG, 10,0)
  'v1Field = Field.Make("Val1", #FIELD_LONG, 5,0)
  'v2Field = Field.Make("Val2", #FIELD_LONG, 5,0)
  'v3Field = Field.Make("Val3", #FIELD_LONG, 5,0)
  'v4Field = Field.Make("Val4", #FIELD_LONG, 5,0)
  'v5Field = Field.Make("Val5", #FIELD_LONG, 5,0)
  'v6Field = Field.Make("Val6", #FIELD_LONG, 5,0)
  'v7Field = Field.Make("Val7", #FIELD_LONG, 10,0)
  'v8Field = Field.Make("Val8", #FIELD_CHAR, 15,0)
  'cropField = Field.Make("Crop", #FIELD_CHAR, 30,0)
  'varField = Field.Make("Variety", #FIELD_CHAR, 30,0)
  tbl.AddFields({idField,clIDField,xField,yField})
  tbl.SetEditable(False)
  newTheme = FTheme.Make(tbl)
"-------------------------------------------------------------------------
'-- Add new shapefile to view
  theView.AddTheme(newTheme)
  newTheme.SetVisible(TRUE)
  av.GetProject.SetModified(true)
'-------------------------------------------------------------------------
'-- Cycle for each polyline segment to develop transects perpendicular to each line
  for each rec in clFTab
    '---------------------------------------------------------------------
    '-- Clear any previous selections
      clFTab.GetSelection.ClearAll
    '---------------------------------------------------------------------
    '-- Set the selection to the current record
      clFTab.GetSelection.Set(rec)
    '---------------------------------------------------------------------
    '-- Clear any existing graphics from the view
```

```
  gLst = theView.GetGraphics
  if (gLst.Count > 0) then
    gLst.Empty
  end
'-------------------------------------------------------------------------
'-- Create empty list to hold temporary centerline
  plylnList = {}
'-------------------------------------------------------------------------
'-- Get the current selected polyline segment of the centerline
  clPLine = clFTab.ReturnValue(clFTab.FindField("Shape"), rec)
  clID = clFTab.ReturnValue(clFTab.FindField("ID"), rec)
  thePlyLn = Polyline.MakeNull
  plylnList.Add(clPline.Clone)
  thePlyLn = plylnList.Get(0)
'-------------------------------------------------------------------------
'-- Return the total length of the centerline
  totalLength = thePlyLn.ReturnLength
'-------------------------------------------------------------------------
'-- Select the points in the Offset_UTM theme that intersect the segment
  ptFTab.SelectByFTab(clFTab, #FTAB_RELTYPE_ISWITHINDISTANCEOF ,0.1, #VTAB_SELTYPE_NEW)
  theView.Invalidate
'-------------------------------------------------------------------------
'-- Determine what names are used for X/Y coordinates
  xName = "None"
  yName = "None"
  fieldList = ptFTab.GetFields
  for each n in fieldList
    fldName = n.AsString

    if ((fldName = "Longitude") or (fldName = "X") or
      (fldName = "X-Coordinate") or (fldName = "X-Coord")) then
        xName = fldName
    elseif ((fldName = "Latitude") or (fldName = "Y") or
      (fldName = "Y-Coordinate") or (fldName = "Y-Coord")) then
        yName = fldName
    end
  end

  if ((xName = "None") or (yName = "None")) then
    Msgbox.Error("Coordinates could not be identified","Coordinate Error")
    exit
  end
'-----------------------------------------------------------
'-- Now run the transect portion with the selected centerline as the plyln
  '-- Initialize the previous bearing variable
    prevBearing = 0

  '-- For each point, get the point information
  for each rec in ptFTab.GetSelection
    thePoint = ptFTab.ReturnValue(ptFTab.FindField("Shape"), rec)
    xVal = ptFTab.ReturnValue(ptFTab.FindField(xName), rec)
    yVal = ptFTab.ReturnValue(ptFTab.FindField(yName), rec)
    'v0Val = ptFTab.ReturnValue(ptFTab.FindField("Val0"), rec)
    'dateVal = ptFTab.ReturnValue(ptFTab.FindField("DateStamp"), rec)
    'v1Val = ptFTab.ReturnValue(ptFTab.FindField("Val1"), rec)
    'v2Val = ptFTab.ReturnValue(ptFTab.FindField("Val2"), rec)
    'v3Val = ptFTab.ReturnValue(ptFTab.FindField("Val3"), rec)
    'v4Val = ptFTab.ReturnValue(ptFTab.FindField("Val4"), rec)
    'v5Val = ptFTab.ReturnValue(ptFTab.FindField("Val5"), rec)
    'v6Val = ptFTab.ReturnValue(ptFTab.FindField("Val6"), rec)
    'v7Val = ptFTab.ReturnValue(ptFTab.FindField("Val7"), rec)
    'v8Val = ptFTab.ReturnValue(ptFTab.FindField("Val8"), rec)
```

```
'crop = ptFTab.ReturnValue(ptFTab.FindField("Crop"), rec)
'variety = ptFTab.ReturnValue(ptFTab.FindField("Variety"), rec)
'-----------------------------------------------------------------------
'-- Calc distance along line
  ptPos = thePlyLn.PointPosition(thePoint)
  distAlong = totalLength * (ptPos/100)
'-----------------------------------------------------------------------
'-- Calc distance ahead of point where cross section will go
  thePnt = thePlyLn.Along(ptPos)
  xPt1 = thePnt.GetX
  yPt1 = thePnt.GetY

  newPnt = thePlyLn.Along(ptPos + 0.0001)
  xPt2 = newPnt.GetX
  yPt2 = newPnt.GetY
  deltaX = xPt2 - xPt1
  deltaY = yPt2 - yPt1
'-----------------------------------------------------------------------
'-- Calc bearing
  allowNeg = False
  bearing1 = (deltaY / deltaX).ATan
  if (deltaX < 0) then
    if (deltaY >= 0) then
      bearing1 = bearing1 + Number.GetPi
    else
      bearing1 = bearing1 - Number.GetPi
    end
  end

  if ((bearing1 < 0) and (not allowNeg)) then
    bearing1 = (Number.GetPi *2) + bearing1
  end
'-----------------------------------------------------------------------
'-- Compare bearing to previous bearing for break in operation check
'-- First check if rec is first or last record
  if (rec = 0) then
    prevBearing = bearing1
  else
    if (bearing1 - prevBearing > 20) then
      bearing1 = prevBearing
    else
      prevBearing = bearing1
    end
  end
'-----------------------------------------------------------------------
'-- Calc angle from bearing that is 90 degrees from direction of travel
  bearing2 = ((number.GetPi/2) - bearing1)
'-----------------------------------------------------------------------
'-- Set point positions for the new endpoints of the transect
  xCoord1 = (theDist * bearing2.Cos)
  yCoord1 = (theDist * bearing2.Sin)
  xCoord2 = (theDist * bearing2.Cos)
  yCoord2 = (theDist * bearing2.Sin)
'-----------------------------------------------------------------------
'-- Calc the new endpoints
  nwPnt = Point.Make((xPt1-xCoord1),(yPt1+yCoord1))
  nwPnt2 = Point.Make((xPt1+xCoord2),(yPt1-yCoord2))
'-----------------------------------------------------------------------
'-- Draw polyline graphic based on the 2 points
  lin = Line.Make(nwPnt, nwPnt2)
  plin = lin.AsPolyline
'-----------------------------------------------------------------------
```

```
      '-- Cut line into new temporary line shapefile
        theView.SetEditableTheme(newTheme)
        shpField = newTheme.GetFTab.FindField("Shape")
        newTheme.GetFTab.BeginTransaction
        rec = newTheme.GetFTab.AddRecord
        newTheme.GetFTab.SetValue(shpField, rec, plin)
        newTheme.GetFTab.EndTransaction
        newTheme.GetFTab.GetSelection.ClearAll
        newTheme.GetFTab.GetSelection.Set(rec)
        newTheme.GetFTab.UpdateSelection
        newTheme = theView.FindTheme(shpFileName)
      '-----------------------------------------------------------------------
      '-- Add other feature attributes to FTab
        newFTab = newTheme.GetFTab
        if (newFTab.IsEditable = "FALSE") then
          newFTab.SetEditable(True)
        end

        for each rec in newFTab.GetSelection
          newFTab.SetValue(idField,rec,rec+1)
          newFTab.SetValue(clIDField,rec, clID)
          newFTab.SetValue(xField,rec,xVal)
          newFTab.SetValue(yField,rec,yVal)
          'newFTab.SetValue(v0Field,rec,v0Val)
          'newFTab.SetValue(dateField,rec,dateVal)
          'newFTab.SetValue(v1Field,rec,v1Val)
          'newFTab.SetValue(v2Field,rec,v2Val)
          'newFTab.SetValue(v3Field,rec,v3Val)
          'newFTab.SetValue(v4Field,rec,v4Val)
          'newFTab.SetValue(v5Field,rec,v5Val)
          'newFTab.SetValue(v6Field,rec,v6Val)
          'newFTab.SetValue(v7Field,rec,v7Val)
          'newFTab.SetValue(v8Field,rec,v8Val)
          'newFTab.SetValue(cropField,rec,crop)
          'newFTab.SetValue(varField,rec,variety)
        end
      '-----------------------------------------------------------------------
      '-- Toggle editing off
        theView.SetEditableTheme(nil)
      '-----------------------------------------------------------------------
    end
  end

  theView.Invalidate
'------------------------------ End of Script ---------------------------
```

Create and clip harvest area polygons based on transect locations

```
'-- Initialize the transects theme and create the FTab
  theView = av.GetActiveDoc
  theThemes = theView.GetThemes
  lnTheme = theView.FindTheme("Transects.shp")
  lnFTab = lnTheme.GetFTab
  lnFTab.SetEditable(True)
'-------------------------------------------------------------------
'-- Select all records
  lnFTab.GetSelection.SetAll
'-------------------------------------------------------------------
'-- Determine the number of records in FTab
  numRecs = (lnFTab.GetSelection.Count) -1
'-------------------------------------------------------------------
'-- Create the polygon shapefile and set-up for entry of the polygons
'-- as drawn below.
  newThemeName = av.Run("CreatePolygonOutputFile",nil)
  for each t in theView.GetThemes
    if (t.GetName = newThemeName) then
      newTheme = t
    end
  end
  shpFileName = newTheme.GetName
'-------------------------------------------------------------------
'-- Select transects that correspond to each centerline segment
'   before processing
    '-- Determine the number of centerline segments
    clTheme = theView.FindTheme("Centerline.shp")
    clFTab = clTheme.GetFTab
    clNum = clFTab.GetNumRecords
    for each i in 1..clNum
      theBitmap = lnFTab.GetSelection
      theBitmap.ClearAll
      theQuery = "[CL_ID] = " + i.AsString
      lnFtab.Query(theQuery,theBitmap, #VTAB_SELTyPE_NEW)
      lnFTab.UpdateSelection
      selNum = lnFTab.GetSelection.Count
      recNum = 0
      '-------------------------------------------------------------
      '-- For each line and the next line
        for each rec in lnFTab.GetSelection
          recNum = recNum + 1
          '---------------------------------------------------------
          '-- Set up the graphics list
            gl = theView.GetGraphics
            gl.Empty
          '---------------------------------------------------------
          '
            lin1 = lnFTab.ReturnValue(lnFTab.FindField("Shape"), rec )
            lnID = lnFTab.ReturnValue(lnFTab.FindField("ID"), rec)
            'acre = lnFTab.ReturnValue(lnFTab.FindField("Acres"), rec)
          '---------------------------------------------------------

            if (recNum < selNum) then
              lin2 = lnFTab.ReturnValue(lnFTab.FindField("Shape"), rec + 1)
            else
              lin2 = lnFTab.returnValue(lnFTab.FindField("Shape"), rec - 1)
            end

            '-- Derive corner points for new polygon
```

```
  pt1 = lin1.AsLine.ReturnStart
  pt2 = lin1.AsLine.ReturnEnd
  pt3 = lin2.AsLine.ReturnEnd
  pt4 = lin2.AsLine.ReturnStart
'-----------------------------------------------------
'-- Remove old graphic shape
  theGraphicList = theView.GetGraphics
  theGraphicList.SelectAll
  theGraphicList.ClearSelected

'-- Now draw the new polygon from points
  newPoly = Polygon.Make({{pt1,pt2,pt3,pt4}})
  gp = GraphicShape.Make(newPoly)
  theView.GetGraphics.UnselectAll
  gp.SetSelected(TRUE)

'-- Paste the new graphic into the view
  theView.GetGraphics.Add(gp)

'-- Run subtration routine
  'if (recNum = 1) then
   '  'do nothing
  'else
    theView.SetEditableTheme(newTheme)

    '-- Does the graphic intersect any of the shapefile's
    '-- polygon features
    newFTab = newTheme.GetFTab
    for each rec in newFTab
      '-- Get the graphic shape
      '-- Change later to make sure there is only one
      '-- selected graphic
      theGraphicList = theView.GetGraphics
      theGraphicShape = theGraphicList.Get(0)
      theShape = theGraphicShape.GetShape

      '-- Remove old graphic shape
      theGraphicList.SelectAll
      theGraphicList.ClearSelected

      thePoly = newFTab.ReturnValue(newFTab.FindField("Shape"), rec)
      answer = thePoly.Intersects(theShape)
      if (answer = true) then
        '-- Subtract the temp shape from the selected feature
        '-- of the FTab
        newShape = theShape.ReturnDifference(thePoly)
        newGraphicShape = GraphicShape.Make(newShape)
       theGraphicList.Add(newGraphicShape)
      else
        newGraphicShape = GraphicShape.Make(theShape)
        theGraphicList.Add(newGraphicShape)
      end
    end

    '-- Reset the polygon theme to uneditable
    theView.SetEditableTheme(Nil)

  theGraphicList = theView.GetGraphics
  theGraphicShape = theGraphicList.Get(0)
  theShape = theGraphicShape.GetShape
  newPlygn = theShape.AsPolygon
```

```
            '-----------------------------------------------------
            '-- Put polygon into new shapefile
              theView.SetEditableTheme(newTheme)
              shpField = newTheme.GetFTab.FindField("Shape")
              ptIDField = newTheme.GetFTab.FindField("PointID")

              newTheme.GetFTab.BeginTransaction
              rec = newTheme.GetFTab.AddRecord
              newTheme.GetFTab.SetValue(shpField, rec, newPlygn)
              newTheme.GetFTab.EndTransaction
              newTheme.GetFTab.GetSelection.ClearAll
              newTheme.GetFTab.GetSelection.Set(rec)
              newTheme.GetFTab.UpdateSelection
            '-----------------------------------------------------
                 '-- Add other feature attributes to FTab
              newFTab = newTheme.GetFTab
              if (newFTab.IsEditable = "FALSE") then
                newFTab.SetEditable(True)
              end

            for each rec in newFTab.GetSelection
              newFTab.SetValue(ptIDField,rec,lnID)
            end
            '-----------------------------------------------------
            '-- Toggle editing off
            theView.SetEditableTheme(nil)
            '-----------------------------------------------------
        end
      '-------------------------------------------------------------
      i = i + 1
    end
'---------------------------------------------------------------------
'-- Stop editing, save edits and clear selections
  lnFTab.SetEditable(False)
  lnFTab.GetSelection.ClearAll
  lnFTab.UpdateSelection
  lnTheme.SetVisible(True)
'---------------------------------------------------------------------
'-- Clear the graphics list
  gl = theView.GetGraphics
  gl.Empty
'---------------------------------------------------------------------
'-- Refresh the view
  theView.Invalidate
'---------------------------------------------------------------------
'-- Remove temporary transect theme from view
  theThemes = theView.GetThemes
  for each t in theThemes
    if (t.GetName = "Transects.shp") then
      tempTheme = t
    end
  end

  'theView.DeleteTheme(tempTheme)
  av.GetProject.SetModified(true)
  av.PurgeObjects
'-------------------------- End of script -------------------------
```

Calculate Harvest Polygon Acreage

```
'-- Get the view and its projection if any.
  theView = av.GetActiveDoc
  thePrj = theView.GetProjection
  if (thePrj.IsNull) then
    hasPrj = false
  else
    hasPrj = true
  end
'-----------------------------------------------------------------
'-- Activate the newly created polygon theme and deactive all others
  theThemes = theView.GetThemes
  for each t in theThemes
    theFTab = t.GetFTab
    '-------------------------------------------------------------
    '-- Make the FTAB editable, and find out which type of feature it is.
    theType = theFTab.FindField("Shape").GetType
    if (theType = #FIELD_SHAPEPOLY) then
      t.SetActive(True)
      theFTab.SetEditable(True)
      '---------------------------------------------------------
      '-- Create the fields "Area" & "Acre"
        theAreaField = Field.Make("Area",#FIELD_DOUBLE,16,4)
        theAcreField = Field.Make("Acres", #FIELD_DOUBLE,16,4)
        theFTab.AddFields({theAreaField,theAcreField})
      '
      '-- Loop through the FTab and find the projected area and perimeter
      '   of each shape and set the field values appropriately.
        for each rec in theFTab
          theArea = 0
          theAcres = 0
          theShape = theFTab.ReturnValue(theFTab.FindField("shape"),rec)
          theFTab.QueryShape(rec,thePrj,theShape)
          theArea = theShape.ReturnArea
          theAcres = theArea*0.0002471044
          theFTab.SetValue(theAreaField,rec,theArea)
          theFTab.SetValue(theFTab.FindField("Acres"),rec,theAcres)
        end
      '-----------------------------------------------------------------
    else
      t.GetFTab.GetSelection.ClearAll
      t.SetActive(False)
    end
  end
'------------------------ End of Script ---------------------------
```

References

Al-Mahasneh, M.A. and T.S. Colvin. 2000. Verification of yield monitor performance for on-the-go measurement of yield with an in-board electronic scale. Transactions of the ASABE. 43(4):801-807.

Andersen, P.B. 1963. Combine control systems. U.S. Patent No. 3,073,099. January 14, 1963.

Arslan, S. and T.S. Colvin. 2002a. An evaluation of the response of yield monitors and combines to varying yields. Precision Agriculture. 3:107-122.

Arslan, S. and T.S. Colvin. 2002b. Grain yield mapping: yield sensors, yield reconstruction, and errors. Precision Agriculture. 3:135-154.

Beal, J. P. and L. F. Tian. 2001. Time shift evaluation to improve yield map quality. Applied Engineering in Agriculture. 17(3): 385-390.

Beck, A.D., S. W. Searcy, and J. P Roades. 2001. Yield data filtering techniques for improved map accuracy. Applied Engineering in Agriculture 17(4): 423-431.

Birrell, S. J., K. A. Sudduth, and S. C. Borgelt. 1996. Comparison of sensors and techniques for crop yield mapping. Computers and Electronics in Agriculture 14(2–3): 215–233.

Birrell, S. J., S. C. Borgelt, and K. A. Sudduth. 1995. Crop yield mapping: Comparison of yield monitors and mapping techniques. In Site Specific Management for Agricultural Systems. ASA-CSSA-SSSA, Madison, WI., pp. 15-31.

Blackmore, B. S., and C. J. Marshall. 1996. Yield mapping; errors and algorithms. In Proc. of the 3rd Intl. Conf. on Precision Agriculture, 403–415. Minneapolis, Minn. ASA-CSSA-SSSA.

Blackmore, B.S. and M.R. Moore. 1999. Remedial correction of yield map data. Precision Agriculture. 1:53-56.

Borgelt, S.C. 1993. Sensing and measurement technologies for site specific management. In Proc. of 1st Workshop on Soil Specific Crop Management, 141-158. P.C. Robert, R.H. Rust, W.E. Larson eds. Madison, Wisc.:ASA-CSSA-SSSA.

Chaplin, J., N. Hemming, and B. Hetchler. 2003. Comparison of an impact plate and torque based yield sensor. ASABE Paper No. 03-1034. St. Joseph, Minn.: ASABE.

Chung, S.O., K. A. Sudduth, S. T. Drummond. 2002. Determining yield monitoring system delay time with geostatistical and data segmentation approaches. Transactions of the ASABE 45(4): 915-926.

Coers, B. A., J.A. Teijido, D.J. Burke, T.S. Tsunemori, J.V. Peterson, W. F. Cooper, J.D. Littke, and J. Kis. 2002. Throughput control from combines having a variable torque sensing drive. U.S. Patent No. 6,475,081. November 5, 2002.

Colvin, T.S., D.L Karlen, J.R. Ambuel, and F. Perez-Munoz. 1995. Yield monitoring for mapping. In Site Specific Management for Agricultural Systems. ASA-CSSA-SSSA, Madison, WI., pp. 3-14.

Devore, J.L. 1999. *Probability and statistics for engineering and the sciences, 4th ed*. Duxbury Press. Pacific Grove, CA.

Diker, K., D.F. Heermann, W.C. Bausch, and D.K. Wright. 2002. Relationship between yield monitor and remotely sensed data for corn. ASABE Paper No. 02-1164. St. Joseph, Minn.: ASABE.

Doerge, T.A. 1999. Yield map interpretation. J. Prod. Agr. 12:57-61.

Doerge, T.A. 1996. Weigh wagon vs. yield monitor comparison. Crop Insights. 7(17):1-5.

Drummond, S. T., C. W. Fraisse, and K. A. Sudduth. 1999. Combine harvest area determination by vector processing of GPS position data. Transactions of the ASABE 42(5): 1221–1227.

ESRI. 2001. ArcView GIS®, version 3.3. Redlands, Cal.: Environmental Systems Research Institute, Inc.

Friesen, O.H., G.C. Zoerb, and F.W. Bigsby. 1966. For combines: Controlling feedrates automatically. Agricultural Engineering 47(8):434-435.

Fulton, J.P., S.A. Shearer, T.S. Stombaugh, M.E. Anderson, T.F. Burks, and S.F. Higgins. 2003. Simulation of fixed and variable-rate application of granular materials. Transaction of ASABE. 46(5):1311-1321.

Grisso, R., M. Alley, and P. McCellan. 2003. Precision farming tools: yield monitor. Publication No. 442-502. Virginia Cooperative Extension, Blacksburg, VA.

Grisso, R.D., P.J. Jasa, M.A. Schroeder, and J.C. Wilcox. 2002. Yield monitor accuracy: successful farming magazine case study. Applied Engineering in Agriculture. 18(2):147 – 151.

Han, S., S.M. Schneider, S.L. Rawlins, and R.G. Evans. 1997. A bitmap method for determining effective combine cut width in yield mapping. Transactions of the ASABE. 40(2):485-490.

Hoffman, R. 1996. A perception architecture for autonomous harvesting. ASABE Paper No. 96-3068. St. Joseph, Minn.: ASABE.

Howard, K.D., J.L. Pringle, M.D. Shrock, D.K. Kuhlman, and D. Oard. 1993. An elevator-based grain flow sensor. ASABE Paper No. 93-1504. St. Joseph, Minn.: ASABE.

IEEE. 1979. Programs for Digital Signal Processing, Algorithm 5.2. IEEE Press, New York

Karlen, D.L., E.J. Sadler, and W.J. Busscher. 1990. Crop yield variation associated with costal plain soil map units. Soil Sci. Soc. Am. J. 56:1249-1256.

Lamb, J.A., J.L., Anderson, G.L. Malzer, J.A. Vetch, R.H. Dowdy, D.S. Onken, and K.I .Ault. 1995. Perils of monitoring grain yield on-the-go. In Site-Specific Management for Agricultural Systems, 87-90. P.C. Roberts R.H. Rust, and W.E. Larson, eds. Madison, Wisc.: ASA, CSSA, and SSSA..

Lark, R.M., J.V. Stafford, and H.C. Bolam. 1997. Limitations on the spatial resolution of yield mapping for combinable crops. Journal of Agricultural Engineering Research. 66:183-193.

Lowenberg-DeBoer, J. and S.M. Swinton. 1997. Economics of site-specific management in agronomic crops. In Site-Specific Management for Agricultural Systems, 369-396. P.C. Robert R.H. Rust, and W.E. Larson, eds. Madison, Wisc.: ASA, CSSA, and SSSA..

Maertens, K., P. Reyns, and J. De Baerdemaeker. 2003. Double adaptive notch filter for mechanical grain flow sensors. Journal of Sound and Vibration. 266: 645-654.

The Mathworks. 2005. Matlab®, version 7.0.1. Natick, MA. The Mathworks.

Missotten, B., G. Strubbe, and J. De Baerdemaeker. 1996. Accuracy of grain and straw yield mapping. In Proc. 3rd Int'l. Conf. on Precision Agriculture, 713-722. P.C. Robert, R.H. Rust, and W.E. Larson, eds. Madison, Wisc.: ASA., CSSA, and SSSA.

Moore, M.R. 1998. An investigation into the accuracy of yield maps and their subsequent use in crop management. PhD diss. Silsoe, UK.: Cranfield University, Silsoe College.

Nelson, R.G. 2002. Resource assessment and removal analysis for corn stover and wheat straw in the Eastern and Midwestern United States – rainfall and wind-induced soil erosion methodology. Biomass and Bioenergy. 22:349-363.

Nolan, S. C., G. W. Haverland, T. W. Goddard, M. Green, D. C. Penney, J. A. Henriksen, and G. Lachapelle. 1996. Building a yield map from geo–referenced harvest measurements. In Proc.3rd International Conference on Precision Agriculture, 885–892. Madison, Wisc.: ASA,CSSA, and SSSA.

Pierce, F.J., N.W. Anderson, T.S. Colvin, J.K. Schueller, D.S. Humburg, and N.B. McLaughlin. 1997. Yield mapping. In The State of Site-Specific Management for Agriculture, 211-245. F.J. Pierce and E.J. Sadler, eds. Madison, Wisc.: ASA, CSSA, and SSSA.

Rietz, P., and H.D. Kutzbach. 1996. Investigation on a particular yield mapping system for combine harvesters. Computers and Electronics in Agriculture. 14:137-150.

Schueller, J.K., M.P. Mailander, G.W. Krutz. 1985. Combine feedrate sensors. Trans. of the ASABE. 28(1):2-5.

Schnug, E., D. Murphy, E. Evans, S. Haneklaus, and J. Lamp. 1993. Yield mapping and application of yield maps to computer-aided local resource management. In Proc. of 1st Workshop on Soil Specific Crop Management, 141-158. P.C. Robert, R.H. Rust, W.E. Larson eds. Madison, Wisc.:ASA-CSSA-SSSA.

Schrock, M.D., D.L. Oard, R.K. Taylor, E.L. Eisele, N. Zhang, Suhardjito, J.L. Pringle. 1999. A diaphragm impact sensor for measuring combine grain flow. Applied Engineering in Agriculture. 15(6):639-642.

Searcy, S.W., J.K. Schueller, Y.H. Bae. S.C. Borgelt, and B.A. Stout. 1989. Mapping of spatially variable yield during grain combining. Transactions of the ASABE. Vol. 32(3): 826-829.

Stafford, J. V., B. Ambler, and H. C. Bolam. 1997. Cut width sensors to improve the accuracy of yield mapping systems. In Proc. Precision Agric. '97. Vol. II: Technology, IT, and Management, 2: 519-527. Milan, Italy BIOS Scientific Publishing Ltd.

Stafford, J. V., B. Ambler, and H.C Wheeler. 1994. Mapping yield variation to aid crop management. In Proc. of the XII World Congress on Agricultural Engineering, 1: 88-96. London, UK: SCI.

Stout, B.L., S.C. Borgelt, and K.A. Sudduth. 1993. Yield determination using an instrumented Claas Combine. ASABE Paper No. 93-1057. St. Joseph, Minn.:ASABE.

Sudduth,K.A., S.T. Drummond, W. Wang, M.J. Krumpelman, and C.W. Fraisse. 1998. Ultrasonic and GPS measurement of combine swath width. ASABE Paper No. 98-3096. St. Joseph, Minn.: ASABE.

Taylor, R.K. H.M. Hobby, and M.D. Shrock. 2005. Evaluation of an automatic feedrate control system for a grain combine. ASABE Paper No. 05-1134. St. Joseph, Minn.: ASABE.

Taylor, R. K., M. D. Schrock, and S. A. Staggenborg. 2002. Extracting machinery management information from GPS data. ASABE Paper No. 02-1008. St. Joseph, Minn.: ASABE.

Vansichen, R. and J. De Baerdemaeker. 1991. Continuous wheat yield measurement on a combine. In Proceedings ASABE Symposium on Automated Agriculture for the 21st Century, Chicago, IL, 16-17 Dec 1991. ASABE, St. Joseph, MN, pp. 346-355.

Veal, M.W., S.A. Shearer, J.P. Fulton. 2004. Improved mass flow sensing for yield monitoring in grain combines. ASABE Paper No. 04-1101. St. Joseph, Minn.: ASABE.

Whelan, B. M., and A. B. McBratney. 1997. Sorghum grain flow convolution within a conventional combine harvester. In 1st European Conference on Precision Agriculture, Vol. II: Technology, IT, and Management, 759–766. Oxford, U.K.: BIOS Scientific Publishers.

Whelan, B.M. and A.B. McBratney. 2002. A parametric transfer function for grain-flow within a combine conventional harvester. Precision Agriculture. 3(2):123-134.

Wild, K., S. Ruhland, and S. Haedicke. 2003. Performance of pulse radar systems for crop yield monitoring. ASABE Paper No. 03-1038. St. Joseph, Minn.: ASABE.

Vita

Matthew W. Veal

PERSONAL INFORMATION

Born 27 December 1977 in Atlanta, GA

EDUCATION

M.S., Auburn University, Mechanical Engineering, Auburn, AL, August, 2003

Thesis:	*Improving Forest Machine Operator Protective Structures: Modeling the Behavior of Excavator Roll/Tip-Overs*
Advisor:	Steve E. Taylor

B.S. Magna Cum Laude, Auburn University, Forest Engineering, Auburn, AL May, 2001

EMPLOYMENT

2003 - Present	**Biosystems and Agricultural Engineering Department, University of Kentucky; Lexington, KY** *Engineer Associate*
2001 - 2003	**Department of Biosystems Engineering, Auburn University, AL** *Graduate Research Assistant*
1999 – 2001	**Department of Biosystems Engineering, Auburn University, AL** *Research Assistant*

TEACHING EXPERIENCE

2005 - Present	**Biosystems and Agricultural Engineering Department, University of Kentucky; Lexington, KY** *Instructor - Embedded Controls for Agriculture*
2001 - 2003	**Biosystems Engineering Department, Auburn University; Auburn, AL** *Graduate Teaching Assistant – Spatial Technologies*

PROFESSIONAL LICENSURE

- E.I.T. State of Alabama

PROFESSIONAL ASSOCIATIONS

- American Society of Agricultural Engineers
- Council on Forest Engineering
- Society of Automotive Engineers
- Tau Beta Pi Engineering Honor Society
- Gamma Sigma Delta Agriculture Honor Society
- Xi Sigma Pi Forestry Honor Society

PROFESSIONAL SERVICE

- 2006 ASABE AETC Planning Committee
- 2000-01 ASABE Southeast Region Student President

AWARDS

- Auburn University Graduate Research Forum – FIRST PLACE 2003
- Named one of Auburn University's Top 10 Master's Students, 2003
- Council on Forest Engineering Student Communication Award 2002
- Auburn University Presidential Fellowship 2001-2002, 2002-2003
- Forest Engineering Student of the Year 2001
- ASABE Preprofessional Poster Competition – FIRST PLACE 2000

RECENT FUNDING

Precision Placement of Granular Material via Distributed Control. **M.W. Veal**, S.A. Shearer, T. S. Stombaugh. 2005 USDA-CSREES Special Grants Program, $45,823. 10/05 – 10/07.

CAN-Based Precision Seed Placement. S.A. Shearer, T. S. Stombaugh, **M.W. Veal**, C. Dillon, M. Darr. 2004 USDA-CSREES Special Grants Program, $65,525. 10/04 – 10/07.

REFEREED and PEER-REVIEWED ARTICLES

Veal, M.W., S.E. Taylor, and R.B. Rummer. 2005. Modeling Excavator Rollovers with ADAMS. Journal of Agricultural Safety and Health. ASABE, St. Joseph, MI. Submitted 1/31/2005.

Veal, M.W., S.A Shearer, and J.P. Fulton. 2005. Improved Mass Flow Sensing for Yield Monitoring in Grain Combines. Transactions of ASABE. ASABE, St. Joseph, MI. In Review. Submitted 8/12/2005

Veal, M.W., S.E. Taylor, R.B. Rummer, R.L. Raper. 2005. Evaluation of site preparation plow energy requirements. International Journal of Forest Engineering 16(2):129-136.

Veal, M.W., S.E. Taylor, R.B. Rummer. 2004. The Use of Multi-Body Dynamic Computer Simulation to Investigate the Likelihood of Excavator-Based Forest Machine Rollover. Proceedings of the 27th Annual Meeting of the Council on Forest Engineering. COFE, Corvallis, OR. 5 pp.

Veal, M.W., S.E. Taylor, R.B. Rummer, J.W. Baier. 2003. Development of a test device for evaluation of thrown object hazards. Journal of Agricultural Safety and Health. 9(2):119-131

Veal, M.W., S.E Taylor, T.P. McDonald, D.T. McLemore, and M.R. Dunn. 2001. Accuracy of Tracking Forest Machines with GPS. Transactions of ASABE 44(6):1903-1911. ASABE, St. Joseph, MI.

Taylor, S.E., T.P. McDonald**, M.W. Veal**, T.E. Grift. 2001. Using GPS to Evaluate Productivity and Performance of Forest Machine Systems. *In* Proceedings of the First International Symposium on Precision Forestry. University of Washington, Seattle, WA. p. 151-155.

PUBLISHED PROCEEDINGS

Shearer, S.A., **M. Veal**, and J.P. Fulton. 2004. Post-Processing Correction to Improve the Accuracy of Yield Monitor Data in Grain Crops. Proceedings of the Seventh Annual Conference on Precision Agriculture. July 25-28, 2004. Minneapolis, Minnesota.

Veal, M.W., S.E. Taylor, R.B. Rummer. 2004. The Use of Multi-Body Dynamic Computer Simulation to Investigate the Likelihood of Excavator-Based Forest Machine Rollover. Proceedings of the 27th Annual Meeting of the Council on Forest Engineering. COFE, Corvallis, OR. 5 pp.

Rummer, R.B., S.E. Taylor, M.W. Veal. 2003. New developments in operator protection for forest machines. In Proceedings of the 2nd International Conference on Forest Engineering. Skogforsk. Vaxjo, Sweden. 8 pp.

Rummer, R.B., S.E. Taylor, M.W. Veal. 2003. Thrown object testing of forest machine operator protective structures. In Proceedings of the 2nd International Conference on Forest Engineering. Skogforsk. Vaxjo, Sweden. 5 pp

Veal, M.W., S.E. Taylor, R.B. Rummer. 2003. Modeling rollover behavior of excavator-based forest machines. In Proceedings of the 2nd International Conference on Forest Engineering. Skogforsk. Vaxjo, Sweden. 5 pp.

Taylor, S.E., T.P. McDonald, M.W. Veal, F.W. Corley, T.E. Grift. 2002. Precision Forestry: Operational tactics for today and tomorrow. *In*: Forest engineering challenges: a global perspective. Proceedings of the 25th Annual Meeting of the Council on Forest Engineering. COFE, Corvallis, OR. 6 pp.

Veal, M.W., S.E. Taylor, R.B. Rummer, R.L. Raper. 2002. Evaluation of site preparation plow energy requirements. *In*: Forest engineering challenges: a global perspective. Proceedings of the 25th Annual Meeting of the Council on Forest Engineering. COFE, Corvallis, OR. 5 pp.

Veal, M.W., S.E Taylor, T.P. McDonald. 1999. Effects of Forest Canopy on GPS. *In* Proceedings of the 22nd Annual Meeting of the Council on Forest Engineering. COFE, Corvallis, OR. 12 pp.

ABSTRACTS AND MEETING PAPERS

Veal, M.W., S.A. Shearer, R.M. Prewitt. 2005. The Use of Multiple Mass Flow Sensing Techniques to Improve the Accuracy of Yield Monitor Data. ASABE Technical Paper No. 05-1128. ASABE, St. Joseph, MI.

Veal, M.W., S.A. Shearer, T.S. Stombaugh, B.K. Koostra. 2005. Assessment of GPS Guidance System Accuracy using Multiple RTK-GPS Receivers. ASABE Technical Paper No. 05-1089. ASABE, St. Joseph, MI.

Shearer, S.A., T.S. Stombaugh, **M.W. Veal**. 2005. Distribution and Directional Dependence of GPS Receiver Dynamic Cross-Track Errors Under Constant Acceleration. ASABE Technical Paper No. 05-5085. ASABE, St. Joseph, MI.

Koostra, B.K., T.S. Stombaugh, S.A. Shearer, **M.W. Veal**. 2005. GIS Analysis of Dynamic GPS Test Data. ASABE Technical Paper No. 05-1084. ASABE, St. Joseph, MI.

Stombaugh, T.S., J. Cole, B.K. Koostra, S.A. Shearer, **M.W. Veal**. 2005. Comparison of GPS Receiver Dynamic Performance Using a Test Fixture. ASABE Technical Paper No. 05-1086. ASABE, St. Joseph, MI.

McDonald, B. M., S.A. Shearer, **M.W. Veal**. 2005. CAN-Based Planter Control Development and Performance. ASABE Technical Paper No. 05-1124. ASABE, St. Joseph, MI.

Veal, M.W., S.E. Taylor, R.B. Rummer. 2004. Evaluating the rollover potential of Excavator-based Machines. ASABE Technical Paper No. 04-5011. ASABE, St. Joseph, MI.

Veal, M.W., S.E. Taylor, R.B. Rummer, and J.W. Baier. 2002. Development of a Test Device for Evaluation of Thrown Object Hazards. ASABE Technical Paper No. 02-8018. ASABE, St. Joseph, MI.

Veal, M.W., S.E Taylor, T.P. McDonald. 2001. Evaluation of Forestry Site Preparation Equipment Using GPS. ASABE Technical Paper No. 01-8018. ASABE, St. Joseph, MI.

Veal, M.W., S.E Taylor, T.P. McDonald, D.K. McLemore, and M.R. Dunn. 2000. Accuracy of Tracking Forest Machines with GPS. ASABE Technical Paper No. 00-5015. ASABE, St. Joseph, MI.

PROFESSIONAL PRESENTATIONS

Veal, M.W. On Farm Data Management in 2025. 2006 Agricultural Equipment Technology Conference. Louisville, KY. February 12-14,2006.

Veal, M.W. and S.A. Shearer. Precision Placement of Crop Inputs and Management Resolution. 2006 Kansas Agricultural Research Association 7th Annual Precision Agriculture Conference. McPherson, KS. January 24-25,2006.

Veal, M.W. and S.A. Shearer. Evaluation of Auto-Guidance System Accuracy. 2005 Agricultural Machinery Conference. Cedar Rapids, IA. May 3-4,2005.

Veal, M.W. and S.A. Shearer. Assessment of AutoTrac Cross-Track Error. John Deere AMS. Des Moines, IA. July 21-22, 2004.

Veal, M.W. *Multi-body Dynamic Simulation of Forestry and Construction Excavator Rollovers.* SAE MTC SC4, Forest Committee Meeting. Auburn, Alabama, July 15-17, 2003.

Veal, M.W. *Rigid-body analysis of Hydraulic Excavator Rollover.* Society of Automotive Engineers MTC SC4, Forestry Committee Meeting. Eugene, Oregon, February 19, 2003.

Veal, M.W. *Improving forest machine operator protective structures.* Society of Automotive Engineers MTC SC4, Forestry Committee Meeting. Woodstock, Ontario, October 16-17, 2002.

Veal, M.W. *Evaluation of forestry plow energy requirements for site Preparation.* 25th Annual Council on Forest Engineering Meeting. Auburn, AL, June 16-19, 2002.

Veal, M.W. and S.E. Taylor. *Protecting forest machine operators from flying debris: A demonstration of THOR.* 25th Annual Council on Forest Engineering Meeting. Auburn, AL, June 16-19, 2002.

Veal, M.W. *Drawbar pull of tillage implements used in forestry.* Forest industry site preparation working group. Auburn, AL, December 6, 2001.

Veal, M.W. *Optimizing forest site preparation operation*. Forest industry site preparation working group. Auburn, AL, October 25, 2001.

Matthew W. Veal

4 August 2006